

**Faculty of Science and Engineering
Department of Petroleum Engineering**

**Numerical Modelling to Evaluate Temperature Profile along an
Injection or Production Wellbore**

Nematollah Tarom

This thesis is presented for the Degree of

Doctor of Philosophy

of

Curtin University

September 2013

Declaration

To the best of my knowledge and belief this thesis contains no material previously published by any other person except where due acknowledgment has been made. This thesis contains no material which has been accepted for the award of any other degree or diploma in any university.

Name:

Nematollah Tarom

Signature:

Date:

26/09/2013

Abstract

Well surveillance involves investigation and analysis of problematic wells or fields that cause substantial production and operating cost problems; and then taking corrective measures. Appropriate action thereafter must identify the causes of the problem through the monitoring process of the reservoir's performance, well maintenance, functions of surface production and treating equipment from the technical and economic viewpoints. The temperature profile is a measurement of the flowing well temperature and is a function of depth along the wellbore in a producing, injection and/or shut-in well, which has been used as a popular tool in the industry that may help to identify the causes of many injection and production related well problems.

Wellbore flowing temperature can be measured through work-over or well intervention operations using a Production Logging Tool (PLT) and/or from an intelligent well completed with permanent down-hole sensors, such as a Distributed Temperature Sensing (DTS) system. However, because of many mechanical and technical limitations; and involvement of high CAPEX and OPEX costs for each project, numerical methods of predicting wellbore flow temperatures may be considered a viable alternative option. Most of the work relevant to temperature analysis found in the literature is dedicated to certain scenarios, such as single phase liquid or gas flow either for the injection or production cases. As result, most of these models have very limited use/capability to address the real field case. Our contribution to new knowledge found in this thesis is focused on developing a multi-purpose practical numerical simulator that can potentially be used to address a wide range of cases such as single phase liquid, single phase gas, multiphase flow for both injection and production wells.

A numerical model is developed which has been based on an overall heat transfer coefficient which accounts for all modes of the heat transferring mechanism for single and multiphase flow, in order to predict the temperature profile along the injection and production wellbore (temperature log). Because of the wellbore complexity, different issues are considered in the process of the wellbore heat

transmission evaluation. A wellbore typically consists of a complex configuration of parameters, including different layers of casing, tubing, annulus, cement sheaths and ground. These layers may have different thermal properties. This thesis then considers the presence of different mechanisms of heat transfer in the evaluation of the wellbore heat transmission process during the passage of different types of fluid such as gas, liquid and multiphase fluid flowing through the production and injection wells.

A computer simulator, named as WTP (wellbore temperature profile) is developed as the numerical model. The potential application of this model has been tested for accuracy: by comparison and validation of the numerical results with many published field cases for injection and production wells; and results from sensitivity studies in response to different production cases that might occur in a real situation. It is demonstrated that the numerical simulator has wide capabilities to deal with single and multiphase fluid flow; and can potentially be used as a powerful tool to analyse many injection/production scenarios with reasonable accuracy, especially for the routine industry case.

This thesis demonstrates that the behaviour and nature of the dependency of the wellbore flowing temperature profile for injection and production wells is very complex, specifically in the case of multiphase flow. Such behaviour is further influenced by many parameters such as the thermal properties of the wellbore surroundings, types of flowing fluid, fluid compositions; impurities carried by flowing fluid, production rate, size of production string, wellbore configuration/schematic, in-situ reservoir temperature and/or geothermal temperature gradient; and heat transfer mechanisms. For instance, impurities such as water, N₂, CO₂, H₂S and so on produced during gas production can substantially influence the behaviour of the temperature profile. A comprehensive discussion on many issues associated with injection and production wells is continued throughout this thesis.

Acknowledgment

Throughout this research, I have been supported by many people whom I would like to thank them.

Firstly, I would like to convey my sincere gratitude to my supervisor, Dr. Mofazzal Hossain for his generous help, support and encouragements throughout the course of this study. Also, I am deeply indebted to my associate supervisor, Dr. David Parks for his constructive comments and suggestions. I would not be able to complete this study without your sincere support.

I wish to thank to people at the Department of Petroleum and Engineering, Curtin University, Professor Brian Evans, chairperson of this thesis committee, Dr. Vamegh Rasouli, head of department, Professor Reza Rezaei and Dr Ali Saeedi for their technical supports and advises throughout of the accomplishment of this research.

I thank the Office of Research and Development at Curtin University for financial support (CIPRS) through this study. I would also like to acknowledge and express my appreciation to Mr Simon Roy for his help and supports.

Also, I would like to thank Dr. Christina Houen, the editorial, for her concise and thorough work.

Very special and lovingly thanks to my wife, Azar Rohi, and my gorgeous daughter, Golshid Tarom for their love, commitment, encouragement and patience which support me work harder every day. They have made my life joyful and have always been my great motivation to live.

Lastly, I wish I could thank my father, who passed away just a few days before my thesis submission, and special thanks go to my mother and parents in law giving me their immense support, encouragement and love. Also, I appreciate from Masoud Zaeim for his enormous supports and encouragement throughout of this study.

I am happy to enjoy the relationship, friendship and support of many people.

Lovingly dedicate to:

My wife Azar

and

My daughter Golshid

who supported me each step of the way.

Contents

Abstract	iii
Acknowledgment	v
Contents	vii
List of Figures	xi
List of Tables	xv
Nomenclature	xvi
Chapter 1 Introduction.....	1
1.1 Background	1
1.1.1 Temperature Profile.....	2
1.1.2 Application of Temperature Profile	3
1.1.3 Heat Transfer Mechanism Through a Wellbore.....	4
1.2 Objectives of the study.....	7
1.3 Significants of this research	8
1.4 Outline of Thesis	9
Chapter 2 Literature Review	11
2.1 Literature Review	11
2.2 General Energy Balance Equation	13
2.3 Theoretical factors.....	15
2.4 Technical factors	19
2.5 Financial factors	21
Chapter 3 Analytical Model Predict the Temperature Distribution Surrounding the Wellbore.....	22

3.1	Introduction	22
3.2	Governing equation	24
3.2.1	Conservation of Mass.....	24
3.2.2	Momentum Balance.....	26
3.2.3	Energy Balance	29
3.2.4	Pressure/Volume/Temperature (PVT) relation	32
3.3	Temperature Model	34
3.3.1	Basic concept of heat transfer	34
3.3.2	Overall heat transfer coefficient	36
3.3.3	Analytical model for temperature prediction at tubing and casing surfaces	38
3.3.4	Algorithm of temperature loss profile	40
3.4	ANSYS software and Excel spread sheet	42
3.4.1	Pre-processing ANSYS Fluent Model.....	45
3.4.2	Fluent definitions	47
3.4.3	Excel spread sheet	48
3.5	Validation and discussion of results.....	50
3.6	Summary	56

Chapter 4 Numerical Modelling of the WTP Simulator58

4.1	The WTP Simulator.....	58
4.2	Single phase liquid flow	59
4.2.1	Temperature profile calculation along a liquid producing wellbore	60
4.2.2	Laminar flow	62
4.2.3	Turbulent flow.....	63
4.3	Single phase gas flow	64
4.3.1	Temperature profile calculation along a gas producing wellbore	64
4.3.2	Temperature loss calculation of flowing gas	67
4.3.3	Pressure loss calculation of flowing gas.....	67
4.3.4	Gas properties.....	69
4.3.5	Gas mixtures	70
	• Gas mixtures with known components.....	71

○	Calculation of pseudo-critical properties of a real gas	71
○	Peng-Robinson equation of state (PR EOS).....	73
○	Mixing rules	74
○	Evaluation of term $(\partial Z/\partial T)_p$	75
●	Gas mixtures with unknown components.....	76
○	Compressibility factor (Z).....	76
○	Evaluation of term $(\partial Z/\partial T)_p$	78
●	Joule-Thomson Coefficient.....	82
4.3.6	Temperature loss at perforations.....	85
4.4	Multiphase fluid flow.....	88
4.4.1	Temperature profile calculation along a multiphase producing wellbore	89
4.4.2	Multiphase flow definitions.....	90
4.4.3	Multiphase flow regimes	93
4.4.4	Multiphase fluid flow pressure gradient.....	95
4.4.5	Flash calculation.....	97
4.5	Summary	100

Chapter 5 Numerical Simulation, Case Studies and Sensitivity Analysis 105

5.1	Introduction.....	105
5.2	Single Phase Liquid Production.....	106
5.2.1	Case study #1 (Example from Hasan and Kabir):	108
5.2.2	Case study #2 (Oil Producing Well).....	113
5.2.3	Case study #3 (Thompson Well Data).....	117
5.3	Single Phase Gas Production	119
5.3.1	Case study #4(Joule-Thomson Effect).....	122
5.3.2	Case Study #5 (Buttress-1 Well CO2CRC Otway project).....	131
5.3.3	Case Study #6 (EnCana’s Gas Wells, Western Canada).....	134
5.3.4	Case Study #7 (Gas Producing Well)	138
5.4	Multi-Phase Fluid Production	140
5.4.1	Case Study #8 (Well Name: GC-17).....	141

5.4.2	Case Study #9 (Tah Field, China)	146
5.5	Injection.....	151
5.5.1	Case Study #10 (CRC-1 Well CO2CRC Otway project).....	152
5.5.2	Case Study #11 (Water Injection Well)	155
5.6	Summary	158

Chapter 6 Conclusions and recommendations 161

6.1	Overview	161
6.2	Conclusion	162
6.2.1	The analytical model	162
6.2.2	Features of the WTP simulator	163
6.2.3	Performance of the WTP Simulator	164
6.2.4	Research Outcomes and Findings	164
6.3	Recommendations	166

_Toc367873875

References 167

Appendices

Appendix A	185
Appendix B	189
Appendix C	191
Appendix D	193
Appendix E	201
Appendix F	206

List of Figures

Figure 1-1 Direction of heat transfer from/to wellbore to/from surrounding area during production and injection operation	5
Figure 1-2 Wellbore schematic and the surroundings contributing to heat transference	6
Figure 2-1 Production Logging	12
Figure 2-2 A typical horizontal well equipped with DTS	14
Figure 3-1 Illustration of modelling concept	23
Figure 3-2 Mass, momentum and energy balances	25
Figure 3-3 Typical phase envelope for a multicomponent mixture (Tarom et al., 2002).	33
Figure 3-4 Heat Distribution from wellbore towards surroundings area.....	36
Figure 3-5 Transient heat conduction in an infinite radial system (RAMEY JR., 1962)	42
Figure 3-6 Heat transfer calculation algorithm	44
Figure 3-7 Wellbore schematic which is designed and meshed by ANSYS/DesignModular	46
Figure 3-8 Wellbore schematic including boundaries definition.....	47
Figure 3-9 Wellbore schematic surrounded by different layers.....	49
Figure 3-10 Input information in the Excel spread sheet.....	49
Figure 3-11 Results gathered in the Excel spread sheet.....	50
Figure 3-12 Heat loss profile around a wellbore.....	51
Figure 3-13 Transient temperature profile around a wellbore for a simple case study	52
Figure 3-14 Comparison of heat loss around a wellbore with and without the application of a radiation heat transfer mechanism through an annulus.....	54
Figure 3-15 Transient temperature profile around a wellbore	55
Figure 3-16 Comparison of temperature profile of this work and FLUENT after 7 days of production.....	55

Figure 3-17 Comparison of temperature profile of this work and FLUENT after 10 days of production.....	57
Figure 3-18 Comparison of temperature profiles calculated by this work and FLUENT after 21 days of production.	57
Figure 4-1 The flow diagram of the WTP Simulator.....	59
Figure 4-2 Flow diagram to design a wellbore through the WTP Simulator.....	60
Figure 4-3 Flow diagram of single phase liquid flow of the WTP simulator.	65
Figure 4-4 Prediction of correction factor C as a function of specific gravity of gas mixture	83
Figure 4-5 Schematic representation of Joule-Thomson effect (modified from Smolen, 1996 (Smolen, 1996))	84
Figure 4-6 Flow diagram of single phase gas flow of the WTP simulator.	87
Figure 4-7 Schematic of multiphase flow	89
Figure 4-8 Flow diagram of temperature loss calculation between two nodes.....	90
Figure 4-9 Flow regimes in upward vertical gas-liquid flow.....	94
Figure 4-10 Schematic of the flash of the wellbore fluid.....	100
Figure 4-11 Flow diagram of multi-phase flow of the WTP simulator.	102
Figure 4-12 Flow diagram of injection section of the WTP simulator.	103
Figure 5-1 Wellhead temperature at different rates (Hasan et al., 1997) (case study #1)	109
Figure 5-2 Comparison of wellbore temperature profiles (case study #1).....	110
Figure 5-3 Temperature profiles for case study #1 at different production rates.....	111
Figure 5-4 Temperature profiles for case study #1 with different production tubing sizes	112
Figure 5-5 Comparison of wellbore temperature profiles (case study #2).....	114
Figure 5-6 Temperature profiles for case study #2 at different production rates for tubing size of 4.5 inches.....	115
Figure 5-7 Temperature profiles for case study #2 with different production tubing sizes for a production rate of 3000 STB/d.	116
Figure 5-8 Comparison of wellbore temperature profiles.....	117
Figure 5-9 Temperature profiles for case study #3 and API sensitivity analysis.....	118

Figure 5-10 Calculation of Joule Thomson effect for gas mixture 1 (case study #4)	122
Figure 5-11 Calculation of Joule-Thomson effect for gas mixture 2 (case study #4)	123
Figure 5-12 Calculation of Joule-Thomson effect for gas mixture 3 (case study #4)	124
Figure 5-13 Calculation of Joule-Thomson effect for gas mixture 4 (case study #4)	124
Figure 5-14 Calculation of Joule-Thomson effect for gas mixture 5 (case study #4)	125
Figure 5-15 Calculation of Joule-Thomson effect for gas mixture 6 (case study #4)	125
Figure 5-16 Calculation of Joule-Thomson effect for gas mixture 7 (case study #4)	126
Figure 5-17 Calculation of Joule-Thomson effect for gas mixture 8 (case study #4)	126
Figure 5-18 Typical well schematic (Case study #4)	128
Figure 5-19 Evaluation of temperature profile and Joule-Thomson effect for mixture 1 of Table 3-1 (case study #4)	129
Figure 5-20 Prediction of temperature profile and the Joule-Thomson effect at different flow rates of gas mixture number 1 in Table 3.1 for a typical wellbore schematic in Figure 5-18 (case study #4)	130
Figure 5-21 The CO2CRC Otway project location (case study #5)	132
Figure 5-22 Comparison of wellbore temperature profiles (case study #5)	133
Figure 5-23 Temperature data over the reservoir interval (after Huebsch et al. (Huebsch et al., 2008)) (case study #6)	135
Figure 5-24 Flowing and shut-in wellbore temperature (after Huebsch et al. (Huebsch et al., 2008)) (case study #6)	136
Figure 5-25 Comparison of wellbore temperature profiles (case study #6)	137
Figure 5-26 Joule-Thomson effect at the entry point to the wellbore (case study #6)	137
Figure 5-27 Surface temperature (case study #6)	138

Figure 5-28 Comparison of wellbore temperature profiles (case study #7).....	139
Figure 5-29 Comparison of predicted wellbore temperature profile by Farshad et al., Beggs-Shiu and Kirkpatrick with the actual field data (case study #8)	144
Figure 5-30 Comparison of wellbore temperature profiles (case study #8).....	145
Figure 5-31 Comparison of wellbore temperature profiles (case study #9).....	149
Figure 5-32 Sensitivity study for oil production well in Tah Fiedl (case study #9)	150
Figure 5-33 CO2CRC Otway project (Cook, 2010) (case study #10)	153
Figure 5-34 Downhole and surface temperature records in CRC-1 well (Paterson et al., 2010) (case study #10)	154
Figure 5-35 Wellbore temperature profile for CRC-1 well (case study #10)	155
Figure 5-36 Wellbore temperature profile (case study #11)	156
Figure 5-37 Predicted temperature profile for different injection rates (case study #11)	157
Figure C1. C_1 coefficient for bubbles rising in static liquid column vs. bubble Reynolds number	198
Figure C2. C_2 coefficient vs. total Reynolds number	199

List of Tables

Table 3-1 Time function $f(t)$ for the radiation boundary condition model	41
Table 3-2 Tubular, thermal and physical properties information	46
Table 3-3 Model and thermal and heat properties data	51
Table 4-1 Compositions of gas mixtures	80
Table 4-2 Comparison of the value of compressibility factor (Z) of gas mixtures in Table 4-1.	80
Table 4-3 Comparison of the value of term $(\partial Z/\partial T)_p$ of gas mixture in Table 3-1 ...	82
Table 5-1 Data calculation for case studies #1 to #3	107
Table 5-2 Production data for case study #1	109
Table 5-3 Data calculation for case studies #4 to #7	121
Table 5-4 The value of impurities in the gas mixture (case study #6).....	136
Table 5-5 Data calculation for case studies #8 to #9.	141
Table 5-6 Production data for well GC-17 (case study #8)	142
Table 5-7 Comparison of temperature profiles for the different models (Case study #8)	143
Table 5-8 Production data for a well of Tah field in China (case study #9)	147
Table 5-9 Data calculation for case studies #10 to #11	152

Nomenclature

ΔL	Increment length, ft
$\Delta T_{overall}$	Overall temperature difference, °F
Δz	Increment depth, ft
A_{ic}	Inside surface area of casing, ft ²
A_{ot}	Outside surface area of tubing, ft ²
C	Correction factor
C_p	Fluid heat capacity, Btu/(lbmole.oF)
C_p	Joule Thomson coefficient
d	Diameter, in
E	Energy
ε_c	Casing emissivity, dimensionless
E_k	Kinetic energy
E_p	Potential energy
ε_t	Tubing emissivity, dimensionless
f	friction factor
$f(t)$	Ramey's transient time function, dimensionless
f'	Fanning friction factor
f_g	Fraction of gas
f_l	Fraction of liquid
g_c	gravity, ft/hr ²
Gr	Grashof number, dimensionless
h_{avg}	Average heat transfer coefficient, Btu/(hr. ft ² . °F)
h_{cv}	Convection heat transfer coefficient, Btu/(hr. ft ² . °F)
h_j	Enthalpy
h_w	Convection heat transfer coefficient, Btu/(hr. ft ² . °F)
i, j	Component number
J_j	Diffusion flux
k	Thermal conductivity coefficient of pipe, Btu/(hr. ft. °F)
k_a	Thermal conductivity coefficient of annulus fluid, Btu/(hr. ft. °F)

k_c	Thermal conductivity coefficient of casing, Btu/(hr. ft. °F)
k_{cmt}	Thermal conductivity coefficient of cement sheath, Btu/(hr. ft. °F)
K_{eff}	Effective conductivity
k_g	Thermal conductivity coefficient of ground/formation, Btu/(hr. ft. °F)
k_{ij}	Binary interaction coefficient
$k_{overall}$	Overall thermal conductivity coefficient, Btu/(hr. ft. °F)
k_p	Thermal conductivity coefficient of pipe, Btu/(hr. ft. °F)
k_t	Thermal conductivity coefficient of tubing, Btu/(hr. ft. °F)
L	Length, ft
N_{Re}	Reynolds number
Nu_δ	Nusselt number, dimensionless
P	Pressure, psi
P_c	Critical pressure, psia
PLT	Production logging tool
P_{pc}	Pseudo critical pressure, psia
P_{pr}	Pseudo reduced pressure
Pr	Prandtl number, dimensionless
P_{wf}	Wellbore flowing pressure, psia
Q	Heat flow rate, Btu/hr
q	Heat flow rate, Btu/hr
Q_{cv}	Convection heat flow rate in annulu, Btu/hr
Q_r	Radiation heat flow rate in annulus, Btu/hr
R	Universal gas constant, (ft) ³ (psia)(lbmole) ⁻¹ (oR) ⁻¹
Ra	Rayleigh number, dimensionless
R_a	Thermal resistance of annulus, 1/k _a
R_c	Thermal resistance of casing, 1/k _c
R_{cmt}	Thermal resistance of cement sheath, 1/k _{cmt}
R_g	Thermal resistance of ground/formation, 1/k _g
r_{ic}	Inside radius of casing, ft
r_{icmt}	Inside radius of cement sheath surface, ft
r_{ip}	Inside radius of pipe, ft
r_{it}	Inside radius of tubing, ft

r_m	Mean radius of annulus, ft
r_{oc}	Outside radius of casing, ft
r_{ocmt}	Outside radius of cement sheath surface, ft
r_{op}	Outside radius of pipe, ft
r_{ot}	Outside radius of tubing, ft
R_t	Thermal resistivity coefficient of tubing, $1/k_t$
R_{total}	Total thermal resistance, $1/k_{overall}$
R_w	Thermal resistance of wellbore, $1/k_w$
S	Entropy
S_h	Heat exchange due to chemical reaction
T	Temperature, °F
t	Time, hr
T_c	Critical temperature, °R
T_g	Ground/formation temperature, °F
T_{ic}	Temperature at inside of casing surface, °F
T_{icmt}	Temperature at inside of cement sheath surface, °F
T_{it}	Temperature at inside of tubing surface, °F
T_{ocmt}	Temperature at outside of cement sheath surface, °F
T_{ot}	Temperature at outside of tubing surface, °F
T_{pc}	Pseudo critical temperature, °R
T_{pr}	Pseudo reduced temperature
T_w	wellbore temperature, °F
U	Internal energy
$U_{overall}$	Overall heat transfer coefficient, °F
V_c	Average velocity of fluid in the wellbore, ft/min
V_c	Critical volume, $ft^3/mole$
W	Work
w_i	Mole fraction
WTP	Wellbore temperature profile
Z	Compressibility factor
z	Unit length, ft
B	Thermal volumetric expansion coefficient of annulus fluid, $1/°R$

γ_g	Gas specific gravity
δ	Increment length, ft
θ	Angle
μ	Viscosity, lb mass/(ft. hr)
μ_{JT}	Joule Thomson Coefficient, F/psi
v	Molar volume, ft ³ /mole
ρ	Fluid density, lbm/ft ³
P	Multi-phase fluid density, lb/ft ³
ρ_a	Density of annulus fluid, lb/ft ³
ρ_g	Density of gas phase, lb/ft ³
ρ_l	Density of liquid phase, lb/ft ³
σ	Stefan-Boltzmann constant, Btu/(hr. ft ² . °R)
τ_w	Viscous stress tensor
ω	Acentric factor

Publications of this thesis

Tarom N, Hossain M M (2013). Investigation of Joule Thomson Effect on Flowing Temperature Profile in Gas Producing Wells. Prepared to submit in Journal of Petroleum Exploration and Production Technology.

Tarom N, Hossain M M (2012). Using ANSYS to Realize a Semi-Analytical Method for Predicting Temperature Profile in Injection/Production Well. Published in WASET Journal, 2012(72): p. 1006-1015.

Tarom N, Hossain M M (2012). Improving reservoir performance using intelligent well completion sensors combined with surface wet-gas flow measurement. Published in Australian Petroleum Production Exploration Association (APPEA) Journal, Page 181

1

Introduction

1.1 Background

Well surveillance, including the process of monitoring a reservoir performance, well maintenance, functioning of surface production and treating equipment can be considered from technical and commercial viewpoints. Conventionally, the Production Logging Tool(s) (PLT) are designed to provide a full set of data measurements during the process of well production, in order to evaluate well and reservoir performance. Nowadays, permanently installed downhole pressure and temperature sensors are also a widespread technology, due to their ability to measure downhole production information with reasonable accuracy as well as reliability. However, all of these methods have their own failures, and there are always other methods for solving the problem (Al-Beaiji et al., 2005).

Moreover, many theoretical works have been reported in the literatures related to the prediction of temperature profiles; wellbore heat flow mechanism; and its potential use for the investigation to identify the potential causes of many injection and production related issues. However, most of the works are dedicated for certain scenarios, such as single phase liquid or gas flow either for injection case or

production cases. As result, most of these models have very limited use/capability to address the real field case. In this view, this study aims to develop a multi-purposes the numerical model that can potentially be used to address a wide range of cases such as single phase liquid, single phase gas, multiphase flow for both injection and production wells.

There follows a brief explanation of temperature profile and its application for well maintenance and reservoir performance. This is followed by the major part of this thesis, which deals with the mechanism of wellbore heat transference, leading to the new method of well and reservoir surveillance. A comprehensive literature review is provided in the next part of this chapter, and the aims of this study will be summarised in the objectives.

1.1.1 Temperature Profile

Temperature profile is the measurement of well temperature as a function of depth of the wellbore in a producing, injection and/or shut in-well. Temperature profile can be applied either through using mechanical techniques such as PLTs and downhole sensors or calculation methods.

Temperature profile can be a powerful tool for: the evaluation of a well and/or reservoir performance; and identification of the causes many injection/production related problems based on temperature anomalies. However, accurate prediction of temperature profile is paramount as it can be a waste of time and resource when poorly and inappropriately applied using either mechanical techniques or calculation methods. This study emphasises on the development of a numerical tool that can be used to predict temperature profile along a flowing wellbore (injection/production) in a most accurate manner.

1.1.2 Application of Temperature Profile

Temperature logs, the continuous recording of wellbore temperature versus depth, have been widely used for reliable diagnosis of many injection/production-related well problems. Some of the vitally informative applications of temperature logs are to evaluate the distinct production rates from separate layers in multi-layer production wells, as well as for inflow profile programming and evaluation of flow behind the casing (Barrett et al., 2012; Curtis and Witterholt, 1973; Hearst et al., 2000; Izgec et al., 2010; Kuchuk et al., 1998; Petricola and Watfa, 1993; Rasoul, 2012; Salehi-moorkani and Mohamadipour, 2011; Sharafutdinov, 2012; Tariq and Avestaran, 1991; Wade et al., 1965; Witterholt and Tixier, 1972; Zhu et al., 2008). Reports from the field logs also show this measurement's ability to indicate the gas cooling anomalies as a result of gas expansion at the entry point into the wellbore (Steffensen and Smith, 1973; Yoshioka et al., 2006; Yoshioka et al., 2007; Zhu et al., 2008). Therefore, some applications of temperature logs may be qualitative and quantitative indications of the fluid distribution along the wellbore, and identification of the root causes for many anomalies encountered during the production/injection process.

Temperature profiles may also help petroleum engineers to study the design of accurate production facilities. For instance, the design of gas lift valves can be improved by adequate temperature prediction at valve depth (Fryer et al., 2005; Mitchell and Wedelich III, 1989; Sagar et al., 1991; Wood et al., 2010). Moreover, the accurate prediction of temperature profiles help to calculate adequate prediction of multi-phase flow liquid hold-up and pressure-drop (Pourafshary et al., 2008) which may improve the design of surface facilities.

In addition, indication of flow behind casing, leakage at top of production packer, fluid entry point, top of cement location are some of the other applications that were

soon discovered (Elshahawi et al., 1999; Johnson et al., 2006). Therefore, the interpretation of temperature profile along a wellbore, which is the heat transferred between a wellbore and its surroundings, can be used in a wide range of diagnoses of production/injection anomalies. Also, quantitative knowledge of wellbore and reservoir heat transfer processes to the surrounding rock formation is important for accurate interpretation and prediction of this temperature profile.

1.1.3 Heat Transfer Mechanism Through a Wellbore

Heat transfer mechanism in a wellbore is the science, which seeks to explain the energy transfer that may take place between a wellbore and the surrounding area as a result of a temperature differential (Brown, 2006; Durrant and Thambynayagam, 1986; Elshahawi et al., 1999; Pacheco and Farouq Ali, 1972; RAMEY JR., 1962; Sagar et al., 1991; SATTER, 1965; Spindler, 2011; Willhite, 1967; Wu and Pruess, 1990). Therefore, depending on the temperature difference between the borehole fluid and the surrounded area within a production/injection operation, heat might normally be lost or gained to/from the ground, which surrounds the wellbore. Figure 1- 1 shows the direction of heat transferred from/to wellbore fluid to/from the surrounding area during a production and injection operation.

A wellbore is generally surrounded by different layers of tubing, annulus, casings, cement sheaths and ground/formation (Figure 1- 2). During the production/injection process, heat is usually conducted throughout all these layers (Alves et al., 1992; Hagoort, 2005; Hasan et al., 2009). From the thermodynamics viewpoint, each of these media has individual thermal properties, which make the process of heat transmission prediction more complex. Additionally, in the case of the annulus, which is filled with fluid, the heat transfer mechanism is more complicated, because the radiation heat transfer will result in additional convection heat transfer (Huygen and Huitt, 1966; Pacheco and Farouq Ali, 1972).

The mechanism of heat transference may be more complicated in different scenarios of production and injection operations. For instance, consider the case of gas injection where gas is injected from the annulus and fluid is produced through the wellbore. In this case, the injected gas through the annulus generally has a lower temperature than the temperature of wellbore fluid and the ground temperature. Therefore, in this case the process of heat transfer would be more complicated, acting like a forced convection heat transfer mechanism. The same problem would also rise in cases of annulus/tubing production and drilling operation.

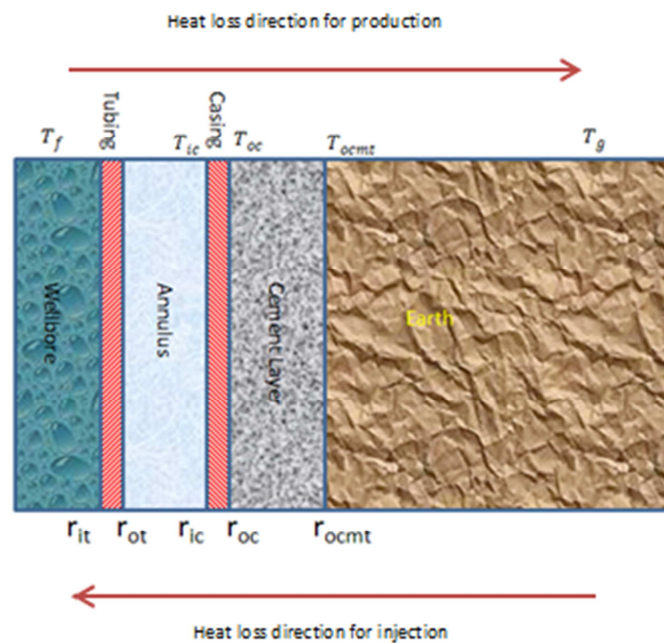


Figure 1- 1 Direction of heat transfer from/to wellbore to/from surrounding area during production and injection operation

The process of opening, shutting, restarting and changing the production schedule often makes up the normal daily program of a well-run operation. Each of these operations may affect transient heat losses through the surrounding media. Kabir et al. (Kabir et al., 1996a; Kabir et al., 1996b), Hagoor (Hagoort, 2005), and Hasan et al. (Hasan and Kabir, 2012) discuss the complexity of the heat transfer mechanism in

transient conditions. Different conditions and mechanisms of heat loss from the wellbore to the surroundings result in complex and cumbersome mathematical models to predict the temperature profile, and require the use of expensive numerical simulators, which are often impractical for industry standard routine engineering calculations.

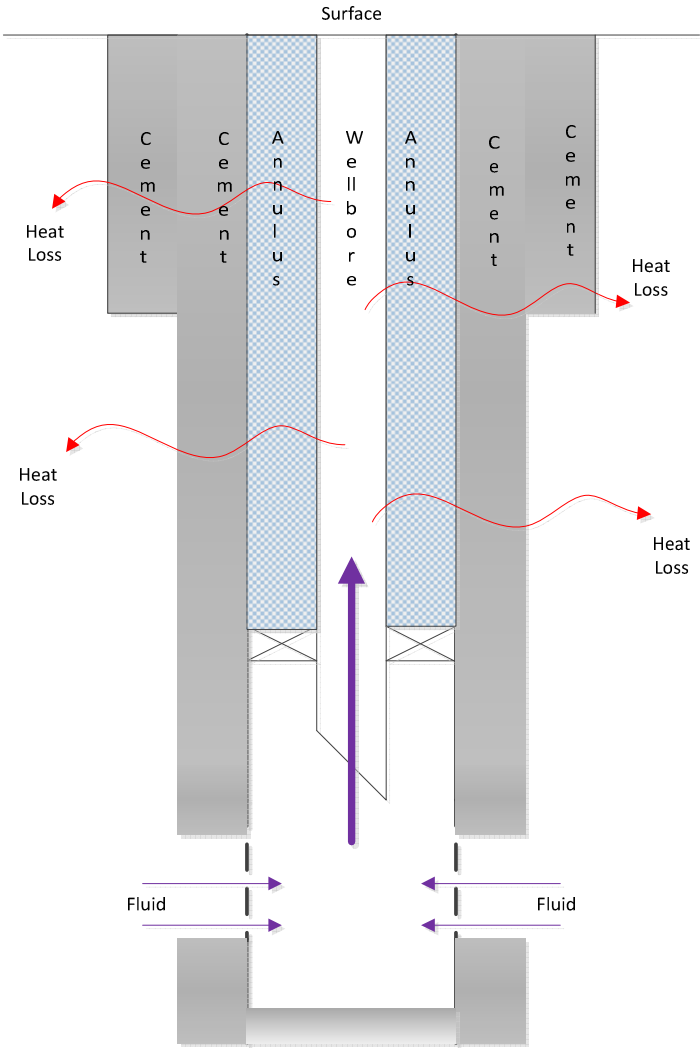


Figure 1- 2 Wellbore schematic and the surroundings contributing to heat transference

1.2 Objectives of the study

Primarily, governing equations are relevant for application to wellbores because they aid the consideration of complexities, which might surround a wellbore in real situations. For instance, a wellbore surrounded with different layers of annulus, cement sheaths and pipes which have different thermal resistances may complicate the problem. Additionally, the problem may seem more complicated when the mechanism of radiation heat transfer is considered while calculating heat loss through annulus. Based on the statement of the problem briefly stated in the above sections, the major objectives of this research are summarized as follows:

- Review the past and latest literatures in predicting temperature profile along a producing wellbore.
- Use of governing equations to develop an alternative method of analysing wellbore production data to predict a temperature profile along a production/injection wellbore.
- Development of practical Wellbore Temperature Profile Numerical Simulator (WTP Simulator) using FORTRAN language employing the developed model, which will predict the temperature profile along a dynamic wellbore for fluid, gas and multi-phase flow systems, and address the issue of producing wellbore temperature measurements. The developed model includes an overall heat transfer coefficient that accounts for all modes of heat transfer process, and focuses on the prediction of a temperature profile as a function of depth for the injection/production wells.
- Validate the results of the developed simulator by comparing with the result of ANSYS commercial software the results of HYSYS commercial software field data obtained from published literature.
- Conduct sensitivity studies in investigate factor influencing the wellbore temperature profile and its consequences on injection and production well.

1.3 Significants of this research

As discussed earlier that the temperature profiles, are used for analysing different kinds of anomalies relating to oil and gas production/injection wellbores. Production logging tools (PLT) and intelligent well completion equipment are some mechanical tools to calculate the temperature profiles. Physical limitations of these methods, and the matter of time and cost involved lead the researchers towards the application of analytical and numerical tools that can be used as an alternative to overcome these limitation. Many research works relevant to the prediction of wellbore temperature found the in literatures were mostly limited for certain cases/scenarios as well as for the case of single phase fluid flow. These works hardly addressed the real field problems in a practical manner. This work; however, may be distinguished from the other similar works based on following basis:

- In this study, the general energy balance equation has been applied to simulate the transfer of energy (heat) from wellbore towards the surroundings or vice versa. The main advantage of this simulation is the WTP simulator can cover a wide range of production and injection scenarios as well as different type of fluid flow (e.g. single phase liquid, single phase gas and multiphase) flowing through a desired wellbore.
- This study introduced a practical approach for the evaluation of gas compressibility factor as a function of the temperature change at constant pressure, $\left(\frac{\partial Z}{\partial T}\right)_p$, to study the Joule Thomson effect. A simplified semi-analytical model was developed, which can applicable to predict Thomson effect for producing gases even when their components are unknown. A correction factor is developed to evaluate the term $\left(\frac{\partial Z}{\partial T}\right)_p$ based on the gas gravity of producing gas. The study has been done for eight different gas

samples and the results have been compared and validated by widely used industry standard commercial software HYSYS.

- Another major advantage of the WTP program is the ability to study the sensitivity analysis of the different production parameters that can affect the profile of wellbore temperature.
- Time is another major consideration through this study. It is worth mentioning that using WTP simulator; the evaluated temperature profiles along the wellbores for different case studies as presented in chapter 5 are predicted in a matter of seconds rather than days or weeks required by software such as ANSYS.

These innovative concepts are going to be practiced through this research and the results are expected to improve the prediction of wellbore temperature profiles along a production and injection wellbore.

1.4 Outline of Thesis

This thesis is organised in six chapters. Chapter 1 introduces the mechanisms of temperature logging and wellbore temperature profile as well as the objectives of the research. Chapter 2 reviews the literature on this subject based on the theoretical, technical and financial factors separately.

Chapter 3 identifies an appropriate theoretical model and implementation of a suitable algorithm to simulate the profile of heat loss around a wellbore at any single point. In this chapter, a governing general energy equation is investigated as a basic concept of the WTP simulator following the description of mass, energy and momentum equations, along with the thermodynamics principles (pressure, volume

and temperature analysis) of the fluids, which are usually used to create a temperature analysis equation through a flowing wellbore. In considering the scientific aspects of the wellbore temperature profile and evaluation method, the basic theoretical model and overall heat transfer coefficient describing heat exchange between wellbore fluid, annulus, tubing, casings, cement sheaths and formation are explored. Then an algorithm is proposed for a heat exchange calculation method at any single point along the wellbore, and the application of ANSYS software to validate the proposed algorithm is described.

In chapter 4, the WTP simulator is extended for prediction of heat exchange along the whole of a flowing wellbore. In this chapter, a semi-analytical model has been developed, and the developed model is applied to cover all types of phases of fluid flow through the wellbore. This chapter divides the simulator into three different sections for formulation of single phase liquid, single phase gas and multiphase fluid flow simulation. It is also explained that the single phase gas flow section includes two subdivisions that are applied for cases in which the components of gas are known or unknown. In addition, in the single phase gas flow section, the Joule-Thomson effect is another important factor which is evaluated through the WTP simulator calculation.

Chapter 5 provides the results of the WTP simulator which has been developed for eleven different production and injection scenarios that reveal the broad application of the simulator. For validation of the achieved results, the predicted temperature profiles are compared with the actual field data. This chapter also explains the importance and relevance of the selected case in each case study.

Finally, Chapter 6 summarises the research findings and presents recommendations for further research in this field.

2

Literature Review

2.1 Literature Review

Discussions around temperature issues along a dynamic wellbore – dynamic in the sense of producing or injecting wells – have been on the desk of researchers for many decades. For instance, production logging (Figure 2-1) with the aim of temperature measurements in producing oil and gas wells began in the late 1930s (Millikan, 1941; Schlumberger et al., 1937). Since then, production logging tools (PLT) have been designed for providing a full set of data measurements in producing wells in order to evaluate well and reservoir performance. However, referring to many mechanical limitations associated with running the PLT through the wellbore, these tools are not efficient enough to achieve production information and forecast production scenarios. Some of these mechanical limitations are related with the cases that the well is completed with artificial completion equipment such as ESP (Electrical Submersible Pump), PCP (Processing Cavity Pump) or intelligent well completion tools. The other worth mentioning cases is when the wellbore is partially blocked by paraffin and sand. The other limitations against the PLT application may relate to any kinds of pipe damage. In addition, the PLT operation may also require undertaking expensive work-over and well intervention operations, which can

significantly increase the production downtime, substantially increase the operational expenditure and reduce the value of the asset.

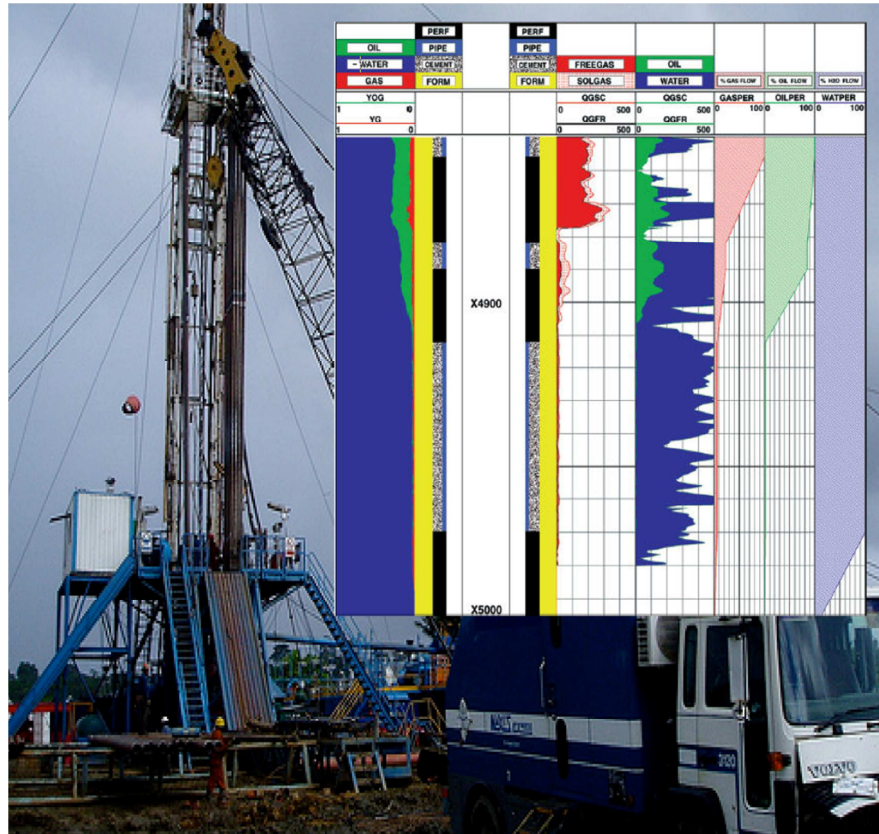


Figure 2-1 Production Logging.

The application of intelligent well completion tools such as the installation of permanent downhole pressure and temperature gauges, fiber-optic system and distribution temperature systems (DTS) may become a solution to overcome the problem (Figure 2-2). Therefore, since the first application of in-well fibre-optic sensors in Shell's Sleen Field in 1993 (Kragas et al., 2001), modern and technological tools such as downhole temperature/pressure sensors, distributed temperature system (DTS) and fibre-optic sensing tools (Al-Beaiji et al., 2005; Arnaout et al., 2008; Brown, 2006; Camilleri et al., 2010; Cox and Molenaar, 2013;

Gao et al., 2007; Hasan et al., 2009; Holley et al., 2012; Li and Zhu, 2009; Reyes et al., 2011; Sun et al., 2011; Sun et al., 2012) have increasingly become common in wellbore temperature monitoring. However, many considerable theoretical, technical and financial aspects have still kept the temperature issues in a wellbore an ongoing challenge for petroleum researchers.

The other solution to the problem might be using general energy balance equation to develop an analytical method of analysing production data, and consequently prediction of temperature profile along a wellbore. In this method the energy balance equation is combined with thermodynamics principles to analyse the mechanism of heat flow between wellbore fluid and the surroundings. This study focuses on developing a semi-analytical method for analysing temperature issues along a producing wellbore and the development of a computer program fully written in FORTRAN language has been designed to predict temperature profile applicable for different production cases and different type of fluid flowing along the wellbore. As a result, a temperature profile along a wellbore can be predicted without the challenging problem of running the PLT or using expensive intelligent well completion equipment. Or, it may also applied in parallel with the intelligent well completion equipment as a supplementary tool among the production time. In this chapter, the energy balance equation and the above mentioned aspects are reviewed throughout the previous studies, and an analytical solution is provided through the study which may help to overcome the above mentioned limitations and issues.

2.2 General Energy Balance Equation

Modelling heat flow in wellbores is vital for analysing different anomalies along producing wellbore as well as for designing of downhole and surface well completion equipment. For most heat equations in oil and gas industry, general energy balance equation, an expression for the balance and conservation of

temperature between two desired points, is the fundamental concept (Beggs, 2003; Shiu and Beggs, 1980a). The developed energy balance equation in combination with thermodynamic principles may apply for analysing temperature anomalies along wellbores.

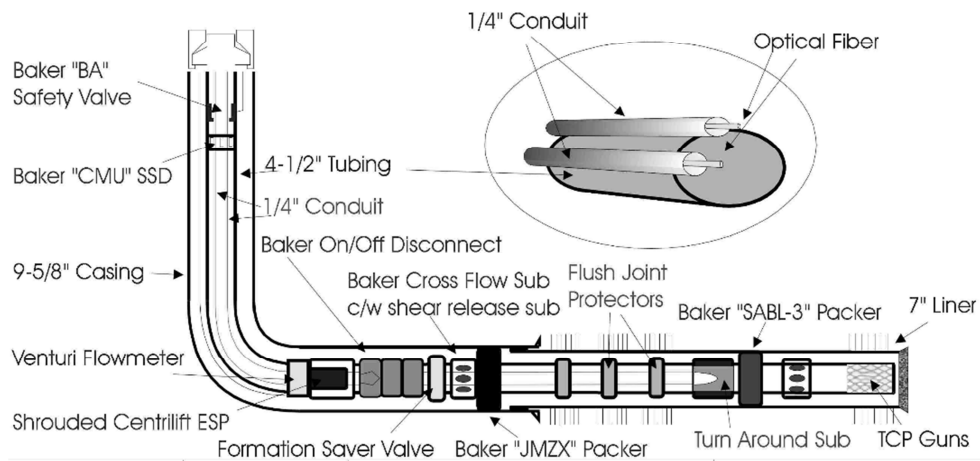


Figure 2-2 A typical horizontal well equipped with DTS.

Considering steady state conditions and no work done, the general energy balance equation applied for estimation of heat transfer between wellbore and surrounding can be summarised as follows:

$$\frac{dh}{dL} = \frac{dQ}{dL} - \frac{v}{Jg_c} \frac{dv}{dL} - \frac{g \sin \theta}{Jg_c}$$

Where:

$$dh = TdS + \frac{dP}{\rho}$$

In these equations, the term Q is heat rate, h is enthalpy, S is entropy, v is fluid velocity and L is length increment.

A brief and detail discussion about how the general energy balance equation is applied for prediction of heat transfer between wellbore fluid and the surrounding as well as its application for prediction of temperature profile along a wellbore have been investigated through this research.

2.3 Theoretical factors

In order to analyse temperature profile along a wellbore theoretically, steady-state energy balance equations are the common procedure (Beggs, 2003). Various mathematical models or tools are used to predict the temperature distribution along the wellbore. These models are mostly analytically or semi-analytically developed, based on energy balance equations for steady state conditions, which hardly describe the real conditions as observed in typical oil and gas flowing wells during production operation. This literature review will offer an overview of the theoretical issues of previous studies in applying energy balance equations for the estimation of a flowing well temperature profile.

Nowak (1953) (Nowak, 1953) applied temperature surveys for estimation of water injection profiles. He claimed that water injection profiles in wellbores had previously been determined from water velocity measurements; however, he applied temperature surveys to determine water injection profiles in water injection wells. He also said the significant feature of using temperature surveys is not only the determination of water entry points into the strata, but they can also determine the

thickness and the rate of injection into various strata. It is believed that the Nowak study opened a new window on the application of temperature profiles to the understanding of wellbore anomalies.

A few years later, Kirkpatrick (1959) (C.V.Kirkpatrick, 1959) applied the previous tasks on the prediction of temperature profiles along a flowing wellbore. He was able to predict temperatures at the injection depth of gas lift valves using flowing-temperature-gradient charts. At the same time (1959), the fundamental features of linear diffusion of heat in a rod and flow of heat towards the surrounding area of a cylinder were being investigated by Carslaw and Jaeger (Carslaw and Jaeger, 1959). Later, Carslaw and Jaeger's study was modified and extended to the determination of heat loss in oil, gas and geothermal wells.

Ramey (1962) (RAMEY JR., 1962) applied Carslaw and Jaeger's proposal (Carslaw and Jaeger, 1959) and developed the first classical and formulated application of energy balance equations to demonstrate an analytical solution to estimate the temperature of fluid, tubing and casing in a hot water injection well as a function of depth and time. He neglected the frictional pressure drop, assumed the mechanism of steady-state heat transfer along the wellbore, and considered transient heat conduction from the formation. With these assumptions, Ramey achieved a semi-analytical model to determine temperature profile along a water injection well (RAMEY JR., 1962). However, since that time, many significant studies by other researchers have built on Ramey's pioneering work (RAMEY JR., 1962) in order to model wellbore temperature.

Satter (1965) improved on Ramey's work considering the occurrence of phase changes for a steam injection project (Satter, 1965). Satter investigated the effect of condensation on heat losses along a wellbore, which is significant for a superheated, saturated and under-saturated steam injection project. Satter explained that the

development of correlation for steam injection is not feasible, because the possible conditions for steam injection are extremely variable. Therefore, Satter developed correlations for some specific cases and apply them to provide approximate results. The author investigated the effect of time, rate, injection temperature and pressure, and provide to plots for approximate calculation of steam temperature along a wellbore. Willhite (1967) (Willhite, 1967) also explained a method for predicting overall heat transfer coefficients in steam injection wells. The author estimated an overall heat transfer coefficient based upon the temperature difference between fluid and cross-sectional area perpendicular to the heat flow direction. He has established that different kinds of heat transfer mechanisms such as conduction, convection and radiation are considered in the calculation of an overall heat transfer coefficient.

Estimation of heat transfers between wellbore and its surroundings are more complicated during drilling and circulation operations, because of the existence of fluids with different temperatures inside the inner pipe and the annulus. A technique for prediction of bottomhole temperature in a drilling mud circulating system was developed by Raymond (1969) (Raymond, 1969). Raymond developed some charts applicable for determination of ΔT and prediction of bottom hole fluid temperature based on fluid rate and geothermal temperature gradient. However, the matter of friction and the mechanism of radiation heat transfer between pipes which may affect the profile of heat loss between wellbore and the surroundings are not considered. In addition, the approach of applying steady state heat transfer in the wellbore and transient heat loss to the formation, used by Ramey (RAMEY JR., 1962) and Willhite (Willhite, 1967), was also applied for describing the fluid temperature in circulating wellbores by Keller et al. (1973) (Keller et al., 1973), Wooley (1980) (Wooley, 1980) and Arnold (1990) (Arnold, 1990).

The extension of Ramey's work for inclined wellbores was done by Sagar, et al (1991) (Sagar et al., 1991) for two-phase flowing wells considering thermodynamics principles. Sagar et al considered the terms Joule Thomson and kinetic energy are

smaller than the other terms into general energy balance equation, and combined this two terms into a one terms as F_c for simplicity. However, to integrate the general energy balance equation over a fixed-length interval, they suggested that the terms F_c , geothermal gradient, specific heat of fluid and inclination angle are constant. Also, an unified equation was developed by Alves et al. (1992) (Alves et al., 1992) to predict flowing wellbore temperature profiles in wellbores and pipelines under single- or two-phase flow conditions for the quite range of inclination angels.

All efforts of Hasan et al. (1991, 1998) (Hasan and Kabir, 1991; Hasan and Kabir, 1994; Hasan et al., 1998; Kabir and Hasan, 1998; Kabir et al., 1996a; Kabir et al., 1996b) on the development of this subject are strong and of considerable merit. They revised Ramey's concepts, and developed models for estimating circulating fluid temperature and formation distribution temperature. Also, Hearst et al (2000) (Hearst et al., 2000a) and Beggs (2003) (Beggs, 2003) describe the application of general energy balance equations and heat flow equations comprehensively. A development of Ramey's work has been carried out by Hagoort (2005) (Hagoort, 2005), applying the model for real gas situations; and Hasan et al. (Hasan and Kabir, 2012; Kabir et al., 2012) indicate that energy balance equations may still play a vital role for the prediction of temperature profiles along a dynamic wellbore.

Due to the flow behaviours and the lack of geothermal temperatue changes along the horizontal wellbore, the behaviour of wellbore temperature profiles along a horizontal wellbore is varied compared to temperature behaviours in vertical and slightly deviated wellbore. The extension of heat transfer modelling through the horizontal section of producing wellbore has been discussed by Yoshioka et al (2005) for steady-state flow. In this study, Yoshioka et al couples mass, momentum and energy balances for horizontal sections to model pressure and temperature profiles along the wellbore. An interpretation technique has been also presented by Pimenov et al (2005) to analyse the temperature profile using distributed temperature sensors (DTS) along the horizontal section of producing wellbore. Muradov and

Davies (2008) apply analytical formulas to describe temperature distribution along vertical and horizontal wellbores separately. However, the consideration of well bore flowing temperature profile for horizontal well is beyond the scope of current study. The current study has considered for vertical well and slightly inclined wellbore.

In this study, the WTP simulator written in FORTRAN language considers all mechanisms of heat transferring such as conduction, convection and radiation between wellbore fluid and the formation. In addition, the effect of friction loss as a cause of fluid movement and its effect on the generation of heat along the wellbore is also considered. In cases of gas production, this friction effect is neglected, but the effect of the Joule Thomson on the temperature of fluid along the wellbore is considered.

2.4 Technical factors

Technically, temperature logs have widely been used to diagnose many injection/production-related well problems reliably. They are also used to obtain a qualitative indication of fluid distribution along the wellbore, and identify the root causes for many anomalies encountered during the production/injection processes. Therefore, quantitative knowledge of the processes of wellbore and reservoir heat transfer to the surrounding rock formation is important for accurate interpretation and prediction of temperature profile along a dynamic well. However, factors such as natural formation (geothermal) temperature, mechanism of heat conduction between the well and surroundings, complexity of heat transfer through annulus, heat generation along wellbore, and thermal changes of fluids should be considered.

During the production process, heat is usually conducted throughout surrounding formations, cement sheaths, casing, annulus and tubing(s), which are known as multi-layer media. Each of these media has individual thermal properties, which

make the process of heat transmission prediction more complex. Therefore, the application of overall heat transfer coefficients is the most common technique used to calculate the profile of heat loss through a multi-layer system (Brown, 2006; Durrant and Thambynayagam, 1986; Hasan et al., 2007; Holman, 1989; Izgec et al., 2008; Spindler, 2011; Wu and Pruess, 1990). Shiu and Beggs (Shiu and Beggs, 1980b) investigated the heat loss from wellbore towards the earth surrounding the well according to multi-layered heat transfer method. Also, Tansev et al (Tansev et al., 1975) applied the mechanism of multi-layered heat transfer for calculation of heat transferred between wellbore fluid and the surrounding area.

In addition, opening, shutting, restarting and changing the production schedule are often part of the normal and daily program of a well producing operation. Each of these operations may cause transient heat losses through surrounding media. Kabir et al. (Kabir et al., 1996a; Kabir et al., 1996b), Hasan et al. (Hasan and Kabir, 2012; Hasan et al., 2007) discussed the complexity of the heat transfer mechanism of transient conditions. Hearst et al (Hearst et al., 2000b) discussed the upsets of thermal equilibrium in and around wellbore when a warm and cool fluid move through a wellbore.

Heat generation, as a cause of fluid movement along a producing/injecting wellbore, is another factor that should be considered through the process of developing a temperature profile along a dynamic wellbore. Generation of heat in pipes due to friction loss in viscous fluid movement is discussed by Atesmen (Atesmen, 2009). This phenomenon might also be discussed as entropy generation due to thermodynamic irreversibility in the flow system (Al-Zaharnah and Yilbas, 2004). Moreover, the entropy generation due to pressure drop is different for oil and gas systems. For instance, the effect of pressure on the entropy of liquid and gas flowing systems is small and large, respectively (Donald and Robert, 1990). Therefore, the result appears as a temperature rise in the oil flowing systems, and inversely a temperature drop in the gas flowing system.

2.5 Financial factors

Production Logging Tool(s) (PLT) are conventionally applied to provide a full set of data measurements in producing wells in order to evaluate well and reservoir performance. To achieve the same purpose, fibre optic sensors, distribution temperature systems (DTS) and downhole pressure and temperature sensors have been used as temporary runs or permanent installations along the completion string. All these normal actions during an oil and gas project add some financial burden onto the project. Also, while running these tasks, factors such as risks, safety, time and failures may add some extra financial costs to the project. Prediction of temperature profiles along a flowing wellbore for different scenarios of production, and discussion about the production-related anomalies by developing numerical and analytical methods using computing tools, may considerably reduce the financial cost of a project.

3

Analytical Model Predict the Temperature Distribution Surrounding the Wellbore

3.1 Introduction

Since 1930, the first year that production logging applications were developed (Millikan, 1941; Shlumberger et al., 1937), temperature measurements in hydrocarbon producing wells, usually in term of wellbore temperature profiles (WTP), have become common for monitoring wellbore conditions during production or injection. Now, modern technologies such as fibre-optics and Distributed Temperature Systems (DTS) (Brown, 2006; Camilleri et al., 2010; Hasan et al., 2009) which aim to measure temperature along the wellbore are applied to assist with this matter. WTP is the measurement of well temperature as a function of depth, and can be used as a powerful tool for monitoring, maintaining and identifying many issues related to producing and injection wells. Many considerable theoretical, technical and financial challenges have been addressed by these methods so far; however, temperature profile issues in a wellbore are still a significant challenge discussed in the literature by petroleum researchers. The aim of this chapter is to identify an appropriate theoretical model and a suitable algorithm to simulate the profile of heat loss around a wellbore at any single point.

In this study, an analytical wellbore temperature model is developed using the mass, energy and momentum equations along with thermodynamics principles (pressure, volume and temperature analysis of fluids). The objectives of this work are based on science and engineering research methodology:

- To identify an appropriate set of semi-analytical equations to simulate the profile of heat loss at any single point around a wellbore.
- To identify a set of necessary data required for numerical simulation. In this analysis, formation properties and well completion details are necessary. Data acquisition techniques, such as downhole pressure/temperature gauges (P/T DHG), distributed temperature system (DTS), fibre-optic sensors at reservoir conditions, and surface production information, can be considered to be adequate for the validation of results.
- ANSYS fluent numerical simulator with broad capabilities to model flow, turbulence and heat transfer is used to validate the results. The modelling concept of this work is illustrated in Figure 3-1.

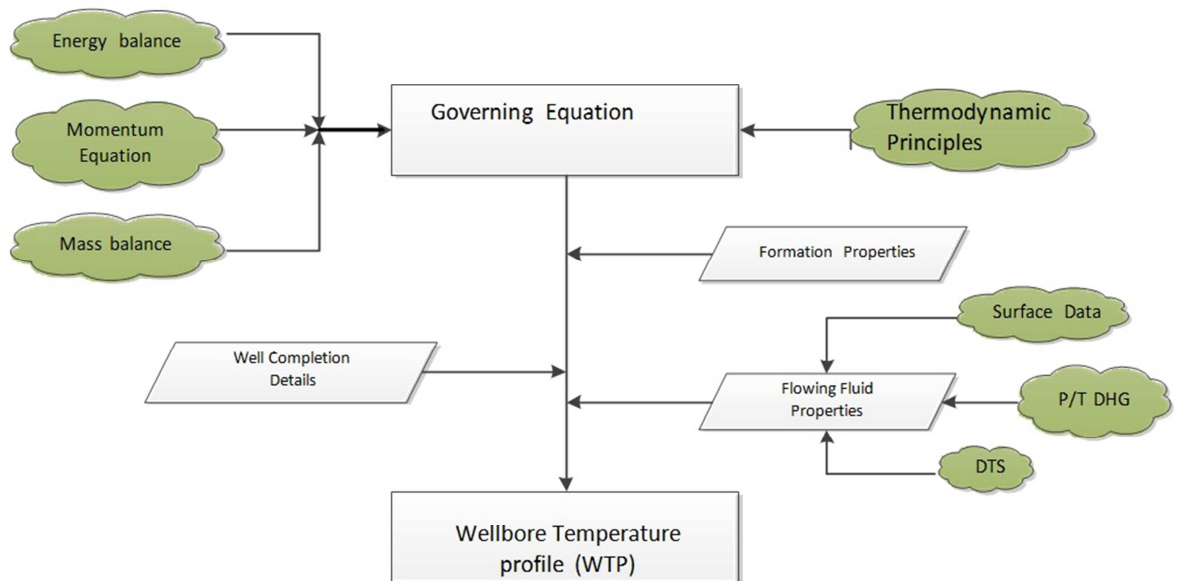


Figure 3-1 Illustration of modelling concept.

3.2 Governing equation

The governing equation is derived for analysing the wellbore temperature parameters in a flowing or static wellbore following the principle of conservation or balancing of energy between two desired points. Figure 3-2 demonstrates the basis of energy balance applied for a unit length of a production string (control volume).

In order to develop the governing equation for a single- and/or multi-phase flowing wellbore, the conservations of mass, momentum and energy along with pressure/volume/temperature (PVT) relations are considered for a control volume along the wellbore. In the following section there are separate descriptions for each of these terms required to obtain a general form of an energy balance equation for a desired control volume.

3.2.1 Conservation of Mass

The conservation of mass for a given control volume simply expresses an accumulation of mass for desired control volume. It is the difference in the rate of fluid in and out that can be explained as follows.

$$\left\{ \begin{array}{l} \text{Rate of mass} \\ \text{accumulation for} \\ \text{a given} \\ \text{control voume} \end{array} \right\} = \left\{ \begin{array}{l} \text{Rate} \\ \text{of} \\ \text{mass} \\ \text{in} \end{array} \right\} - \left\{ \begin{array}{l} \text{Rate} \\ \text{of} \\ \text{mass} \\ \text{out} \end{array} \right\} \quad 3.1$$

Equation 3.1 can be expressed as:

$$\frac{\partial \rho}{\partial t} + \nabla \cdot (\rho \vec{v}) = 0 \quad 3.2$$

In case of flowing fluid through a wellbore, Equation 3.2 can be expressed as:

$$\frac{\partial \rho}{\partial t} + \frac{\partial(\rho v)}{\partial z} = 0 \quad 3.3$$

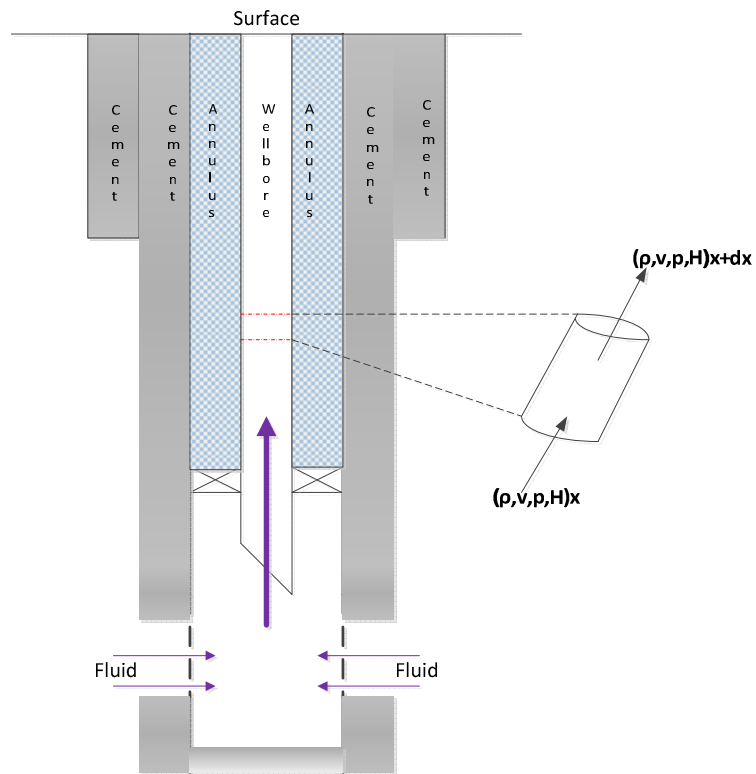


Figure 3-2 Mass, momentum and energy balances.

Where, ρ is density of fluid, v is specific volume of fluid and z is the unit length of the producing string.

3.2.2 Momentum Balance

In a general form, the momentum balance on the motion of fluids such as liquid or gas can be expressed as:

$$\left\{ \begin{array}{l} \text{Rate of} \\ \text{momentum} \\ \text{change} \\ \text{in a given} \\ \text{control volume} \end{array} \right\} = \left\{ \begin{array}{l} \text{Rate of} \\ \text{momentum} \\ \text{in} \end{array} \right\} - \left\{ \begin{array}{l} \text{Rate of} \\ \text{momentum} \\ \text{out} \end{array} \right\} + \left\{ \begin{array}{l} \text{External} \\ \text{force on the} \\ \text{fluid} \end{array} \right\} \quad 3.4$$

Momentum is a vector property, and is the product of mass and velocity on the object. For the explanation of fluids motion and changes in the momentum of fluid particles, the Navier-Stokes equations are used:

$$\rho \left[\frac{\partial \vec{v}}{\partial t} + (\vec{v} \cdot \nabla) \vec{v} \right] = -\nabla p + \nabla \tau + \rho \vec{f} \quad 3.5$$

Where ρ is density, v is the velocity vector, τ is the viscous stress tensor, p is pressure and f is the body force per unit mass. The body force f can be replaced by gravitational force (g) when the weight of fluid is the only body force on the fluid.

During a wellbore flow, most viscous shear happens at the wall. Also, pressure drops and energy is lost in fluid flowing through a producing string as a result of change in kinetic energy and friction loss. It is defined as the ratio of wall shear stress (τ_w) to kinetic energy per unit volume ($\rho v^2/2$) that reflects a dimensionless group known as friction factor f (Beggs, 2003):

$$f = \frac{2\tau_w}{\rho v^2} \quad 3.6$$

By substituting Equation 3.6 in Equation 3.5, then rearranging and summarising Equation 3.5 for a one-dimensional flow through an inclined wellbore, Equation 3.5 becomes:

$$\frac{1}{\rho} \frac{\partial p}{\partial z} = -\frac{\partial v}{\partial t} - v \frac{\partial v}{\partial z} - g \sin\theta - \frac{2f'v^2}{d} \quad 3.7$$

Where f' is Fanning friction factor which in terms of Moody friction factor, $f = 4f'$.

In Equation 3.7, the friction factor (f) plays an important role, which needs to be calculated accurately. Many equations are developed for smooth pipes, and are valid for various ranges of the Reynolds number ($N_{Re}=(\rho v d)/\mu$). However, pipes are not smooth, and wall roughness affects flow significantly and needs to be taken into consideration (Beggs, 2003).

The value of the friction factor depends on the velocity of fluid flowing through a pipe, and type of the flow. For a laminar flow, (when $N_{Re} < 2000$), f can be calculated using:

$$f = \frac{64}{N_{Re}} \quad 3.8$$

From the lack of uniformity of roughness along the pipes, Nikuradse (Beggs, 2003) considered the effect of roughness on prediction of the friction factor. Since then,

many investigators have proposed numerous correlations. Among these studies, Colebrook and White's equation (1939) (Equation 3.9) is widely used.

$$\frac{1}{\sqrt{f}} = 1.74 - 2 \log \left(\frac{2\varepsilon}{d} + \frac{18.7}{N_{Re} \sqrt{f}} \right) \quad 3.9$$

Equation 3.9 is an explicit equation in which the friction factor f requires solving iteratively.

Jain (Beggs, 2003) proposed an implicit equation (Equation 3.10) for calculating the friction factor (f), and compared its achievements with the Colebrook equation. He claimed that the error of his work in comparison with the Colebrook equation was within $\pm 1.0\%$ for a range of relative roughness of 10^{-6} to 10^{-2} and a range of Reynolds numbers of 5×10^3 to 10^8 .

$$\frac{1}{\sqrt{f}} = 1.14 - 2 \log \left(\frac{\varepsilon}{d} + \frac{21.25}{N_{Re}^{0.9}} \right) \quad 3.10$$

In Equation 3.7, another important factor to be determined is the density (ρ) of multiphase flowing fluids, which depends on the gas and liquid densities, and can be calculated by:

$$\rho = f_g \rho_g + f_l \rho_l \quad 3.11$$

Where f_g and f_l are the fraction of gas and liquid phases, respectively.

3.2.3 Energy Balance

The total energy balance equation for a desired control volume of flowing fluid is the sum of internal, potential and kinetic energy of the system.

$$E = U + E_p + E_k \quad 3.12$$

Internal energy, U , corresponds to all the translational, rotational and vibrational energy of molecules, atoms and sub-particles of mass in a system. At the microscopic level, internal energy contains both potential and kinetic energy. The internal energy is also explained as a state of function of a system, and an increase in internal energy causes an increase in temperature or a change in phase of the system. From a thermodynamics viewpoint, the absolute value of the internal energy of a system cannot be determined. Therefore, only the difference in the internal energy, ΔU , is considered by thermodynamics, which is related to some standard state and can be determined experimentally.

Potential energy (E_p) is a kind of energy that is stored in a system, and has the potential to convert to another kind of energy. Potential energy is important for fluid systems, as the mass of fluid at a specified position can be utilised and do some work when its elevation changes. On the other hand, kinetic energy (E_k) is related to the energy of motion of a body, and it equals to work done when it is brought to rest.

By definition, closed and open systems are two different kinds of thermodynamic systems. In a closed system, mass does not cross the boundaries, whereas an open system allows the mass to cross the boundaries. Therefore, as there is no flow through a closed system, the closed system can be explained as:

$$\left\{ \begin{array}{l} \text{Rate of} \\ \text{total energy} \\ \text{accumulation} \\ \text{in a closed system} \end{array} \right\} = \left\{ \begin{array}{l} \text{Net rate of} \\ \text{heat added to} \\ \text{system from} \\ \text{surroundings} \end{array} \right\} - \left\{ \begin{array}{l} \text{Net rate of} \\ \text{work done by} \\ \text{system on} \\ \text{surroundings} \end{array} \right\} \quad 3.13$$

Mathematically, it can be expressed as:

$$\Delta E = Q_h - W \quad 3.14$$

Therefore, the energy balance for a closed system can be expressed by:

$$\Delta U + \Delta E_p + \Delta E_k = Q_h - W \quad 3.15$$

The statement of energy balance for a steady-state open system is expressed by:

$$\left\{ \begin{array}{l} \text{Rate of total} \\ \text{energy} \\ \text{out} \end{array} \right\} - \left\{ \begin{array}{l} \text{Rate of total} \\ \text{energy} \\ \text{in} \end{array} \right\} = \left\{ \begin{array}{l} \text{Net rate of} \\ \text{heat added to} \\ \text{system from} \\ \text{surroundings} \end{array} \right\} - \left\{ \begin{array}{l} \text{Net rate of} \\ \text{work done by} \\ \text{system on} \\ \text{surroundings} \end{array} \right\} \quad 3.16$$

Mathematically, it is explained:

$$\left(\frac{dE}{dt} \right)_{out} - \left(\frac{dE}{dt} \right)_{in} = \frac{dQ_h}{dt} - \frac{dW}{dt} \quad 3.17$$

Based on the steady-state condition, as the mass flow rate through the open system is constant, therefore:

$$(e)_{out} - (e)_{in} = q_h - w \quad 3.18$$

Substituting Equation 3.12 into Equation 3.18:

$$\left(u + \frac{gZ}{g_c} + \frac{v^2}{2g_c}\right)_{out} - \left(u + \frac{gZ}{g_c} + \frac{v^2}{2g_c}\right)_{in} = q_h - w \quad 3.19$$

The term ‘work’ has three different aspects, which are the work done by a system at the entrance, at the exit, and shaft work (w_s). At the entrance of the control volume, the work done per unit mass is the required work to push a unit mass of fluid at pressure p_1 and specific volume v_{s1} into the open system. Therefore, the exerted force is p_1A_1 , and the total displacement per unit mass is v_{s1}/A_1 . A_1 is the surface area of the entrance side of the control volume. The same definition can be applied for the exit side (point 2) of a control volume which has the same surface area ($A_2=A_1$) in this case. Therefore, p_2A_2 and v_{s2}/A_2 show the exerted force and total displacement per unit mass at exit point, respectively. So, it can be stated that:

$$w = p_2v_{s2} - p_1v_{s1} + w_s \quad 3.20$$

Substituting Equation 3.20 into Equation 3.19 and rearranging them defines the energy balance for a homogenous steady-state flowing fluid condition, expressed by:

$$\Delta u + \Delta \left(\frac{gZ}{g_c}\right) + \Delta \left(\frac{v^2}{2g_c}\right) = q_h - \Delta(pv_s) - w_s \quad 3.21$$

The term of internal energy in Equation 3.21 can be eliminated from mechanical energy balance. From the second law of thermodynamics:

$$dU = dh - d\left(\frac{p}{\rho}\right) \quad 3.22$$

$$dh = TdS + \frac{dp}{\rho} \quad 3.23$$

Then:

$$dU = TdS + \frac{dp}{\rho} - d\left(\frac{p}{\rho}\right) \quad 3.24$$

Where, h is enthalpy, S is entropy and T is temperature.

Substituting Equation 3.24 into Equation 3.21, writing in differential form and rearranging it gives:

$$TdS + \frac{dp}{\rho} + \frac{v dv}{g_c} + \frac{g}{g_c} dz + dq + dw_s = 0 \quad 3.25$$

Applying the definition of Clausius inequality for an irreversible process gives:

$$dS \geq \frac{-dq}{T} \quad 3.26$$

Assuming no work is done, considering $dz = dL \cdot \sin\theta$ and substituting Equation 3.26 into 3.25, the energy balance equation can be solved for pressure gradient:

$$\frac{dp}{dL} = \frac{g}{g_c} \rho \sin\theta + \frac{\rho v dv}{g_c dL} + \left(\frac{dp}{dL}\right)_f \quad 3.27$$

3.2.4 Pressure/Volume/Temperature (PVT) relation

Produced fluids are in gas and liquid phases. In the process of production, there are pressure and temperature drops in the path of fluid transfer from the reservoir to the surface. The cause of these pressure and temperature drop is the change in phase

behaviour, physical properties, thermodynamic properties and composition of the phases. Therefore, the determination of the mixture properties at any pressure and temperature are paramount in the oil and gas industry.

Plotting pressure as a function of temperature for any mixture, known as a phase diagram or envelope (as shown in Figure 3-3), is used to determine the fluid production path from the reservoir to oil and gas units at the surface. The produced fluid can be classified according to pressure and temperature conditions plotted on the phase envelope. The phase envelope for a desired mixture can be plotted from data gathered experimentally and/or achieved through analytical methods using appropriate equation of states.

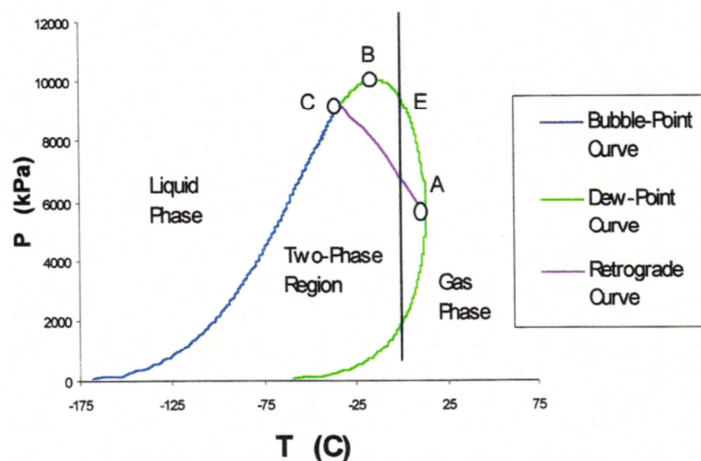


Figure 3-3 Typical phase envelope for a multicomponent mixture (Taron et al., 2002).

Thermodynamic functions are used to determine pressure/volume/temperature (PVT) properties of a flowing fluid. These functions relate volumetric properties to entropy, enthalpy, the Joule-Thomson coefficient, compressibility factor (Z) and specific heat. Many practical correlations are available in the literature to calculate these properties

for specific fluid system. Further details including the application of all these properties will be elaborated in Chapter 4.

3.3 Temperature Model

During the hydrocarbon production process, the temperature of fluid typically drops to some extent along the production string. This temperature is lost from the produced fluid to the surrounding earth, and it depends on the thermodynamic properties of the produced fluid, the thermal properties of tubing and casing, the thermal resistance of cement sheaths and earth, and the length of producing time. The temperature profile along a wellbore can be evaluated if all of these parameters are known. In this section, the fundamental concepts of heat loss calculation from wellbore to the surroundings applied in this work are discussed.

3.3.1 Basic concept of heat transfer

During the petroleum production process, heat is usually conducted throughout the surrounding formation, cement sheaths, casing, annulus and tubing(s). The process is illustrated in Figure 3-4. In addition to heat conduction, the heat is also transferred from the flowing fluid by a convection process to the innermost tubing. In the case of the annulus which is filled with fluid, the radiation heat transfer mechanism will also result in the action of the convection heat transfer mechanism (Holman, 1986; Mills).

To predict a temperature profile accurately, it is necessary to evaluate the wellbore heat loss considering all different heat transfer mechanisms, which is always a challenging issue faced by petroleum engineers. The calculation of wellbore heat loss and overall heat transfer coefficient has been discussed by many authors (Chin and Wang, 2004; Hasan and Kabir, 1994). They believe that in a vertical fluid flow,

the mechanism of convection is the process of heat transfer from the flowing fluid to the innermost pipe of the well. The process of heat transfer is also dependent on the type of flowing fluid, and the physical and thermal properties of fluid in the annulus. In this study, to ease the calculation process, the overall heat transfer coefficient concept has been applied to deal with this problem. The overall heat transfer coefficient has been calculated based on the heat resistivity of all the layers around a wellbore that determine the overall rate of heat loss per unit area.

The ratio of temperature difference between the borehole and the ground to the total thermal resistance is called the overall heat transfer through any unit section of desired well (Holman, 1986).

$$q = \frac{\Delta T_{overall}}{R_{total}} \quad 3.28$$

In Equation 3.28, the total thermal resistance is the summation of the thermal resistivity of all layers. For a well surrounded by different layers of tubing, annulus, casings, cement layers and the surrounding ground, which have different physical and thermal properties. The total thermal resistance per unit area of surface may be calculated by:

$$R_{total} = R_w + R_t + R_a + R_c + R_{cmt} + R_g \quad 3.29$$

Further details for the estimations of thermal resistivity for each layer are provided in appendix A.

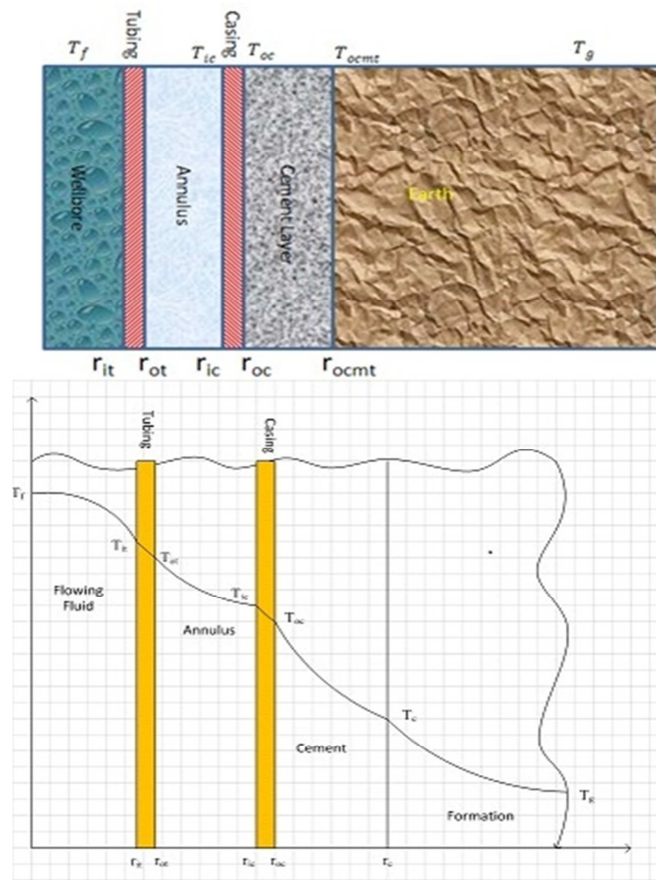


Figure 3-4 Heat Distribution from wellbore towards surroundings area

3.3.2 Overall heat transfer coefficient

By definition, the overall heat transfer coefficient can be estimated by Equation 3.30:

$$U_{overall} = \frac{1}{R_{total}} \quad 3.30$$

Where, terms $U_{overall}$ and R_{total} indicate the overall heat transfer coefficient and total thermal resistance, respectively.

By neglecting the thermal resistivity of tubing and casing, and assuming that the outer surface of tubing (T_{ot}) is equal to wellbore temperature (T_w), then in accordance with Equation 3.29 and Equations A16 and A18 of appendix A the total thermal resistance between tubing and cement sheath can be expressed by Equation 3.31:

$$R_{total} = \frac{1}{2\pi\Delta L} \left(\frac{1}{r_m h_{avg}} + \frac{\ln\left(\frac{r_{ocmt}}{r_{icmt}}\right)}{k_{cmt}} \right) \quad 3.31$$

Where, terms r_{ocmt} and r_{icmt} denote the outer and inner radius of cement sheath respectively. Also k_{cmt} shows the thermal conductivity coefficient of the cement layer, and h_{avg} is the average heat transfer coefficient of the annulus.

At the steady state condition, the equation expressed by Hassan et al. (1994) can be applied to calculate the heat flow rate per unit length of wellbore:

$$Q = 2\pi r_{ot} U_{overall} (T_w - T_{ocmt}) \Delta L \quad 3.32$$

Where, terms T_w and T_{ocmt} are the temperature of media at the wellbore and cement sheath, respectively.

Combining Equations 3.28 to 3.32 will result in an expression for calculation of overall heat transfer coefficient, which is expressed by Equation 3.33:

$$U_{overall} = [R_{total}]^{-1} / 2\pi r_{ot} \Delta L = \left[\frac{r_{ot}}{r_m h_{avg}} + \frac{r_{ot} \ln\left(\frac{r_{ocmt}}{r_{icmt}}\right)}{k_{cmt}} \right]^{-1} \quad 3.33$$

Where, terms r_{ot} and r_m are defined as the outer radius of the tubing and mean radius of the annulus, respectively.

3.3.3 Analytical model for temperature prediction at tubing and casing surfaces

In Equations 3.30 to 3.31, knowledge of the tubing and casing temperature is required to calculate the average heat transfer coefficient (h_{avg}) for the annulus. The temperature of casing and cement-ground interface can be determined using Equations 3.34 to 3.40, by assuming that the temperature of the tubing is known (i.e. $T_{ot}=T_w$) (Willhite, 1967).

Overall heat loss:

$$Q = \frac{2\pi k_{overall}}{\ln\left(\frac{r_{ocmt}}{r_{it}}\right)} (T_w - T_{ocmt})\Delta L \quad 3.34$$

Heat loss through casing:

$$Q = \frac{2\pi k_c}{\ln\left(\frac{r_{oc}}{r_{ic}}\right)} (T_{ic} - T_{oc})\Delta L \quad 3.35$$

Heat loss through cement sheath:

$$Q = \frac{2\pi k_{cmt}}{\ln\left(\frac{r_{ocmt}}{r_{icmt}}\right)} (T_{icmt} - T_{ocmt})\Delta L \quad 3.36$$

Where,

- Q and ΔL are heat flow rate and length increment.
- $k_{overall}$, k_c and k_{cmt} are thermal conductivity coefficient of overall casing and cement sheath.

- r_{ib} , r_{ic} , and r_{icmt} show the inner radius of tubing, casing and cement sheath.
- r_{oc} , r_{ocmt} explain the outer radius of casing and cement sheath.
- T_w is the temperature of wellbore fluid.
- T_{ic} and T_{icmt} define the temperatures at inner surface of casing and cement sheath, and T_{oc} and T_{ocmt} also define the temperatures at the outer radius of casing and cement sheath.

Since heat flow through all layers, Q , is equal, after rearrangement, Equations 3.34 to 3.36 yield:

$$T_{ic} = T_{ocmt} + \left(\frac{k_{overall}}{\ln \frac{r_{ocmt}}{r_{it}}} \right) \left(\frac{\ln \frac{r_{ocmt}}{r_{oc}}}{k_{cmt}} + \frac{\ln \frac{r_{oc}}{r_{ic}}}{k_c} \right) (T_w - T_{ocmt}) \quad 3.37$$

Since the thermal resistance of the casing is negligible due to its physical properties, Equation 3.37 becomes:

$$T_{ic} = T_{ocmt} + \left(\frac{k_{overall}}{\ln \frac{r_{ocmt}}{r_{it}}} \right) \left(\frac{\ln \frac{r_{ocmt}}{r_{oc}}}{k_{cmt}} \right) (T_w - T_{ocmt}) \quad 3.38$$

In Equation 3.38, the unknown term, T_{ocmt} , may be calculated by following Ramy's procedure (Hill, 1990; RAMEY JR., 1962). Therefore;

$$Q = \frac{2\pi k_g (T_{ocmt} - T_g) \Delta z}{f(t)} \quad 3.39$$

Equating the overall heat flow in the well (Equation 3.34) with the radial heat flow through the ground (Equation 3.39), and considering $\Delta z = \Delta L$ results in the following equation.

$$T_{ocmt} = \frac{\left(\frac{k_{overall}}{\ln \frac{r_{ocmt}}{r_{it}}}\right) T_w + \left(\frac{k_g}{f(t)}\right) T_g}{\left(\frac{k_{overall}}{\ln \frac{r_{ocmt}}{r_{it}}}\right) + \left(\frac{k_g}{f(t)}\right)} \quad 3.40$$

Therefore, the calculation of heat transfer profile between production fluid and the surrounding media is predictable by calculating the temperature values at casing surface (T_{ic}) and cement surface (T_{oc}) using Equations 3.38 and 3.40, respectively.

3.3.4 Algorithm of temperature loss profile

Equations 3.34, 3.38 and 3.40 are applied to evaluate the profile of temperature loss from a wellbore fluid towards its surroundings at a single point. However, the logarithmic term in Equation 3.40 makes it non-linear and must be solved iteratively in order to calculate the total thermal resistance. The following iterative steps can be used to calculate the total thermal resistance.

1. Guess a value of $k_{overall}$.
2. Determine $f(t)$.

For the production time more than 7 days (Ramey 1962):

$$f(t) = \ln \frac{2\sqrt{\alpha t}}{r_{ocmt}} - 0.29 \quad 3.41$$

In other cases:

- a) Without annulus in a wellbore schematic: use Figure 3-5 of Ramey (RAMEY JR., 1962).
- b) With annulus in a wellbore schematic: use Table 3-1.

Chapter 3 Analytical Model Predict Temperature Distribution Surrounding the Wellbore

3. Calculate T_{ocmt} using equation 3.40.
4. Calculate T_{ic} using equation 3.38.
5. Estimate Q_r and Q_{cv} using Equation A6 and A8, respectively.
6. Estimate $Q_a = Q_r + Q_{cv}$.
7. Estimate $Q_{overall}$ using equation 3.34.
8. If $Q_a = Q_{overall}$, the calculation will be finished. Otherwise, guess a new value for the $k_{overall}$ and repeat the procedure until $Q_{overall} = Q_a$.

A computer program is developed employing the proposed analytical model using FORTRAN language. The algorithm of this program for the estimation of total thermal resistance and temperatures at casing and cement sheaths are also provided in the form of a block diagram as shown in Figure 3-6.

Table 3-1 Time function f(t) for the radiation boundary condition model

$\frac{r_{ocmt} U_{ocmt}}{k_g}$	0.01	0.02	0.05	0.1	0.2	0.5	1	2	5	10	20	50	100	∞
0.1	0.313	0.313	0.314	0.316	0.318	0.323	0.33	0.345	0.373	0.396	0.417	0.433	0.438	0.445
0.2	0.423	0.423	0.424	0.427	0.43	0.439	0.452	0.473	0.511	0.538	0.568	0.572	0.578	0.588
0.5	0.616	0.617	0.619	0.623	0.629	0.644	0.666	0.698	0.745	0.772	0.79	0.802	0.806	0.811
1	0.802	0.803	0.806	0.811	0.82	0.842	0.872	0.91	0.958	0.984	1	1.01	1.01	1.02
2	1.02	1.02	1.03	1.04	1.05	1.08	1.11	1.15	1.2	1.22	1.24	1.24	1.25	1.25
5	1.36	1.37	1.37	1.38	1.4	1.44	1.48	1.52	1.56	1.57	1.58	1.59	1.59	1.59
10	1.65	1.66	1.66	1.67	1.69	1.73	1.77	1.81	1.84	1.86	1.86	1.87	1.87	1.88
20	1.96	1.97	1.97	1.99	2	2.05	2.09	2.15	2.15	2.16	2.16	2.17	2.17	2.17
50	2.39	2.39	2.4	2.42	2.44	2.48	2.51	2.56	2.56	2.57	2.57	2.58	2.58	2.58
100	2.73	2.73	2.74	2.75	2.77	2.81	2.84	2.88	2.88	2.89	2.89	2.89	2.89	2.9

For validation of the developed program based on the proposed semi-analytical model, the industry standard numerical simulator ANSYS-Fluent package has been used. Also, calculations are performed on an Excel spread sheet for cross-checking. All features and applications of ANSYS and Excel will be further elaborated in the next section.

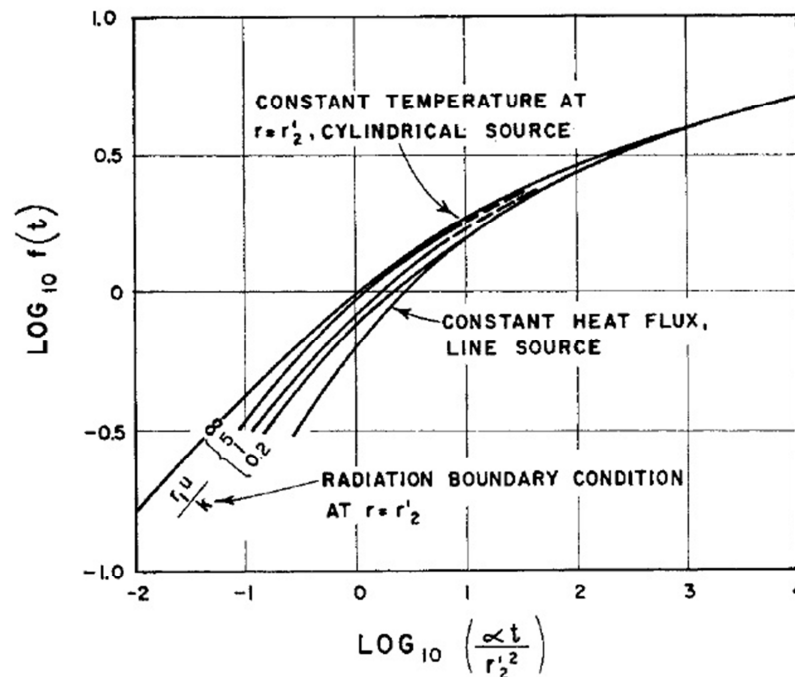


Figure 3-5 Transient heat conduction in an infinite radial system (RAMEY JR., 1962)

3.4 ANSYS software and Excel spread sheet

ANSYS Fluent numerical simulator is a Finite Element and CFD (Computational Fluid Dynamics) based commercial numerical simulator, which has broad capabilities to model flow, turbulence, heat transfer, and so on. It covers a wide

range of industrial applications including fluid and heat flow issues through a wellbore and its surroundings. The main module of this simulator that deals with fluid and heat flow related problems is Fluent, which has been embedded within the ANSYS Fluent package. However, the Fluent module was used to simulate heat loss (gain) through (from) the wellbore surrounding area to validate the semi-analytical method which is developed in this work.

The ANSYS Fluent package also provides complete mesh types including 2D and 3D, and mesh flexibilities including the ability to solve the heat and flow problems. Moreover, some of the capabilities of the heat transmission problem-solving functions of the Fluent software are: natural, forced and mixed heat convection mechanisms; conjugate (fluid/solid) heat transfer; radiation heat transfer mechanism; and transient and steady-state heat transfer. Consequently, ANSYS Fluent can be a powerful and reliable tool to validate the proposed semi-analytical model.

The following section describes how the general energy equation (Equation 3.42) is used in ANSYS Fluent to solve different conditions of energy flow (ANSYS 2010). Section 5.2.1 of the ANSYS (2010) manual comprehensively describes the heat transfer theory used by the ANSYS Fluent simulator, including a wide range of various form of energy terms such as pressure work, kinetic energy, viscous dissipation, diffusion, reaction, radiation, anisotropy conductivity, interphase energy source and energy equation in solid regions. In this work, it is assumed that there are fluids in the wellbore and annulus section and the other parts are solids. Therefore, a solution is provided for the mixing of fluid and solid including different properties for each section.

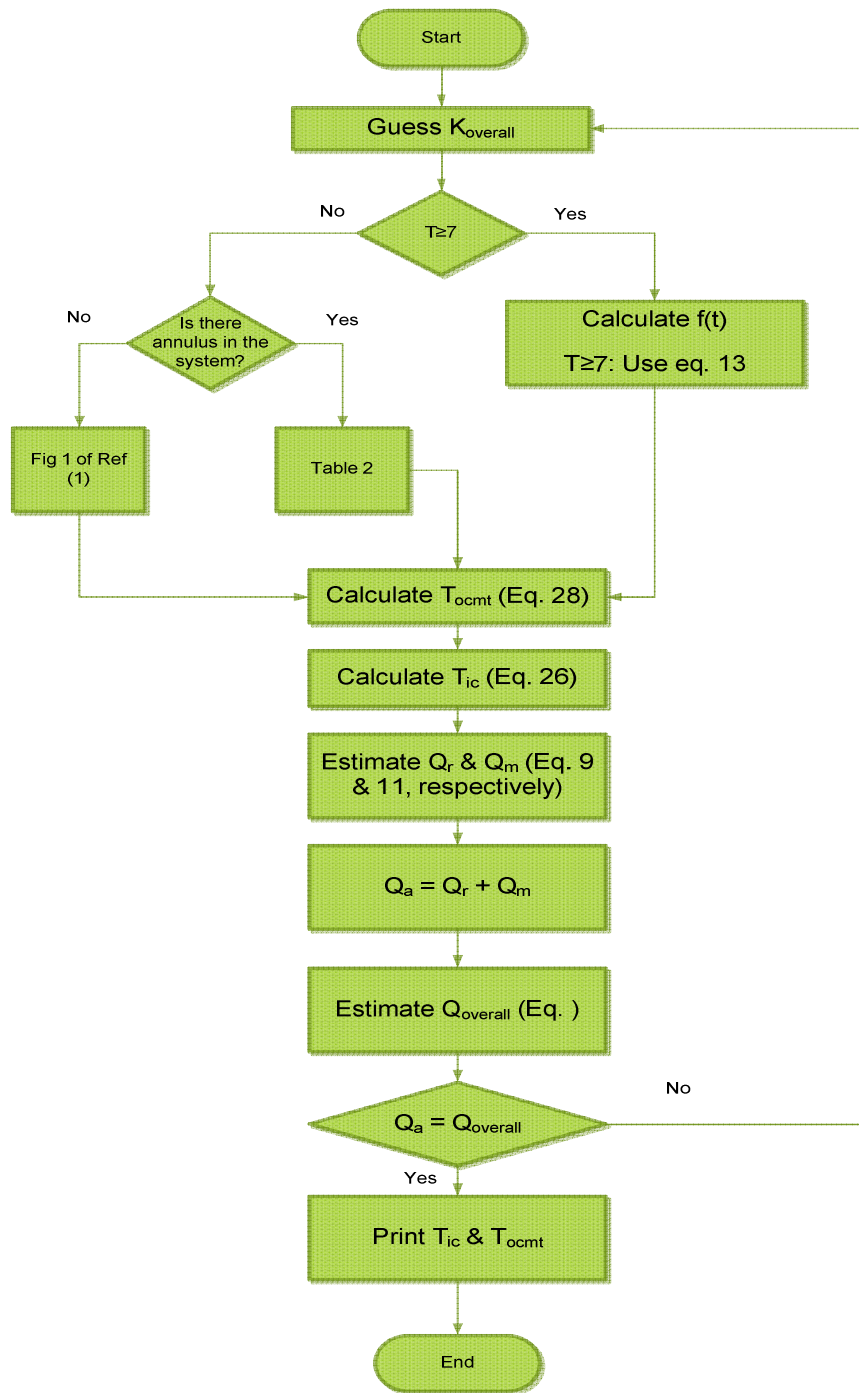


Figure 3-6 Heat transfer calculation algorithm

$$\frac{\partial}{\partial t}(\rho E) + \nabla \cdot (\vec{\vartheta}(\rho E + P)) = \nabla \cdot \left(k_{eff} \nabla T - \sum_j h_j \vec{J}_j + (\overline{\tau}_{eff} \cdot \vec{\vartheta}) \right) + S_h \quad 3.42$$

Here, terms k_{eff} , h_j , J_j and v show effective conductivity, enthalpy, diffusion flux and kinematic viscosity of the desired control system respectively. Also, energy transfer due to conduction, diffusion and viscous dissipation are explained by the first three terms of the right hand side of equation. In this equation, the term S_h describes any heat exchange due to chemical reaction and other volumetric heat sources.

3.4.1 Pre-processing ANSYS Fluent Model

Specification of geometry properties, material definition and meshing are conducted at the pre-processor level in ANSYS/Design Modular. In this stage of the work, a two dimensional (2D) geometry has been created and meshed. Figure 3-7 shows a schematic designed and meshed by Design Modular for wellbore heat calculation, including material properties of each layer. The input data has been summarised in Table 3-1.

Also, all definitions which are necessary to define boundary conditions can be seen in Figure 3-8 using Table 3-2 information. The proposed model and definitions which are considered for ANSYS Fluent simulation are the same as those for the semi-analytical model. Moreover, ANSYS Fluent post-processing tools are easy to use for creating meaningful graphics and reports. For further data analysis, case and data files can be read by other software.

Table 3-2. Tubular, thermal and physical properties information.

Item	Sign	Value	Unit
Tubing	rit	0.4125	ft
	rot	0.4583	ft
Casing	ric	0.7296	ft
	roc	0.8021	ft
Cement	rocmt	1.4	ft
Cement Thermal Conductivity	Kcmt	0.2	Btu/hr sq ft F/ft
Earth Thermal Conductivity	Kg	1	Btu/hr sq ft F/ft
Earth Thermal Diffusivity	α	0.0286	sq ft/hr
Tubing Surface Emissivity	etbg	0.9	
Casing Surface Emissivity	ecsg	0.9	
Heat Capacity	Cp	0.245	Btu/lb F
Fluid Density	ρ_a	0.0388	lb/cu ft
Fluid Viscosity	μ_a	6.90E-02	lb mass/ ft hr
Annulus Fluid Thermal Conductivity	Ka	0.0255	Btu/hr sq ft F/ft
Wellbore	Tf	200	F
Earth	Tg	194.17	F

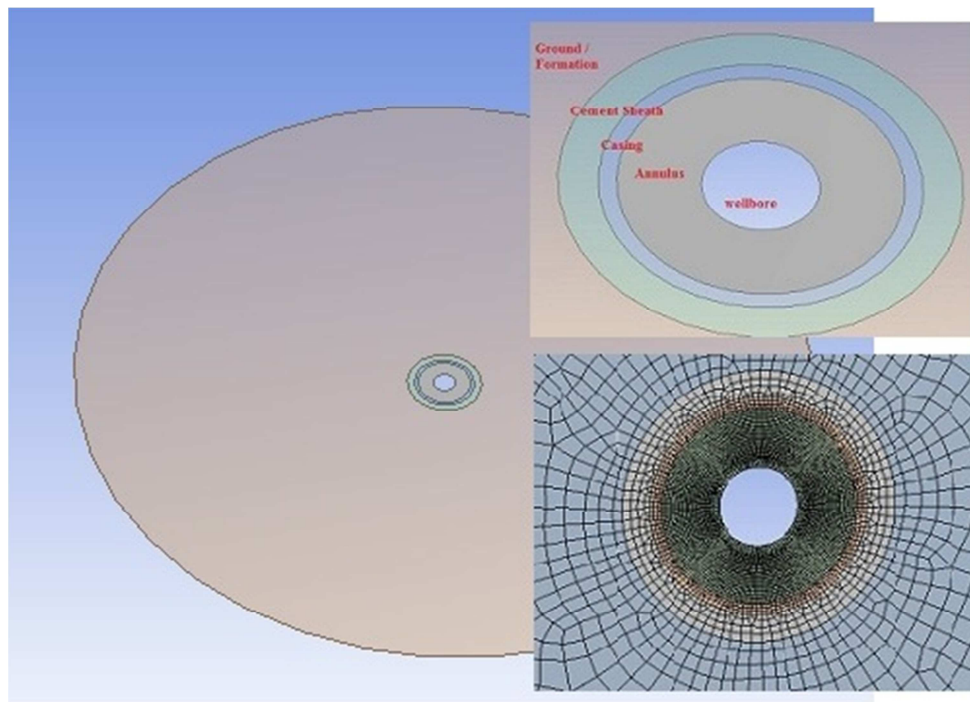


Figure 3-7 Wellbore schematic which is designed and meshed by ANSYS/DesignModular

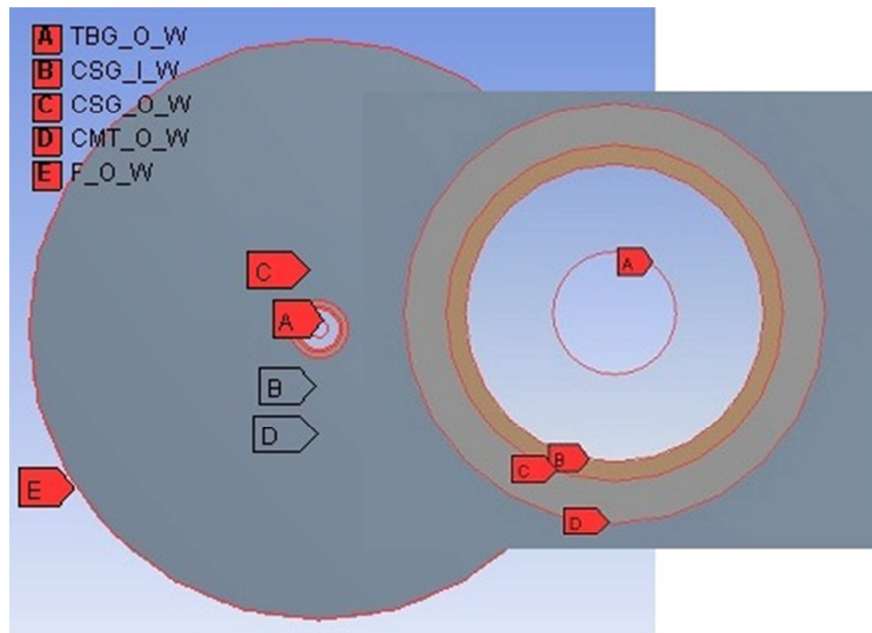


Figure 3-8 Wellbore schematic including boundaries definition

3.4.2 Fluent definitions

When a mesh has been read into Fluent, all operations such as setting boundary conditions, defining fluid properties, executing the solution, refining the mesh, post-processing and viewing the results are executed within Fluent. Optional inputs also allow the user to specify different sources or fixed values such as temperature, mass, flow and so on. In this work, the temperatures at tubing (T_t) and geothermal temperature (T_g) are known, and selected as boundary conditions. Figure 3-9 shows the meshes and different layers surrounding a wellbore designed with Fluent software using information in Table 3-2.

3.4.3 Excel spread sheet

An Excel Spread sheet calculation program was developed for crosschecking all mathematical operations throughout this study using the same data. The block diagram in Figure 3-6 shows the algorithm of the developed program for estimation of the total thermal resistance and the calculation of temperatures at casing and cement sheaths. Figure 3-10 and Figure 3-11 depict the input and output of the developed program designed through the Excel spread sheet.

As can be seen in Figure 3-10, the information required for this program includes: tubular and drilled hole sizes; temperature information at wellbore and ground; production duration; thermal properties of different layers surrounding the wellbore; physical properties of annulus fluid; and constants such as Stefan-Boltzman and gravity acceleration.

Figure 3-12 provides the result obtained by using the Excel program for calculation of the temperature loss profile around a wellbore for different durations of production and at specified points along a wellbore. Later in this chapter, some more results gathered from the Excel program will be discussed while comparing the results with numerical results obtained from ANSYS Fluent simulation.

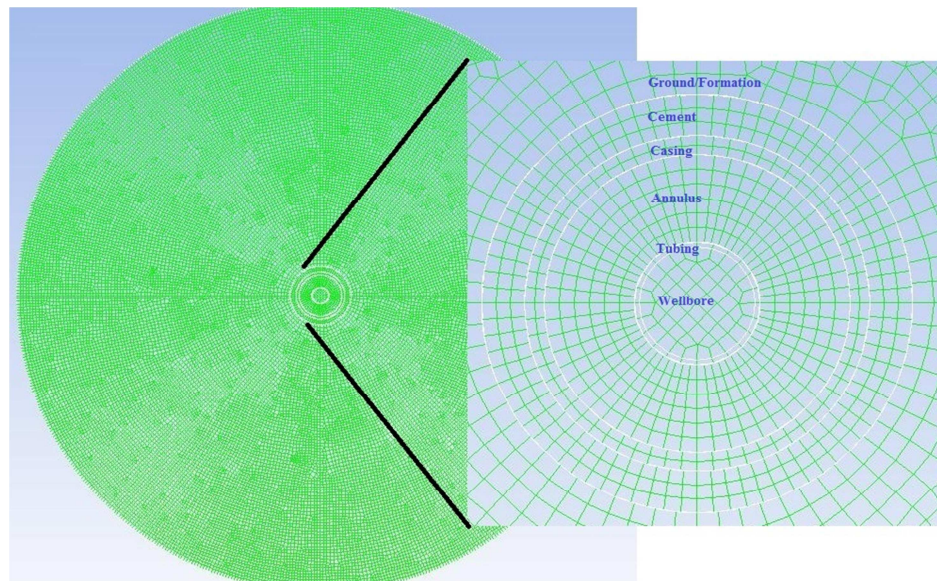


Figure 3-9 Wellbore schematic surrounded by different layers

	A	B	C	D	E	F	G	H
1	Input Required Information							
2								
3	Tubular and Hole Sizes			Thermal Information				
4	Item	Sign	Size (ft)	Item		Sign	Value	Unit
5	Tubing	rit =	0.4125	Cement Thermal Conductivity		Kcmt =	0.2	Btu/hr sq ft F/ft
6		rot =	0.4583	Earth Thermal Conductivity		Kg =	1	Btu/hr sq ft F/ft
7	Casing	ric =	0.7296	Earth Thermal Diffusivity		$\alpha =$	0.0286	sq ft/hr
8		roc =	0.8021	Tubing Surface Emissivity		etbg =	0.9	
9	Cement	rocmt =	1.4	Casing Surface Emissivity		ecsg =	0.9	
10								
11								
12	Temperature Information			Physical Properties of Annulus Fluid				
13	Item	Sign	Deg. F	Item		Sign	Value	Unit
14	Wellbore	Tf =	200	Heat Capacity		Cp =	0.245	Btu/lb F
15	Earth	Tg =	194.17	Fluid Density		$\rho_a =$	0.0388	lb/cu ft
16				Fluid Viscosity		$\mu_a =$	6.90E-02	lb mass/ ft hr
17				Annulus Fluid Thermal Conductivity		Ka =	0.0255	Btu/hr sq ft F/ft
18								
19								
20	Production Time			Constant				
21	Sign	Value	Unit	Item		Sign	Value	Unit
22	t =	7	day	Stefan-Boltzman Constant		$\sigma =$	1.714E-09	Btu/hr ft ² R ⁴
23	t =	168	hr	Gravity Acceleration		g =	4.17E+08	ft/hr ²
24								

Figure 3-10 Input information in the Excel spreadsheet

<u>The process of overall heat transfer coefficient calculation</u>				
	Sign	Value	Unit	
Step 1: Guess a value for Koverall:				
	Koverall =	0.22	Btu/hr sq ft F/ft	
Step 2: Calculation of F(t):				
	f(t) =	0.85		
Step 3: Calculation of Temperatur at the Cement-Formation interface:				
	A =	0.197008423		
	B =	1.174422047		
	Tocmt =	195.01	Deg F	
Step 4: Calculate Temperatur at the Outside Surface of Casing:				
	C =	2.784971136		
	Tic =	197.75	Deg F	
Step 5: Calculate Heat-Loss Value Through Annulus:				
	Qr =	3.74	Btu/hr	Heat loss through annulus as a radiation mechanism.
	Pr =	6.63E-01		
	v^2 =	0.316202478		
	β =	0.001515152	1/R	volume coefficient of expansion
	Gr =	89907.58768		
	Ra =	5.96E+04	(hr ft F)/Btu	
	Nu =	1.85E+00		
	hm =	1.74E-01	Btu/hr sq ft F	
	Qm =	2.46	Btu/hr	Heat loss through annulus as a convection mechanism.
	Qa = Qr+Qm =	6.20	Btu/hr	Total Heat Loss through Annulus.
	havg=	0.75	Btu/hr sq ft F	
Step 6: Calculation of Overall Heat Loss from wellbore to the Surrounding:				
	Qoverall =	3.37	Btu/hr	
Step 7: Overall Heat Transfer Calculation:				
	rm =	0.58	ft	
	Uoverall =	0.43	Btu/hr sq ft F	

Figure 3-11 Results gathered in the Excel spread sheet

3.5 Validation and discussion of results

For the purpose of studying the temperature loss (gain) at any single point of a wellbore to the surroundings, the computer program developed for this study is used to perform several simulations. The simulated results are compared with the

numerical results obtained by Finite Element and CFD (Computational Fluid Dynamics) commercial numerical simulator to validate the proposed analytical model. A model consisting of a wellbore surrounded with a multi-layer media including tubing, annulus, casing, cement and earth/formation is devised using ANSYS Fluent pre-processor, as explained earlier.

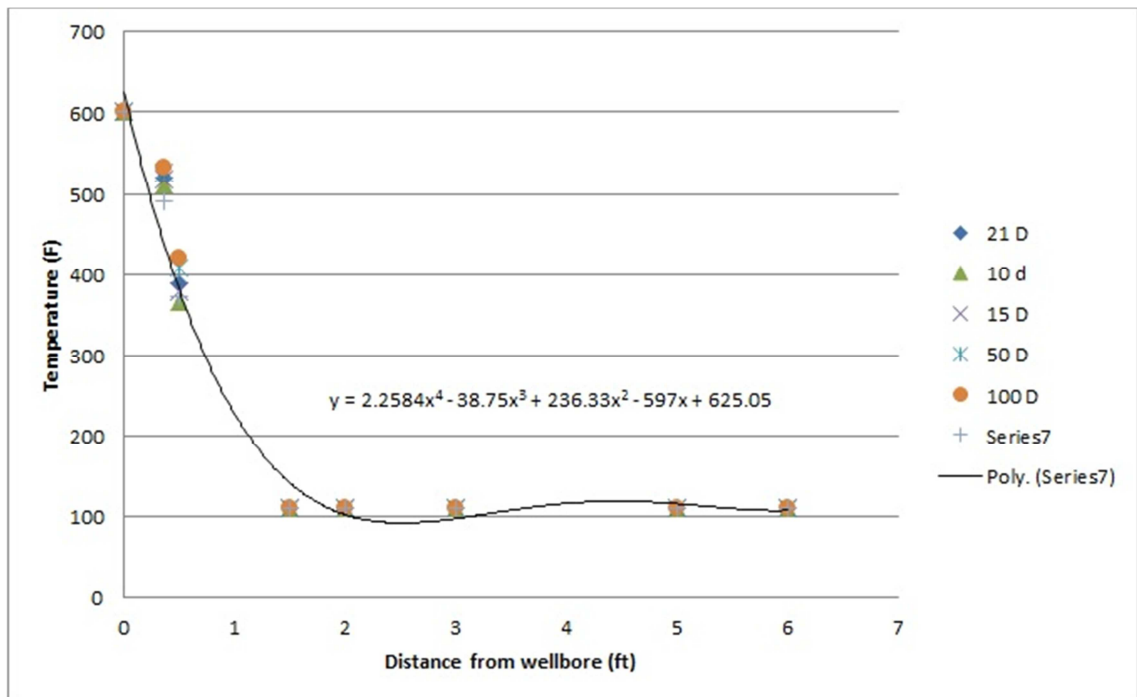


Figure 3-12 Heat loss profile around a wellbore Table 3-3 provides the thermal and physical properties of each layer surrounding the wellbore in this case study. ANSYS Fluent modelling results are used to validate the proposed analytical model through a similar set of calculations done by an Excel spread sheet and computer program. This validation of results will be discussed in a later section. The ANSYS Fluent simulation results are presented in Figure 3-13 through Figure 3-14.

Table 3-3 Model and thermal and heat properties data

Chapter 3 *Analytical Model Predict Temperature Distribution Surrounding the Wellbore*

Tubing	r_{it}	0.14	Ft
	r_{ot}	0.146	Ft
Casing	r_{ic}	0.355	Ft
	r_{oc}	0.4	Ft
Cement	r_{ocmt}	0.5	Ft
Cement thermal conductivity	K_{cmt}	0.2	Btu/hr sq ft F/ft
Earth thermal conductivity	K_e	1	Btu/hr sq ft F/ft
Earth thermal diffusivity	α	0.0286	sq ft/hr
Tubing surface emissivity	ϵ_{tbg}	0.9	
Casing surface emissivity	ϵ_{csg}	0.9	
Heat capacity of annulus fluid	C_p	0.245	Btu/lb F
Fluid density of annulus fluid	ρ_a	0.0388	lb/cu ft
Fluid viscosity of annulus fluid	μ_a	6.90E-02	lb mass/ ft hr
Thermal conductivity of annulus fluid	K_a	0.0255	Btu/hr sq ft F/ft

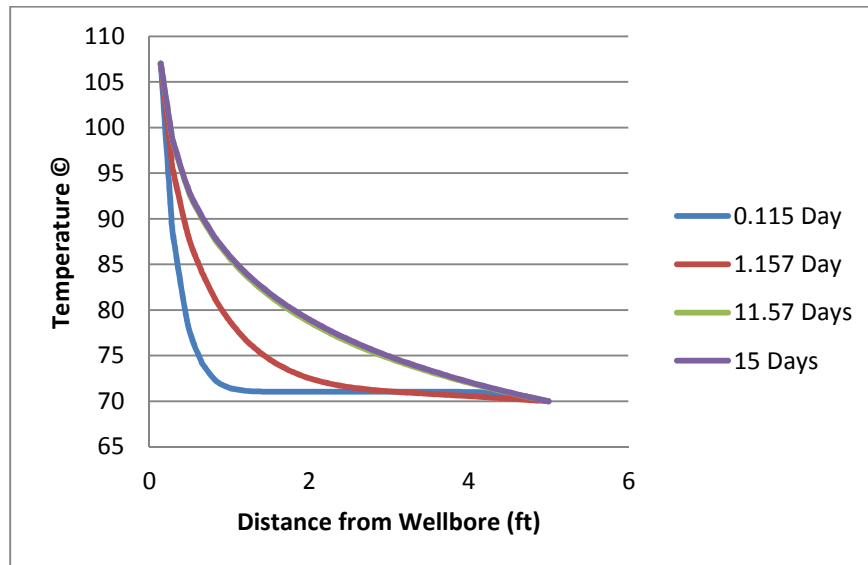


Figure 3-13 Transient temperature profile around a wellbore for a simple case study

Numerical results obtained by ANSYS Fluent, as presented in Figure 3-13, provide temperature loss profile through the surroundings of a wellbore. In this case, the annulus space around the wellbore has not been considered. As can be seen, the temperature profiles have been calculated for different durations of production times. The figure also depicts that the rate of temperature loss reaches a steady state conditions after around 10 days. Therefore, it is possible to predict temperature distribution around a wellbore during transient times using ANSYS.

Figure 3-14 through Figure 3-15 demonstrate temperature profiles around a wellbore when an annulus has been considered within the wellbore schematic. Figure 3-14 compares the profiles of calculated temperature distributions around a wellbore with and without the application of a radiation heat transfer mechanism through an annulus. Figure 3-14 reveals the application of a radiation heat transfer mechanism in addition to other mechanisms should be considered throughout the process of temperature profile calculation around a wellbore including an annulus. Another important point in Figure 3-14 is that the temperature distribution within the fluid-occupied annulus (at a distance of 0.18 - 0.285ft) is considered the same (320°F in this case) by the ANSYS Design Modular.

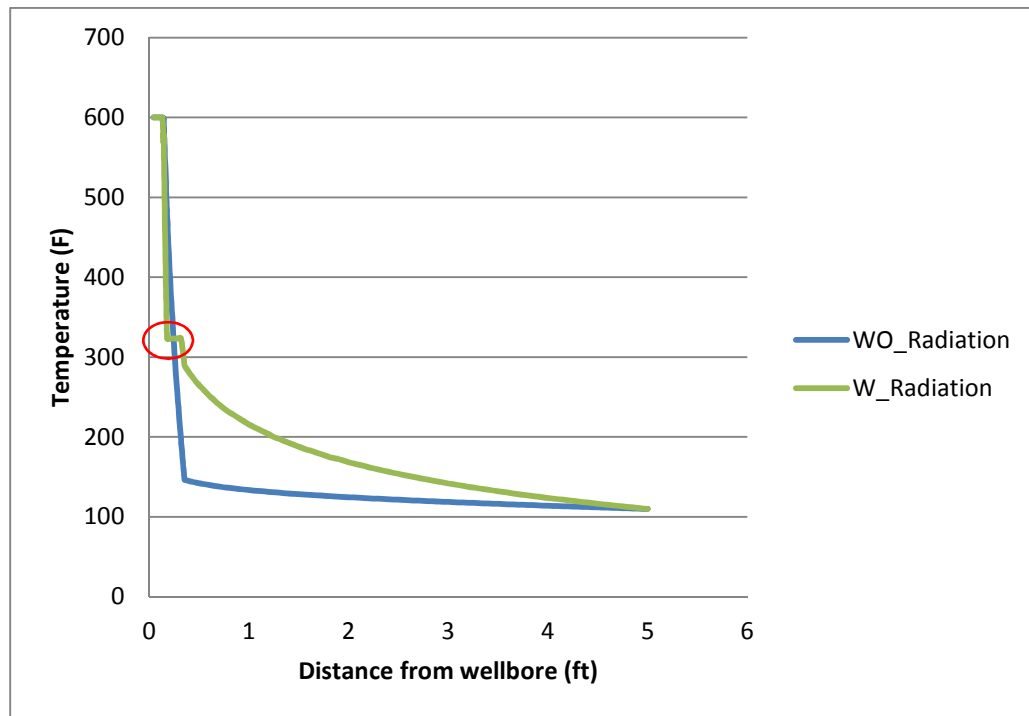


Figure 3-14 Comparison of heat loss around a wellbore with and without the application of a radiation heat transfer mechanism through an annulus.

Figure 3-15 provides the transient temperature profile around a wellbore, in which the results are presented for different times from 1 hour to 21 days after starting production. It is demonstrated in Figure 15 that the system reaches a steady state condition after around 10 days.

The results of temperature distribution around a wellbore for different times after starting the production (as presented in Figure 3-16 through Figure 3-18), obtained from the proposed semi-analytical method using Excel spread sheet calculation and from numerical simulation results using ANSYS Fluent, have shown very good agreement.

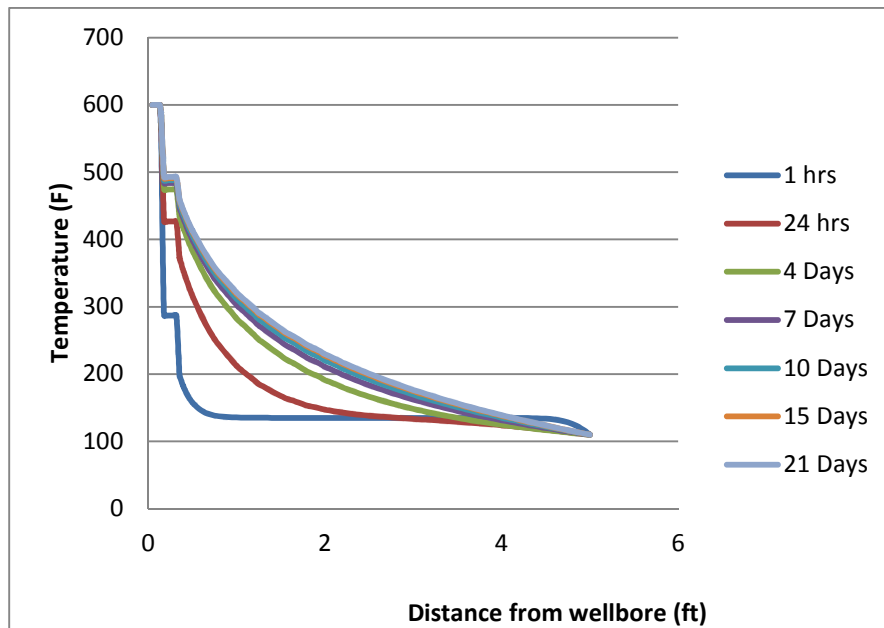


Figure 3-15 Transient temperature profile around a wellbore

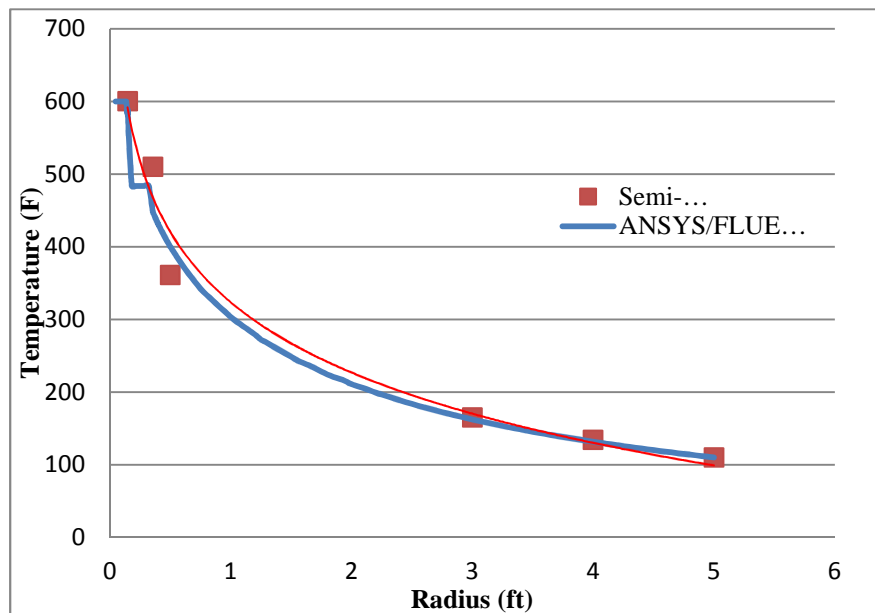


Figure 3-16 Comparison of temperature profile of this work and FLUENT after 7 days of production.

3.6 Summary

A heat loss profile at any single point of a wellbore is modelled by use of energy, momentum and mass balance equations, along with thermodynamics principles of fluid, formation properties, well completion information and flowing fluid properties. In the first part of this chapter, the contribution of different kinds of energy equations in the calculation of overall heat loss from a wellbore to the surroundings, as analysed in this study, has been described in detail.

In this chapter, the concept of the thermal resistance of each layer around a wellbore and the calculation of temperature loss from a wellbore to the surroundings are explained. In simulation, it is supposed (as in real cases) that a wellbore is surrounded with different layers of tubing, annulus, casings, cement sheaths and earth, each of which has different resistivity to the heat loss mechanism. The research project is to write a computation code in FORTRAN with the aim of calculating flowing temperature profiles, or the distribution of flowing temperature along an injection or producing well from the bottom to surface, using the concepts explained in this chapter the algorithm for calculation has been summarised in the form of a block diagram in Figure 3-6.

The widely accepted and reliable FEM- and CFD-based numerical simulator ANSYS Fluent is used to validate the analytical model. Results obtained from numerical simulation show good agreement with the results obtained from the proposed analytical method. This application will be extended to calculate temperature profile along a wellbore in the next chapter.

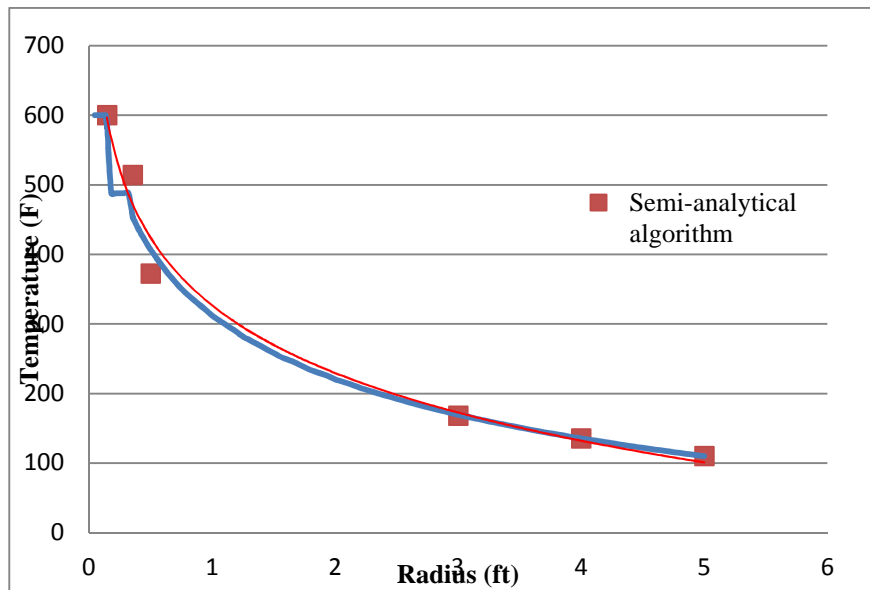


Figure 3-17 Comparison of temperature profile of this work and FLUENT after 10 days of production

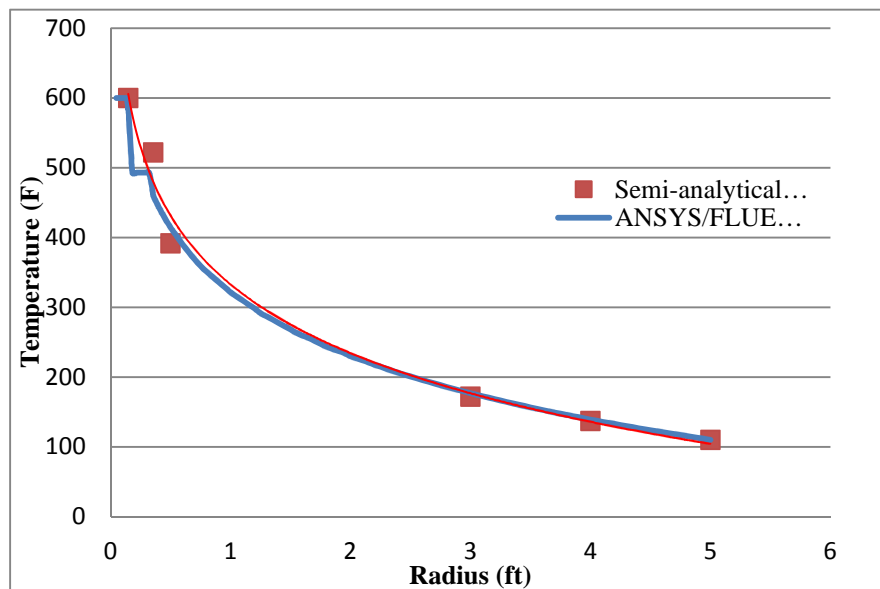


Figure 3-18 Comparison of temperature profiles calculated by this work and FLUENT after 21 days of production.

4

Numerical Modelling of the WTP Simulator

4.1 The WTP Simulator

The analysis of any fluid flow through a wellbore conduit depends on the type of flowing fluid entering into the wellbore from the reservoir, which might be totally liquid, only gas or a multi-phase fluid (e.g. gas, water and oil). The analytical model presented in Chapter 3 has been further extended to predict the wellbore flowing fluid temperature profile. A numerical simulator named Wellbore Temperature Profile (WTP) simulator is developed in this respect using FORTRAN language. The simulator has the capability to deal with all types of fluid flowing through a typical injection and/or production well. Figure 4-1 shows how different cases are considered or selected in the simulator for the prediction of WTP for different fluid phases flowing along a wellbore.

A typical wellbore includes a production string, casings and cement sheaths. It may have different sizes of tubing, casings and liners with different layers of cement sheaths in different depths from surface to bottom. The WTP Simulator is developed to address the complexity of a typical wellbore scenario. Figure 4- 2 provides a flow diagram that portrays the complexities of a wellbore and its surroundings.

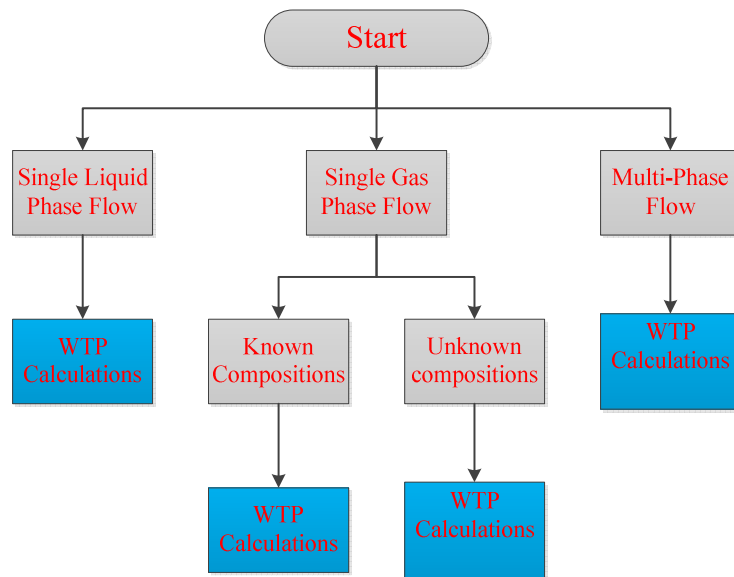


Figure 4-1 The flow diagram of the WTP Simulator

The details of associated numerical models considered to develop this simulator are presented in this chapter. The chapter has four sections. The first section explains a mathematical model for single phase liquid flow through the wellbore. The second section describes the mathematical model for a single phase gas flow. The third section presents mathematical models that developed to deal with the flow of a mixture of phases through the wellbore. And the numerical model for calculation of temperature profile along an injection wellbore using the WTP simulator is provided in section four. This chapter also outlines the algorithms used various calculations.

4.2 Single phase liquid flow

In this section, it is supposed that the fluid flowing along the wellbore is just liquid. Also, it is assumed that physical and thermal properties such as density and heat capacity for the producing fluid and the fluid occupied annulus are known. For

calculations of WTP in this section, reservoir temperature and pressure, geothermal temperature at reservoir depth and geothermal temperature gradient are required.

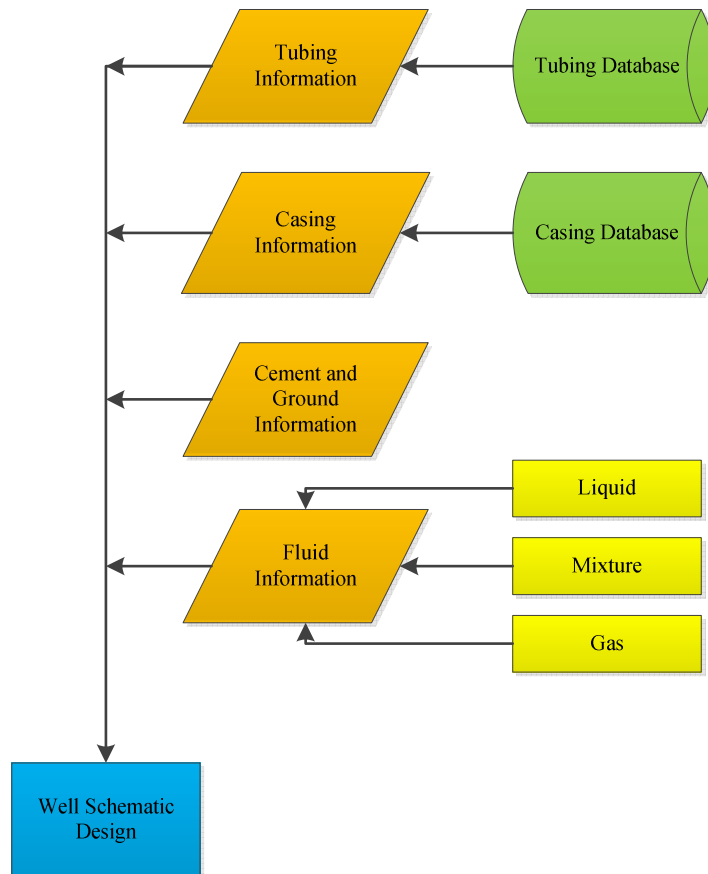


Figure 4- 2 Flow diagram to design a wellbore through the WTP Simulator

4.2.1 Temperature profile calculation along a liquid producing wellbore

Considering the volume of a unit length of liquid flowing along a wellbore, the heat changes through the desired volume of fluid as a result of local and frictional losses may be expressed as follows:

$$\begin{aligned} & \left(\begin{array}{l} \text{Heat changes} \\ \text{in a volume of} \\ \text{a unit length of} \\ \text{a production string} \end{array} \right) & 4.1 \\ & = \left(\begin{array}{l} \text{Heat loss/gain} \\ \text{towards the} \\ \text{surroundings} \end{array} \right) + \left(\begin{array}{l} \text{Heat generation} \\ \text{as a cause of} \\ \text{fluid friction} \end{array} \right) \end{aligned}$$

The summation of local and frictional heat changes of the fluid can be used to determine the temperature of the fluid at any point along the wellbore.

The heat generation process along a wellbore can be explained by the first law of thermodynamics. The amount of heat (Q) generated in a pipe associated with pressure loss due to friction between the flowing fluid and the pipe wall can be expressed accordingly as:

$$Q = (V_m A) \Delta P \quad 4.2$$

Where:

Q = Heat generation due to friction (Btu/min)

V_m = Average velocity of fluid in the wellbore in (ft/min)

A = Cross sectional area of the string (ft²)

ΔP = Pressure drop along the tubing (i.e. production string) in the wellbore (psi)

For calculation of pressure loss along the production string, clarification of the flow mechanism through the wellbore is necessary, which in the case of single liquid flow, depends on the size, roughness and direction of flow along the production

string and the flow rate of fluid produced (fluid production rate). Referring to the physical properties of the production string and the fluid flow rate, the mechanism of fluid flow through a wellbore can be categorised into laminar or turbulence flow conditions. These conditions of flow can be determined using the Reynolds number. Each of these flow regimes requires a different correlation for calculation of the friction factor, as well as the amount of heat generation caused by fluid flow along the production string and wellbore.

An algorithm to calculate the heat loss/gain at any single point for a unit length of the production string, which is known as a node (first parenthesis on the left hand side of Equation 4.1) is explained in section 3.3.4 of Chapter 3. For evaluation of the second parenthesis in Equation 4.1, fluid flow equations are also needed to simulate the flow of fluid to the next node, which appears as a consequence of pressure loss and heat generation. Therefore, heat generation is calculated for the desired section (between two nodes) of the wellbore using the procedure of calculation for heat loss, as explained in Chapter 3 (section 3.3.4) and the fluid flow equations. Then, the calculations for heat loss, pressure loss and heat generation are repeated at any point along the wellbore until the fluid reaches the surface. At each section of the wellbore, the physical properties of the ground surrounding the wellbore are required to predict whether there are any changes caused by these conditions. The concepts of the calculations are the same for injection and production scenarios, except for the effect of gravitational force on the fluid in production cases.

4.2.2 Laminar flow

For a laminar flow, pressure drop along the production string may generally be expressed as the product of friction factor (f), non-dimensional length of string (L/D) and kinetic energy of fluid ($\rho V_m^2/2$) flowing through the wellbore (Atesmen, 2009).

$$\Delta P = f \left(\frac{L}{D} \right) \left(\frac{\rho V_m^2}{2} \right) \quad 4.3$$

Where, in the laminar flow region ($N_{Re} < 2000$), the friction factor is given as follows:

$$f = 64 / N_{Re} \quad 4.4$$

Where N_{Re} is the Reynolds number, and is equal to $(\rho v_m d) / \mu$ (Beggs, 2003).

4.2.3 Turbulent flow

Turbulent flow condition is a function of velocity profile and pressure gradient, which are sensitive to the characteristics of pipe walls. A number of equations have been available in published literatures (Bannister and Bengel, 1981; Cao and Ahmadi, 1995; Millionshchikov, 1971; Pasinato, 2011; Vollmer et al., 2004; Wu et al., 2011) to predict turbulent flow condition behaviours for smooth pipes and a range of Reynolds numbers. This work, however considered the most accurate empirical equations for prediction of flow behaviour under turbulent conditions are presented by Beggs (Beggs, 2003).

Figure 4- 3 shows the flow diagram of temperature profile calculation for a single phase liquid production wellbore. As can be seen, the program start with reading inputs such as tubular data, depth, liquid rate, physical properties of production and annulus fluid, reservoir pressure and temperature and geothermal information. In order to calculate parameters such as determination of flow regimes, heat generation temperature loss and so on, the related sections are referred in the flow diagram. Section 3.3.6 and Figure 3-6 of chapter 3 comprehensively provides the algorithm for calculation of overall heat loss. Also, the list of subroutines and computer codes

for calculation of the wellbore temperature profile along a liquid production wellbore can be seen in Appendix F.

4.3 Single phase gas flow

Clearly, the gas stream in the problem may include known or unknown components, and this section considers both cases. For evaluation of WTP through single phase gas flow systems, the WTP Simulator requires all properties of a real gas, including compressibility factor, density, specific gravity and gas formation volume factor. The methods for calculation of parameters such as pressure drop and Joule Thomson effect are discussed in this section.

4.3.1 Temperature profile calculation along a gas producing wellbore

For a unit volume of wellbore occupied by gas, the heat changes can be written as follows.

$$\left(\begin{array}{l} \text{Heat changes} \\ \text{in a volume of gas} \\ \text{per unit length of} \\ \text{a production string} \end{array} \right) = \left(\begin{array}{l} \text{Heat loss/gain} \\ \text{within the} \\ \text{surroundings} \end{array} \right) + \left(\begin{array}{l} \text{Heat gain/loss} \\ \text{as a cause of} \\ \text{friction loss} \\ \text{and JT effect} \\ \text{during flow} \end{array} \right) \quad 4.5$$

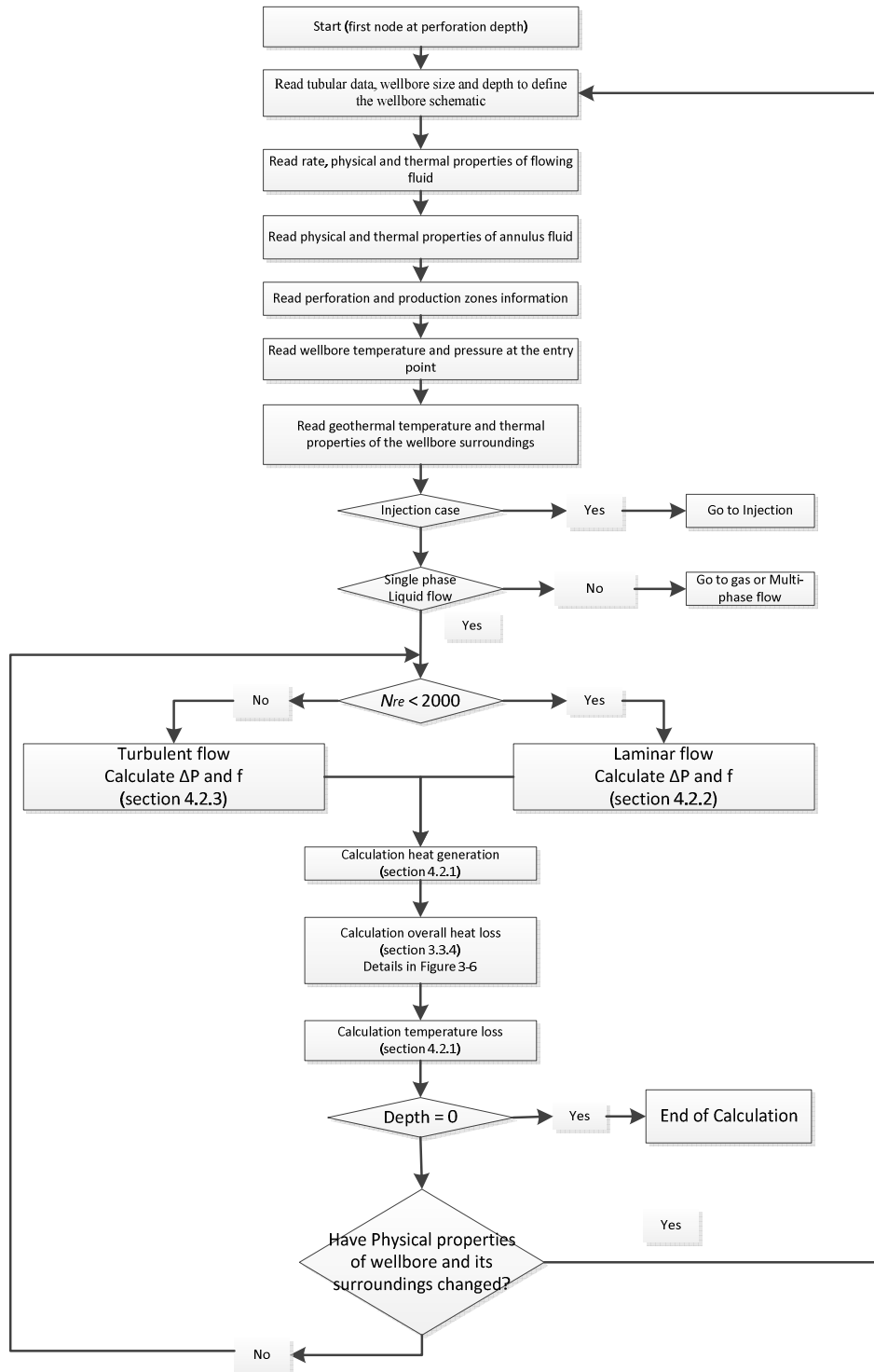


Figure 4- 3 Flow diagram of single phase liquid flow of the WTP simulator.

The contribution of friction loss to generate heat is different for gas and liquid fluids, due to the different physical natures of gas and liquid. This relates to the behaviours of fluids and thermodynamic irreversibility, which can be referred to the amount of entropy generation through the flowing fluid system (Al-Zaharnah and Yilbas, 2004). Katz (Donald and Robert, 1990) explains that the effect of pressure on entropy generation for gas fluids is very large. They say as the pressure drops in gas systems, heat energy is mainly supplied for adding entropy of the thermal system. This is happening in order to maintain the temperature of the system at lower pressure. They finally result that the supplied heat is larger than the contribution of frictional energy to the generated entropy. As a result, the frictional energy does not significantly contribute to raising the temperature of the flowing gas. This phenomenon is antithesis for oil systems, and so most of the consumed frictional energy in a given pressure drop converts to temperature raising through the flowing fluid system (Donald and Robert, 1990). However, the calculation of energy loss as a contribution of friction loss can be not evaluated theoretically, but may be correlated empirically by applying laboratory experimental methods based on the functions of gas flow variables.

On the other hand, some temperature changes may occur in the gas systems, due to the expansion of gas caused by pressure loss, which is known as the Joule-Thomson (JT) effect (Edmister and Lee, 1984; Perry et al., 1997; Smolen, 1996). This temperature change may be positive or negative, and depends on the compositions of gas mixture and also the rate of fluid flow. Katz (Donald and Robert, 1990) refers to the effect of the JT effect on the flowing gas systems and the contribution of pressure to entropy generation. He predicted that there is not enough energy of expansion to maintain the temperature of the system. Therefore, gas pipelines are normally cooler than oil pipelines.

In this study, it is understood that temperature drop at the entry point of gas from reservoir to the wellbore is mainly an effect of the JT. While along the wellbore,

from the entry point to the surface, the temperature mainly drops based on the temperature difference between the flowing fluid and the wellbore surroundings, and there is a minor dependency on the JT effect. However, in this study, the contribution of the JT effect to the temperature loss along the wellbore is considered, and is predicted for a typical gas production well.

4.3.2 Temperature loss calculation of flowing gas

In order to evaluate temperature profile through a flowing gas wellbore, Equation 34.25 of Chapter 3, explaining the mechanical energy balance equation for a homogenous and steady-state single phase fluid, is applied. Therefore, the equation is rewritten for enthalpy and rearranges to the following form:

$$\frac{dH}{dx} + \frac{g \sin\alpha}{g_c J} + \frac{v}{g_c J} \frac{dv}{dx} = \pm \frac{Q}{w} \quad 4.6$$

Also, the following equation is applied for the explanation of enthalpy:

$$dH = C_p dT_f - C_j C_p dP \quad 4.7$$

By substituting Equation 4.7 in Equation 4.6, we obtain the following equation that can be applied for calculation of temperature loss across a desired control volume:

$$dT_f = C_j dP - \frac{1}{C_p} \left[\frac{Q}{w} + \frac{g \sin\alpha}{g_c J} + \frac{v}{g_c J} \frac{dv}{dx} \right] dx \quad 4.8$$

4.3.3 Pressure loss calculation of flowing gas

Pressure loss in a flowing gas wellbore is due to the combination of hydrostatic effect and frictional effect between the fluid and the pipe wall. The following

equation is the final form of the pressure loss calculation equation along a wellbore given by Katz (Donald and Robert, 1990) and Lee (Lee and Wattenbargar, 1996):

$$P_{wf}^2 = e^s P_{tf}^2 + \frac{6.67 * 10^{-4} q_g^2 f \bar{T}^2 \bar{Z}^2}{d^5} (e^s - 1) \quad 4.9$$

Where:

$$s = \frac{0.0375 \gamma_g dx}{\bar{Z} \bar{T}} \quad 4.10$$

In Equations 4.10 and 4.11, the compressibility factor (\bar{Z}) and temperature (\bar{T}) is considered as an average along the wellbore. However, in this work, as the total length of the wellbore is divided into very small increments (nodes), the average value of compressibility and temperature at any node is considered for the whole of the desired increment through the calculation.

Clearly, the calculation of the friction factor (f) in Equation 4.9 depends on the velocity of fluid flowing along the wellbore, flow conditions (laminar or turbulent) and relative roughness of the pipe wall. There are number of correlations widely used for calculating the friction factor covering laminar and turbulent flow conditions. In this work, Equation 4.4 is applied to calculate the friction factor for laminar flow conditions; while the Jane and Swamee correlation (Beggs, 2003; Lee and Wattenbargar, 1996) (Equation 4.11) is applied for turbulent flow conditions.

$$\frac{1}{\sqrt{f}} = 1.74 - 2 \log \left(\frac{2 \epsilon}{d} + \frac{18.7}{N_{Re} \sqrt{f}} \right) \quad 4.11$$

To calculate the gas compressibility factor (Z) in Equation 4.9, considering known and unknown components conditions, the Peng-Robinson equation of state (PR

EOS) and Hall-Yarborough correlation are applied. Both of these methods are elaborated in the following sections.

4.3.4 Gas properties

In this section, the gas properties needed for evaluating the temperature and pressure profile along a wellbore are discussed, and the equations that have been applied through the WTP Simulator to calculate the important gas properties are provided.

For a gas including some components, the molecular weight is defined as:

$$M = \sum_{i=1}^n M_i y_i \quad 4.12$$

Where M is the molecular weight of a mixture, M_i is the molecular weight of component i , and n shows the total number of components.

Specific gravity is explained as:

$$\gamma_g = \frac{M}{M_{air}} \quad 4.13$$

Where, M_{air} denotes the molecular weight of air which is equals to 28.96 lbm/lbmole.

Gas density is expressed as:

$$\rho_g = \frac{PM}{ZRT} \quad 4.14$$

Or,

$$\rho_g = 2.7 \frac{P\gamma_g}{ZT} \quad 4.15$$

Where, ρ is in lbmole/ft³, P is in psia, T is in degrees of Rankin and the universal gas constant (R) is equal 10.73((ft)³(psia)(lbmole)⁻¹(R)⁻¹.

The formation volume factor (B_g), the ratio of volume of one mole of mixture at a given temperature and pressure in a reservoir or down hole condition to the volume of one mole of that mixture at standard conditions (14.7 psi and 520 °R), is defined as:

$$B_g = 0.0282 \frac{ZT}{P} \quad 4.16$$

Where, B_g is in ft³/SCF, T is in degrees of Rankin and P is in psia.

4.3.5 Gas mixtures

Production gases are usually composed of different hydrocarbon and non-hydrocarbon components, which make the prediction of the gas mixture properties and behaviours complex. Laboratories are the normal place for the determination of the components of a gas mixture. When the composition of a gas mixture is known, an appropriate equation of states (EOS) is generally required to evaluate the gas mixture properties and behaviours. This requires an expensive and cumbersome experimental study to quantitatively identify the components and percentage of composition of the gas mixture. However, there are many empirical correlations available in the literatures which are widely used in the industry for particular gas mixture systems when the detailed composition of gas mixtures is not available. Both cases (i.e. gas mixtures with known composition and unknown composition)

are considered in this study to calculate the required gas mixture properties and predict the flowing well temperature profile along a wellbore.

- *Gas mixtures with known components*
 - Calculation of pseudo-critical properties of a real gas

The following equations are used to calculate the pseudo-critical pressure and temperature of a real gas with known compositions.

$$T_{pc} = \sum_{i=1}^n w_i T_{ci} \quad 4.17$$

$$P_{pc} = \sum_{i=1}^n w_i P_{ci} \quad 4.18$$

Where, w_i is mole fraction of gas.

The pseudo-reduced pressure and temperature of the mixture are defined as:

$$T_{pr} = \frac{T}{T_{pc}} \quad 4.19$$

$$P_{pr} = \frac{P}{P_{pc}} \quad 4.20$$

However, some corrections are needed in the presence of impurities such as H₂S, CO₂, N₂, H₂O and C7⁺ components.

In the presence of C7⁺ components in a mixture, the Stewart et al. method for sweet gases is applied to calculate the pseudo-critical properties of the mixture. A

comprehensive explanation of this method can be seen in the literature (Lee and Wattenbargar, 1996) and provided in Appendix B.

To account for the effect of H₂S and CO₂ on the pseudo-critical properties of a mixture, the following correlations are considered, as given by Wichert and Aziz (Donald and Robert, 1990).

$$T'_{pc} = T_{pc} - \psi \quad 4.21$$

$$P'_{pc} = \frac{P_{pc}T'_{pc}}{[T_{pc} + B(1 - B)\psi]} \quad 4.22$$

$$\psi = 120((y_{H_2S} + y_{CO_2})^{0.9} - (y_{H_2S} + y_{CO_2})^{1.6}) + 15(By_{H_2S}^{0.5} - y_{H_2S}^4) \quad 3.23$$

Where, y_{H_2S} and y_{CO_2} are the mole fraction of H₂S and CO₂ components, respectively.

The following semi-empirical equations are also applied to make corrections due to the effect of N₂ and H₂O on the pseudo-critical properties of a mixture.

$$T''_{pc} = \frac{T'_{pc} - (227.2y_{N_2}) - (1165y_{H_2O})}{(1 - y_{N_2} - y_{H_2O})} + \xi_1 \quad 4.24$$

$$P''_{pc} = \frac{P'_{pc} - (493.1y_{N_2}) - (3200y_{H_2O})}{(1 - y_{N_2} - y_{H_2O})} + \xi_2 \quad 4.25$$

Where:

$$\xi_1 = -(246.1y_{N_2}) + (400y_{H_2O}) \quad 4.26$$

$$\xi_2 = -(162y_{N_2}) + (1270y_{H_2O}) \quad 4.27$$

In the case where the composition details of a gas mixture are not known, Standing's correlations are applied for the evaluation of pseudo-critical properties. Standing's correlations are expressed as:

$$T_{pc} = 168 + 325\gamma_g - 12.5\gamma_g^2 \quad 4.28$$

$$P_{pc} = 677 + 15\gamma_g - 37.5\gamma_g^2 \quad 4.29$$

Then, Equations 4.21 through 4.27 are applied to make corrections to account the effect of H₂S, CO₂, N₂ and H₂O, when necessary.

○ Peng-Robinson equation of state (PR EOS)

The simplicity and convenience of using equations of state (EOS), allow users to apply them for modelling the liquid and vapour behaviour of hydrocarbon mixtures. Among them, PR EOS is more accurate for predicting the vapour pressure value of pure substances, when the liquid density value, compressibility factor and the equilibrium ratio of mixtures are compared with the other equations of state such as Soave-Redlich-Kwong (SRK) and van der Waals equations of states (Donald and Robert, 1990; Peng and Robinson, 1976). As a consequence, PR EOS has been selected to evaluate the compressibility factor of gas mixtures in this work.

The PR EOS is written as:

$$P = \frac{RT}{v - b} - \frac{a}{v(v + b) + b(v - b)} \quad 4.30$$

Where, R is the universal gas constant (10.73 (ft)³(psia)(lbmole)⁻¹(R)⁻¹), T is the absolute temperature, and v is the molar volume.

The Peng-Robinson equation of state (Equation 4.30) is used to evaluate the derivative term $\left(\frac{Z}{\partial T}\right)_p$ required to calculate the Joule-Thomson effect, which will be elaborated in a later section (section 3.4.6) as a part of the WTP evaluation. But because Equation 4.30 is not readily explicit for temperature or volume, the cubic polynomial form of the Peng-Robinson equation of state is applied; it is written as:

$$f(Z) = Z^3 + \alpha Z^2 + \beta Z + \gamma = 0 \quad 4.31$$

Where:

$$\alpha = B - 1 \quad 4.32$$

$$\beta = A - 2B - 3B^2 \quad 4.33$$

$$\gamma = B^3 + B^2 - AB \quad 4.34$$

$$A = aP / (RT)^2 \quad 4.35$$

$$B = bP / RT \quad 4.36$$

$$a = a_c \left[1 + m \left(1 - \sqrt{\frac{T}{T_c}} \right) \right] \quad 4.37$$

$$a_c = 0.457235 \frac{R^2 T_c^2}{P_c} \quad 4.38$$

$$m = 0.37464 + 1.54226\omega - 0.26992\omega^2 \quad 4.39$$

$$b = 0.077796 \frac{RT_c}{P_c} \quad 4.40$$

○ Mixing rules

Equations of state are basically used for the description of the volumetric and phase behaviour of pure components. Therefore, mixing rules are applied to extend the application of equations of state for mixed fluids.

For a fluid with n-component compositions, the following empirical relations are applied to calculate the mixture parameters of a and b .

$$a = \sum_{i=1}^n \sum_{j=1}^n w_i w_j (a_i a_j)^{0.5} (1 - k_{ij}) \quad 4.41$$

$$b = \sum_{i=1}^n w_i b_i \quad 4.42$$

Where, k_{ij} in Equation 4.41 is the binary interaction coefficient, and is known as an interaction parameter between non-similar molecules. The value of k_{ij} is equal to zero when $i=j$, and its value is close to zero for hydrocarbon-hydrocarbon interaction. However, the value of k_{ij} is non-zero for non-hydrocarbon-hydrocarbon components. The value for k_{ij} is tabulated in the literature (Danesh, 1998), which also suggests the following equation for evaluation of k_{ij} .

$$(1 - k_{ij}) = \left[\frac{2(V_{ci}^{1/3} V_{cj}^{1/3})^{1/2}}{V_{ci}^{1/3} + V_{cj}^{1/3}} \right]^n \quad 4.43$$

Danesh (Danesh, 1998) suggests the theoretical value of $n=6$; however, Cheuh and Prausnitz (P. L. Chueh and Prausnitz, 1967) believe that $n=3$ gives better results.

○ Evaluation of term $\left(\frac{\partial Z}{\partial T}\right)_p$

Using Equation 4.30, the derivative term $\left(\frac{\partial Z}{\partial T}\right)_p$ can be written as:

$$\left(\frac{\partial Z}{\partial T}\right)_p = \frac{\left(\frac{\partial A}{\partial T}\right)_p (B - Z) + \left(\frac{\partial B}{\partial T}\right)_p (6BZ + 2Z - 3B^2 - 2B + A - Z^2)}{3Z^2 + 2(B - 1)Z + (A - 2B - 3B^2)} \quad 4.44$$

The derivative term of $\left(\frac{\partial A}{\partial T}\right)_p$ can be achieved from Equation 4.35.

$$\left(\frac{\partial A}{\partial T}\right)_p = \frac{P}{R^2 T^2} \left(\frac{da}{dT} - \frac{2a}{T}\right) \quad 4.45$$

Also, using Equation 4.36, the derivative term $\left(\frac{\partial B}{\partial T}\right)_p$ can be rewritten as:

$$\left(\frac{\partial B}{\partial T}\right)_p = \frac{-bP}{RT^2} \quad 4.46$$

Therefore, Equation 4.41 applies for evaluation of term $\frac{da}{dT}$ in Equation 4.37 for an n-components fluid.

$$\frac{da}{dT} = \frac{1}{2} \sum_{i=1}^n \sum_{j=1}^n w_i w_j (a_i a_j)^{0.5} \left[\sqrt{\frac{a_j}{a_i}} \frac{da_i}{dT} + \sqrt{\frac{a_i}{a_j}} \frac{da_j}{dT} \right] \quad 4.47$$

$$\frac{da_i}{dT} = \frac{-m_i a_i}{\left[1 + m_i \left(1 - \sqrt{\frac{T}{T_c}} \right) \right] \sqrt{TT_{ci}}} \quad 4.48$$

- **Gas mixtures with unknown components**

- Compressibility factor (Z)

Gas mixtures are not ideal, and the compressibility factor is applied to show deviations from the ideal condition. In the case where the details of components are not known, there are many correlations, such as Hall-Yarborough (Ikoku, 1984), Dranchuk EOS (Lee and Wattenbarger, 1996) and Beggs and Brill (Golan and

Whitson, 1991), which may be applied to predict the compressibility factor of a gas mixture. Among them, the Hall-Yarborough method is extremely simple and accurate to apply for this purpose (Dake, 1978). Therefore, the Hall-Yarborough correlation is used to evaluate the compressibility factor of a mixture in the case of unknown details of components throughout this work.

The Hall-Yarborough method and Newton-Raphson iterative techniques are applied to calculate the compressibility factor (Z) of producing fluids. To calculate the Z factor using the Hall-Yarborough method, the pseudo-reduced pressure and temperature of the mixture are required. In the case of a mixture with detailed analysis, Equations 4.17 through 4.20 are applied. However, in the case of a mixture without detailed analysis, the density of the mixture is required to apply the following equations to calculate the pseudo-critical pressure and temperature of the mixture.

$$T_{pc} = 326 + (315.5(\rho_g - 0.5) - 240y_{N_2} - 83.3y_{CO_2} + 133.3y_{H_2S}) \quad 4.49$$

$$P_{pc} = 678 + (50(\rho_g - 0.5) - 206.7y_{N_2} - 440y_{CO_2} + 606.7y_{H_2S}) \quad 4.50$$

The Hall-Yarborough equation is expressed as:

$$Z = \frac{0.06125P_{pr}t_r e^{-1.2(1-t_r)^2}}{y} \quad 4.51$$

Where P_{pr} is pseudo-reduced pressure, t_r is the reciprocal of pseudo-reduced temperature and y is the reduced density which can be calculated using the following equation:

$$\begin{aligned}
 & -0.06125P_{pr}t_r e^{-1.2(1-t_r)^2} + \frac{y + y^2 + y^3 - y^4}{(1-y)^3} \\
 & - (14.76t_r - 9.76t_r^2 + 4.58t_r^2)y^2 \\
 & + (90.7t_r - 242.2t_r^2 + 42.4t_r^3)y^{(2.18+2.82t_r)} = 0
 \end{aligned} \tag{4.52}$$

The Newton-Raphson iteration method is used for the calculation of y through the non-linear Equation 4.52.

○ Evaluation of term $\left(\frac{\partial Z}{\partial T}\right)_p$

For the evaluation of the term $\left(\frac{\partial Z}{\partial T}\right)_p$ in the case of unknown details of gas mixtures, the equation can be re-written as:

$$\left(\frac{\partial Z}{\partial T}\right)_p = \left(\frac{\partial Z}{\partial T_{pr}}\right)_p \left(\frac{\partial T_{pr}}{\partial T}\right)_p = \frac{1}{T_{pc}} \left(\frac{\partial Z}{\partial T_{pr}}\right)_p \tag{4.53}$$

Where for the evaluation of the term $\left(\frac{\partial Z}{\partial T_{pr}}\right)_p$, a gas compressibility factor chart (Katz and Standing) (Ahmed, 1946) a function of the pseudo-reduced pressure and temperature of the mixture is used. . Several equations and algorithms are published to summarise the Standing and Katz chart, and to simplify the calculations. One of them is published by Brill and Beggs, and then modified by Standing (Beggs, 2003). While these equations have been checked in this study and found to be erroneous. It is found that calculation of term $\left(\frac{\partial Z}{\partial T_{pr}}\right)_p$ using these equations and comparing them with Katz chart has significant differences. Another correlation published by Bahrami et al (Bahrami et al., 2012), used for the calculation of Z factor was found to be more accurate when $T_{pr} > 1.25$. The correlation is given as follows:

$$Z = C_1 + C_2 P_{pr} + C_3 P_{pr}^2 + C_4 P_{pr}^3 + C_5 P_{pr}^5 \quad 4.54$$

Where the parameters C_1 to C_5 are described in Appendix C.

Therefore, Equation 4.54 may be applied to express $\left(\frac{\partial Z}{\partial T_{pr}}\right)_p$ as follows:

$$\begin{aligned} \left(\frac{\partial Z}{\partial T_{pr}}\right)_p &= \left(\frac{\partial C_1}{\partial T_{pr}}\right)_p + \left(\frac{\partial C_2}{\partial T_{pr}}\right)_p P_{pr} + \left(\frac{\partial C_3}{\partial T_{pr}}\right)_p P_{pr}^2 + \left(\frac{\partial C_4}{\partial T_{pr}}\right)_p P_{pr}^3 \\ &\quad + \left(\frac{\partial C_5}{\partial T_{pr}}\right)_p P_{pr}^4 \end{aligned} \quad 4.55$$

Where, the details of derivatives in Equation 4.55 are provided in Appendix C.

After calculating the term $\left(\frac{\partial Z}{\partial T_{pr}}\right)_p$ for different gas mixtures and comparing them with the PR EOS results, it has been found that Equation 4.53 needs to be adjusted with a correction factor. Therefore, after applying correction factor, Equation 4.53 is can be re-written as:

$$\left(\frac{\partial Z}{\partial T}\right)_p = \frac{C}{T_{pc}} \left(\frac{\partial Z}{\partial T_{pr}}\right)_p \quad 4.56$$

Where C is a correction factor; Figure 4- 4 provides an approach for evaluating the correction factor introduced in Equation 4.56.

For evaluation of the correction factor, Equation 4.56 may be rewritten as:

$$\left(\frac{\partial Z}{\partial T}\right)_p = \frac{C}{T_{pc}} \left(\frac{\partial Z}{\partial T_{pr}}\right)_p = \left(\frac{\partial Z}{\partial T}\right)_{p_{EOS}} \quad 4.57$$

Therefore:

$$C = \frac{T_{pc} * \left(\frac{\partial Z}{\partial T}\right)_{p_{EOS}}}{\left(\frac{\partial Z}{\partial T_{pr}}\right)_p} \quad 4.58$$

Table 4-1 Compositions of gas mixtures

γ_g Comp	(1) 0.68	(2) 0.61	(3) 0.68	(4) 0.73	(5) 0.63	(6) 0.71	(7) 0.66	(8) 0.68
C1	0.880	0.930	0.790	0.758	0.900	0.780	0.847	0.820
C2	0.040	0.028	0.157	0.151	0.050	0.072	0.053	0.054
C3	0.030	0.020	0.015	0.045	0.043	0.024	0.015	0.015
i-C4	0.030	0.004	0.005	0.034	0.003	0.035	0.020	0.023
n-C4	0.020	0.003	0.003	0.002	0.002	0.001	0.005	0.002
i-C5		0.003	0.001	0.001	0.001	0.001	0.005	0.003
n-C5		0.002	0.001	0.001	0.001			0.003
N2		0.010		0.002		0.063	0.050	0.050
H2S			0.018	0.005		0.024	0.005	0.025
CO2			0.010	0.001				0.005

Where $\left(\frac{\partial Z}{\partial T}\right)_{p_{EOS}}$ is the derivative of the Z factor against temperature changes at constant pressure predicted by PR EOS, and the term $\left(\frac{\partial Z}{\partial T_{pr}}\right)_p$ is the same predicted by using the proposed equation (Equation 4.55).

To evaluate the correction factor, a number of gas mixtures with different gas gravity and compositions are considered in this study (Table 4-1).

Table 4-2 Comparison of the value of compressibility factor (Z) of gas mixtures in Table 4-1.

		(1)	(2)	(3)	(4)	(5)	(6)	(7)	(8)
1	PR-EOS	0.7948	0.8401	0.7847	0.7482	0.8171	0.8188	0.8368	0.8529
2	Eq. 7	0.7932	0.8273	0.7932	0.7700	0.8173	0.7792	0.8027	0.7932
3	HYSYS	0.7837	0.8303	0.7909	0.7367	0.8088	0.7948	0.8177	0.8064

In order to validate the proposed model, the value of the Z factor predicted by this study for each mixture shown in Table 4-1 has been initially compared with the ones predicted by HYSYS software using PR-EOS. Where $\left(\frac{\partial Z}{\partial T}\right)_{p_{EOS}}$ is the derivative of the Z factor against temperature changes at constant pressure predicted by PR EOS, $\partial Z / \partial T_{prp}$ is the same predicted by using the proposed equation (Equation 4.55).

To evaluate the correction factor, a number of gas mixtures with different gas gravity and compositions are considered in this study (Table 4-1).

Table 4-2 provides the results; while the first and second row of this table are the Z factors predicted in this study for the conditions of known and unknown components of gas mixtures shown. The third row is the result of the Z factor calculation using HYSYS for the same mixture shown in Table 4-1.

Table 4-3 provides the evaluated result $(\partial Z / \partial T)_p$ for gas mixtures using PR EOS when the components are known, and based on the proposed model when the only known data is the gas gravity. As it can be seen, there is good agreement between

results obtained from PR EOS and the proposed model when a correction factor (as of Equation 4.53) is applied.

Table 4-3 Comparison of the value of term $(\partial Z/\partial T)_p$ of gas mixture in Table 3-1

$(\partial Z/\partial T)_p$	(1)	(2)	(3)	(4)	(5)	(6)	(7)	(8)
PR-EOS	5.083E-5	6.513E-5	5.949E-5	3.843E-5	6.120E-5	5.414E-5	5.911E-5	5.877E-5
This work	5.458E-5	5.504E-5	5.458E-5	5.549E-5	5.483E-5	5.493E-5	5.459E-5	5.458E-5

Finally, the correction factor C predicted for different gas gravities is plotted in Figure 4- 4. From Figure 4- 4, it can be seen that a linear relationship exists between C and gas gravity in the form of

$$C = m\gamma_g + D \tag{4.59}$$

Where m is the slope and D is the intercept. For the particular mixture considered in this study (as shown in Figure 4- 4), m is found to be -0.184 and $D = 0.1799$.

- ***Joule-Thomson Coefficient***

The phenomenon of the Joule-Thomson effect is the temperature change of flowing fluid, specifically gas, as a consequence of pressure drop due to the flowing of fluid through reservoir, perforations and wellbore. This temperature change may be positive, negative or zero, and depends on the fluid composition. The Joule-Thomson effect normally appears in the form of cooling effects in producing gas and warming effects in produced water. The Joule-Thomson coefficient depends on the flow rate and the size of fluid entry point from reservoir to wellbore. The situations for a gas producing well with different flow rates and permeability creating similar

temperature drops are illustrated in Figure 4- 5, in which A and C respectively show the lowest and highest flow rates.

Using the principle of thermodynamics, the phenomenon of Joule-Thomson is defined as a change in flowing fluid temperature due to a pressure drop at constant enthalpy (Al-Beaiji et al., 2005; Hasan et al., 2009; Izgec et al., 2010). Mathematically, it can be expressed as:

$$JTC = \left[\frac{\partial T}{\partial P} \right]_H \quad 4.60$$

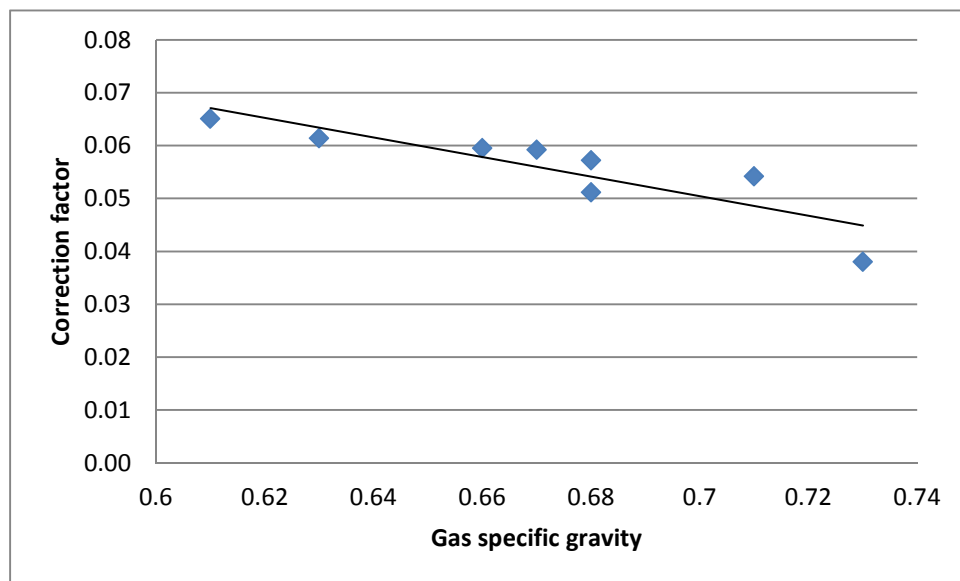


Figure 4- 4 Prediction of correction factor C as a function of specific gravity of gas mixture

In order to solve this mathematical expression, the general energy balance equation and equation of state are generally applied.

Alternatively, the following equation is used to calculate Joule-Thomson Coefficient.

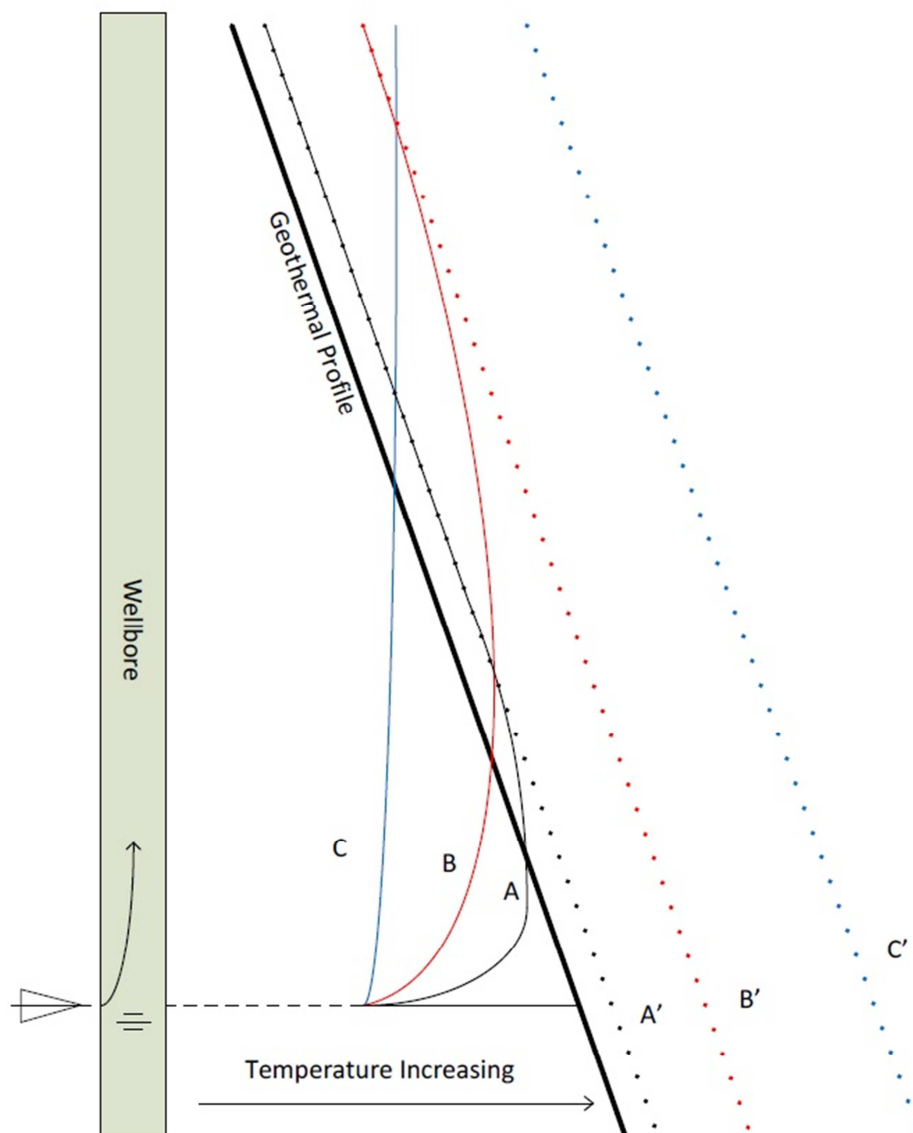


Figure 4- 5 Schematic representation of Joule-Thomson effect (modified from Smolen, 1996 (Smolen, 1996))

$$C_j = \frac{1}{C_p} \left[\frac{T}{Z\rho} \left(\frac{\partial Z}{\partial T} \right)_p \right] \quad 4.61$$

In order to solve terms Z and $\left(\frac{\partial Z}{\partial T} \right)_p$ in Equation 4.61, when the composition of the gas mixture is known, an equation of state can be used. Clearly, there are a number of equations of state such as van der Waals (vdW), Soave-Redlich-Kwong (SRK), Peng-Robinson (PR) and so on, which are applied to calculate the volumetric and phase behaviour of pure and mixed fluids. In this work, the Peng-Robinson equation of state is applied to calculate the terms $Z \left(\frac{\partial Z}{\partial T} \right)_p$ and the Joule-Thomson coefficient is used in the case of known components of the gas mixture. However, in the case of unknown details of the gas mixture, Equation 4.56 is applied throughout this work to calculate the term, $\left(\frac{\partial Z}{\partial T} \right)_p$.

4.3.6 Temperature loss at perforations

In a real situation, the perforations of a wellbore allow the fluid to move from the reservoir into the wellbore. Regarding the difference in diameter size between wellbore and perforations, any single perforation can act like an orifice while producing. Therefore, pressure drop happens as a cause of increase in the gas-stream velocity. Theoretically, a general energy balance equation (Equation 2.25) which explains the mechanical energy balance for a homogenous and steady-state single phase fluid is applied to calculate pressure loss across a perforation. For the condition of gas flowing through an orifice, there is no external work done (i.e., $W_s=0$), there is no elevation change ($\Delta z=0$), and friction loss is negligible ($F=0$). Therefore, equation 2.25 is summarized as:

$$\int_{P_1}^{P_2} v_s dP + \Delta \left(\frac{v^2}{2g_c} \right) = 0 \quad 4.62$$

Therefore:

$$v_2^2 - v_1^2 = 2g_c v_s (P_1 - P_2) \quad 4.63$$

And:

$$\left(\frac{q_2}{A_2} \right)^2 - \left(\frac{q_1}{A_1} \right)^2 = 2g_c v_s (P_1 - P_2) \quad 4.64$$

It is supposed that $q_1=q_2$, and $v_s=(ZRT/PM)$. After rearranging Equation 4.62, the following equation, which presents the calculation of mass flow rate across a restriction under ideal conditions for single phase gas flow is applied to evaluate the Joule-Thomson effect and calculation of temperature loss at any single perforation. It is supposed that the average rate of gas flowing across any perforation is calculated based on total gas flow rate per number of perforations in the wellbore. Therefore:

$$\Delta P = \frac{1152q^2 \left[\frac{d_2^4 - d_1^4}{d_2^4 d_1^4} \right]}{\pi^2 g_c \left(\frac{ZRT}{PM} \right)} \quad 4.65$$

Where, q is in ft^3/sec , and d_1 and d_2 are the diameters of the pipe and perforation, respectively.

Figure 4- 6 provides the flow diagram of the WTP simulator for calculation of temperature profile along a gas production wellbore. Also, the list of subroutines and computer codes for calculation of the wellbore temperature profile along a gas production wellbore can be seen in Appendix F.

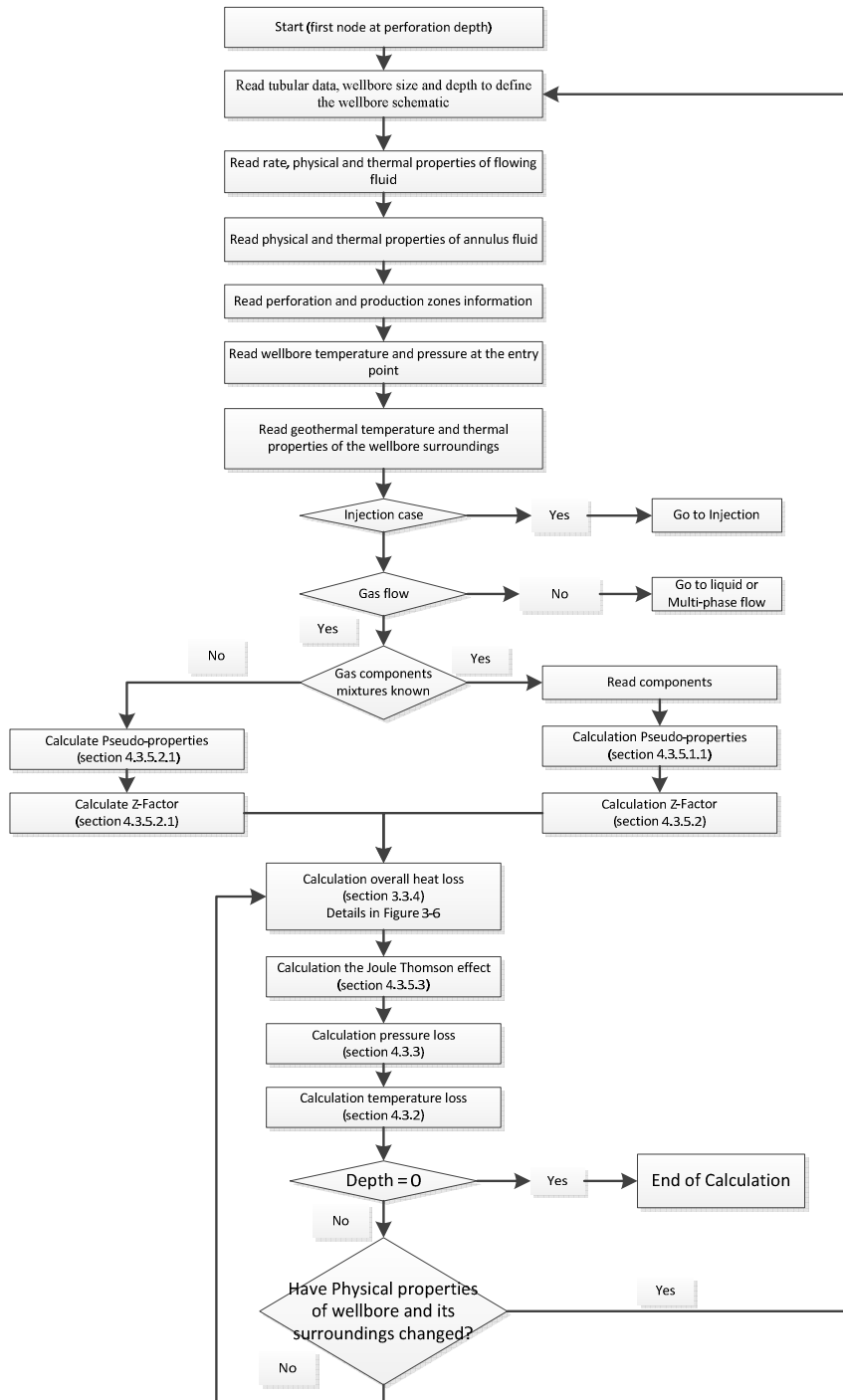


Figure 4- 6 Flow diagram of single phase gas flow of the WTP simulator.

4.4 Multiphase fluid flow

Investigation of multiphase flow – the flow of two or more phases of fluid through a pipe – is of paramount importance to oil and gas production wells as well as to some injection wells. Figure 4- 7 shows a multiphase flow stream, which is the combination of gas and liquid phases flow. Analysis of temperature profile along a multiphase flow wellbore is complex because of the complexity of the nature of phases in the fluid. In multiphase flow streams, because of the difference densities of phases, phases may separate and travel at difference speeds. These complexities make the analysis of pressure gradient along a wellbore more complicated, which can affect the analysis of temperature profile. This section will demonstrate the analysis of evaluation of temperature profile and different properties of multiphase fluids, which can affect the analysis of temperature gradient along a multiphase flowing wellbore.

Fluid enters the wellbore with a mass flow rate of Q lbm/day from reservoir. Then, it moves upward through the wellbore until it reaches the surface. It is assumed that the mass flow rate along the wellbore to the surface is constant. Also, the mass flow rate of gas and liquid and the gas liquid ratio (R_g) at the separator condition is known.

At the entry point, at which fluid enters the wellbore from the reservoir, a flash calculation is performed to evaluate the fraction and density of vapour and liquid phases in the fluid. This evaluation is required to determine the properties of the mixture as well as the type of flow regime necessary to determine the amount of pressure and temperature loss when fluid moves to the next node. In this study, the Orkiszewski method (ORKISZEWSKI, 1967) is applied to determine the flow regime along the vertical upward flowing wellbore. Orkiszewski made a comprehensive literature review, used a few sets of experimental data for testing different methods, and then selected Griffith and Wallis's and Duns and Ros's

methods (Bradley, 1987). The use of this method allows the calculation of the amount of pressure loss and density of multiphase fluid.

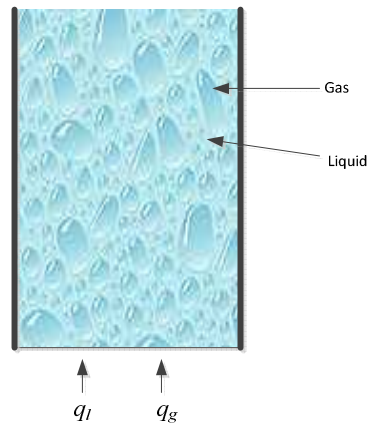


Figure 4- 7 Schematic of multiphase flow

4.4.1 Temperature profile calculation along a multiphase producing wellbore

For calculation of temperature loss between any two nodes, the conceptual idea of Equation 4.1 is applied, with the exception that the whole of the fluid is not liquid. The fraction of liquid has been evaluated through the procedure of flash calculation.

The calculated temperature and pressure at the next node will be applied to repeat the flash calculation procedure and calculate other properties for determination of pressure and temperature for the next node along the wellbore. This procedure is repeated until the flow reaches the surface. The flow diagram of this calculation can be seen in Figure 4- 8. In the following, all steps of the calculations in Figure 4-1 are discussed in detail.

4.4.2 Multiphase flow definitions

Distribution of each phase in the pipe determines the behaviour of multiphase fluid. Each phase has individual properties, which are simply defined for a single phase. However, the multiphase fluid behaves as a mixture of phase behaviours, in which their properties such as density, holdup, volume fraction, superficial velocities, flow rate and so on are more complex. In this section, some definitions of multi-phase fluid which are applied throughout this study are explained.

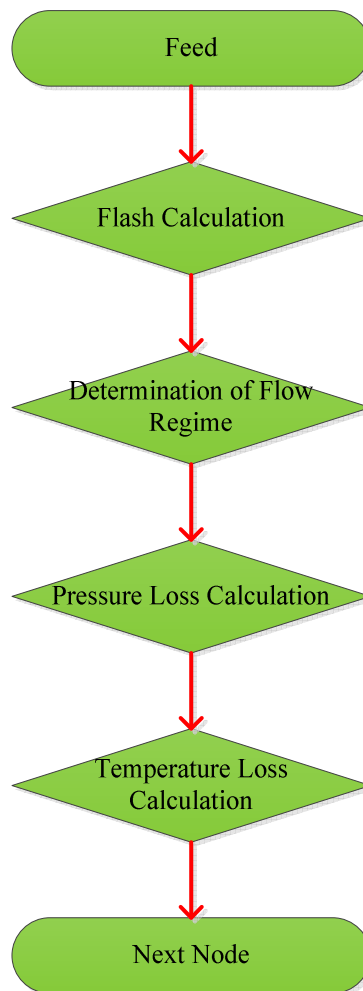


Figure 4- 8 Flow diagram of temperature loss calculation between two nodes.

Clearly, the density of each phase is different, and in the upward flow, the lighter phase moves up faster. Therefore, the phenomenon of holdup comes into play, which is defined as a fraction of the pipe occupied with each of phases.

For a two-phase flow, liquid and gas holdup, H (holdup) is mathematically written as follows:

$$H_l = \frac{V_l}{V} \quad 4.66$$

$$H_g = 1 - H_l \quad 4.67$$

Where, V_l and V are the volume of liquid phase and total volume of phases respectively.

Another vital property of multiphase fluid is the input fraction of each phase, λ , which is also known as a no-slip holdup. For a mixture of gas and liquid phase flow, this fraction is defined as follows:

$$\lambda_l = \frac{q_l}{q_l + q_g} \quad 4.68$$

$$\lambda_g = 1 - \lambda_l \quad 4.69$$

Where, q_l and q_g are the volumetric flow rate of liquid and gas phases respectively. Regarding the density and velocity difference of phases, slip velocity, u_s , is defined as the velocity difference between lighter and denser phases and is another way of measuring the holdup phenomenon.

$$u_s = u_g - u_l \quad 4.70$$

Where, u_g and u_l demonstrate the velocity of gas and liquid phases respectively.

In order to determine u_g and u_l , the superficial velocity of phases is defined, which shows the velocity of each phase when it occupies the total cross section of the pipe alone:

$$u_{sg} = \frac{q_g}{A} \quad 4.71$$

$$u_{sl} = \frac{q_l}{A} \quad 4.72$$

Therefore, it can be written that:

$$u_g = \frac{u_{sg}}{H_g} \quad 4.73$$

$$u_l = \frac{u_{sl}}{H_l} \quad 4.74$$

As a result, slip velocity may be written as follows:

$$u_s = \frac{1}{A} \left(\frac{q_g}{1 - H_l} - \frac{q_l}{H_l} \right) \quad 4.75$$

The density of a multiphase fluid behaves as a mixture of all phase densities. Considering the slip or no-slip velocity between phases, the following equations are written:

$$\rho_s = \rho_l H_l + \rho_g H_g \quad 4.76$$

$$\rho_n = \rho_l \lambda_l + \rho_g \lambda_g \quad 4.77$$

Where, ρ_s and ρ_n stand for multiphase fluid density in slippage and no-slippage conditions, respectively.

When the liquid phase is a mixture of oil and water, the ρ_l is written as follows:

$$\rho_l = \rho_o f_o + \rho_w f_w \quad 4.78$$

Where:

$$f_o = \frac{q_o}{q_o + q_w} \quad 4.79$$

And:

$$f_w = 1 - f_o \quad 4.80$$

Where, f_o and f_l show the mole fraction of oil and water in the fluid respectively.

4.4.3 Multiphase flow regimes

Flow regimes or flow patterns are applied to describe the phase distribution along a wellbore qualitatively. In the literature (Beggs, 2003; Bradley, 1987; Economides et al., 1993; Mukherjee and Brill, 1985; Vilaseca et al., 2010), there are four generally agreed different flow configurations for gas-liquid vertical upward flow, namely bubble, slug, churn (slug-mist transition) and annular (mist) flow. Figure 4- 9 shows these flow configurations, and they are briefly described as follows:

1. Bubble flow: A small amount of gas bubbles is dispersed into a continuous liquid flow. The amount of gas is small and it has small effect on the pressure gradient. However, the dispersed gas can affect the density of the fluid.
2. Slug flow: The rate of gas is higher than bubble flow, and both gas and liquid phases have a significant effect on the pressure gradient of the fluid. The gas

bubbles are large, and between the bubbles are slugs of liquid that contain dispersed gas.

3. Churn flow: This type of flow regime has larger bubbles of gas and slugs of liquid disappear between gas bubbles. In some cases, the liquid phase is discontinuous and the gas phase becomes continuous. The pressure losses in this type of flow happen mostly as a result of the gas phase and partly as a result of the liquid phases.
4. Mist flow: At higher rate of gas flow, the gas phase becomes continuous, containing droplets of liquid, and only the pipe wall is wetted by a film of liquid.

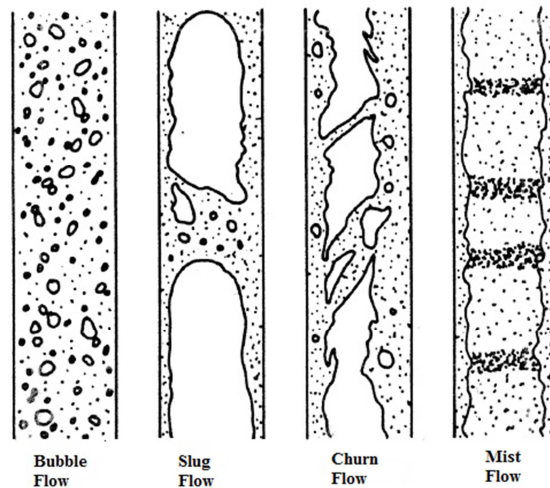


Figure 4- 9 Flow regimes in upward vertical gas-liquid flow.

Duns and Ros (Jr. and Ros, 1963) provide a map for the determination of the flow regimes of gas-liquid vertical upward flow, and they divide the various flow configurations into three main regions. They determine that bubble flow is covered by the first region, slug flow is covered by the second region, and the third region covers mist flow. Also, a transition region is defined between region two and three. However, Orkiszewski (ORKISZEWSKI, 1967), through a review of the literature, found that the Griffith and Wallis method is accurate for boundary determination of

a bubble-slug flow, and the method of Duns and Ros is accurate for boundary determination of other flow regimes. These boundaries are listed as follows.

1. Bubble flow: $q_g/q_t < L_b$
2. Slug flow: $q_g/q_t > L_b, v_{gd} < L_b$
3. Transition flow: $L_m > v_{gd} > L_s$
4. Mist flow: $v_{gd} > L_m$

The above dimensionless variables for determination of flow regimes are fully explained in Appendix D.

4.4.4 Multiphase fluid flow pressure gradient

As with single phase flow, the mechanical energy balance equation is generally applied for the calculation of pressure loss along a multiphase fluid flow. However, because the fluid flow properties may significantly change along the flow path, the calculation of pressure loss for any particular part of the pipe should be considered. Therefore, the pressure gradient for each section of pipe may change, even though all physical properties of the pipe remain unchanged.

The mechanical energy balance equation may be written as follows:

$$\frac{dp}{dz} = \left(\frac{dp}{dz}\right)_{PE} + \left(\frac{dp}{dz}\right)_{KE} + \left(\frac{dp}{dz}\right)_F \quad 4.81$$

Where, the potential pressure gradient for most of the multiphase flow can be written as follows:

$$\left(\frac{dp}{dz}\right)_{PE} = \frac{g}{g_c} \bar{\rho} \sin\theta \quad 4.82$$

And Equation 4.76 and 4.77 may be applied for calculation of multiphase fluid density($\bar{\rho}$).

The term of kinetic pressure gradient or acceleration term in Equation 4.81 is ignored by many investigators (Beggs, 2003) except for large flow rates (Bradley, 1987). Duns and Ros (Jr. and Ros, 1963) believe this term is significant in a mist flow regime. This is the equation for calculation of kinetic pressure gradient in multiphase flow when $v_g \gg v_l$ (Bradley, 1987).

$$\left(\frac{dp}{dz}\right)_{KE} = \frac{\rho v}{g_c} dv = -\frac{W_t Q_g}{g_c A^2 P} dp \quad 4.83$$

Where:

A = Pipe area, sq ft

W_t = Total mass flow rate, lbm/esc

Q_g = gas volumetric flow rate, cu ft/sec.

The term of frictional pressure gradient in Equation 4.81 is the most complicated term in the calculation of multiphase flow pressure gradients. This term becomes the following:

$$\left(\frac{dp}{dz}\right)_f = \frac{f \rho v^2}{2 g_c d} = \tau_f \quad 4.84$$

Many correlations have been investigated to calculate the frictional pressure gradient term. However, in this study, the Orkiszewski method which covers all flow regimes (bubble, slug, transition and mist flow regimes) in vertical flow pipes has been selected. This method has been selected, because of its accuracy in simulation of

multi-phase flow (Adeyemi, 2009; Lawson and Brill, 1974), easy computer coding and covering all type of flow regimes. Lawson and Brill tested this method against 148 wells and compared with the other methods such as Poettmann and Carpenter (Poettman and Carpenter, 1952), Baxendell and Thomas (BAXENDELL and THOMAS, 1961), Fancher and Brown (FANCHER JR. and BROWN, 1963), Ros (ROS, 1961), Duns and Ros (Ros, 1963), and Hagedorn and Brown (Hagedorn and Brown, 1965). Finally, they reported that the error of 0.8% for estimation of pressure loss using Orkiszewski method.

Orkiszweski defines the flow regime and then applies Griffith's procedure for bubble flow, a modified form of the Griffith and Wallies method for slug flow, a modified form of the Griffith method combined with the Duns and Ros method for transition flow, and the Duns and Ros method for mist flow regimes. A comprehensive description of the Orkiszweski method for calculation of τ_f can be found in Appendix D.

4.4.5 Flash calculation

Multi-phase fluid is composed as a contribution of a number of phases along the path of flow. As the temperature and pressure of fluid through the path of flow change, the contribution of phases may vary. The flash calculation procedure at constant pressure and temperature is frequently applied to determine the phase of the mixture of known total components. This concept has guided this research to the application of the flash calculation along the wellbore to determine the contribution of each phase along the wellbore, allowing the prediction of the value of fluid temperature at any point along the wellbore.

At the entry point of fluid from reservoir to the wellbore, the fluid (F) has the mole fraction of components z_i , $i = 1, \dots, n_c$ (i.e., $\sum_{i=1}^{n_c} z_i = 1$), at reservoir pressure and

temperature, which is a compounded of liquid phase (L) and vapour phase (V). It is assumed that any unit volume of the production string is occupied with a liquid mole fraction of x_i , $i = 1, \dots, n_c$ (i.e., $\sum_{i=1}^{n_c} x_i = 1$), and a vapour mole fraction of y_i , $i = 1, \dots, n_c$ (i.e., $\sum_{i=1}^{n_c} y_i = 1$). Figure 4- 10 provides the schematic of the flash process for wellbore fluid.

At any point of the wellbore, according to the law of mass conservation, the material balance for components can be written as follows.

$$Fz_i = x_iL + y_iV \quad 4.85$$

Also,

$$\sum_{i=1}^{n_c} x_i = 1 \quad 4.86$$

$$\sum_{i=1}^{n_c} y_i = 1 \quad 4.87$$

Equalising the fugacity of components in each phase is a traditional method for solving flash (Ahmed, 1946; Bünz et al., 1991; Firoozabadi, 1999; Nelson, 1987; Ohanomah and Thompson, 1984; Sofyan et al., 2003). Therefore, based on the equilibrium condition, the equality of chemical potentials or components can be written as follows.

$$f_i^L(T, P, x) = f_i^V(T, P, y), \quad i = 1, \dots, n_c \quad 4.88$$

The flash starts with assuming the number of phases, and then estimates the vaporisation equilibrium ratio (K_i). Wilson's approximation (Wilson, 1964) is used for the initial assumption of equilibrium ratios at the given pressure and temperature.

$$K_i = \frac{P_{ci}}{P} \exp \left[5.37(1 - \omega_i) \left(1 - \frac{T_{ci}}{T} \right) \right], \quad i = 1, \dots, n_c \quad 4.89$$

Generally, EOSs, a set of non-linear equations, are used for computation of the mathematical formulation of phase equilibrium. This set of equations can be solved by the successive iterative technique and Newton's method; both methods are believed to be the best approach to solving such a problem (Firoozabadi, 1999). Convergence is reached when changes in equilibrium ratios and mole fractions are below the specified tolerance.

Equations 4.85 through 4.87 of chapter 3 are the conceptual equations for the procedure of flash calculation. A comprehensive description of flash calculation for multi-component hydrocarbon mixtures is provided in Appendix E and can be found in the literature (Ahmed, 1946; Firoozabadi, 1999).

Figure 4- 11 provides the flow diagram of wellbore temperature profile calculation for a multi-phase flow production wellbore. Also, the list of subroutines and computer codes for calculation of the wellbore temperature profile along a multi-phase fluid production wellbore can be seen in Appendix F.

Moreover, the Figure 4- 12 provides the flow diagram of wellbore temperature profile for an injection cases. Also, the list of subroutines and computer codes for calculation of the wellbore temperature profile along an injection wellbore can be seen in Appendix F.

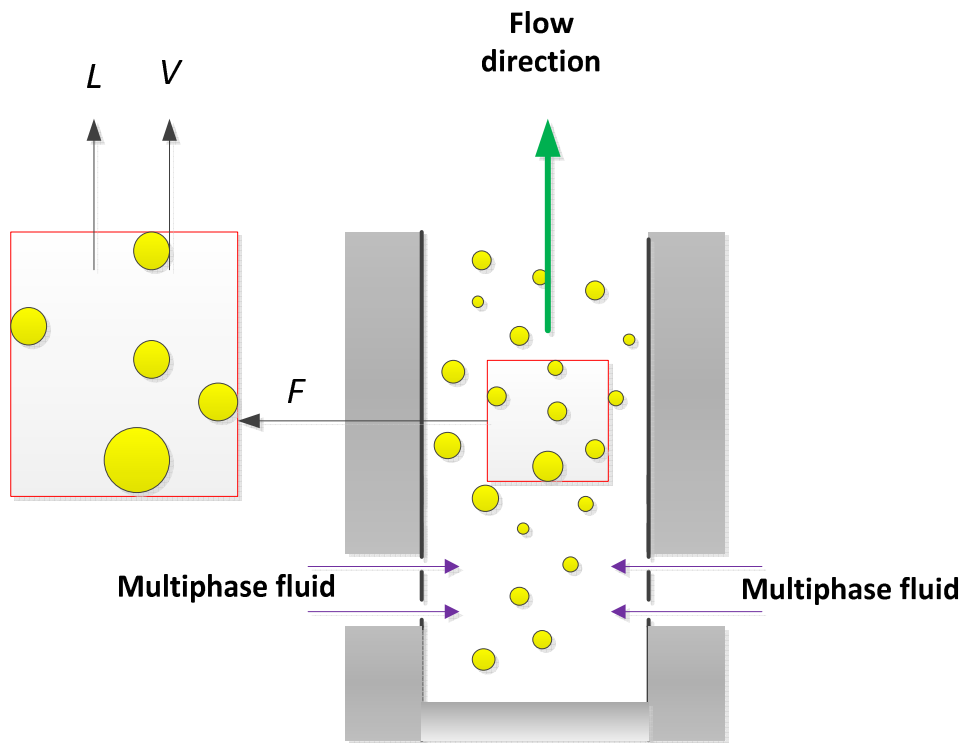


Figure 4- 10 Schematic of the flash of the wellbore fluid

4.5 Summary

A mathematical model along with the tubular information, thermal properties of surrounding area and thermodynamics properties are the fundamental aspects of the WTP simulator for prediction of wellbore temperature profile. The details of mathematical model that are employed in the developed WTP simulator to predict and analyse the wellbore flowing temperature profile for the injection and/or production wells are elaborated for single phase liquid, single phase gas and multiphase flow regimes.

The simulator is developed based on the prediction of wellbore heat transmission and generation at any single point of well depth. Therefore, the summation of heat change due to the heat transfer between flowing fluid and the surrounding area and the frictional heat change are used to calculate the temperature of fluid at any depth along the wellbore. Clearly, the frictional heat changes depend on the type of fluid flows through the wellbore.

In case of gas production, as the components of the gas stream in the problem may be known or unknown, the WTP simulator deals with both conditions. When gas components are known, the PR-EOS is applied for prediction of gas mixture properties. Also, the Hall-Yarborough method is applied for calculation of pseudo-critical properties of gas mixtures when gas components are unknown. A correction factor (C) has also been developed for estimation of term $\left(\frac{\partial Z}{\partial T}\right)_p$ in cases of unknown components. This term is applied for prediction of the Joule Thomson effect at the entry point of produced gas into wellbore.

Finally, Figure 4- 3, Figure 4- 6, Figure 4- 11 and Figure 4- 12 provide the flow charts and algorithm of wellbore temperature profile for single phase liquid production, single phase gas production, multi-phase fluid production and liquid injection scenarios.

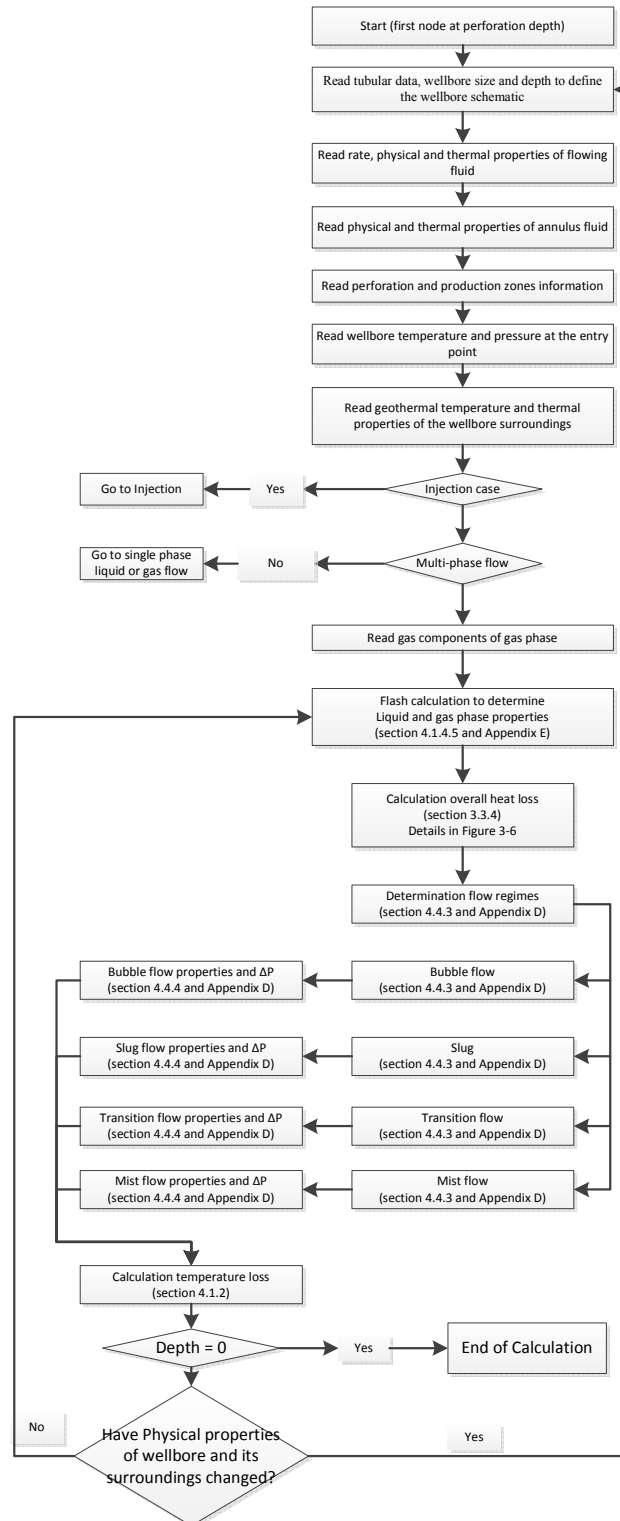


Figure 4- 11 Flow diagram of multi-phase flow of the WTP simulator.

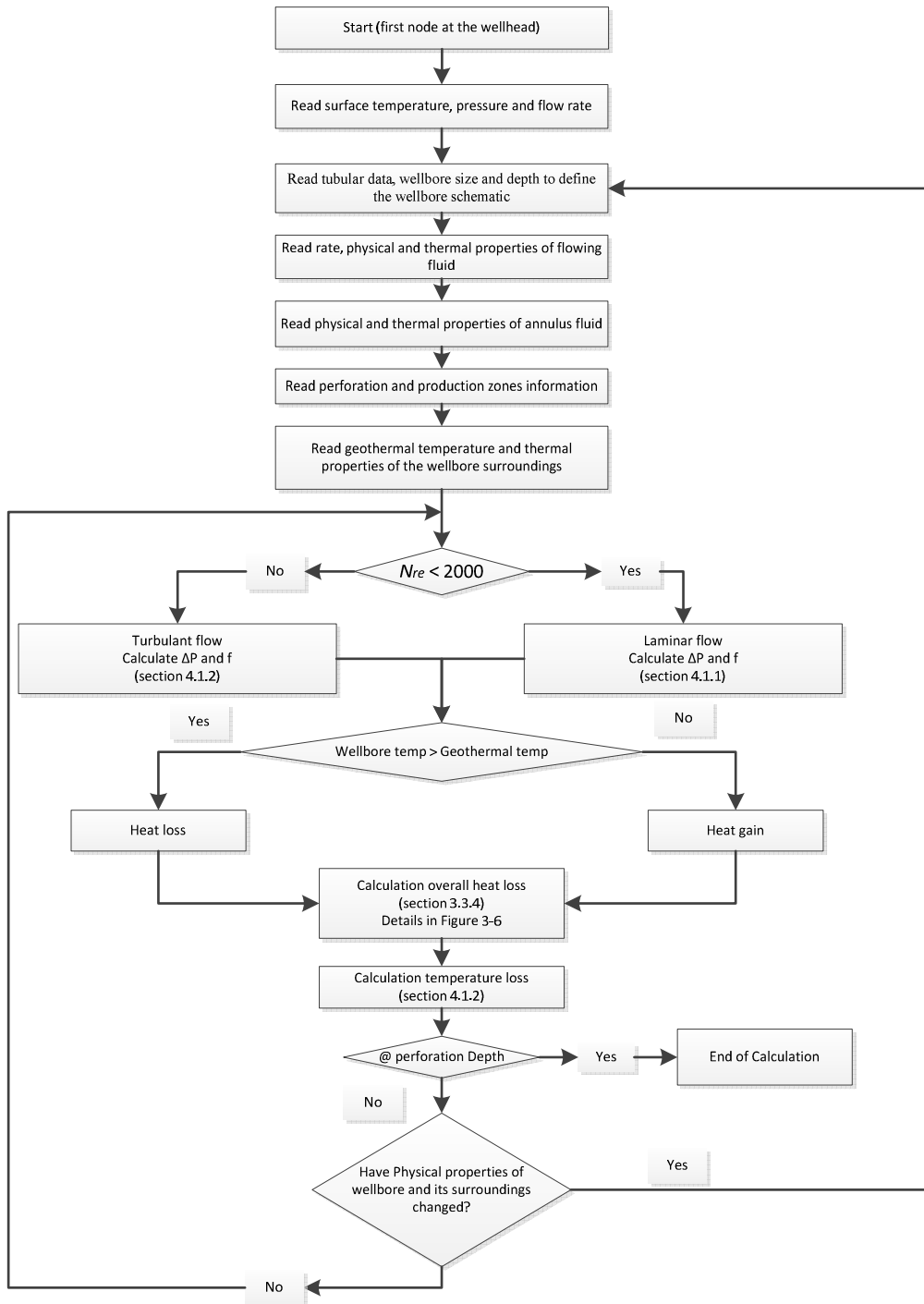


Figure 4- 12 Flow diagram of injection section of the WTP simulator.

5

Numerical Simulation, Case Studies and Sensitivity Analysis

5.1 Introduction

As hydrocarbon or injected fluids flow through a wellbore temperature loss or gain happens due to the temperature differentials with the surroundings and friction of the flowing fluid. Correct estimation of wellbore temperature may optimise the design of production scenarios, the solving of wellbore anomalies and the design of surface facilities. The WTP Simulator has been developed to model heat flow and temperature profile along production and injection wellbores. In chapters two and three, the details of the modelling have been discussed. Briefly, it can be said that the developed model has been designed with an entry section and four main sections. The first section is called the entry section which is designed for defining the wellbore; the thermal properties of the environment surrounded the wellbore; the geothermal gradient; and the type of flowing fluid. The four main sections vary from each other according to the fluid type and direction of which fluid flow through the wellbore. The sections are called: single phase liquid production; single phase gas production; multi-phase production; and fluid injection. Each of these sections also includes the validation of the results of this work. This chapter, however, explains how the developed WTP Simulator covers all types of fluid and flow regimes that can flow through the desired wellbore, as well as how the developed model is applied for injection cases.

Eleven suitable case studies have been considered, and several simulation runs have been performed for different cases of production and injection scenarios in order to validate the developed simulator. Three case studies refer to single phase liquid production, four apply to single phase gas production, and two double case studies are considered for multi-phase production and injection sections. In addition, sensitivities that can affect the profile of wellbore temperature are studied within each case study. The results of this work are compared with the actual field data as well as the data predicted by some other works. Overall, the chapter reveals the broad production fields and difficulties that can be analysed through the WTP Simulator.

5.2 Single Phase Liquid Production

In order to validate this part of the WTP Simulator, three different case studies have been considered. Necessary data used for case studies #1 to case studies #3 are presented in Table 5-1. In each case the results evaluated from this study are compared with the actual data. For each case study, the sensitivities of flow rate and parameters related with wellbore (e.g. tubing, annular and openhole diameter) influence the wellbore temperature profile are also investigated.

The first case study has been considered from Hasan and Kabir (Hasan and Kabir, 2002) for the validation of this work. The study considered an oil producing well which was simulated by Hasan and Kabir. The sensitivity studies are conducted to investigate the influence of production rate and tubing size on the wellbore temperature profile and the wellhead temperature.

Table 5-1 Data calculation for case studies #1 to #3

Data	Description	Case study #1			Case study #2			Case study #3		
		Size (in)	Weight (ppf)	Depth (ft)	Size (in)	Weight (ppf)	Depth (m)	Size (in)	Weight (ppf)	Depth (ft)
Well Schematic	Outer Casing	13 5/8	54.4	480	13 5/8	54.4	110	13 5/8	54.4	340
	Inner Casing	9 5/8	43.5	8500	9 5/8	43.5	2000	9 5/8	43.5	3550
	Liner	7	26	10000	7	26	5000	7	26	5100
	Tubing	3 1/2	9.2	9900	4 1/2	12.75	4900	2 7/8	6.5	5900
	Total Depth (ft)	10000			5000			5019		
Wellhead		Temperature (F)	Pressure (psig)	Rate (bbl/d)	Temperature (F)	Pressure (psig)	Rate (bbl/d)	Temperature (F)	Pressure (psig)	Rate (bbl/d)
	Wellhead	220	7000	2000	90		3000			2080
Wellbore		Produced fluid properties			Produced fluid properties			Produced fluid properties		
	Type	Liquid <input checked="" type="checkbox"/>	Gas <input type="checkbox"/>	Mixture <input type="checkbox"/>	Liquid <input checked="" type="checkbox"/>	Gas <input type="checkbox"/>	Mixture <input type="checkbox"/>	Liquid <input checked="" type="checkbox"/>	Gas <input type="checkbox"/>	Mixture <input type="checkbox"/>
	%Oil	100%			67%			100%		
	%Gas									
	%Water				33%					
	Specific Gravity (API)	28			40			40		
Annulus		Annulus fluid properties			Annulus fluid properties			Annulus fluid properties		
	Density (lb/cu.ft)	0.0388			0.0388			0.04		
	Heat Capacity (Btu/ lb.F)	0.245			0.245			0.25		
	Viscosity (cp)	0.069			0.069			0.07		
	Thermal resistivity (Btu/hr.ft.F)	0.2			0.2			0.2		
Formation		Thermal resistivity (Btu/hr.ft.F)			Thermal resistivity (Btu/hr.ft.F)			Thermal resistivity (Btu/hr.ft.F)		
	Ground	2.5			1			3.33		
	Cement	0.38			0.38			0.625		
Geothermal		Geothermal Temperature			Geothermal Temperature			Geothermal Temperature		
	Surface (F)	70			70			70		
	Reservoir (F)									
	Gradient (F/ft)	0.015			0.01			0.0137		

The second case study considered is from Ouyang and Belanger (Ouyang and Belanger, 2006), which is a multi-zone oil producing well. From The aim of considering this case study are to: compare the WTP Simulator results with the actual field data; and show the potential application of this simulator for a complex production system. Also, the sensitivities of wellbore temperature profile with the size of production string and the rate of producing fluid are considered in this case study.

Thomson Well field data from Wang's study [4] is considered as the third case study, with the aim of comparing the results obtained from WTP Simulator study with actual field data. The Thomson well was drilled for producing oil from a depth of 5019 ft, and was completed with 2 7/8" production tubing. The sensitivity of wellbore temperature profile with the API gravity of producing fluid is also investigated in this case study.

5.2.1 Case study #1 (Example from Hasan and Kabir):

An oil well production data considered in this case study are extracted from Hasan and Kabir's paper (Hasan and Kabir, 2002; Hasan et al., 1997). An oil production rate of 2000 bbl/d with a temperature at reservoir and surface conditions of 220 and 138 degrees Fahrenheit respectively was considered in this case study. The wellhead temperature at the oil production rates of 1000 and 2000 stb/d provided by Hasan et al. (Hasan et al., 1997) are shown in Figure 5-1. Table 5-1 provides wellbore and reservoir data for this case study, and other required data can be seen in Table 5-2.

Figure 5-2 compares the wellbore temperature profile predicted by the WTP Simulator and the data extracted from Hasan and Kabir's work. As it can be seen, the predicted temperature profiles are a good match with the accuracy of surface

temperature calculated using the developed simulator, which is closer to the reported surface temperature. The surface temperature reported by Hasan et al. (Hasan et al., 1997) is 138°F, and the surface temperature calculated by the WTP Simulator is 138.224°F, which shows the accuracy of this work.

Table 5-2 Production data for case study #1

Case study #:	1	
<u>Well and Fluid Parameter</u>	<u>Value</u>	<u>Unit</u>
Well depth	10000	ft
Reservoir Pressure	7000	psia
Reservoir Temperature	220	°F
Formation Permeability	500	md
Formation Thickness	100	ft
Oil Gravity	28	API
Gas Gravity	0.75	
Formation Heat Capacity	0.625	Btu/lbm. °F
Formation Density	165	lbm/ft ³

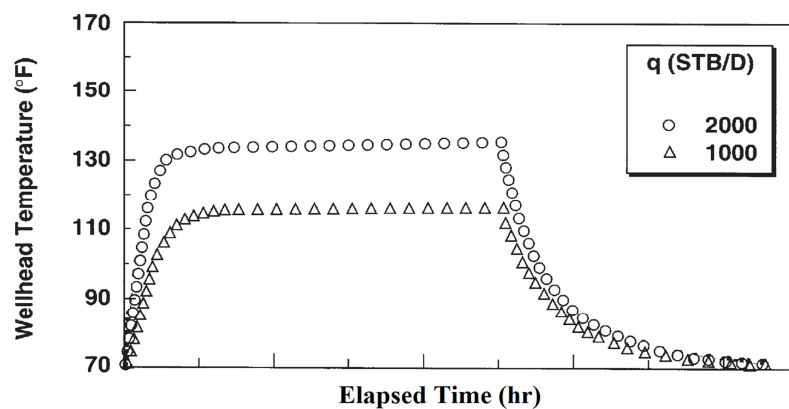


Figure 5-1 Wellhead temperature at different rates (Hasan et al., 1997) (case study #1)

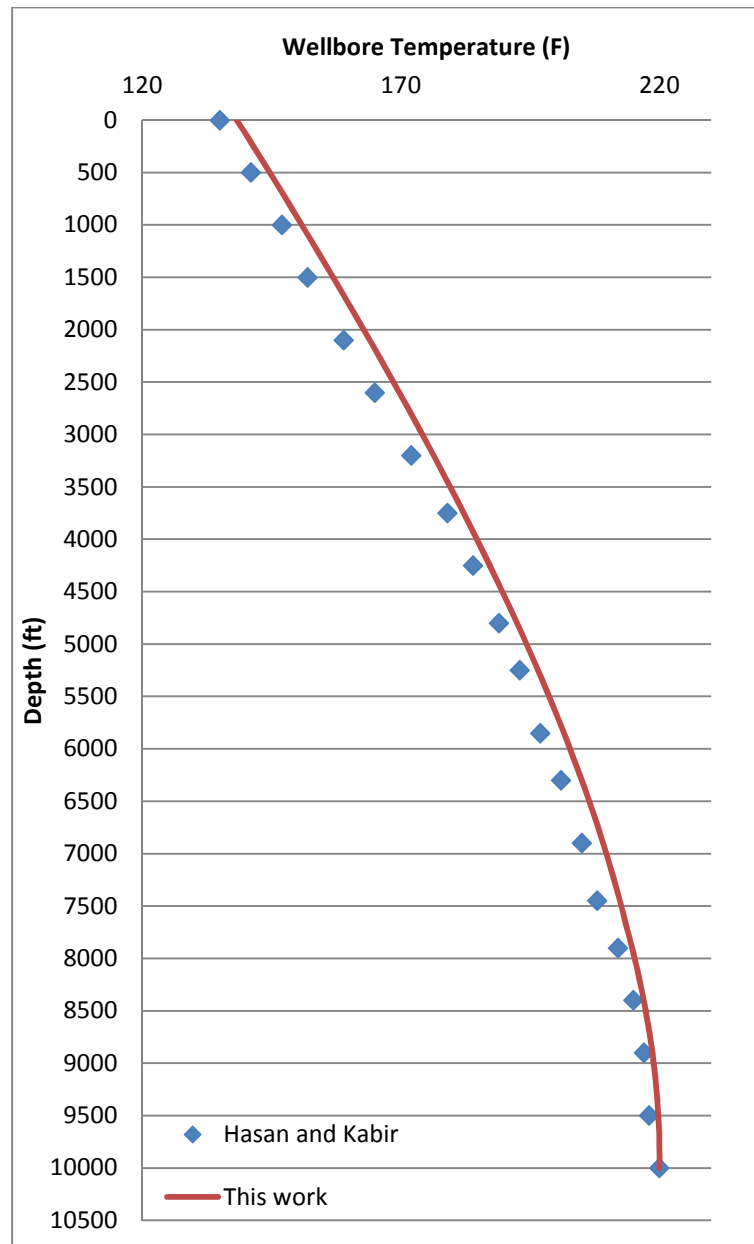


Figure 5-2 Comparison of wellbore temperature profiles (case study #1)

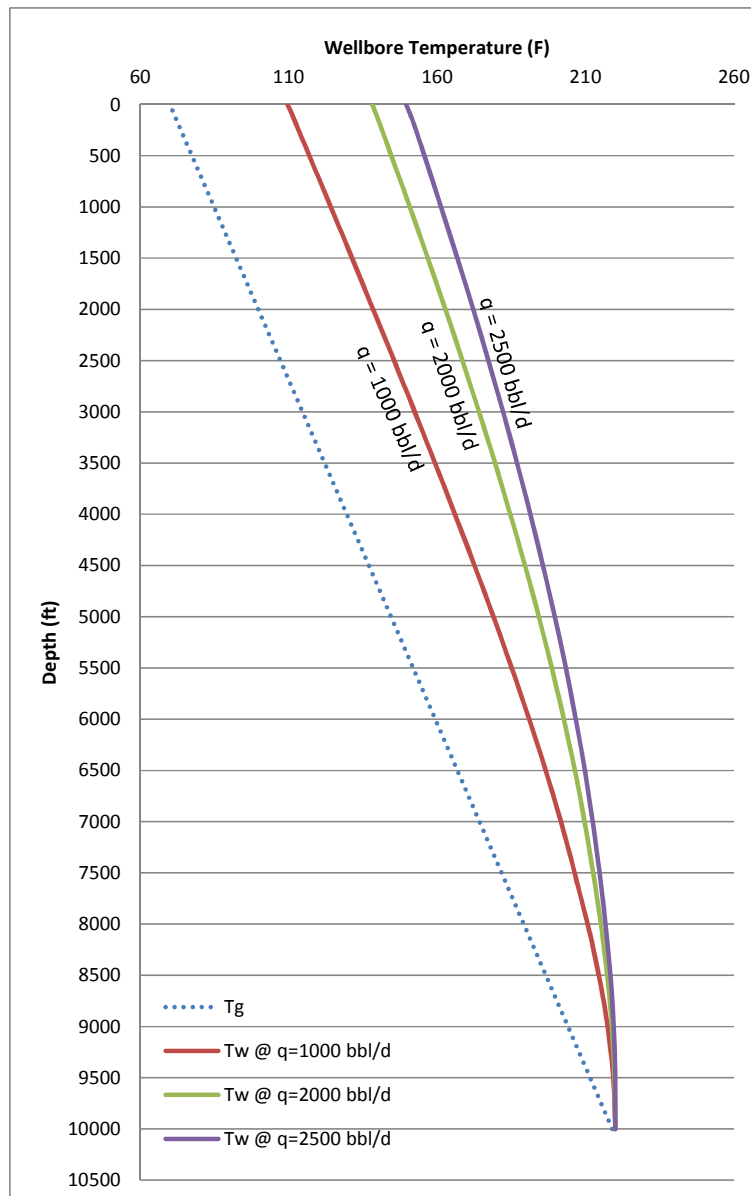


Figure 5-3 Temperature profiles for case study #1 at different production rates

In order to investigate the influence of production rate, and production tubing size on the wellbore temperature profile, sensitivity study is also performed.

Simulation results run for the rates of 1000, 2000 and 2500 bbls/d are plotted in Figure 5-3 for a given tubing size of 3.5 inches. As can be seen in Figure 5-3 that the increase in production rate increases surface temperature which is mainly due to the fact that the increase in rate increases the enthalpy of produced fluid; and the friction between the fluid and conduit. This higher production rate results higher temperature at the surface. From Figure 5-3, it can be seen that the surface temperature is 109.654, 138.224 and 149.598°F for conditions of 1000, 2000 and 2500 bbls/d oil production rate respectively.

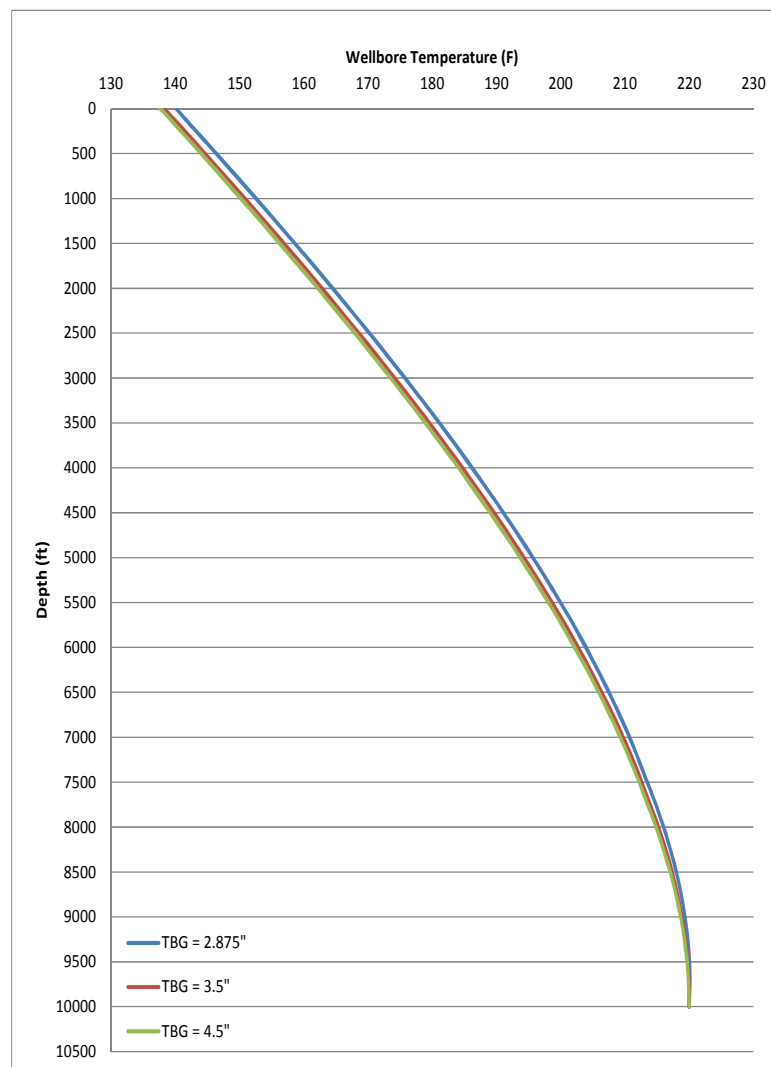


Figure 5-4 Temperature profiles for case study #1 with different production tubing sizes

Simulation results, run for different tubing size for a given production rate of 2000 bbls/d, are presented in Figure 5-4. It can be seen in Figure 5-4 that the wellbore flowing temperature decreases as the tubing diameter increases resulting a lower temperature at the surface. This is because the larger tubing diameter means the pipe has a larger surface area for transferring heat from the fluid towards the surroundings in production scenarios; while in injection scenarios, it may conversely cause temperature gain. Figure 5-4 shows that the surface temperatures for production tubing sizes of 2.875", 3.5" and 4.5" are 140.159, 138.224 and 137.529°F respectively.

5.2.2 Case study #2 (Oil Producing Well)

The second case study has been based on Ouyang and Belanger's work (Ouyang and Belanger, 2006), which considered mixture of oil and water production from a multi-zone production wellbore. The well has three perforated production zones; all zones contributed in production, with the production contribution rates for intervals of 2000 to 2600 ft MD, 2900 to 3500 ft MD and 4400 to 4900 ft MD reported as 600 STB/D, 1200 STB/D and 200 STB/D respectively. The study also reported a production rate of 1000 STB/D water from the interval of 4400 to 4900 ft MD. The total production of 3000 STB/D liquid had a reported wellhead temperature of 90°F. The wellbore, production and reservoir data are provided in Table 5-1.

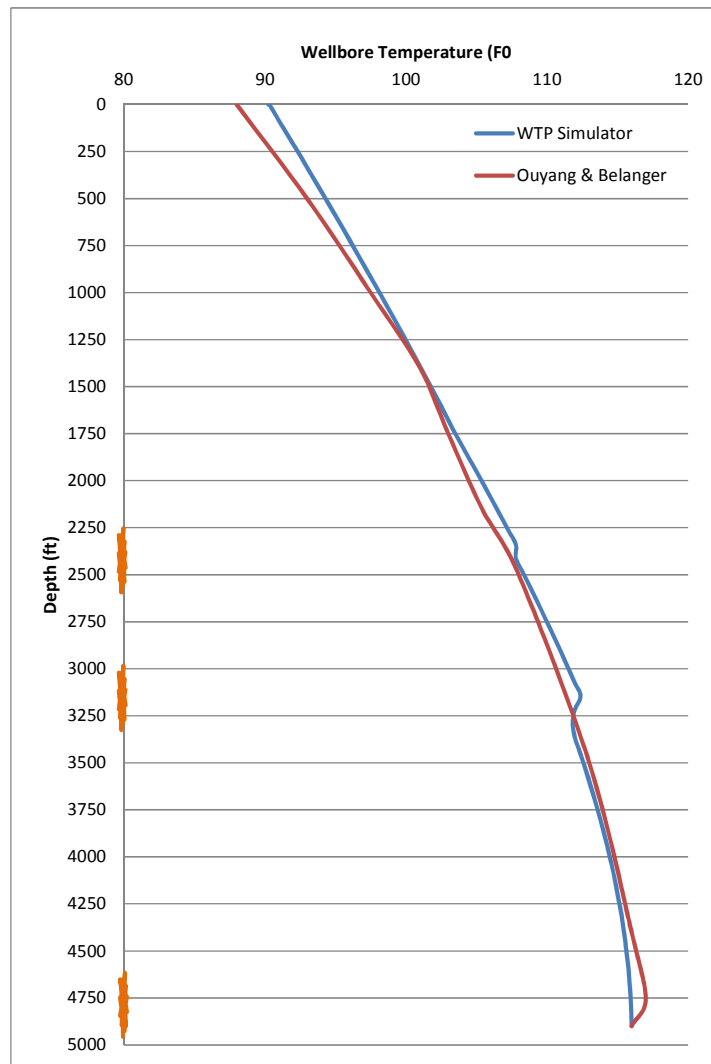


Figure 5-5 Comparison of wellbore temperature profiles (case study #2)

The comparison between the results obtained from the WTP Simulator and presented in Ouyang and Belanger’s work are shown in Figure 5-5. In Figure 5-5, the red curve is the flowing wellbore temperature predicted by Ouyang and Belanger whereas the blue curve is that predicted by the WTP Simulator. A reasonably close agreement is noticed. As shown in Figure 5-5 the wellhead temperature predicted by the WTP Simulator (90.245°F) is very close to the wellhead temperature (90°F) reported in Ouyang and Belanger’s work.

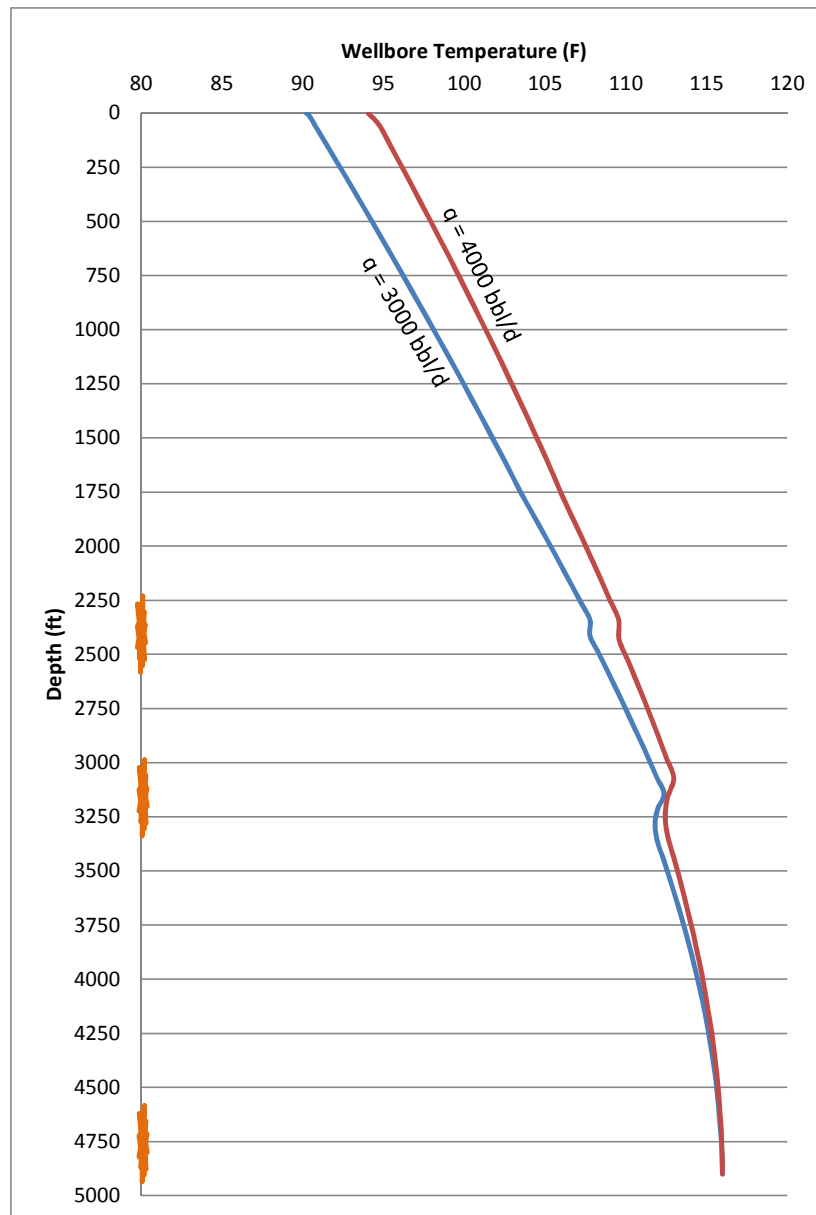


Figure 5-6 Temperature profiles for case study #2 at different production rates for tubing size of 4.5 inches

Figure 5-6 and Figure 5-7 present the sensitivity results of flowing wellbore temperature profiles for different the production rate and the wellbore tubing size. For this case study, the flow rates considered are 3000 and 4000 STB/D (Figure 5-6) of the total liquid with tubing sizes of 3.5” and 4.5” (Figure 5-7). As can be seen, in

the case of higher production rates through the same tubing size, the wellbore temperature and consequently the wellhead temperature is higher (Figure 5-6). The same scenario also happens in the case of a smaller tubing diameter with the same production rate (Figure 5-7). Figure 5-7 also shows that when the total liquid production rate is 3000 STB/D, the wellhead temperature for 3.5" and 4.5" tubing diameter is 91.682 and 90.245°F respectively.

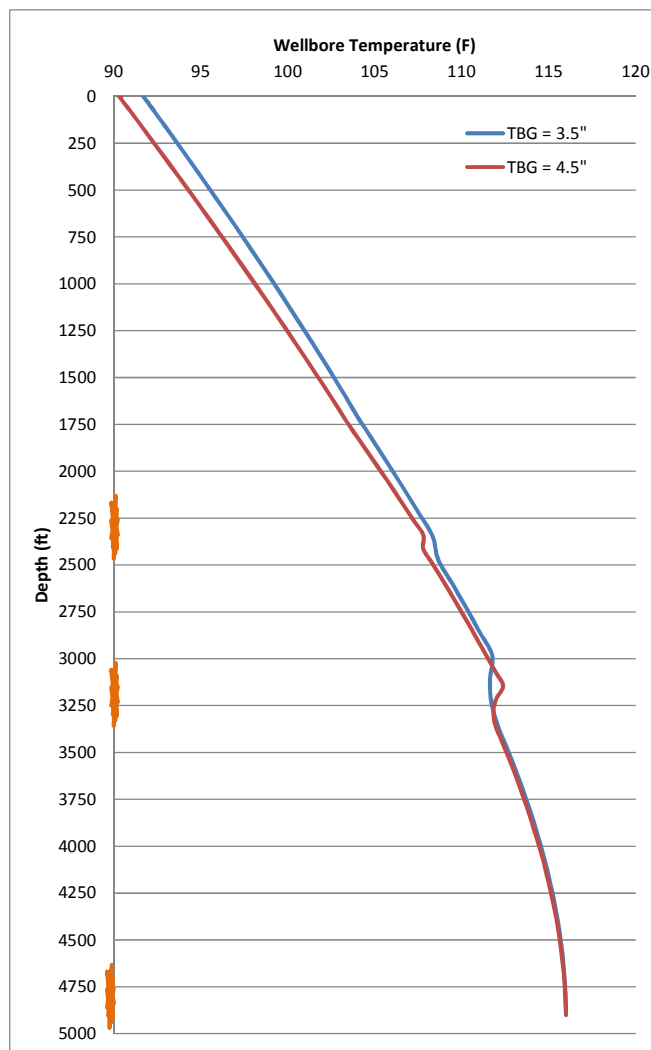


Figure 5-7 Temperature profiles for case study #2 with different production tubing sizes for a production rate of 3000 STB/d.

5.2.3 Case study #3 (Thompson Well Data)

Thomson Well field data from Wang’s study (Wang et al., 2008) are considered as an another example for validating the results of this research. The well depth is 5019 ft and the production rate is 2080 STB/D. Fluid properties, geothermal information and well completion data are provided in Table 5-1.

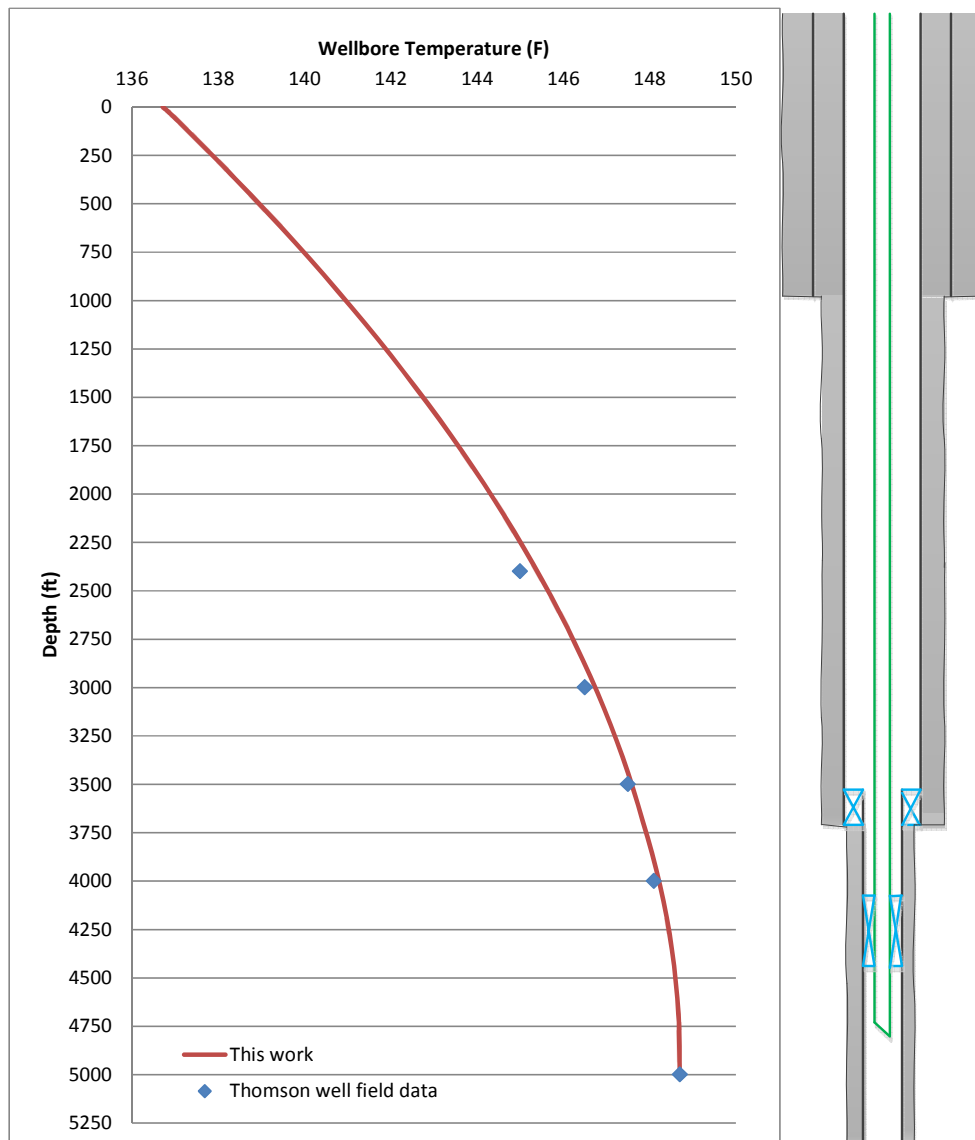


Figure 5-8 Comparison of wellbore temperature profiles

Figure 5-8 compares the field and the predicted temperature profile, and a good agreement between the result of the WTP Simulator and the field data can be seen. Figure 5-9 explores the wellbore temperature profile and the effect of API gravity on the profile of the wellbore temperature for case study #3. As can be seen, the calculated surface temperature for 10.3, 25 and 40 °API is 136.15, 135.61 and 134.525°F respectively. Therefore, produced oil with higher degrees of API has a lower surface temperature. It can be explained that hydrocarbon with higher degrees of API has lower viscosity, and consequently has less friction with the wall of tubing, which is the cause for heat generation along a fluid flowing wellbore.

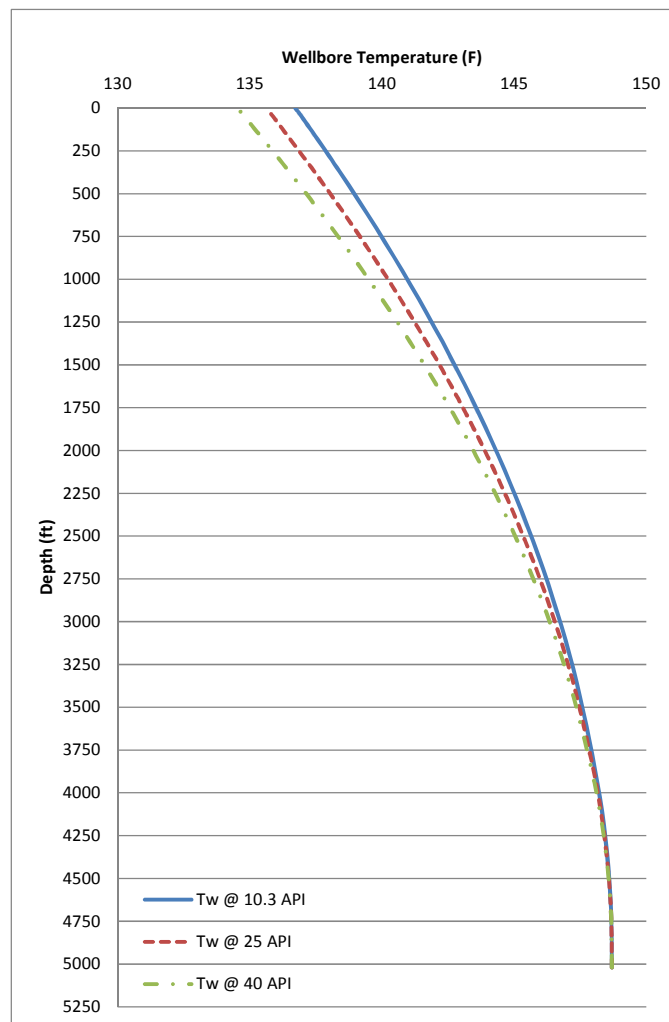


Figure 5-9 Temperature profiles for case study #3 and API sensitivity analysis

5.3 Single Phase Gas Production

To validate the simulation in cases of single phase gas flow through a wellbore using the WTP Simulator, four different case studies are considered (case studies #4 through 7). In case study #4, the Joule-Thomson (JT) effect has been studied that may happen at the entry point of gas from reservoir into the wellbore. The aim of this section is to demonstrate the accuracy of the result of this study and its ability to calculate the Joule-Thomson effect for a gas production well. Evaluation of the JT effect may be important because inaccurate calculation of temperature at the bottom hole may affect the whole wellbore temperature profile calculation. Also, the evaluation of JT may be relevant for prediction of the gas flow rate from the reservoir into the wellbore.

Buttress-1 well, a CO₂ production well of the CO₂CRC Otway project, has been considered from Lincoln et al.'s work (Paterson et al., 2010) as case study #5. This case study is important, as the data is from an actual well. Also, the large density change due to pressure and temperature changes along the wellbore may make it different from natural gas wells. Therefore, the aim of this case study is to investigate the ability of this Simulator to be applied to different type of gas production.

Case studies #6 and #7 have been considered from Huebsch et al.'s (Huebsch et al., 2008) and Louis et al.'s (Lesem et al., 1957) work respectively. Both wells are constructed for the purpose of natural gas production. In case study #6, the field data has been gathered from the slick-line DTS (Distributed Temperature System) run through a well in EnCana's multi-zone gas wells in the Deep Basin of Western Canada, which gives an opportunity to compare the results of this study with the results of DTS records. In case study #7, the predicted temperature profile is compared with the actual field data. Both of these case studies are important, as they

provide actual field data from conventional and intelligent well monitoring tools for validation of this study.

Fluid properties, geothermal information and well completion data are tabulated in Table 5-3. In each case the results drawn from this study have been compared with the actual data and discussed.

Table 5-3 Data calculation for case studies #4 to #7

Data	Description	Case study #4			Case study #5			Case study #6			Case study #7		
Well Schematic		Size (in)	Weight (ppf)	Depth (ft)	Size (in)	Weight (ppf)	Depth (ft)	Size (in)	Weight (ppf)	Depth (ft)	Size (in)	Weight (ppf)	Depth (ft)
	Outter Casing	13 3/8	54.5	240	13 3/8	54.5		13 3/8	54.5	385	13 3/8	54.5	270
	Inner Casing	9 5/8	43.5	4400	9 5/8	43.5		9 5/8	43.5	8800	9 5/8	43.5	4000
	Liner	7	26	5200	7	26		7	26	10500	7	26	6830
	Tubing	5 1/2	17	5000	3 1/2	9.2	5200	4 1/2	12.75	10400	2 7/8	4.7	6750
	Total Depth (ft)	5200			5300			10500			6830		
Wellhead		Temperature (F)	Pressure (psig)	Rate (MMscf/d)	Temperature (F)	Pressure (psig)	Rate (MMscf/d)	Temperature (F)	Pressure (psig)	Rate (MMscf/d)	Temperature (F)	Pressure (psig)	Rate (MMscf/d)
	Wellhead	220	7000	2000							107		4.08
Wellbore		Produced fluid properties			Produced fluid properties			Produced fluid properties			Produced fluid properties		
	Type	Liquid <input type="checkbox"/>	Gas <input checked="" type="checkbox"/>	Mixture <input type="checkbox"/>	Liquid <input type="checkbox"/>	Gas <input checked="" type="checkbox"/>	Mixture <input type="checkbox"/>	Liquid <input type="checkbox"/>	Gas <input checked="" type="checkbox"/>	Mixture <input type="checkbox"/>	Liquid <input type="checkbox"/>	Gas <input checked="" type="checkbox"/>	Mixture <input type="checkbox"/>
	%Oil												
	%Gas	100%			100%			100%			100%		
	%Water												
Gas Gravity	0.68			1.31			0.75			0.6127			
Annulus		Annulus fluid properties			Annulus fluid properties			Annulus fluid properties			Annulus fluid properties		
	Density (lb/cu.ft)	0.35			0.25			0.25			0.25		
	Heat Capacity (Btu/ lb.F)	0.1			0.04			0.04			0.04		
	Viscosity (cp)	0.17			0.07			0.07			0.07		
	Thermal resistivity (Btu/hr.ft.F)	0.35			0.03			0.03			0.03		
Formation		Thermal resistivity (Btu/hr.ft.F)			Thermal resistivity (Btu/hr.ft.F)			Thermal resistivity (Btu/hr.ft.F)			Thermal resistivity (Btu/hr.ft.F)		
	Ground	1			4.3			2.5			2.5		
	Cement	0.2			1.28			0.38			0.38		
Geothermal		Geothermal Temperature			Geothermal Temperature			Geothermal Temperature			Geothermal Temperature		
	Surface (F)	70			40			50			75		
	Reservoir (F)	119						207			170		
Gradient (F/ft)				0.015									

5.3.1 Case study #4(Joule-Thomson Effect)

The Joule-Thomson (JT) effect is temperature changes in flowing fluid, in particular, gas, causing pressure drop due to fluid flowing through a reservoir, perforations and wellbore (Edmister and Lee, 1984; Perry et al., 1997; Smolen, 1996). Accurate evaluation of Joule-Thomson effects is paramount for predicting the flowing temperature profile in a gas producing well. The WTP Simulator is able to predict the JT effect, and in order to validate the WTP Simulator for evaluation of JT effects, various computations have been performed drawing on the gas mixtures presented in Table 3.1.

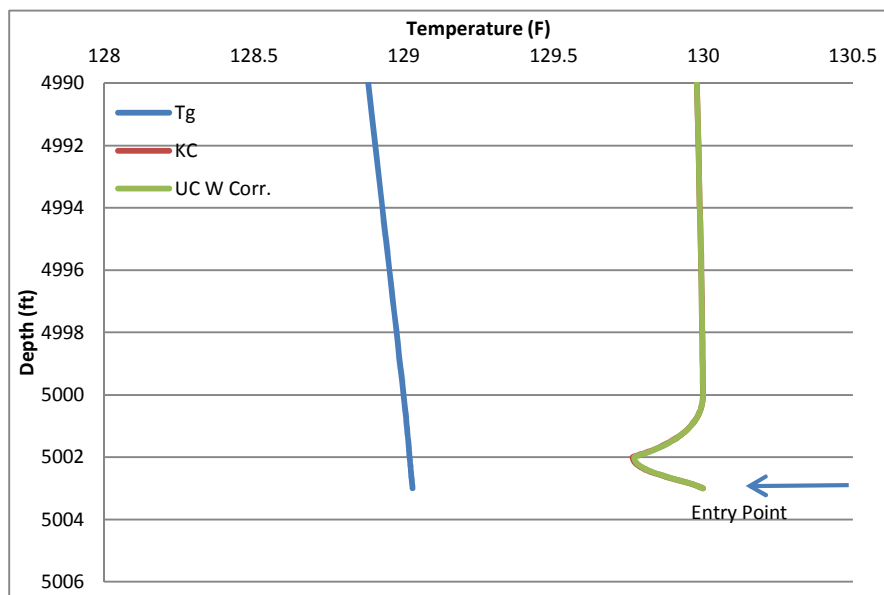


Figure 5-10 Calculation of Joule Thomson effect for gas mixture 1 (case study #4)

The JT effect and predicted temperature profiles of gas producing wells at the entry point for gas mixtures, as shown in Table 3.1, are plotted in Figure 5-10 through Figure 5-17. In these figures the blue curve shows the geothermal temperature. The red and green curve provide the JT effect as well as wellbore temperature profiles at the entry point of gas from the reservoir into the wellbore in cases of known and

unknown components respectively. For calculation of the red curve, where the components of the gas mixture are known, PR EOS has been applied. The method proposed in section 3.2.2.5.5 of chapter 3, including a correction factor, is applied for calculation of the green curve, when the gas gravity of the mixtures is the only given data. In chapter 3 section 3.2.2.5.5 it is also explained that for validity of the results this work, the calculated compressibility factor (Z) for gas mixtures in Table 3.1 have been compared with the ones calculated through HYSYS, and there is a good match between them. Consequently, as can be seen through Figure 5-10 to Figure 5-17, there is a good agreement between the red and green curves. Therefore, when the specific gravity of a gas mixture is known and Equation 3.56 is applied, the term $(\partial Z/\partial T)_p$ can be predicted with reasonable accuracy, and is applicable for prediction of Joule-Thomson effects in gas producing wells.

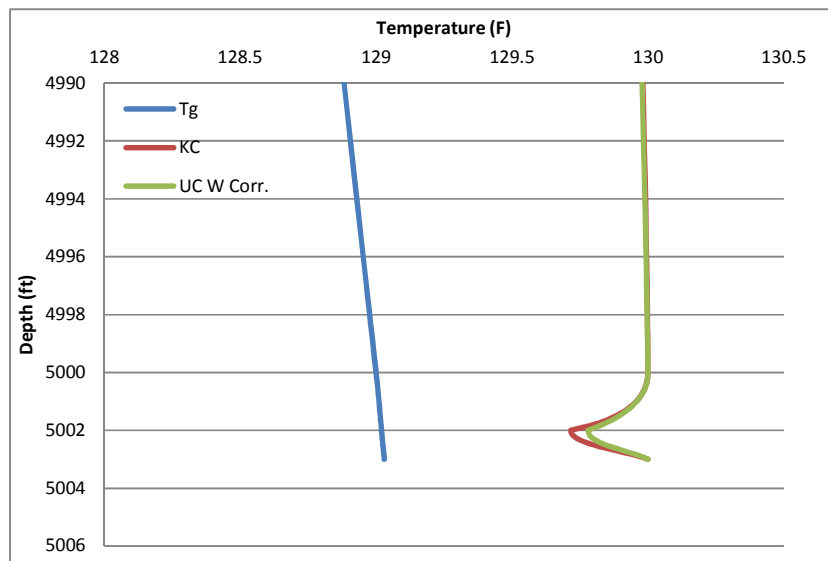


Figure 5-11 Calculation of Joule-Thomson effect for gas mixture 2 (case study #4)

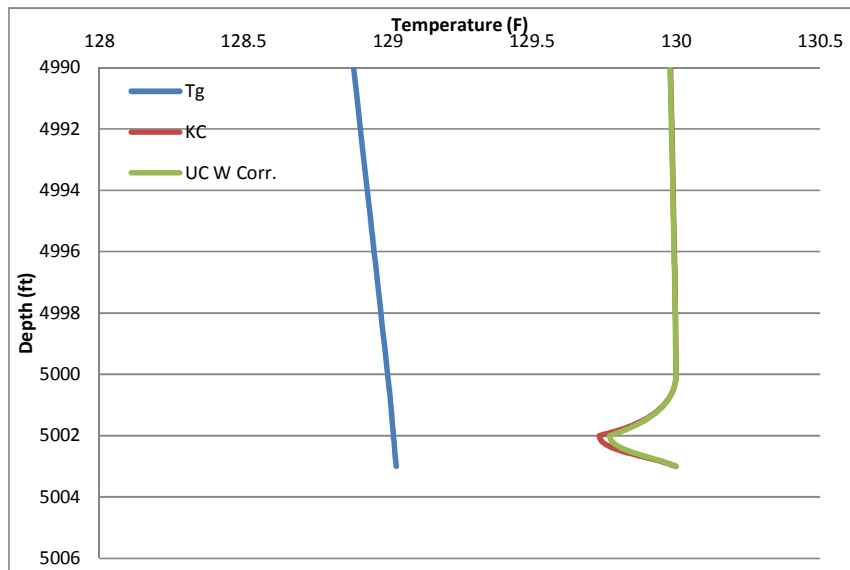


Figure 5-12 Calculation of Joule-Thomson effect for gas mixture 3 (case study #4)

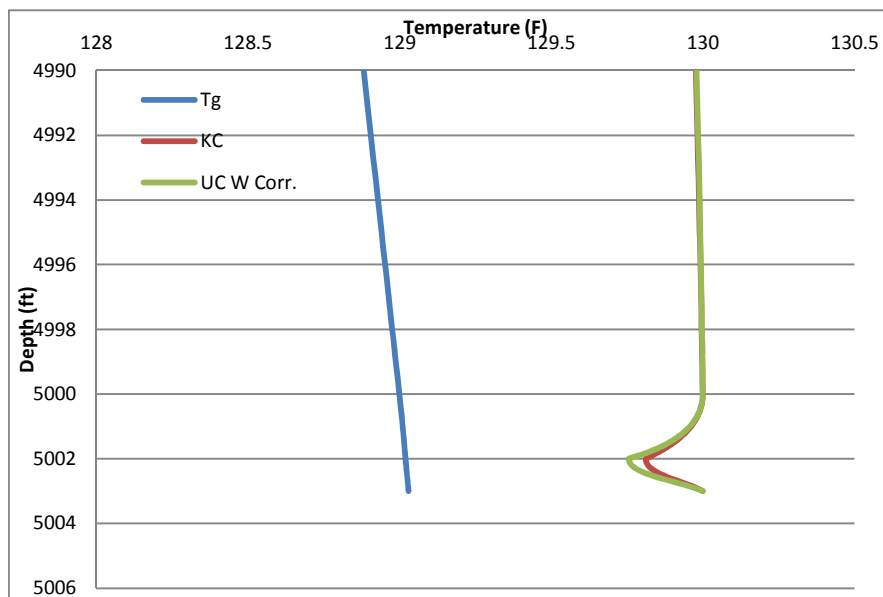


Figure 5-13 Calculation of Joule-Thomson effect for gas mixture 4 (case study #4)

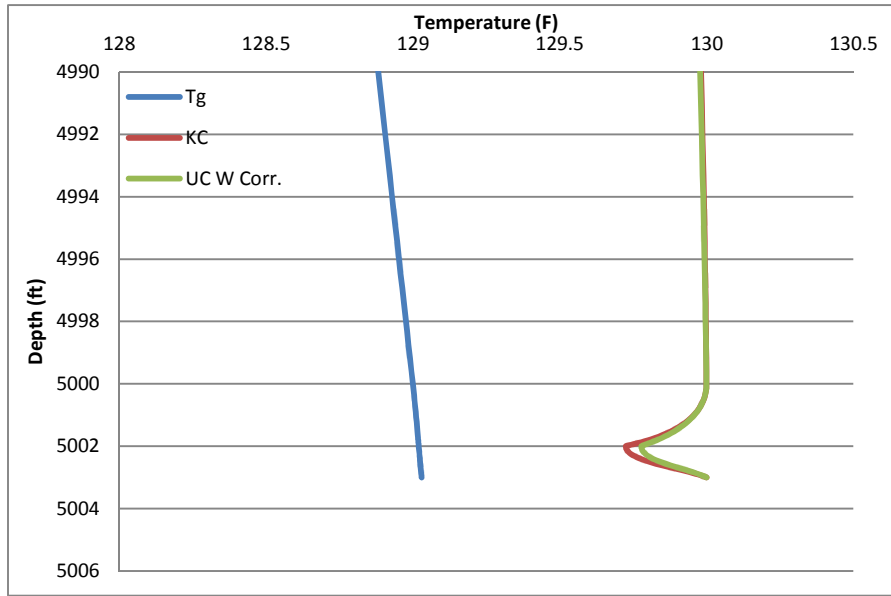


Figure 5-14 Calculation of Joule-Thomson effect for gas mixture 5 (case study #4)

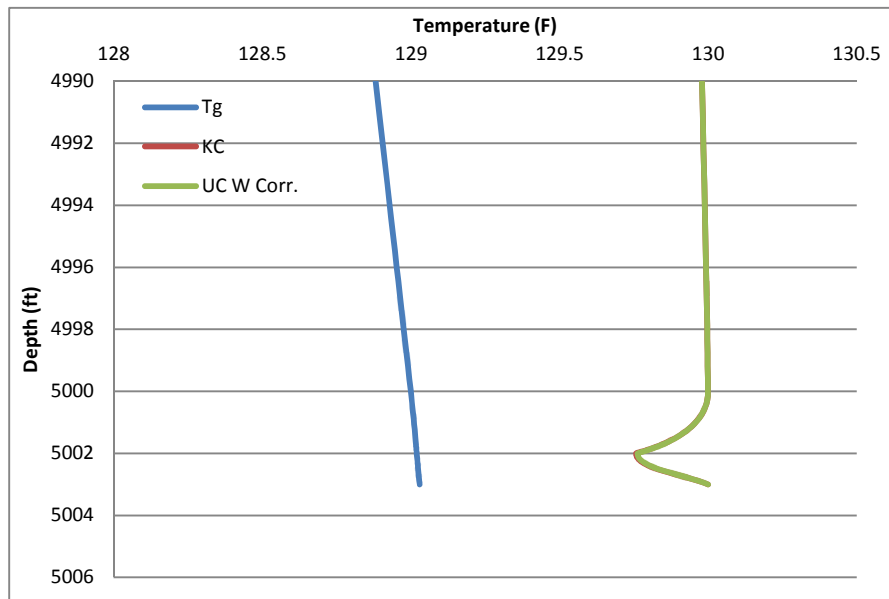


Figure 5-15 Calculation of Joule-Thomson effect for gas mixture 6 (case study #4)

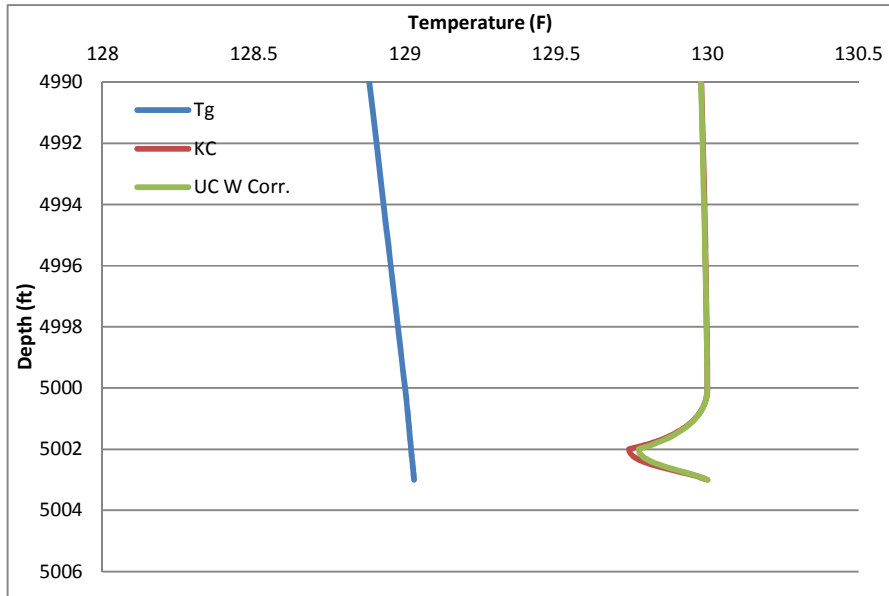


Figure 5-16 Calculation of Joule-Thomson effect for gas mixture 7 (case study #4)

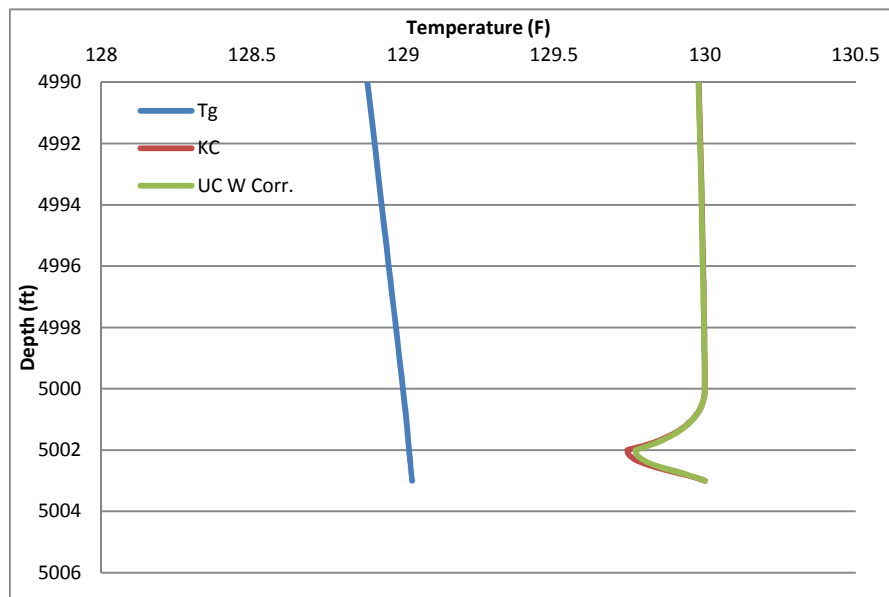


Figure 5-17 Calculation of Joule-Thomson effect for gas mixture 8 (case study #4)

The aim of this study is the theoretical prediction of the flowing temperature profile along a gas producing well from entry point to the surface, where it is necessary to

evaluate the Joule-Thomson effect in gas producing wells. The predicted temperature profile can be used to understand production behaviour, and identify the causes of many problems associated with gas production which are caused by the anomalous behaviour of predicted temperature profile with temperature logs or survey data. In this perspective, a typical gas producing wellbore is considered to be surrounded by different layers of casings, tubing, annulus occupied with a fluid, cement sheaths and ground, as illustrated in Figure 5-18. In such a situation, it is necessary to take into account the physical and thermal properties of all layers around a wellbore for the prediction of temperature profiles. This information is necessary to predict temperature loss at any point along a wellbore, and to evaluate the Joule-Thomson coefficient. Knowing all these parameters, it is possible to predict a temperature profile along a gas producing well. Tarom (2012) provides comprehensive study and detailed mathematical models.

Figure 5-19 shows a predicted temperature profile along the wellbore under consideration (shown in Figure 5-18) for the mixture (1) as provided in Table 3.1. This profile is calculated for a gas producing well with a gas production rate of 40 MMSCFD from a reservoir at the depth of 5000 ft TVD with pressure and temperature of 2500 psig and 130°F, respectively. The other wellbore, casing, and tubing data are shown in Figure 5-18, and the necessary geothermal, physical and fluid properties are provided in Table 5-3. It is interesting to see that the JT effects predominantly affect the behaviour of temperature changes in the case of a gas producing well at the entry point, i.e. near the perforation (shown as inset in Figure 5-19). The effect is found to be very significant, especially for a high producing gas well.

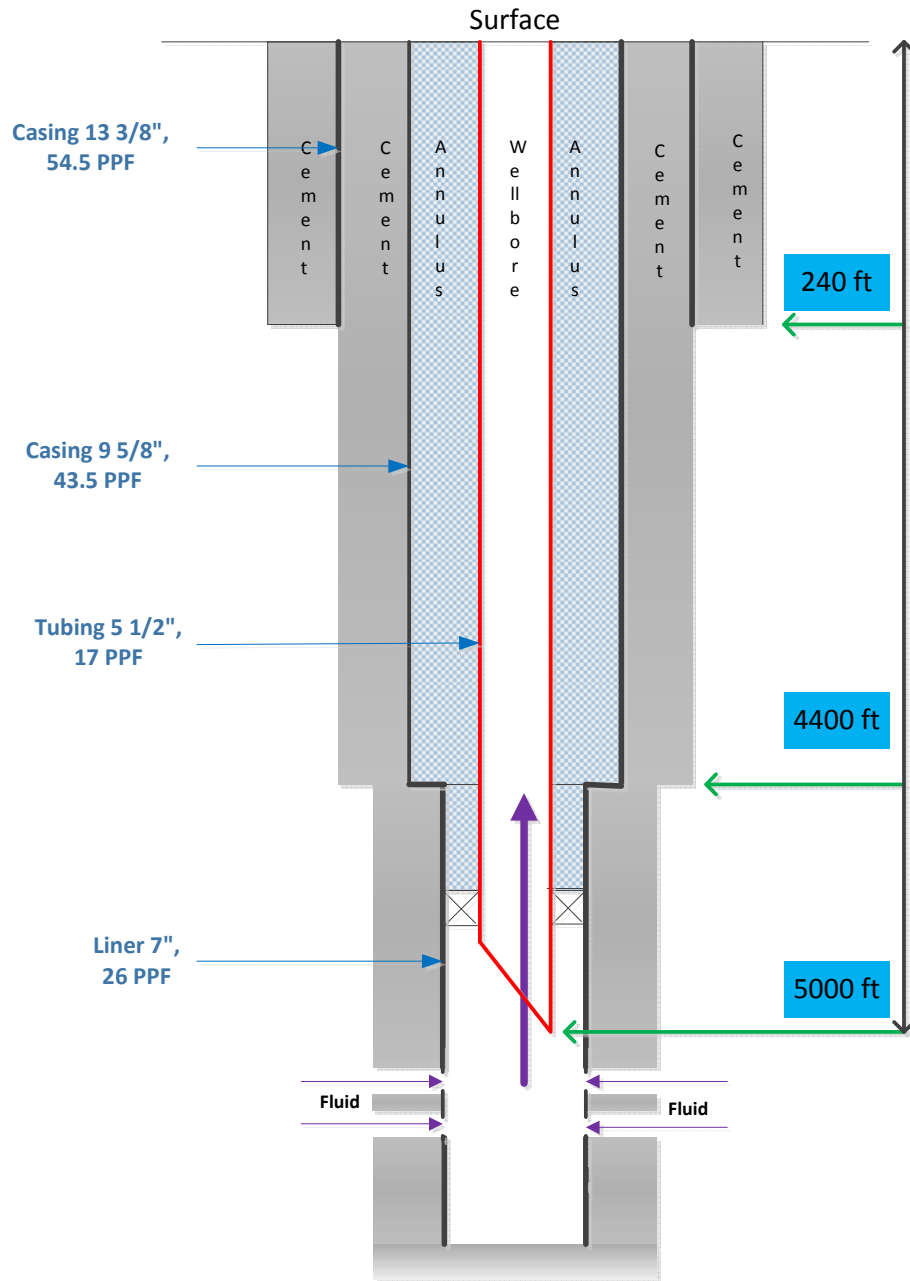


Figure 5-18 Typical well schematic (Case study #4)

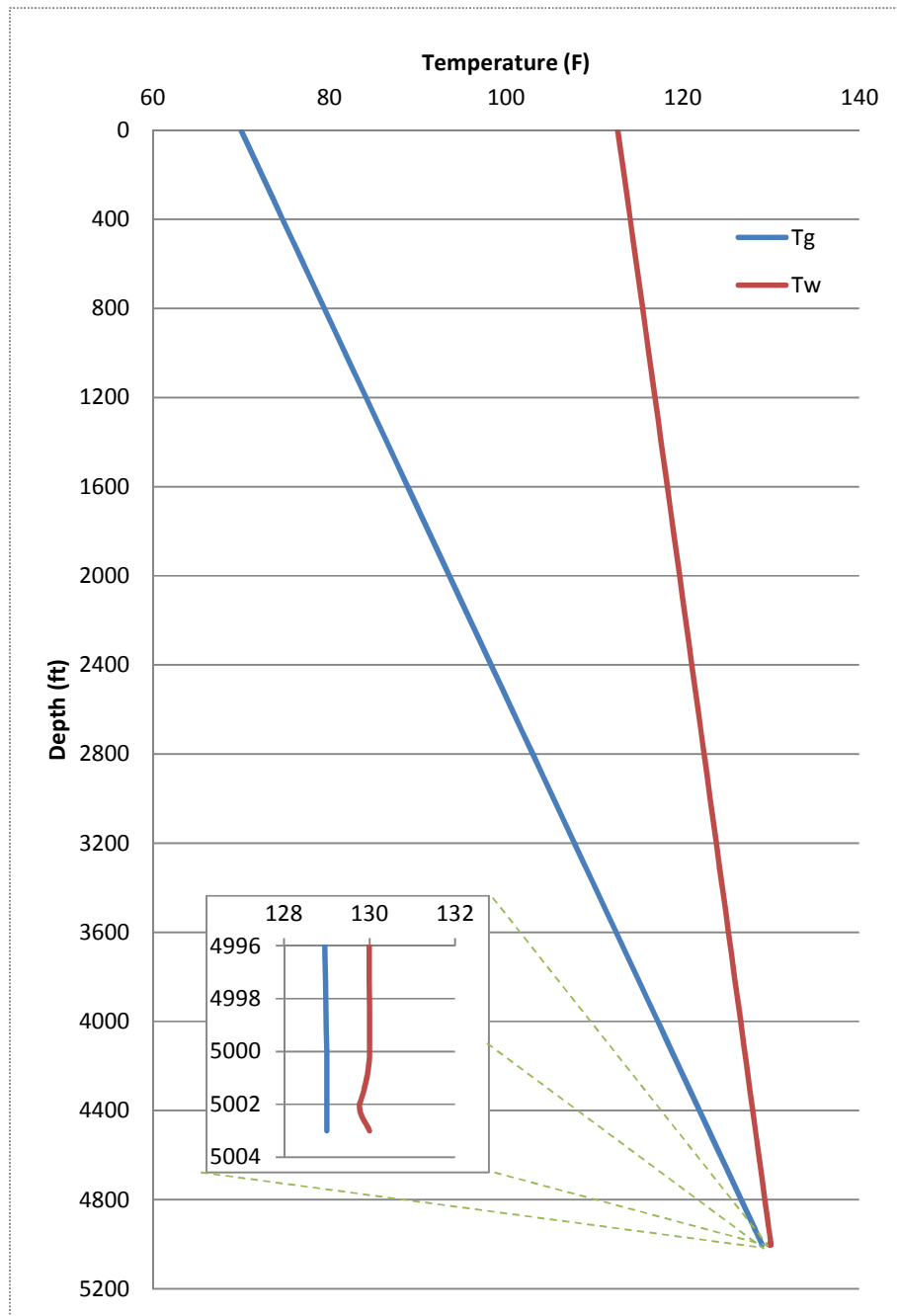


Figure 5-19 Evaluation of temperature profile and Joule-Thomson effect for mixture 1 of Table 3-1 (case study #4)

A sensitivity study has been performed to investigate the effect of the gas production rate on the wellbore temperature profile along a wellbore, and the phenomenon of

the Joule-Thomson (JT) effect at the entry point to the wellbore. All computations are performed for the same wellbore schematic as shown in Figure 5-18, and for the thermal information given in Table 5-3.

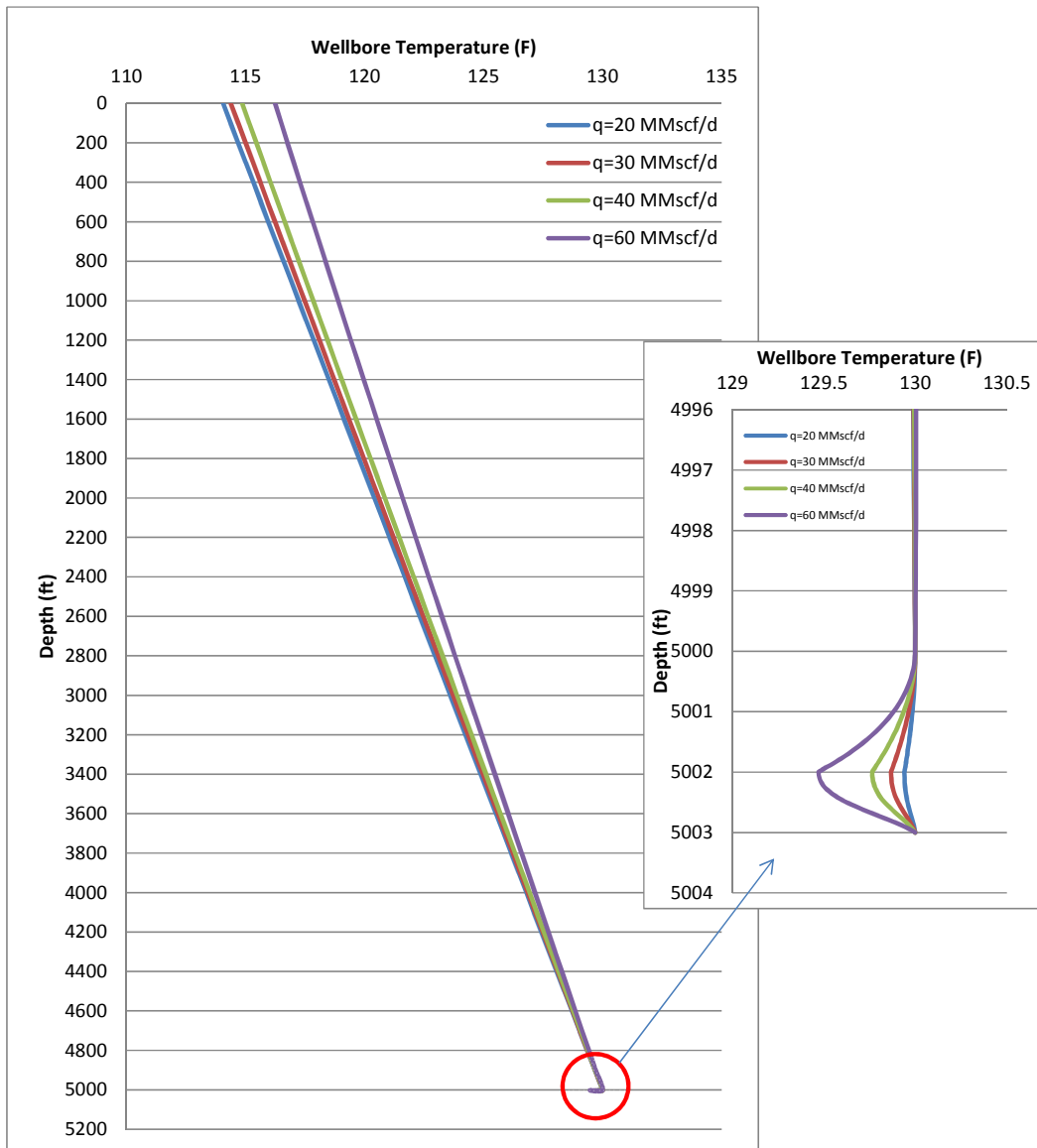


Figure 5-20 Prediction of temperature profile and the Joule-Thomson effect at different flow rates of gas mixture number 1 in Table 3.1 for a typical wellbore schematic in Figure 5-18 (case study #4)

Figure 5-20 provides the predicted temperature profile for various gas flow rates (20, 30, 40 and 60 MMscf/d) with gas components of mixture (1) in Table 3.1. As can be seen, the surface temperature is 114.059, 114.388, 114.863 and 116.245 degrees Fahrenheit for production rates of 20, 30, 40 and 60 MMscf/d respectively. This means that as the production rate increases, the gas mixture travels faster up the wellbore, which allows less time for the loss of heat energy, resulting in a heat gain, mainly from the initial geothermal gradient, as temperature gain due to friction is usually insignificant for a gas production well. As a result, the fluid temperature at the surface is higher, and it increases as the production rate is increased. The inset of **Figure 5-20** also shows that the JT effect on the drop of temperature at the entry point (shown by a red circle) is substantial and increases significantly as the production rate is increased.

5.3.2 Case Study #5 (Buttress-1 Well CO₂CRC Otway project)

The second example for single phase gas flow is the production well, Buttress-1, from CO₂CRC Otway project (Paterson et al., 2010). In this project, the Buttress-1 well was drilled and completed as a 3.5” mono-bore production well for the purpose of carbon dioxide production from a natural source, to demonstrate carbon dioxide storage in a small, depleted gas reservoir in South-Eastern Australia via well CRC-1 (Figure 5-21). Well CRC-1 is an injection well, which is also investigated in the injection section of this chapter (case study #10). After testing the produced gas, it was reported that the production from Buttress-1 well was a gas stream of mole fraction of 77% CO₂, 20% methane and 3% other gas components. The Buttress-1 produced 65,445 tonnes from 18 March 2008 until 29 August 2009, with the rate of 157-166 tonnes/day for the demonstration project. The wellhead temperature, during production, was reported 33-34°C, which was less than the designed temperature of 45-5 °C.

The bottom hole pressure and temperature for Buttress-1 was 16.73 MPa and 65.2°C respectively. The other required information can be found in **Table 5-3**.

The temperature profile calculated by this work is compared with the results of Lincoln et al.'s work (Paterson et al., 2010) in Figure 5-22. As can be seen, the graph shows a good match, and the surface temperature evaluated by this work is 33.016°C, which is in the range of actual data (33-34°C).

This case is important for this study, because it is a chance to observe the thermal profile along a CO₂ production well. This study is not only focused on the production of natural gas, but covers different types of gas production, and can be applied for prediction of wellbore temperature profiles along different gas type flowing wellbores.

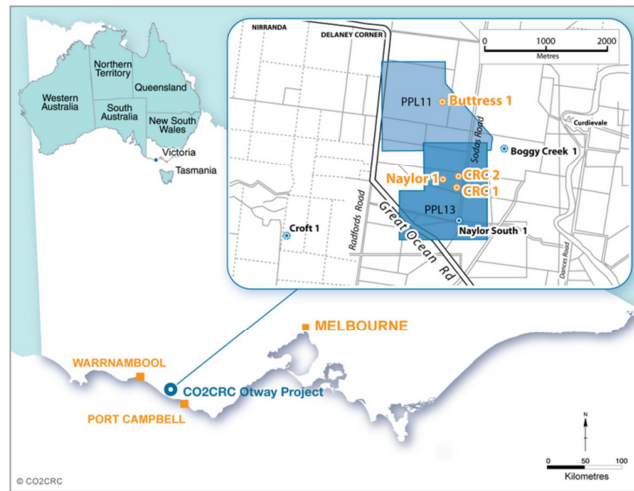


Figure 5-21 The CO₂CRC Otway project location (case study #5)

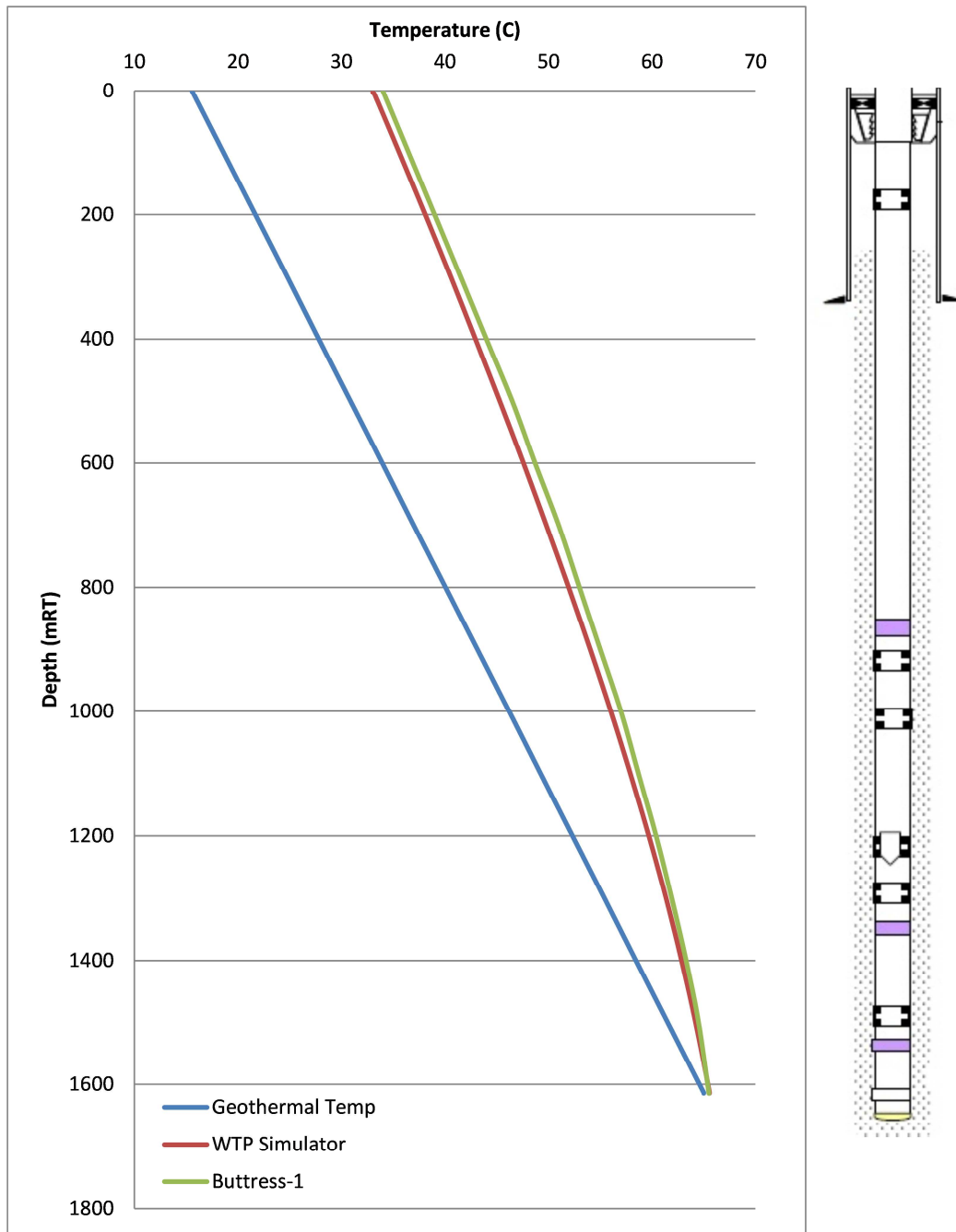


Figure 5-22 Comparison of wellbore temperature profiles (case study #5)

5.3.3 Case Study #6 (EnCana's Gas Wells, Western Canada)

This example has been considered from Huebsch et al.'s (Huebsch et al., 2008) work, in which the slickline DTS was used for wellbore temperature and pressure recording in EnCana's gas wells in the Deep Basin in Western Canada in 2007. The optic fibre was embedded in a 1/8th inch diameter slickline cable. **Figure 5-23** shows the temperature data over the reservoir interval, and **Figure 5-24** provides the wellbore temperature profile for flowing and shut-in conditions gained from DTS records. It is not the purpose of this work to show how the temperature measurements are obtained by a DTS; this is explained in many papers (Barrufet et al., 1995; Brown, 2006; Camilleri et al., 2010; Cox et al., 2006; Hill, 1990; Kabir and Hasan, 1998; Weaver et al., 2005). However, it is worth noting that the recorded data is used as a reference for this study, which aims to establish how accurately the temperature profile along a gas production well can be predicted by developed WTP simulator.

Figure 5-25 compares the wellbore temperature predicted in this study by the WTP simulator and the obtained records from the DTS temperature measurements. The inset figure also shows the temperature drop as the Joule-Thomson effect at the entry point of gas from the reservoir into the wellbore. From these comparisons, a good agreement can be observed between the profiles, which plot a temperature curve for every foot along the gas producing wellbore.

The sensitivity of wellbore temperature to gas impurities has been selected in this example. The gas has a gas gravity of 0.75, with the impurities shown in **Table 5-4**. **Figure 5-26** shows the effect of impurities on the Joule-Thomson effect. As can be seen, when the amount of water increases in the gas mixture, the wellbore temperature at the entry point drops less because of the Joule-Thomson effect. However, the surface temperature for the gas mixture including water is higher,

which may relate to the heat capacity of water, which is higher than the heat capacity of gases.

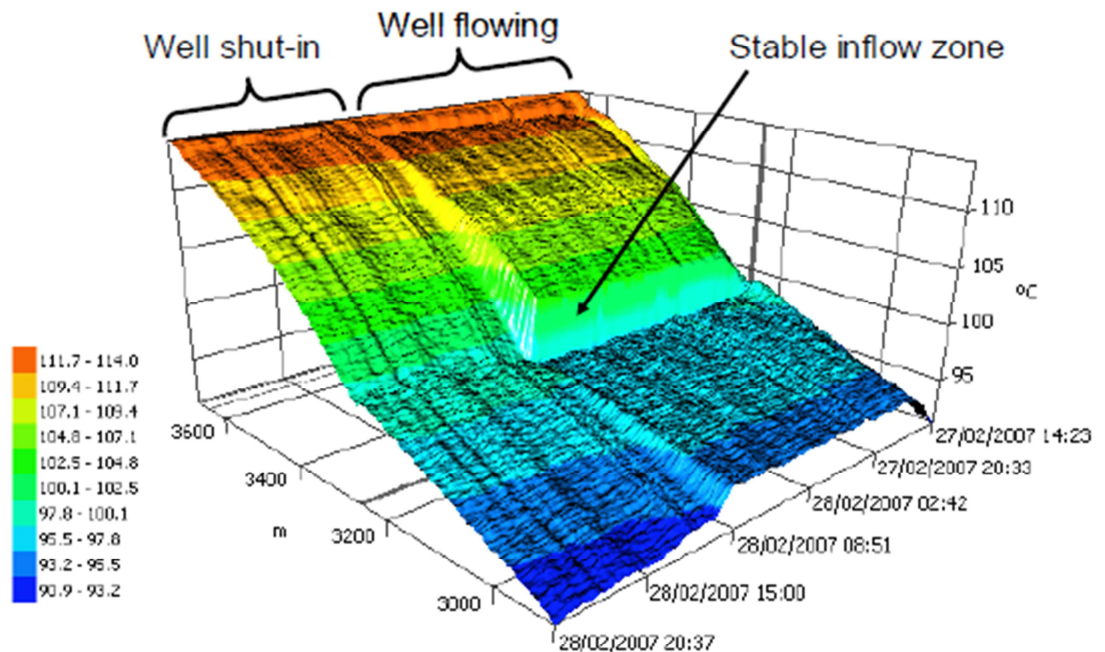


Figure 5-23 Temperature data over the reservoir interval (after Huebsch et al. (Huebsch et al., 2008)) (case study #6)

As the field data has been obtained from a DTS system, there is a chance to compare the results of this work with the intelligent well monitoring systems which are popular nowadays. From this comparison, it can be claimed that this work can be applied in parallel and/or instead of intelligent well monitoring systems such as the DTS and fibre optic cables.

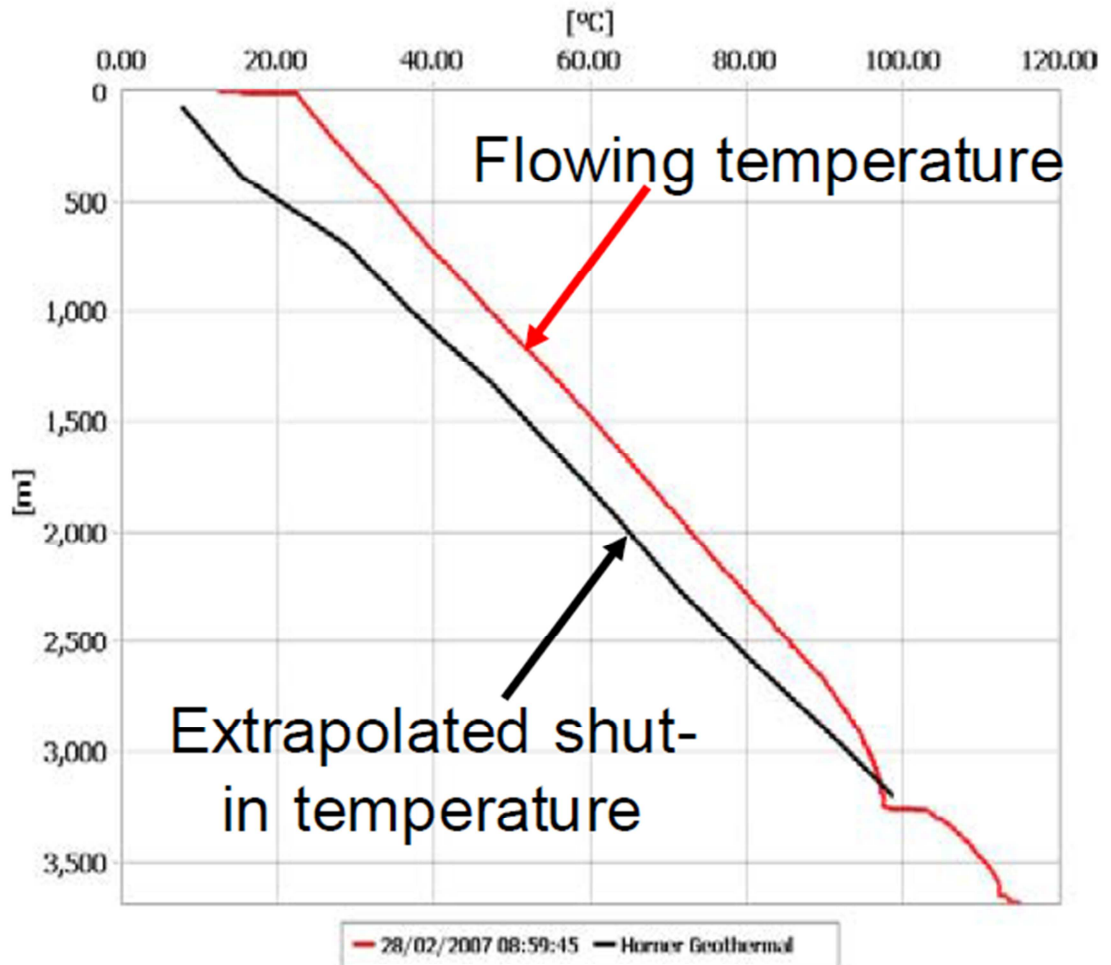


Figure 5-24 Flowing and shut-in wellbore temperature (after Huebsch et al. (Huebsch et al., 2008)) (case study #6)

Table 5-4 The value of impurities in the gas mixture (case study #6)

Impurities	(1)	(2)	(3)
N2	0	0.5	0.5
CO2	0	0	0
H2S	0	0.5	0.5
H2O	0	0	0.15

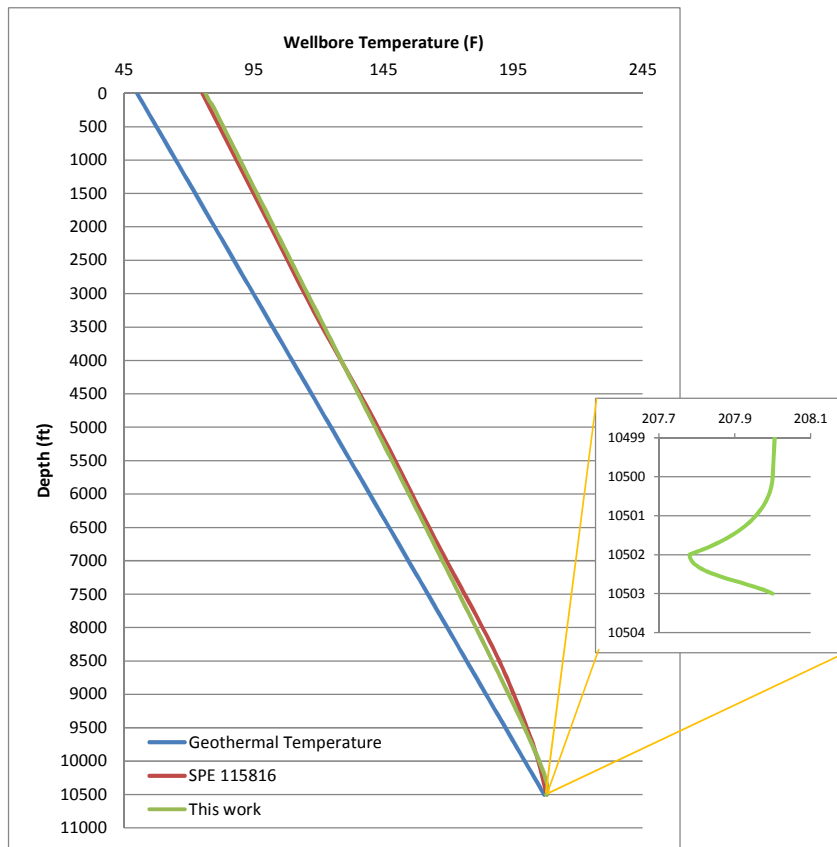


Figure 5-25 Comparison of wellbore temperature profiles (case study #6)

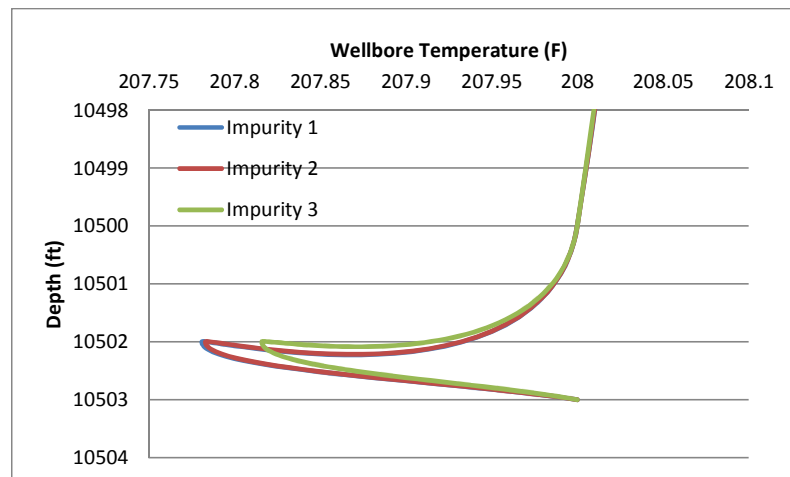


Figure 5-26 Joule-Thomson effect at the entry point to the wellbore (case study #6)

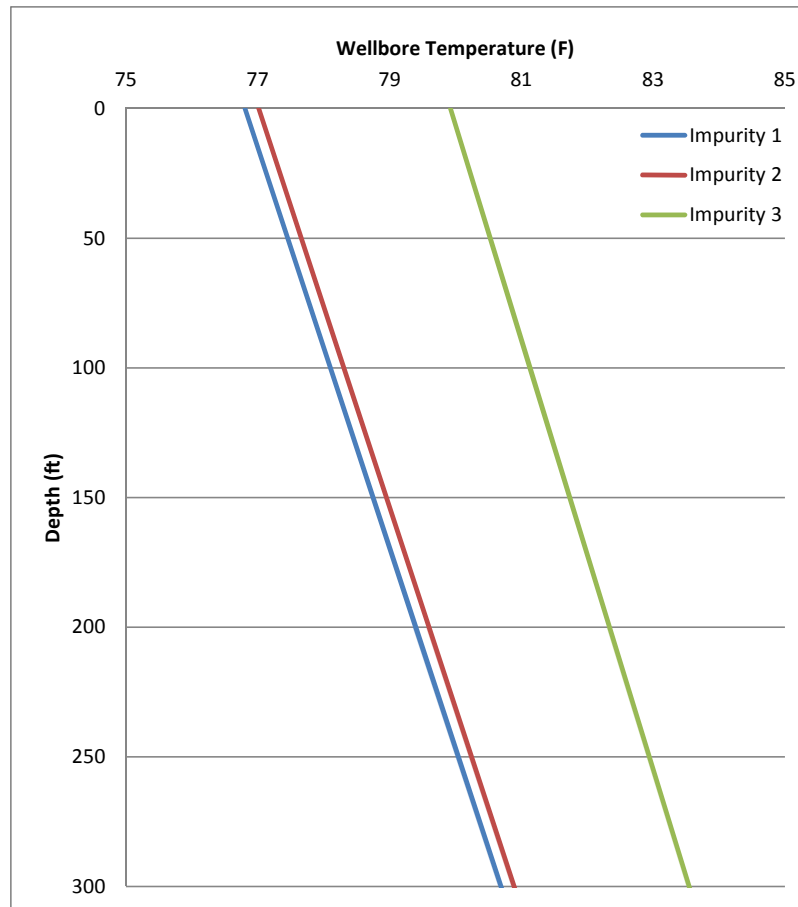


Figure 5-27 Surface temperature (case study #6)

5.3.4 Case Study #7 (Gas Producing Well)

The data for this case has been extracted from Louis et al.'s study (Lesem et al., 1957), which provides observed data from a gas producing well. The well was producing gas with a specific gravity of 0.6127 and flow rate of 4.08 MMscf/d from a depth of 6830 ft. The tubing size was 2 ½", and the bottom temperature and pressure were 171°F and 2934 psia, respectively. The physical properties of the produced gas, geothermal properties and wellbore details are given in Table 5-3.

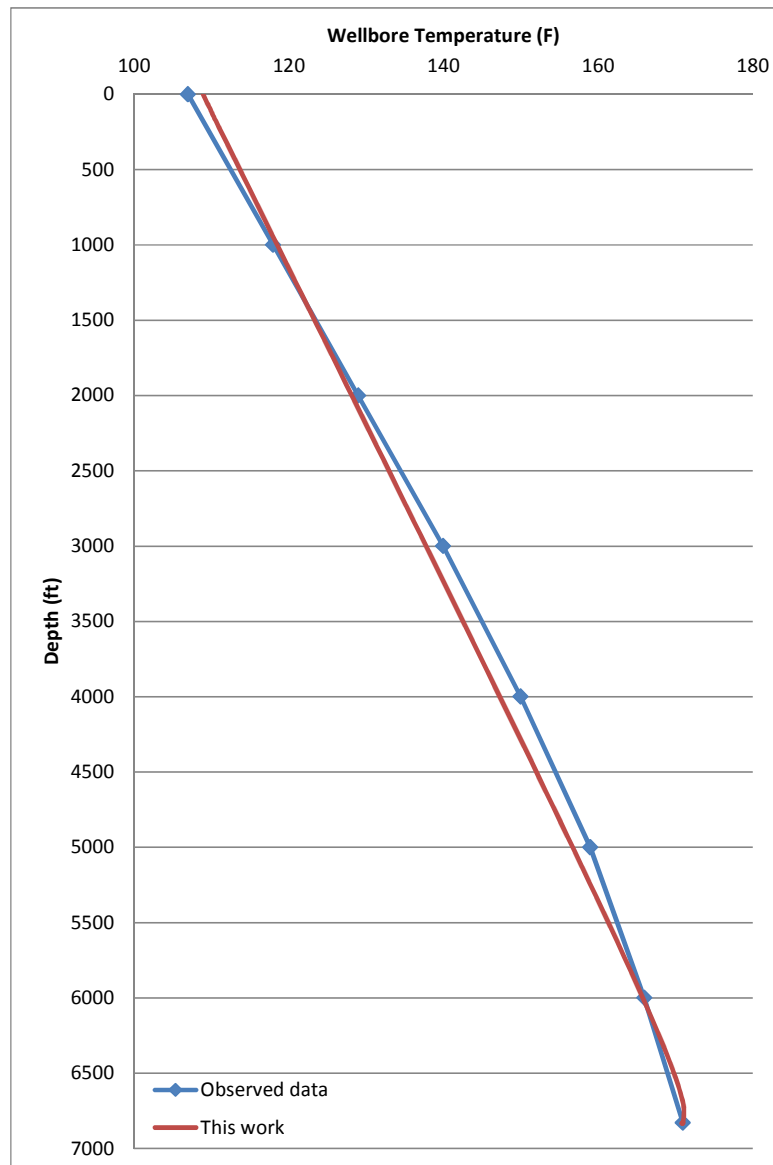


Figure 5-28 Comparison of wellbore temperature profiles (case study #7)

Figure 5-28 compares the result of this work and the observed data from the gas production well. As can be seen, there is a reasonable match between the curves. Also, Louis et al. reported a value of 0.841 for the compressibility factor of produced gas, and the calculated value for the compressibility factor in this study is 0.8623, which is very close.

This data is important because it is from an actual well. Therefore, it supports the claim that this WTP simulator can be applied for the the prediction of wellbore temperature profile along a gas producing wellbore.

5.4 Multi-Phase Fluid Production

Two different examples, well GC-17 (case study #8) and a well from the Tah field in Chaina (case study #9), have been considered to investigate the potential application of developed WTP simulator in case of multiphase flowing production well. GC-17 is a well for multi-phase production from a depth of 12990 ft. Case study #9 is a multi-phase production well from the Tah oilfield in China, which is an ultra-deep and ultra-heavy oil production reservoir. The physical wellbore, geothermal, and fluid data are tabulated in Table 5-5.

Table 5-5 Data calculation for case studies #8 to #9.

Data	Description	Case study #8			Case study #9		
		Size (in)	Weight (ppf)	Depth (ft)	Size (in)	Weight (ppf)	Depth (ft)
Well Schematic	Outer Casing	13 3/8	54.5	480	13 3/8	54.5	
	Inner Casing	9 5/8	43.5	10000	9 5/8	43.5	
	Liner	7	26	12990	7	26	
	Tubing	5 1/2	17	12850	3 1/2	9.2	
	Total Depth (ft)	12990					
Wellhead		Temperature (F)	Pressure (psig)		Temperature (F)	Pressure (psig)	
	Wellhead	226	916				
Production data		Produced fluid properties			Produced fluid properties		
	Type	Liquid <input type="checkbox"/>	Gas <input type="checkbox"/>	Mixture <input checked="" type="checkbox"/>	Liquid <input type="checkbox"/>	Gas <input type="checkbox"/>	Mixture <input checked="" type="checkbox"/>
	Oil rate (bbl/d)	192.00			470.00		
	Gas (MMscf/d)	0.83			0.21		
	Water (bbl/d)	162.00			110.00		
Gas Gravity	0.645			0.715			
Annulus		Annulus fluid properties			Annulus fluid properties		
	Density (lb/cu.ft)	0.04			0.12		
	Heat Capacity (Btu/ lb.F)	0.25			0.38		
	Viscosity (cp)	0.07			0.08		
Thermal resistivity (Btu/hr.ft.F)	0.03			0.5			
Thermal data		Thermal Conductivity (Btu/hr.ft.F)			Thermal Conductivity (Btu/hr.ft.F)		
	Ground	2.5			2.4		
	Cement	0.38			1.74		
Geothermal		Geothermal Temperature			Geothermal Temperature		
	Surface (F)	50			70		
	Reservoir (F)	225			253		
	Gradient (F/ft)						
Surface	Pressure (psia)	916			432		
	Temperature (F)	65			77		
Reservoir	Pressure (psia)	3338			5400		
	Temperature (F)	226			254.19		

5.4.1 Case Study #8 (Well Name: GC-17)

The multi-phase producing well, GC-17 well, from Farshad et al.’s work (Farshad et al., 1999) has been selected as an example to validate the results of multi-phase fluid flow simulation in this work. The rate of oil, gas and water production for this well was 192 bbl/d, 0.832 Mscf/d and 162bbl/d respectively through 2 7/8” wellbore tubing. Geothermal properties and wellbore details are provided in **Table 5-5**, and physical properties of the produced fluid are provided in Table 5-6.

Table 5-6 Production data for well GC-17 (case study #8)

Well ID #:	GC-17	
Description:	Multi-phase oil	
Well and Fluid Parameter		
	Value	Unit
Oil flow rate:	192	bbl/d
Water flow rate:	162	bbl/d
Gas flow rate:	0.832	Mscf/d
Gas-Oil ratio:	4333	scf/bbl
Well depth:	12990	ft (TVD)
Bottom hole pressure:	3338	psia
Wellhead pressure:	916	psia
Wellhead temperature:	65	F
Bottom hole temperature:	226	F
Oil API:	36.9	API
Water specific gravity:	1	
Gas specific gravity:	0.645	
Dead oil viscosity @ 100 F	3.201	cp

Farshad et al. compared their results with that of the Beggs-Shiu and Kirkpatrick’s work, as well as actual field data (**Table 5-7**), and the results are plotted in Figure 5-29. The figure shows that the predicted temperature profile by Beggs-Shiu and Kirkpatrick deviate considerably from the actual data. It can also be seen that the Farshad et al. results deviate from actual data for the bottom section as well as the top section of the wellbore. The reason of such deviations is not clearly explained in their works. It is apparent that such deviations are maybe due to the lake of the data especially thermal properties of rocks surrounding the wellbore. However, this actual data are considered in the current study to predict the temperature profile using the WTP simulator. This study provides a close match between the results of the WTP simulator and the actual data which are discussed in details below.

Table 5-7 Comparison of temperature profiles for the different models (Case study #8)

Well ID#: GC-17									
Tube internal diameter: 2.441 in.		Bottom-hole Pressure: 3338 psi							
Oil flow rate: 192 bbl/D		Wellhead Pressure: 916 psi							
Water flow rate: 162 bbl/D		Wellhead Temperature: 65 °F							
Gas-oil Ratio: 4333 scf/bbl		Oil °API gravity: 36.9							
Depth of well: 12990 ft		Gas specific gravity: 0.645							
Oil viscosity: 3.201 cp									
Depth (ft)	Measured Temperature (°F)	Neural Network 1		Neural Network 2		Beggs-Shiu		Kirkpatrick	
		Predicted Temperature (°F)	Absolute % Relative Error	Predicted Temperature (°F)	Absolute % Relative Error	Predicted Temperature (°F)	Absolute % Relative Error	Predicted Temperature (°F)	Absolute % Relative Error
0	65.0	65.0	0.0	65.0	0.0	72.0	10.7	66.2	1.8
1999	122.0	126.2	3.4	135.0	10.6	97.9	19.7	90.8	25.6
3999	146.0	136.4	6.6	153.9	5.4	123.9	15.1	115.4	21.0
5919	169.0	149.9	11.3	173.3	2.5	148.9	11.9	139.0	17.8
7755	190.0	166.9	12.1	191.5	0.8	172.6	9.1	161.6	15.0
9596	208.0	188.5	9.4	208.2	0.1	196.0	5.8	184.2	11.4
11430	221.0	214.3	3.0	222.4	0.6	216.8	1.9	206.8	6.4
12351	225.0	228.8	1.7	228.5	1.6	224.1	0.4	218.1	3.1
12990	226.0	239.3	5.9	232.3	2.8	226.0	0.0	226.0	0.0
Mean Absolute % Relative Error			5.9		2.7		8.3		11.3

Figure 5-30 compares the results of the WTP Simulator with the actual field data. In this figure, there are four different curves, and the field data (blue) curve provides the actual data. Referring to the field data (blue curve), it can be seen in Figure 5-30, the rate of temperature loss for the top section of the wellbore (from surface to 3500 ft) is higher than for the rest of wellbore. Farshad et al. did not provide any physical and/or geothermal wellbore information for analysis of the rate change of the temperature gradient. But, for example, it can be predicted that if this section of the wellbore is surrounded by the sea, it can cause a higher rate of temperature loss. Therefore, different physical properties are considered in the calculations in this section, which means that the definition of different sections with different thermal conductivity along a wellbore is another capability of this work. Thermal conductivity equal to 4.5 Btu/(hr.ft.F) for the surrounding section above 3500 ft, and 2.5 Btu/(hr.ft.F) for the rest of the wellbore surrounding the bottom of the well is

considered in the calculation. Figure 5-30 shows the wellbore temperature profile predicted by this work, plotted in purple colour. As can be seen, there is good agreement between the results of this work (purple curve) and the actual field data (blue curve).

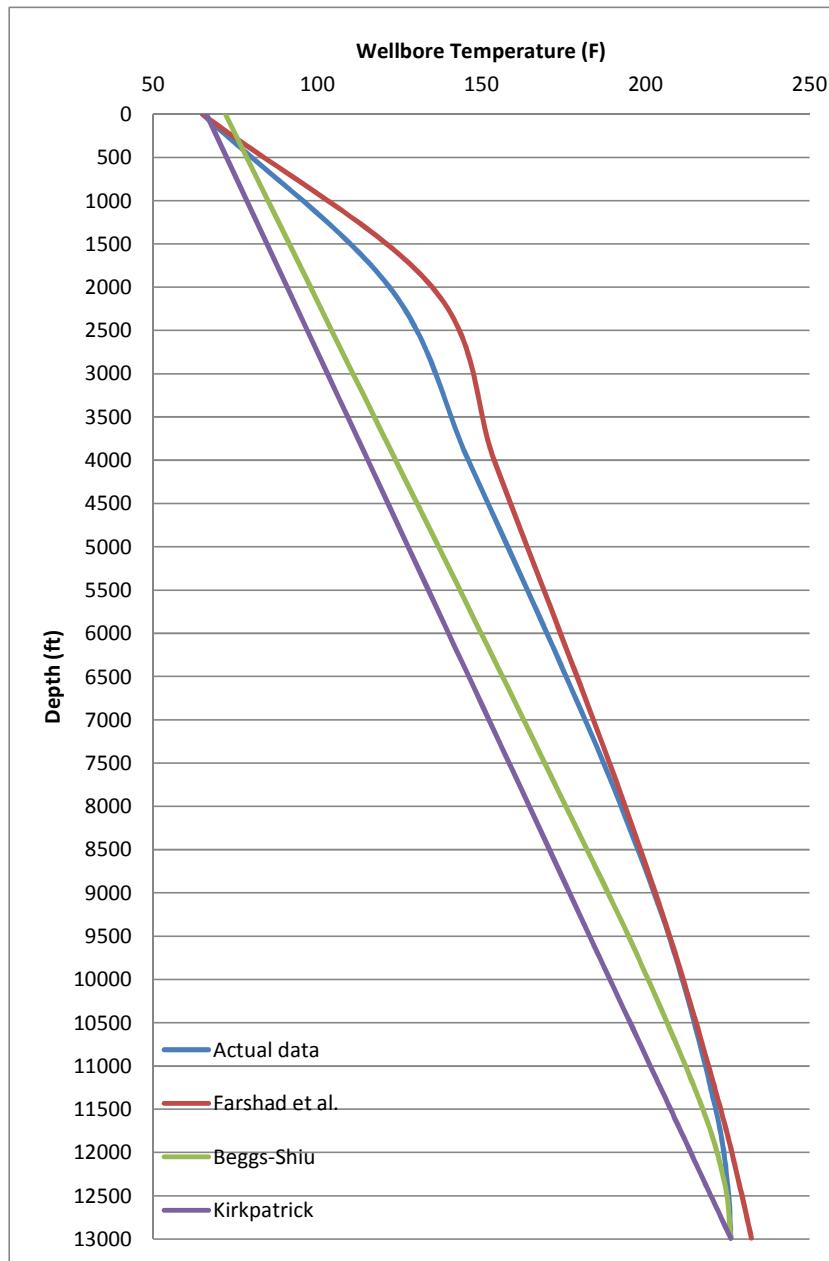


Figure 5-29 Comparison of predicted wellbore temperature profile by Farshad et al., Beggs-Shiu and Kirkpatrick with the actual field data (case study #8)

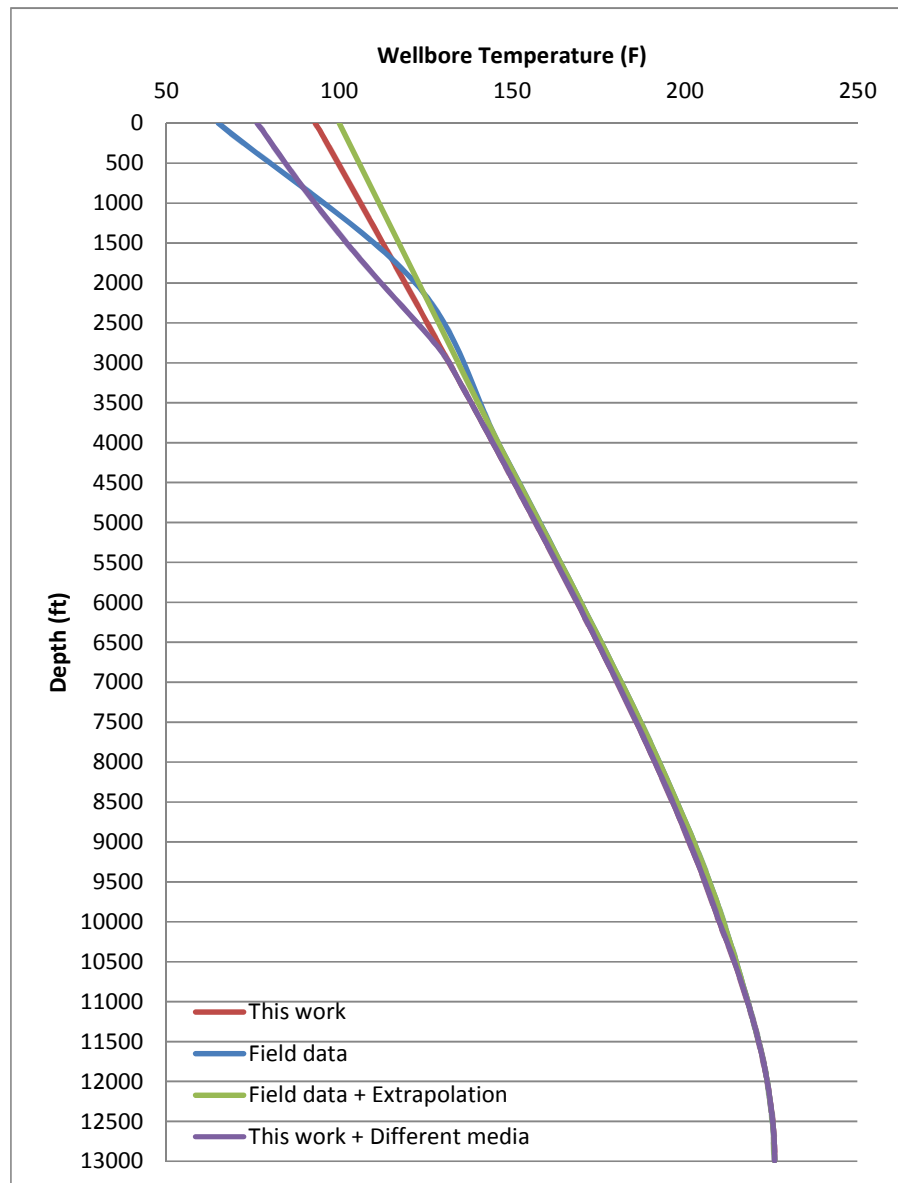


Figure 5-30 Comparison of wellbore temperature profiles (case study #8)

There are two more curves as presented in Figure 5-30, which are red and green curves. The green curve is the same as the field data (blue curve) with the exception of the extrapolation of temperature profile for the top section of the wellbore. The green curve is plotted when the top section of the wellbore has the same thermal conductivity as the other parts of the surrounding wellbore. The red curve shows the

results of this work, when the thermal conductivity of wellbore surroundings is equal to 2.5 Btu/(hr.ft.F). A good agreement can be seen between the predicted wellbore temperature profile in this work (red curve) and the actual wellbore temperature profile, including extrapolation for the top section (green curve).

5.4.2 Case Study #9 (Tah Field, China)

This case study is considered from Yanmin et al.'s work (Yu et al., 2009) which is a well in Tah field in China with ultra-deep and ultra-heavy oil reservoir properties. Yanmin et al. explain that evaluation of wellbore temperature through the wells of this oil field is important, as most of the wells have the problem of high oil viscosity for the upper section of the wellbore due to high temperature loss in this section. The authors state that one solution to the problem is the injection of light oil with lower viscosity through the annulus to help the production. Therefore, accurate prediction of wellbore temperature profile is highly important for the design of a well and in the design of dilution projects.

Table 5-8 Production data for a well of Tah field in China (case study #9)

Field:	Tah, China	
Description:	Multi-phase oil	
Well and Fluid Parameter	Value	Unit
Oil flow rate:	470	bbl/d
Water flow rate:	110	bbl/d
Gas flow rate:	0.21	Mscf/d
Well depth:	18050	ft (TVD)
Bottom hole pressure:	5400	psia
Wellhead pressure:	432	psia
Wellhead temperature:	77	F
Bottom hole temperature:	123.44	F
Oil API:	41	API
Water salinity:	100000	ppm
Gas specific gravity:	0.715	
Dead oil viscosity @ 100 F	0.6	cp

This case study is considered because of the complexity of this field and the challenge of comparing the predictions using developed WTP simulator with the actual field data. Figure 5-31 compares the results of this work with the actual data of Tah field in China. As can be seen, there are four curves in Figure 5-31. The blue curve shows the actual field data, which, as discussed by Yanmin et al., is caused by the property of the media surrounding the top section of the wellbore. In this section of the wellbore, the temperature loss is more than in the other parts of the wellbore. Yanmin et al. did not provide details of the thermal properties of the top section of the wellbore surroundings. Therefore, some thermal data are suggested for the top section of wellbore through this study, and the predicted wellbore temperature profile based on the suggested data for top section of the wellbore can be seen on the red curve. It is suggested that the thermal conductivity of this section is three times that of the other parts of the wellbore.

The green and purple curves are the wellbore temperature profiles predicted by this work without considering the difference in the thermal properties of surrounding

media and Tah field data after extrapolation for the top section of the wellbore respectively. When we look at the curves in Figure 5-31, which are based on the results of the WTP Simulator (red and purple curves) and actual data (blue and green curves), a good agreement can be seen, especially from the depth of 2500 ft to the bottom of the well, where the physical and thermal properties of the surrounding media are obvious.

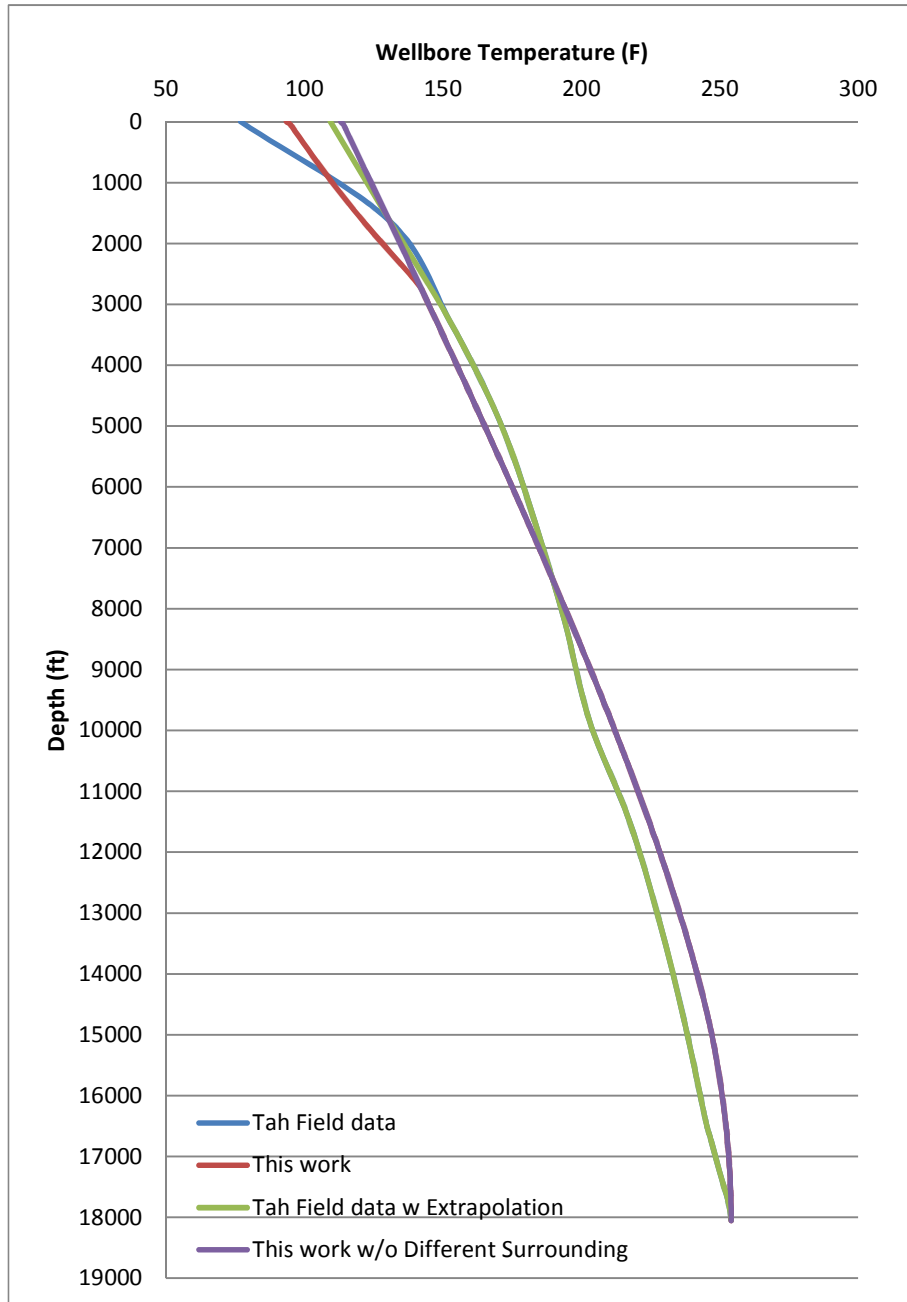


Figure 5-31 Comparison of wellbore temperature profiles (case study #9)

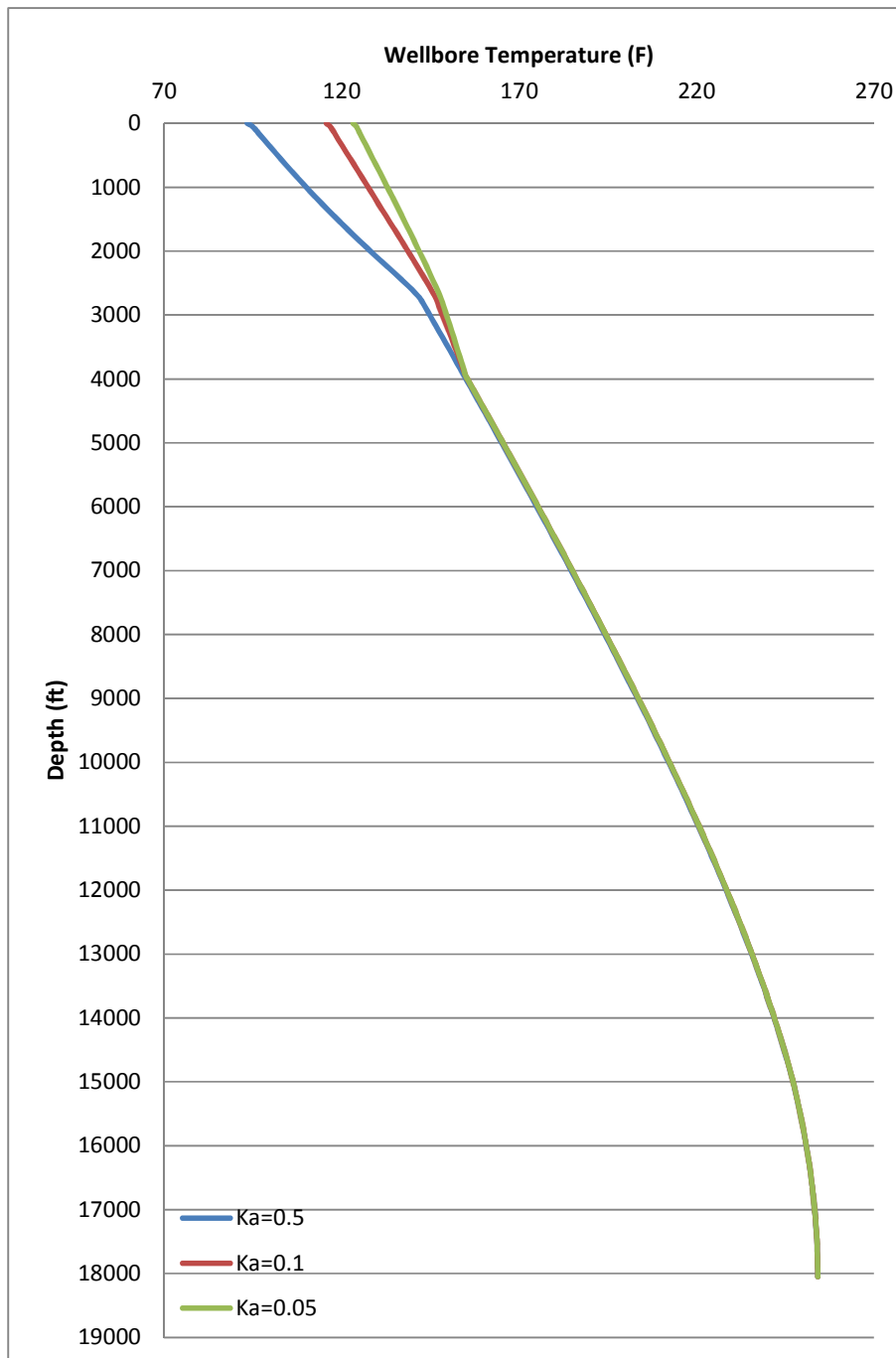


Figure 5-32 Sensitivity study for oil production well in Tah Fiedl (case study #9)

A sensitivity study has been performed on the oil production well in the Tah Field (Figure 5-32). In this study, the effect of thermal conductivity of annulus fluid on the

wellbore temperature profile has been considered. In chapter two (section 2.3) and Appendix A it was explained that temperature loss or gain through the annulus happens because of convection and radiation heat transfer mechanisms. Therefore, it is thought that annulus fluid with lesser thermal conductivity can act to isolate heat loss from the wellbore fluid to the surroundings. In this study, an injection point at the depth of 4000 ft is considered, with the aim of injecting warmer fluid or a gas with lower thermal conductivity into the crude production oil. This injection prevents increase of the viscosity of crude oil, because the annulus space acts as a barrier to the heat loss from the crude oil to the surroundings, as well as mixing the oil with a fluid with lower viscosity. This technique can be a solution to the viscosity problem of crude produced oil, as can be seen in Figure 5-2, where the cases with lower thermal conductivity of annulus fluid (k_a) have a higher temperature profile and higher surface temperature as a result. It is clear that crude oil with a higher temperature has a lower viscosity.

The achievement of this case study is the comparison of the results predicted in this study with the actual field data related to complicated oil production conditions.

5.5 Injection

A primary objective for evaluating the temperature in an injection well is to measure the temperature of injected fluid at the entry point to the reservoir. This may disturb the temperature of the formation that has been caused by fluid injection over a long term.

Two case studies (case study #10 and 11) have been considered to justify the potential application of developed WTP simulator for the injection well. The first one is the well CRC-1 of the CO₂CRC Otway project which has been drilled for the purpose of a CO₂ injection study into a depleted gas reservoir. The second case study has been considered in case of a water injection well studied by Squier et al.

(SQUIER et al., 1962). Further details of these two cases are provided in a later section below. However, in this study, the result of the WTP simulator has also been compared with the above two cases. The geothermal data, physical wellbore information and injected fluid properties for both of these case studies are presented in Table 5-9.

Table 5-9 Data calculation for case studies #10 to #11

Data	Description	Case study #10			Case study #11		
		Size (in)	Weight (ppf)	Depth (ft)	Size (in)	Weight (ppf)	Depth (ft)
Well Schematic	Casing				13 3/8	54.5	2700
	Casing	7 5/8	43.5	270	9 5/8	43.5	5000
	Liner						
	Tubing	4 1/2	17	1900	7	26	6400
	Total Depth (ft)	1990			6400		
Wellhead		Temperature (F)	Pressure (psig)	Rate (bbl/d)	Temperature (F)	Pressure (psig)	Rate (bbl/d)
	Wellhead	48.2	450	500	83	350	900
Wellbore		Produced fluid properties			Produced fluid properties		
	Type	Liquid <input checked="" type="checkbox"/>	Gas <input type="checkbox"/>	Mixture <input type="checkbox"/>	Liquid <input checked="" type="checkbox"/>	Gas <input type="checkbox"/>	Mixture <input type="checkbox"/>
	%Water	100%			100%		
Annulus		Annulus fluid properties			Annulus fluid properties		
	Density (lb/cu.ft)	62.4			54		
	Heat Capacity (Btu/ lb.F)	0.85			1		
	Viscosity (cp)	0.07			1.5		
	Thermal resistivity (Btu/hr.ft.F)	0.5			1.45		
Formation		Thermal resistivity (Btu/hr.ft.F)			Thermal resistivity (Btu/hr.ft.F)		
	Ground	1			2.5		
	Cement	2.6			0.38		
Geothermal		Geothermal Temperature			Geothermal Temperature		
	Surface (F)	60			70		
	Reservoir (F)	160			198		
	Gradient (F/ft)						

5.5.1 Case Study #10 (CRC-1 Well CO2CRC Otway project)

As mentioned, Well CRC-1 was selected for the injection of produced CO2 (Buttress-1 well, case study #5) into a depleted gas reservoir in Southern Australia in the CO2CRC Otway project (Paterson et al., 2010). In this project the CO2 source is a natural source about 2 km from the injection well (Figure 5-21). The gas produced

was 157-166 tonnes/day via Buttress-1 well, and the produced gas composed of 77% CO₂ and 23% other gases. The CO₂ was purified from other gases, compressed and injected via CRC-1 well into a small and depleted gas reservoir. The concept of CO₂CRC research project is shown in **Figure 5-33**.

The CRC-1 well was drilled and completed as a 4.5” mono-bore production well for the purpose of carbon dioxide injection produced from a natural source via Buttress-1 well, to demonstrate carbon dioxide storage in a small, depleted gas reservoir in South-Eastern Australia (Paterson et al., 2010). The geothermal data, physical wellbore information and injected fluid property used for evaluation of the wellbore temperature profile can be seen in Table 5-9.

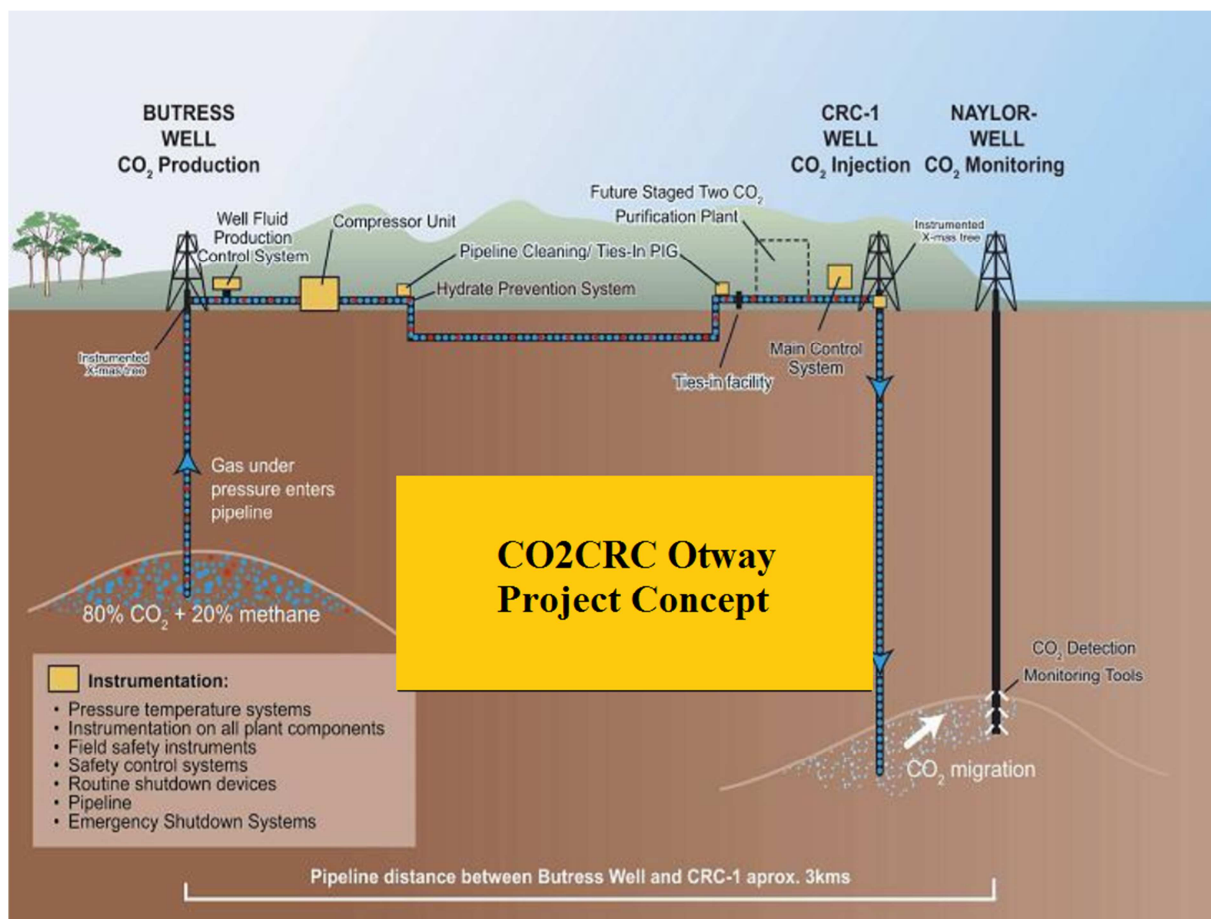


Figure 5-33 CO₂CRC Otway project (Cook, 2010) (case study #10)

Permanent downhole gauge and surface temperature recorders have been used throughout this project for recording downhole and surface injection temperature, respectively. Figure 5-34 provides the downhole and surface temperature records in CRC-1 well (Paterson et al., 2010). As can be seen, for example, downhole and surface temperature on July 2009 are 29°C (84.2°F) and 62°C (143.6°F), respectively.

The predicted wellbore temperature profile, which is evaluated for July 2009 using the WTP Simulator, are presented in Figure 5-35. The figure provides the injected fluid loss temperature through the top section of the well until the fluid temperature and the surroundings have the same temperature, and conversely gains temperature through the bottom section of the well. It is worth mentioning that the evaluated bottom hole temperature in this study is 143.833°F. Therefore, the predicted and measured bottom hole temperature are very close.

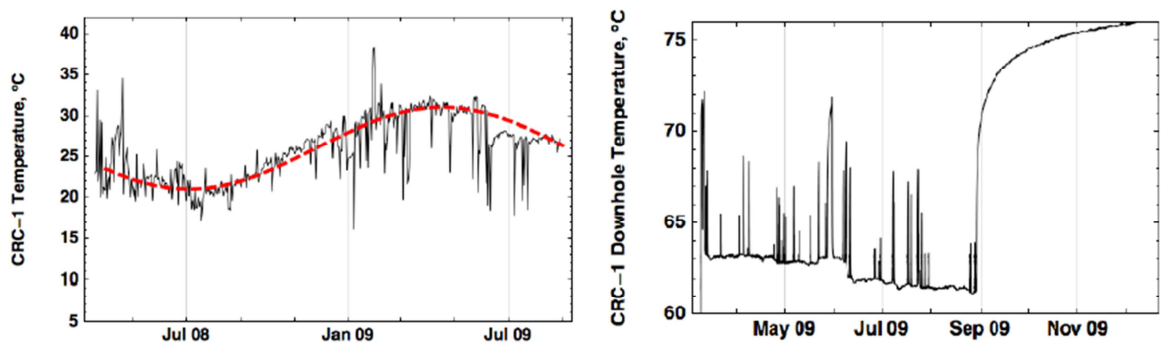


Figure 5-34 Downhole and surface temperature records in CRC-1 well (Paterson et al., 2010) (case study #10)

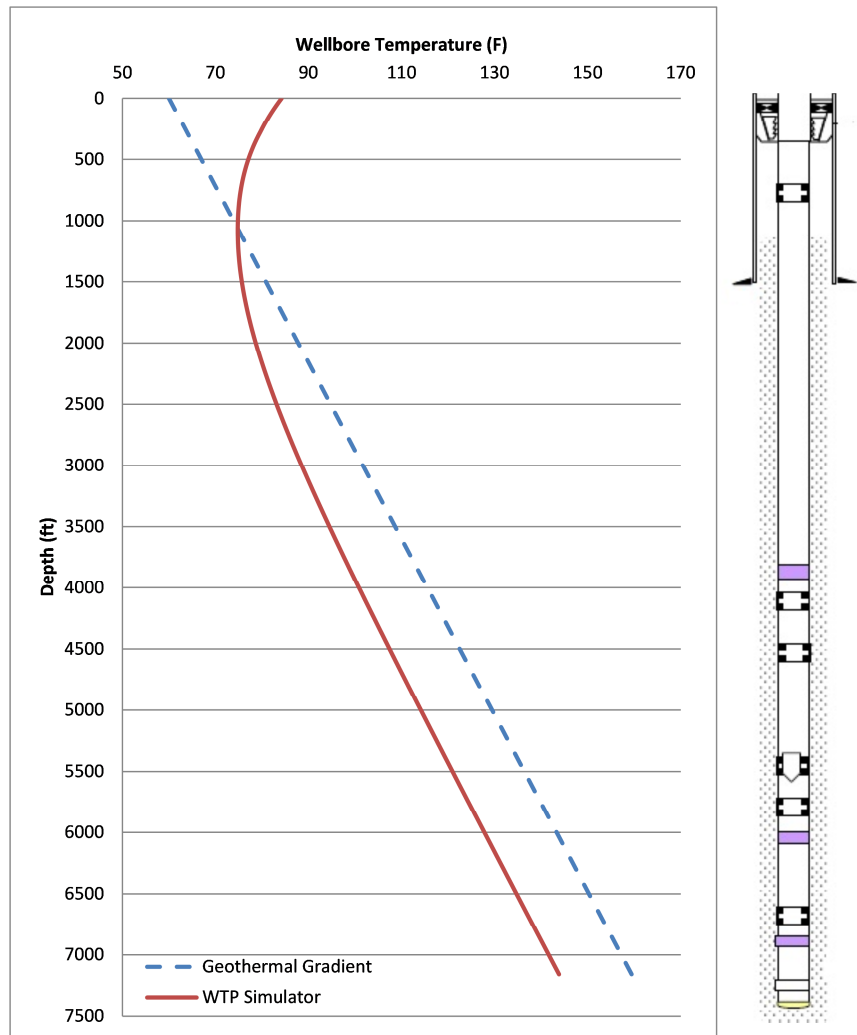


Figure 5-35 Wellbore temperature profile for CRC-1 well (case study #10)

5.5.2 Case Study #11 (Water Injection Well)

As mentioned, the field data for this case study has been taken from Squier et al. (SQUIER et al., 1962). Water at 83°F at the surface was injected at a rate of 900 bbl/d through 7" casing. The physical properties of injected water such as heat capacity and thermal conductivity are not given in the reference; however, these values are calculated at 1 (Btu/lb.F) and 1.45 (Btu/hr.ft.F) respectively in this study. The wellbore data, fluid information and geothermal gradient provided in Table 5-9.

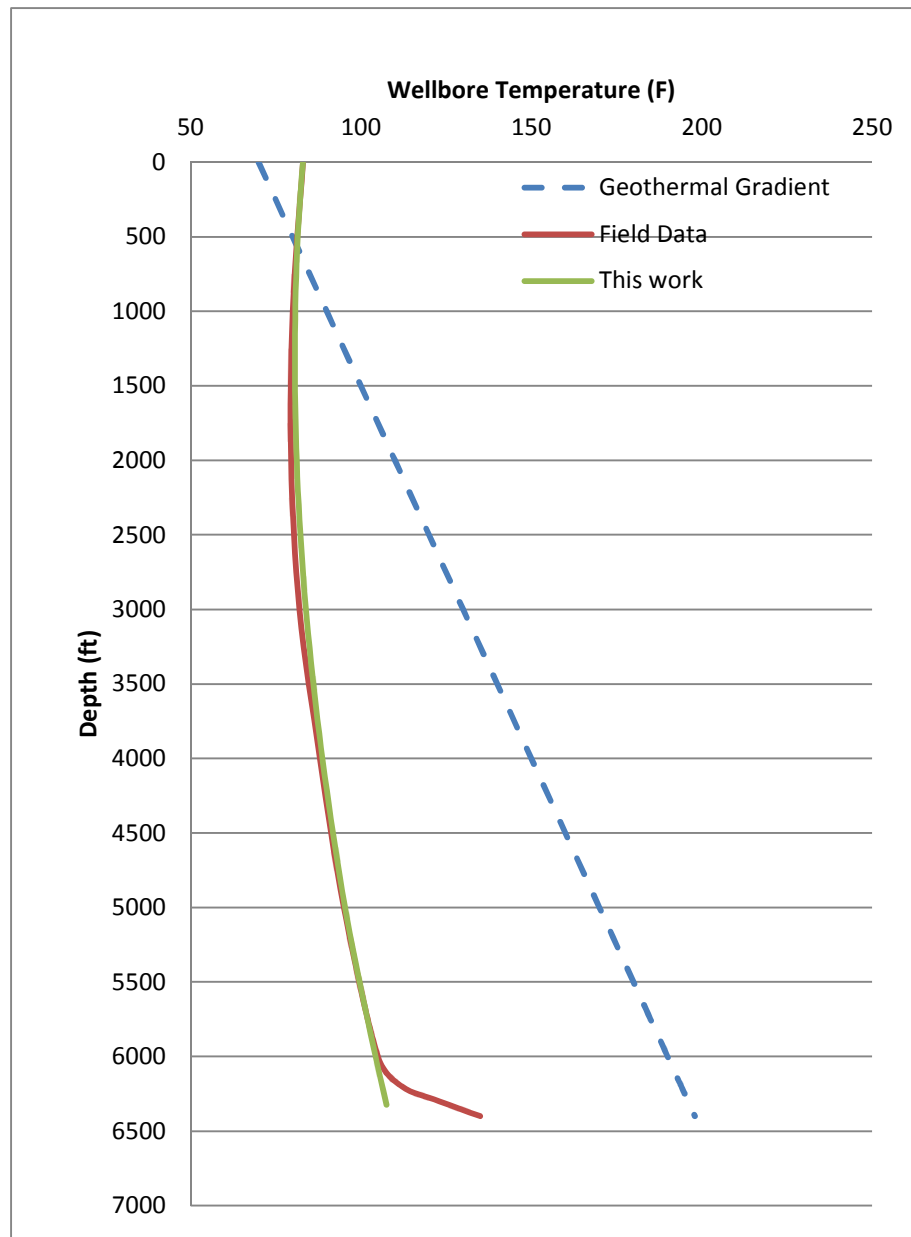


Figure 5-36 Wellbore temperature profile (case study #11)

In **Figure 5-36**, the temperature profile predicted by the WTP Simulator has been compared with the field data, showing a good agreement. A sensitivity study results are also presented in **Figure 5-37**. In **Figure 5-37**, the predicted wellbore temperature profiles are shown for 500, 900 and 1500 bbl/d injections of water. As it can be seen that the bottom hole temperature of injected water is higher for a slower injection

rate. In this calculation 122.192, 107.523 and 98.154°F are the temperatures of fluid at the entry point to the reservoir for injection rates of 500, 900 and 1500 bbl/d respectively. Thus, fluid with a slower rate of flow has more time to gain temperature from the surrounding media.

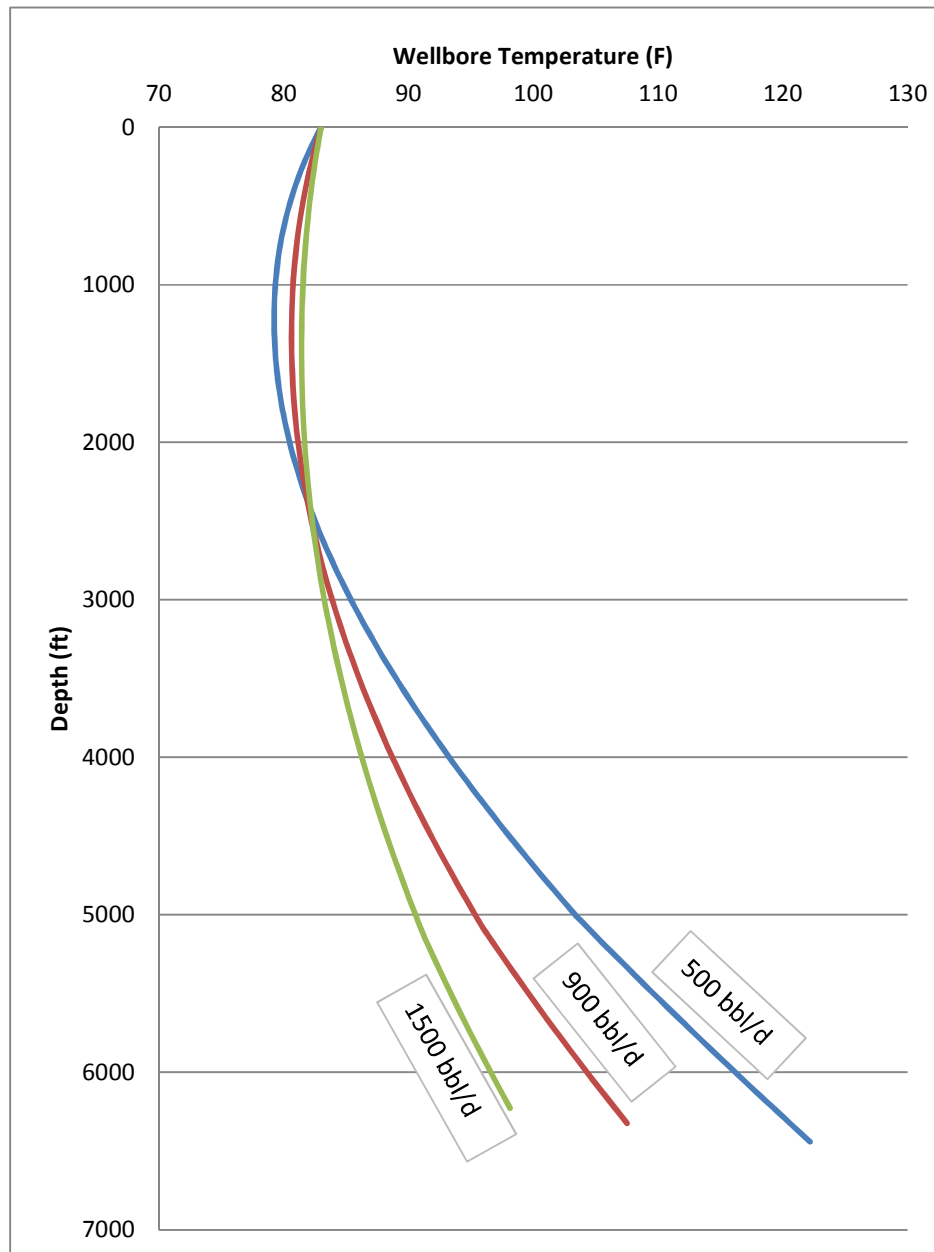


Figure 5-37 Predicted temperature profile for different injection rates (case study #11)

5.6 Summary

The key objectives of this chapter are to justify the potential application of the developed WTP simulator (the main outcome of this study) and its level of accuracy to deal with real field cases through validation of predicted results with field specific scenarios using field data and/or typically published field representative data. Eleven case studies have been considered in this study, which cover all types of fluid flow through the wellbore as well as fluid injection cases. Among these studies, three cases are used to justify the prediction of wellbore temperature profile in single phase liquid production. To justify the temperature profile of single phase gas production well, four cases are examined. Further, two cases for multi-phase fluid production wells, and two cases for injection scenarios are also studied to justify the results of this study. Based on the study it can be inferred that developed simulator can be used to predict the wellbore flowing temperature profiles for both injection and production wells flowing single phase gas, single phase liquid and multiphase fluids.

It is worth mentioning that computation time required by WTP Simulator for generating the flowing temperature profile for any of the cases discussed above is extremely confirming that this simulator is very practical especially for the theoretical prediction of flowing wellbore flowing temperature profile in a routine industry environment. Using the theoretically predicted profile in comparison with temperature survey data obtained by PLT or DTS system, it would be possible to identify many well problems associated with injection and production from anomalies.

Sensitivity analysis studies are also performed to investigate Joule Thompson effects and the effects of some key parameters such as injection and production rate, tubing size, oil gravity on the behaviour of wellbore following temperature profile in case of

single and multiphase fluids. The effects are highlighted in following conclusions based on the results of sensitivity study:

- The JT effect plays a vital role and influence substantially on the behaviour flowing temperature profile, especially for gas wells (both injection and production), and accurate prediction of this effect is very critical.
- Impurities such as water, N₂, CO₂, H₂S and so on produced with gas production can affect the JT effect. However, among these impurities, water production has more influence than the others on the JT effect. As the amount of water increases with produced gas, the temperature drop at the entry point decreases due to Joule Thomson effects, whereas for the same production case, the surface temperature increases due to the presence of water.
- Rate is another important production features that influences significantly the profile of wellbore temperature. For wells with the same well completion profile, the surface and wellbore temperatures are higher for higher oil production rate, which is due to the increase in produced fluid enthalpy, and heat gain from higher friction between fluid and tubing wall.
- The wellbore flowing temperature for production cases decreases with increase in the size of tubing diameter (i.e. internal diameter of tubing), as the larger tubing diameter facilitates larger surface area for transferring heat between wellbore fluid and its surroundings. However, the effect is opposite in case injection scenarios, where it may conversely cause temperature gain.
- The produced oil with higher degrees of API gravity has a lower surface temperature. This is due to the fact that hydrocarbon with higher degrees of API gravity has lower viscosity, and thereby the producing fluid has less friction with the tubing wall causing lesser heat gain due to friction, which results in lower temperature at the surface.
- Increasing injection rate increases the temperature at the entry point to the reservoir. This is due to the fact that the fluid with lower injection rate has

more time to gain heat from surrounding while moving from surface to the reservoir.

6

Conclusions and recommendations

6.1 Overview

This study aims to investigate the wellbore temperature profile along a flowing hydrocarbon production and injection wellbore, and its application for well maintenance and reservoir performance through development of a numerical tool. In the current study, a numerical model is developed which is a combination of flow equations, energy balance equations and thermodynamics principles. The model can simulate the heat transmission between wellbore and its surroundings, which enables the prediction of temperature profile along a flowing wellbore for production and injection well. A computer simulator named as WTP Simulator is developed in the FORTRAN language employing the developed numerical model. The potential application of the developed simulator and its accuracy are justified based on series of simulation results using actual field data obtained from a variety of published results; and through case studies. This chapter presents a summary of research findings and recommends possible new research areas for further investigation.

6.2 Conclusion

The main research features and results arising from the research and the simulator performance are summarised as follows.

6.2.1 The analytical model

A numerical model has been developed for calculation of heat transmission at any single point along a well depth. The algorithm of calculation has been expressed in section 3.3.4, and the major findings can be summarised as follows:

- The application of basic heat transfer mechanisms along with energy, momentum and conservation of mass equation as well as thermodynamics principles produce an applicable analytical model. The analytical model is applied throughout this study to develop a tool for prediction of heat transmission at any single point of a wellbore.
- Thermal resistivity of each layer surrounding the wellbore controls the rate of heat transmission between the wellbore fluid and the earth. For example, the thermal resistivity of different layers around a wellbore such as annulus fluid, cement sheaths and earth affect the overall heat transfer coefficient and finally the rate of heat transmission between wellbore fluid and the earth. In this study a method for calculation of overall heat transfer coefficient based on the heat resistivity of different layers around a wellbore has been developed.
- The study investigates and reveals the significant effect of radiation heat transfer caused by the annulus. For a typical case study(detailed in chapter three) the temperature of the casing at the surface when considering radiation heat transfer mechanism is about 39% more than when radiation effects are ignored.

- In the current study, it is investigated that ANSYS software may be a useful tool for evaluation of temperature loss at any single point in the wellbore. ANSYS may be useful to analyse the temperature effects in the localized area in the wellbore. However, it not convenient to generate the temperature along the long wellbore, which requires a very long computational time involving with very cumbersome modelling process. In this study, the ANSYS was used for the purpose of validating the results from the study of temperature loss (gain) at any single point in a wellbore to its surroundings.

6.2.2 Features of the WTP simulator

The WTP simulator can be used as a powerful tool to general flowing temperature profile theoretically; and applicable to analyse injection production scenarios to identify many issues, and/or well problems based on temperature anomalies. Followings are main features of this simulator. .

- This simulator can simulate a wide range of production and injection scenarios as well as covering different types of fluid flow along a wellbore such as gas, liquid and multiphase fluid.
- The simulator simply requires very basic information related to wellbore such as tubular sizes and its material properties (i.e. mechanical and heat transfer properties), well depth, size and geothermal properties of wellbore surroundings (e.g. rocks), injection/production related parameters such as production rate, pressure, geothermal temperature, and PVT properties of flowing fluids, to generate the temperature profile for a given condition. .
- The simulator has the capability of dealing with the any gas mixture regardless whether the composition of that gas mixture is known or unknown.

- The simulator has the capacity to predict the flowing wellbore temperature profile for both injection and production case.
- The simulator works based on simplified numerical model which requires significantly low computation time and hence very appropriate for routine industry works.

6.2.3 Performance of the WTP Simulator

Eleven cases are simulated to justify the capability, applicability and accuracy of calculations and the performance of this WTP simulator. It is established from the case study that the WTP simulator is capable of dealing with various production/injection situations for single and multiphase for the prediction of wellbore temperature profile. This simulator also has the potentials to simulate CO₂ injected well.

6.2.4 Research Outcomes and Findings

The main findings of this research have been summarized below:

- As a major outcome of this study, the Wellbore Temperature Profile (WTP) simulator has been developed, which can be successfully used to predict flowing temperature profile of injection/production well with reasonable accuracy and have wide capabilities to deal with single and multiphase fluid flow.
- For the case of gas production, a wide range of study has been done to investigate the Joule Thomson (JT) effect on the wellbore temperature profile as well as the surface flowing temperature. It is inferred that the Joule Thomson effect has significant impact on the flowing temperature, especially in the case of gas flow. The JT effect increases significantly specifically at

the high gas production rate, which can cause a substantial drop in temperature especially at the entry point.

- In case of a well producing water and gas, as the amount of water increases with produced gas, the temperature drop at the entry point decreases due to Joule Thomson effects, whereas for the same production case, the surface temperature increases due to the presence of water.
- In case of gas well producing with impurities such as water, N₂, CO₂, H₂S and so on can affect the JT effect. However, among these impurities, water production has more influence than the others on the JT effect.
- In case of a production well producing single oil and/or liquid (i.e. oil plus water), the behaviour flowing temperature profile along the wellbore and final surface temperature would vary depending on well completion profile and the rate of production. For instance, wells with the same well completion profile, the surface and wellbore temperatures are higher for higher oil production rate.
- Obviously the wellbore flowing temperature for production cases decreases with increase in the size of tubing diameter (i.e. internal diameter of tubing), as the larger tubing diameter facilitates larger surface area for transferring heat between wellbore fluid and its surroundings. However, the effect is opposite in case injection scenarios, where it may conversely cause temperature gain.
- The produced oil gravity (API number) plays a significant role on the behaviour of flowing temperature profile. For instance, higher the degrees of API gravity is lower the surface temperature.
- In case of liquid (e.g. liquefied N₂) injection, increasing injection rate increases the temperature at the entry point to the reservoir due to the fact that the fluid with lower injection rate has more time to gain heat from surrounding while moving from surface to the reservoir.
- In case of multiphase flow, the phase contribution effects the temperature profiles substantially.

6.3 Recommendations

The following recommendations are suggested for further studies:

1. In this study emphasis is given in the case of injection or production well flowing single or multiphase flow. This study does not include some complex production cases where the both injection and production takes place in the same well (e.g. production well with gas lift). Further study is required to extend the capability of the developed simulator for dealing with such complex production conditions.
2. PR-EOS is the only equation of state which is applied for evaluation of fluid properties through this study, since it is mostly appropriate for typical petroleum fluid and reliably used in the industry. However, extension of the simulator to support alternative equations of state would be beneficial to cover range of hydrocarbon mixture.
3. The current study has been focused on only for vertical well flowing multiphase fluid; and the program is designed for vertical and near vertical well bores. However, horizontal well technology is the key technology especially for the exploitation of unconventional resources such as tight gas, shale gas, as well as geothermal resources. Flowing behaviour and temperature profile along the horizontal well differs many ways. It is strongly recommended to conduct further research in this area. An extension of current resreach to simulate temperature profile along highly deviated and horizontal wellbores for different production scenarios would be advantageous.

The WTP Simulator considers the reservoir temperature as at the entry point temperature. However, the simulation of temperature distribution in the reservoir can be added to the WTP Simulator so that the temperature study can be managed from the reservoir to the surface.

References

- Adeyemi, W., 2009. Predicting Two-Phase Flow Regimes in Segments of a Gas/Condensate Well.
- Ahmed, T.H. (Editor), 1946. Reservoir Engineering Handbook. Gulf Professional Pub., Boston.
- Al-Beaiji, T.M., Al-Abdullatif, M.M., Al-Dossari, S.M. and Zeybek, M., 2005. Identification of Water Entry with New Integrated Production Logging Tool in Challenging Horizontal Wells, International Petroleum Technology Conference. International Petroleum Technology Conference, Doha, Qatar.
- Al-Zaharnah, I. and Yilbas, B., 2004. Thermal Analysis in Pipe Flow: Influence of Variable Viscosity on Entropy Generation. *Entropy*, 6(3): 344-363.
- Alves, I.N., Alhanati, F.J.S. and Shoham, O., 1992. A Unified Model for Predicting Flowing Temperature Distribution in Wellbores and Pipelines. *SPE Production Engineering*, 7(4): 363-367.
- Arnaut, I. et al., 2008. Optimizing Production in Maximum Reservoir Contact Wells with Intelligent Completions and Optical Downhole Monitoring System, Abu Dhabi International Petroleum Exhibition and Conference. Society of Petroleum Engineers, Abu Dhabi, UAE.
- Arnold, F.C., 1990. Temperature Variation in a Circulating Wellbore Fluid. *J. Energy Resources Technology*, 112: 79 - 83.

- Atesmen, A.K., 2009. Everyday Heat Transfer Problems: sensitivities to governing variables. ASME Press, New York, 235 pp.
- Bahrami, H., Rezaee, R., Hossain, M.M., Alizadeh, N. and Fathi, A., 2012. Effect of Sand Lens Size and Hydraulic Fractures Parameters on Gas In Place Estimation Using 'P/Z vs Gp Method' in Tight Gas Reservoirs, SPE/EAGE European Unconventional Resources Conference and Exhibition. Society of Petroleum Engineers, Vienna, Austria.
- Barrett, E.E., Abbasy, I., Wu, C.R., You, Z. and Bedrikovetsky, P., 2012. Improved Determination of Well Rate From Temperature and Pressure Distributions Along the Well, North Africa Technical Conference and Exhibition. Society of Petroleum Engineers, Cairo, Egypt.
- Barrufet, M.A., Rasool, A. and Aggour, M., 1995. Prediction of Bottomhole Flowing Pressures in Multiphase Systems Using a Thermodynamic Equation of State, SPE Production Operations Symposium, Oklahoma City, Oklahoma.
- Bannister, C.E. and Bengel, O.G., 1981. PIPE FLOW RHEOMETRY: RHEOLOGICAL ANALYSIS OF A TURBULENT FLOW SYSTEM USED FOR CEMENT PLACEMENT, SPE Annual Technical Conference and Exhibition. 1981 Copyright 1981, Society of Petroleum Engineers of AIME, San Antonio, Texas.
- BAXENDELL, P.B. and THOMAS, R., 1961. The Calculation of Pressure Gradients In High-Rate Flowing Wells.
- Beggs, H.D., 2003. Production Optimization Using NODALTM Analysis. OGCI and Petroskills, Tulsa, 411 pp.

- Bradley, H.B., 1987. Petroleum Engineering Handbook. Society of Petroleum Engineers, Texas.
- Brown, G.A., 2006. Monitoring Multilayered Reservoir Pressures and Gas/Oil Ratio Changes Over Time Using Permanently Installed Distributed Temperature Measurements, SPE Annual Technical Conference and Exhibition, San Antonio, Texas, USA.
- Bünz, A.P., Dohrn, R. and Prausnitz, J.M., 1991. Three-phase flash calculations for multicomponent systems. *Computers & Chemical Engineering*, 15(1): 47-51.
- C.V.Kirkpatrick, 1959. *Advances in Gas-lift Technology*. American Petroleum Institute.
- Camilleri, L.A.P., Akram, A.H. and Bravo, M.E.Q., 2010. Combining the use of ESPs and Distributed Temperature Sensors to Determine Layer Water Cut, PI and Reservoir Pressure, SPE Production and Operations Conference and Exhibition, Tunis, Tunisia.
- Carslaw, H.S. and Jaeger, J.C. (Editors), 1959. *Conduction of heat in solids*. Oxford University Press, London.
- Chin, Y.D. and Wang, X., 2004. Mechanics of Heat Loss in Dry Tree Top-Tensioned Risers.
- Cox, B. and Molenaar, M., 2013. Field Cases of Hydraulic Fracture Stimulation Diagnostics Using Fiber Optic Distributed Acoustic Sensing (DAS) Measurements and Analyses, 2013 SPE Middle East Unconventional Gas

Conference & Exhibition. Society of Petroleum Engineers, Muscat, Sultanate of Oman.

CO2CRC Otway project webpage. <http://www.co2crc.com.au/otway/>

Camilleri, L.A.P., Akram, A.H. and Bravo, M.E.Q., 2010. Combining the use of ESPs and Distributed Temperature Sensors to Determine Layer Water Cut, PI and Reservoir Pressure, SPE Production and Operations Conference and Exhibition, Tunis, Tunisia.

Cook, P.J., 2010. CO2CRC Otway Project.

Cox, S.A., Sutton, R.P. and Blasingame, T.A., 2006. Errors Introduced by Multiphase Flow Correlations on Production Analysis, SPE Annual Technical Conference and Exhibition, San Antonio, Texas, USA.

Curtis, M.R. and Witterholt, E.J., 1973. USE OF THE TEMPERATURE LOG FOR DETERMINING FLOW RATES IN PRODUCING WELLS, Fall Meeting of the Society of Petroleum Engineers of AIME. 1973 Copyright 1973, American Institute of Mining, Metallurgical, and Petroleum Engineers, Inc., Las Vegas, Nevada.

Dake, L.P., 1978. Fundamentals of Reservoir Engineering. Elsevier, Amsterdam, 433 pp.

Danesh, A., 1998. PVT and phase behaviour of petroleum reservoir fluids. Elsevier, New York.

- Donald, L.K. and Robert, L.L., 1990. Natural gas engineering: production and storage. McGraw-Hill Book Co, Singapore, 751 pp.
- Durrant, A.J. and Thambynayagam, R.K.M., 1986. Wellbore Heat Transmission and Pressure Drop for Steam/Water Injection and Geothermal Production: A Simple Solution Technique. SPE Reservoir Engineering, 1(2): 148-162.
- Economides, M.J., Hill, A.D. and Ehlig-Economides, C., 1993. Petroleum Production Systems. Prentice Hall PTR, New Jersey, 611 pp.
- Edmister, W.C. and Lee, B.I. (Editors), 1984. Applied hydrocarbon thermodynamics, 1. Gulf Pub. Co., Houston.
- Elshahawi, H., Osman, M.S. and Sengul, M., 1999. Use Of Temperature Data in Gas Well Tests, SPE Annual Technical Conference and Exhibition, Houston, Texas.
- FANCHER JR., G.H. and BROWN, K.E., 1963. Prediction of Pressure Gradients for Multiphase Flow in Tubing.
- Farshad, F., Garber, J.D. and Lorde, J.N., 1999. Predicting Temperature Profiles in Producing Oil Wells Using Artificial Neural Networks, Latin American and Caribbean Petroleum Engineering Conference. Society of Petroleum Engineers, Caracas, Venezuela.
- Firoozabadi, A., 1999. Thermodynamics of Hydrocarbon Reservoirs. McGraw-Hill, New York, 353 pp.

- Fryer, V.I., Dong, S., Otsubo, Y., Brown, G.A. and Guilfoyle, P., 2005. Monitoring of Real-Time Temperature Profiles Across Multizone Reservoirs during Production and Shut in Periods Using Permanent Fiber-Optic Distributed Temperature Systems, SPE Asia Pacific Oil and Gas Conference and Exhibition. Society of Petroleum Engineers, Jakarta, Indonesia.
- Gao, C.H., Rajeswaran, R.T. and Nakagawa, E.Y., 2007. A Literature Review on Smart Well Technology, Production and Operations Symposium. Society of Petroleum Engineers, Oklahoma City, Oklahoma, U.S.A.
- Golan, M. and Whitson, C.H. (Editors), 1991. Well Performance. Prentice Hall Co., 669 pp.
- Hagedorn, A.R. and Brown, K.E., 1965. Experimental Study of Pressure Gradients Occurring During Continuous Two-Phase Flow in Small-Diameter Vertical Conduits.
- Hasan, A.R. and Kabir, C.S., 2002. Fluid Flow and Heat Transfer in Wellbores. Society of Petroleum Engineers, Richardson, Texas, 181 pp.
- Hasan, A.R., Kabir, C.S. and Wang, X., 1997. Development and Application of a Wellbore/Reservoir Simulator for Testing Oil Wells. SPE Formation Evaluation, 12(3): 182-188.
- Hasan, A.R. and Kabir, C.S., 1991. Heat Transfer During Two-Phase Flow in Wellbores; Part I-Formation Temperature, SPE Annual Technical Conference and Exhibition. 1991 Copyright 1991, Society of Petroleum Engineers, Inc., Dallas, Texas.

- Hasan, A.R. and Kabir, C.S., 1994. Aspects of Wellbore Heat Transfer During Two-Phase Flow (includes associated papers 30226 and 30970). SPE Production & Operations(08).
- Hasan, A.R., Kabir, C.S. and Wang, X., 1998. Wellbore Two-Phase Flow and Heat Transfer During Transient Testing. SPE Journal(06).
- Hasan, A.R., Kabir, C.S. and Wang, X., 2007. A Robust Steady-State Model for Flowing-Fluid Temperature in Complex Wells, SPE Annual Technical Conference and Exhibition. Society of Petroleum Engineers, Anaheim, California, U.S.A.
- Hagoort, J., 2005. Prediction of wellbore temperatures in gas production wells. Journal of Petroleum Science and Engineering, 49(1–2): 22-36.
- Hasan, A.R. and Kabir, C.S., 2012. Wellbore heat-transfer modeling and applications. Journal of Petroleum Science and Engineering, 86–87(0): 127-136.
- Hasan, A.R., Kabir, C.S. and Wang, X., 2009. A Robust Steady-State Model for Flowing-Fluid Temperature in Complex Wells. SPE Production & Operations(05).
- Hearst, J.R., Nelson, P.H. and Paillet, F.L., 2000. Well logging for physical properties. John Wiley & Sons.
- Hearst, J.R., nelson, P.N. and Paillet, F.L. (Editors), 2000b. Well Logging for Physical Properties. John Wiley & Sons Ltd, Chichester.

- Hill, A.D., 1990. Production Logging - Theoretical and Interpretive Elements, 154 pp.
- Holley, E.H., Molenaar, M.M., Fidan, E. and Banack, B.M., 2012. Interpreting Uncemented Multistage Hydraulic-Fracturing Completion Effectiveness Using Fiber-Optic DTS Injection Data, SPE Middle East Unconventional Gas Conference and Exhibition. Society of Petroleum Engineers, Abu Dhabi, UAE.
- Holman, J.P., 1989. Heat Transfer. McGraw-Hill Book Co, Singapore, 676 pp.
- Huebsch, H.T. et al., 2008. Monitoring Inflow Distribution in Multi-zone, Velocity String Gas Wells Using Slickline Deployed Fiber Optic Distributed Temperature Measurements, SPE Annual Technical Conference and Exhibition. Society of Petroleum Engineers, Denver, Colorado, USA.
- Huygen, H.H.A. and Huitt, J.L., 1966. Wellbore Heat Losses and Casing Temperatures during Steam Injection. American Petroleum Institute.
- Izgec, B., Hasan, A.R., Lin, D. and Kabir, C.S., 2010. Flow-Rate Estimation From Wellhead-Pressure and -Temperature Data. SPE Production & Operations(02).
- Johnson, D.O., Sierra, J.R., Kaura, J.D. and Gualtieri, D., 2006. Successful Flow Profiling of Gas Wells Using Distributed Temperature Sensing Data, SPE Annual Technical Conference and Exhibition. Society of Petroleum Engineers, San Antonio, Texas, USA.
- Jr., H.D. and Ros, N.C.J., 1963. Vertical flow of gas and liquid mixtures in wells. World Petroleum Congress.

- Ikoku, C.U., 1984. Natural gas reservoir engineering. John Wiley and Sons, New York.
- Lawson, J.D. and Brill, J.P., 1974. A Statistical Evaluation of Methods Used To Predict Pressure Losses for Multiphase Flow in Vertical Oilwell Tubing. *Journal of Petroleum Technology*, 26(8): 903-914.
- Lee, J. and Wattenbargar, R.A., 1996. Gas Reservoir Engineering, 5. Society of Petroleum Engineers, Texas, 349 pp.
- Kabir, C.S., Hasan, A.R., Jordan, D.L. and Wang, X., 1996a. A Wellbore/Reservoir Simulator for Testing Gas Wells in High-Temperature Reservoirs. *SPE Formation Evaluation*, 11(2): 128-134.
- Kabir, C.S., Hasan, A.R., Kouba, G.E. and Ameen, M., 1996b. Determining Circulating Fluid Temperature in Drilling, Workover, and Well Control Operations. *SPE Drilling & Completion*, 11(2): 74-79.
- Kabir, C.S. and Hasan, A.R., 1998. Does Gauge Placement Matter in Downhole Transient-Data Acquisition? *SPE Reservoir Evaluation & Engineering*(02).
- Kabir, C.S., Izgec, B., Hasan, A.R. and Wang, X., 2012. Computing flow profiles and total flow rate with temperature surveys in gas wells. *Journal of Natural Gas Science and Engineering*, 4(0): 1-7.
- Keller, H.H., Couch, E.J. and Berry, P.M., 1973. Temperature Distribution in Circulating Mud Columns. *Society of Petroleum Engineers Journal*, 13(1): 23-30.

- Kragas, T.K., Williams, B.A. and Myers, G.A., 2001. The Optic Oil Field: Deployment and Application of Permanent In-well Fiber Optic Sensing Systems for Production and Reservoir Monitoring, SPE Annual Technical Conference and Exhibition. Society of Petroleum Engineers, New Orleans, Louisiana.
- Kuchuk, F.J., Lenn, C., Hook, P. and Fjerstad, P., 1998. Performance Evaluation of Horizontal Wells, SPE Asia Pacific Conference on Integrated Modelling for Asset Management. 1998 Copyright 1998, Society of Petroleum Engineers, Inc., Kuala Lumpur, Malaysia.
- Lesem, L.B., Greytok, F., Marotta, F. and Jr., J.J.M., 1957. A Method of Calculating the Distribution of Temperature in Flowing Gas Wells.
- Li, Z. and Zhu, D., 2009. Predicting Flow Profile of Horizontal Wells by Downhole Pressure and DTS Data for Infinite Waterdrive Reservoir, SPE Annual Technical Conference and Exhibition, New Orleans, Louisiana.
- Mitchell, R.F. and Wedelich III, H.F., 1989. Prediction of Downhole Temperatures Can Be Key for Optimal Wellbore Design, SPE Production Operations Symposium. 1989 Copyright 1989, Society of Petroleum Engineers, Inc., Oklahoma City, Oklahoma.
- Millikan, C.V., 1941. Temperatures surveys in oil wells. Trans. AIME, 142: 15-23.
- Mills, A., Basic heat and mass transfer / A.F. Mills.

- Mukherjee, H. and Brill, J.P., 1985. Empirical equations to predict flow patterns in two-phase inclined flow. *International Journal of Multiphase Flow*, 11(3): 299-315.
- Muradov, K.M. and Davies, D.R., 2008. Prediction of Temperature Distribution in Intelligent Wells, SPE Russian Oil and Gas Technical Conference and Exhibition. Society of Petroleum Engineers, Moscow, Russia
- Nelson, P.A., 1987. Rapid phase determination in multiple-phase flash calculations. *Computers & Chemical Engineering*, 11(6): 581-591.
- Nowak, T.J., 1953. The Estimation of Water Injection Profiles From Temperature Surveys.
- Ohanomah, M.O. and Thompson, D.W., 1984. Computation of multicomponent phase equilibria—Part I. Vapour-liquid equilibria. *Computers & Chemical Engineering*, 8(3–4): 147-156.
- Orkiszewski, J., 1967. Predicting Two-Phase Pressure Drops in Vertical Pipe.
- Ouyang, L.-B. and Belanger, D.L., 2006. Flow Profiling by Distributed Temperature Sensor (DTS) System—Expectation and Reality. *SPE Production & Operations*, 21(2): pp. 269-281.
- P. L. Chueh and Prausnitz, J.M., 1967. Vapor-liquid equilibria at high pressures: Calculation of partial molar volumes in nonpolar liquid mixtures. *AIChE*, 13(6): 1099-1107.

- Pacheco, E.F. and Farouq Ali, S.M., 1972. Wellbore Heat Losses and Pressure Drop In Steam Injection. SPE Journal of Petroleum Technology(2): 139-144.
- Paterson, L., Ennis-King, J.P. and Sharma, S., 2010. Observations of Thermal and Pressure Transients in Carbon Dioxide Wells, SPE Annual Technical Conference and Exhibition. Society of Petroleum Engineers, Florence, Italy.
- Pasinato, H.D., 2011. Velocity and temperature dissimilarity in fully developed turbulent channel and plane Couette flows. International Journal of Heat and Fluid Flow, 32(1): 11-25.
- Peng, D.-Y. and Robinson, D.B., 1976. A New Two-Constant Equation of State. Industrial & Engineering Chemistry Fundamentals, 15(1): 59-64.
- Perry, R.H., Green, D.W. and Maloney, J.O. (Editors), 1997. Perry's chemical engineers' handbook. . McGraw-Hill, New York.
- Petricola, M.F.J. and Watfa, M., 1993. Multiwell Application of Downhole Temperature Profiles for Crossflow Analysis, Middle East Oil Show. 1993 Copyright 1993, Society of Petroleum Engineers, Inc., Bahrain.
- Pimenov, V., Brown, G.A., Tertychnyi, V.V., Shandrygin, A. and Popov, Y., 2005. Injectivity Profiling in Horizontal Wells via Distributed Temperature Monitoring, SPE Annual Technical Conference and Exhibition. Society of Petroleum Engineers, Dallas, Texas
- Poettman, F.H. and Carpenter, P.G., 1952. The Multiphase Flow of Gas, Oil, and Water Through Vertical Flow Strings with Application to the Design of Gas-lift Installations. American Petroleum Institute.

- Pourafshary, P., Varavei, A., Sepehrnoori, K. and Podio, A., 2008. A Compositional Wellbore/Reservoir Simulator to Model Multiphase Flow and Temperature Distribution, International Petroleum Technology Conference. International Petroleum Technology Conference, Kuala Lumpur, Malaysia.
- RAMEY JR., H.J., 1962. Wellbore Heat Transmission. SPE Journal of Petroleum Technology, 14(4).
- Rasoul, R.R.A., 2012. Novel Applications of Distributed Temperature Measurements to Estimate Zonal Flow Rate and Pressure in Offshore Gas Wells, SPE International Production and Operations Conference & Exhibition. Society of Petroleum Engineers, Doha, Qatar.
- Raymond, L.R., 1969. Temperature Distribution in a Circulating Drilling Fluid.
- Reyes, R.P., Yeager, V.J., Glasbergen, G., Parrish, J.L. and Tucker, R., 2011. DTS Sensing: An Introduction To Permian Basin With A West-Texas Operator, SPE Annual Technical Conference and Exhibition. Society of Petroleum Engineers, Denver, Colorado, USA.
- Ros, D., 1963. Vertical flow of gas and liquid mixtures in wells. World Petroleum Congress.
- ROS, N.C.J., 1961. Simultaneous Flow of Gas and Liquid As Encountered in Well Tubing.
- Sagar, R., Doty, D.R. and Schmidt, Z., 1991. Predicting Temperature Profiles in a Flowing Well. SPE Production Engineering, 6(4): 441-448.

Salehi-moorkani, R. and Mohamadipour, M., 2011. Application of Production Logging and Noise Logging for Well Leak Detection, Case Study in Persian Wells, SPE Project and Facilities Challenges Conference at METS. Society of Petroleum Engineers, Doha, Qatar.

SATTER, A., 1965. Heat Losses During Flow of Steam Down a Wellbore.

Sharafutdinov, R.F., 2012. Application of active temperature logging at oilfields of Russia, SPE Russian Oil and Gas Exploration and Production Technical Conference and Exhibition. Society of Petroleum Engineers, Moscow, Russia.

Shiu, K.C. and Beggs, H.D., 1980a. Predicting temperatures in flowing oil wells. *Journal of Energy Resources and Technology*, 102(1).

Shlumberger, M., Doll, H.G. and Perebinossoff, A.A., 1937. Temperature measurements in oil wells. *J. Ints. Pet. Technologists*, 23(159): 1-25.

Smolen, J.J., 1996. Cased Hole and Production Log Evaluation. PennWell, Tulsa.

Sofyan, Y., Ghajar, A.J. and Gasem, K.A.M., 2003. Multiphase Equilibrium Calculations Using Gibbs Minimization Techniques. *Industrial & Engineering Chemistry Research*, 42(16): 3786-3801.

Spindler, R.P., 2011. Analytical Models for Wellbore-Temperature Distribution. *SPE Journal*, 16(1): pp. 125-133.

SQUIER, D.P., SMITH, D.D. and DOUGHERTY, E.L., 1962. Calculated Temperature Behavior of Hot-Water Injection Wells.

- Steffensen, R.J. and Smith, R.C., 1973. The Importance of Joule-Thomson Heating (or Cooling) in Temperature Log Interpretation, Fall Meeting of the Society of Petroleum Engineers of AIME. 1973 Copyright 1973, American Institute of Mining, Metallurgical, and Petroleum Engineers, Inc., Las Vegas, Nevada.
- Sun, K., Guo, B. and Saputelli, L., 2011. Multinode Intelligent-Well Technology for Active Inflow Control in Horizontal Wells. *SPE Drilling & Completion*, 26(3): pp. 386-395.
- Sun, K., Omole, O., Saputelli, L. and Gonzalez, F., 2012. Transferring Intelligent-Well-System Triple-Gauge Data Into Real-Time Flow Allocation. *SPE Drilling & Completion*, 27(2): pp. 264-281.
- Tansev, E., Startzman, R.A. and Cooper, A.M., 1975. Predicting Pressure Loss and Heat Transfer in Geothermal Wellbores, Fall Meeting of the Society of Petroleum Engineers of AIME. 1975 Copyright 1975, Dallas, Texas.
- Tariq, S.M. and Ayestaran, L.C., 1991. Analyses and Applications of Pressure, Flow Rate, and Temperature Measurements During a Perforating Run. *SPE Production Engineering*, 6(1): 83-92.
- Tarom, N., Moshfeghian, M., Jalali, F. and Mashat, A., 2002. Determination of Retrograde Condensation Region of Reservoir Fluids by MNM EOS, Tehran and Qatar Universities, Tehran and Doha.
- Vilaseca, O., Llovel, F., Yustos, J., Marcos, R.M. and Vega, L.F., 2010. Phase equilibria, surface tensions and heat capacities of hydrofluorocarbons and their mixtures including the critical region. *The Journal of Supercritical Fluids*, 55(2): 755-768.

- Vollmer, D.P., Fang, C.S., Ortego, A.M. and Lemoine, E., 2004. Convective Heat Transfer in Turbulent Flow: Effect of Packer Fluids on Predicting Flowing Well Surface Temperatures, SPE International Symposium and Exhibition on Formation Damage Control. Society of Petroleum Engineers, Lafayette, Louisiana.
- Wade, R.T., Cantrell, R.C., Poupon, A. and Moulin, J., 1965. Production Logging-The Key to Optimum Well Performance.
- Wang, X., Lee, J. and Vachon, G., 2008. Distributed Temperature Sensor (DTS) System Modeling and Application, SPE Saudi Arabia Section Technical Symposium. Society of Petroleum Engineers, Al-Khobar, Saudi Arabia.
- Weaver, M.A. et al., 2005. Installation and Application of Permanent Downhole Optical Pressure/Temperature Gauges and Distributed Temperature Sensing in Producing Deepwater Wells at Marco Polo, SPE Annual Technical Conference and Exhibition, Dallas, Texas.
- Willhite, G.P., 1967. Over-all Heat Transfer Coefficients in Steam And Hot Water Injection Wells. SPE Journal of Petroleum Technology(05).
- Wilson, G.A., 1964. A modified Redlich-Kwong equation of state applicable to general physical data calculations. AIChE.
- Witterholt, E.J. and Tixier, M.R., 1972. TEMPERATURE LOGGING IN INJECTION WELLS, Fall Meeting of the Society of Petroleum Engineers of AIME. 1972 Copyright 1972 American Institute of Mining, Metallurgical, and Petroleum Engineers, Inc., San Antonio, Texas.

- Wood, P. et al., 2010. Monitoring Flow and Completion Integrity of a North Sea Subsea HPHT Appraisal Well During an Extended Well Test Using Permanently Installed Fiber-Optic Temperature Sensors, SPE Deepwater Drilling and Completions Conference. Society of Petroleum Engineers, Galveston, Texas, USA.
- Wooley, G.R., 1980. Computing Downhole Temperatures in Circulation, Injection, and Production Wells. *Journal of Petroleum Technology*, 32(9): 1509-1522.
- Wu, Y.-S. and Pruess, K., 1990. An Analytical Solution for Wellbore Heat Transmission in Layered Formations (includes associated papers 23410 and 23411). *SPE Reservoir Engineering*, 5(4): 531-538.
- Yoshioka, K., Zhu, D., Hill, A.D., Dawkrajai, P. and Lake, L.W., 2006. Detection of Water or Gas Entries in Horizontal Wells From Temperature Profiles, SPE Europec/EAGE Annual Conference and Exhibition. Society of Petroleum Engineers, Vienna, Austria.
- Yoshioka, K., Zhu, D., Hill, A.D., Dawkrajai, P. and Lake, L.W., 2007. Prediction of Temperature Changes Caused by Water or Gas Entry Into a Horizontal Well. *SPE Production & Operations*, 22(4): pp. 425-433.
- Yoshioka, K., Zhu, D., Hill, A.D., Dawkrajai, P. and Lake, L.W., 2005. A Comprehensive Model of Temperature Behavior in a Horizontal Well, SPE Annual Technical Conference and Exhibition. Society of Petroleum Engineers, Dallas, Texas.
- Yu, Y., Lin, T., Xie, H., Guan, Y. and Li, K., 2009. Prediction of Wellbore Temperature Profiles During Heavy Oil Production Assisted With Light Oil,

SPE Production and Operations Symposium. Society of Petroleum Engineers, Oklahoma City, Oklahoma.

Zhu, D., Achinivu, O.I. and Furui, K., 2008. An Interpretation Method of Downhole Temperature and Pressure Data for Flow Profiles in Gas Wells, SPE Russian Oil and Gas Technical Conference and Exhibition. Society of Petroleum Engineers, Moscow, Russia.

“Every reasonable effort has been made to acknowledge the owners of copyright material. I would be pleased to hear from any copyright owner who has been omitted or incorrectly acknowledged”.

APPENDICES

Appendix A: Calculation of heat transferred between the wellbore fluid and the surrounding

This appendix is intended to provide information about the applied mathematical equations for the calculation of heat transferred between the wellbore fluid and its surrounding which is as a contribution of convection, conduction and radiation of heat transfer mechanisms. As it mentioned within the thesis, in case of annulus, radiation heat transfer mechanism will be added to the others mechanisms, and will make more complex situation for calculation of heat transferred from the wellbore fluid towards the surrounding. The main purpose of this appendix is to show how different heat transfer mechanisms are applied to calculate the heat resistance of each layer that surrounds a wellbore.

Convective heat transfer between flowing fluid and innermost pipe

The heat energy transfers between flowing fluid and inside tubing wall based on the convective heat transfer mechanism, which can be determined by the following equation.

$$Q = 2\pi r_{it} h_w (T_f - T_{it}) \Delta L \quad \text{A-1}$$

Therefore;

$$R_w = \frac{1}{2\pi r_{it} \Delta L h_w} \quad \text{A-2}$$

The term h_w is the heat transfer film coefficient which is a function of the flowing fluid properties. For a two phase flow, the term h_w is dependent to the flow regime.

Conductive heat transfer equation for pipes

The steady-state, radial and one-dimensional heat conduction equation for pipes is expressed by:

$$R_p = \frac{\ln\left(\frac{r_{op}}{r_{ip}}\right)}{2\pi\Delta Lk_p} \quad \text{A-3}$$

Tubing resistivity modifications are required to account for the build-up of scale or paraffin on the pipe wall.

Heat transfer mechanisms through annulus

The total heat flux through annulus (between outside of tubing and inside of casing surfaces) may explain by:

$$Q = Q_r + Q_{cv} = 2\pi r_m h_{avg}(T_{ot} - T_{ic})\Delta L \quad \text{A-4}$$

At the following, step by step procedure of Q_r and Q_{cv} estimations can be seen.

- **Radiation heat transfer mechanism (Q_r) through annulus**

In case of annulus around a wellbore, because of tubing and casing physical properties, radiation heat transfer mechanism may apply. Therefore, the radiation heat exchange between tubing and casing may calculate by Holman (1986):

$$Q_r = \frac{\sigma A_{ot}(T_{ot}^4 - T_{ic}^4)}{\frac{1}{\epsilon_t} + \left(\frac{A_{ot}}{A_{ic}}\right)\left(\frac{1}{\epsilon_c} - 1\right)} \quad \text{A-5}$$

The area ratio $\frac{A_{ot}}{A_{ic}}$ of Equation A-5 may be replaced by the radius ratio $\frac{r_{ot}}{r_{ic}}$.

Therefore, the heat exchange per unit area of pipe may rewrite as following:

$$Q_r = \frac{\sigma(T_{ot}^4 - T_{ic}^4)}{\frac{1}{\epsilon_t} + \left(\frac{r_{ot}}{r_{ic}}\right)\left(\frac{1}{\epsilon_c} - 1\right)} \quad \text{A-6}$$

Where, the term σ is the Stefan-Boltzmann constant. The terms ϵ_t and ϵ_c refer to the emissivity of tubing and casing, respectively.

$$\sigma = 5.669 * 10^{-8} (W/m^2 \cdot K^4) = 0.1714 * 10^{-8} (Btu/h \cdot ft^2 \cdot R^4) \quad A-7$$

- **Convection heat transfer mechanism (Q_{cv}) through annulus**

The heat transfer through annulus is a function of temperature difference between tubing and casing, the gap width and height of annulus and the fluid properties such as viscosity, thermal capacity and thermal conductivity. Therefore:

$$Q_{cv} = 2\pi r_m h_{cv} (T_{ot} - T_{ic}) \Delta L \quad A-8$$

The convection heat transfer coefficient is explained by:

$$h_{cv} = \frac{K}{\delta} Nu_{\delta} \quad A-9$$

Nu_{δ} is the Nusselt number which is defined by:

$$Nu_{\delta} = 0.049 Ra^{0.333} Pr^{0.074} \quad A-10$$

Where, Equation A-10 is valid for the range of $5 * 10^4 < Ra < 7.17 * 10^4$.

Ra, Pr and Gr are the Rayleigh, Prandtl and Grashof numbers, respectively.

$$Ra = Gr \cdot Pr \quad A-11$$

$$Pr = \frac{C_p \mu}{k} \quad A-12$$

$$Gr = \frac{g \beta (T_{ot} - T_{ic}) \delta^3}{\nu^2}$$

Where β is the volume coefficient of expansion, c_p is the thermal capacity, μ is the dynamic viscosity and ν is the kinematic viscosity of the annulus fluid.

Also, r_m is the mean area for cylindrical annulus defined by:

$$r_m = \frac{r_{ic} - r_{ot}}{\ln(r_{ic}/r_{ot})} \quad A-13$$

Therefore, as a result of Equations A-4 to A-13, the resistance to radiation, natural convection and conduction heat transfer through the annulus may explain by:

$$R_a = \frac{1}{2\pi r_m \Delta L h_{avg}} \quad \text{A-14}$$

Heat transfer mechanism through the cement sheath

The steady-state, radial and one-dimensional heat transferred per unit surface area between the outer surface of the last casing and the cement sheath may apply by:

$$Q = \frac{2\pi k_{cmt}}{\ln\left(\frac{r_{ocmt}}{r_{oc}}\right)} (T_{ocmt} - T_{oc}) \quad \text{A-15}$$

Therefore, the resistance of conductive heat transfer through the ground may explain by:

$$R_{cmt} = \frac{\ln\left(\frac{r_{ocmt}}{r_{oc}}\right)}{2\pi \Delta L k_g} \quad \text{A-16}$$

Heat transfer mechanism through the ground

The process of heat transfer through ground may be the same as for cement sheath.

Therefore:

$$Q = \frac{2\pi k_g}{\ln\left(\frac{r_g}{r_{ocmt}}\right)} (T_{ocmt} - T_g) \quad \text{A-17}$$

And:

$$R_g = \frac{\ln\left(\frac{r_g}{r_{ocmt}}\right)}{2\pi \Delta L k_g} \quad \text{A-18}$$

Appendix B: Stewart et al mixing rules for the calculation of pseudo-critical properties of a sweet natural gas

Mole fraction, molecular weight, temperature and pressure critical properties of each component, and specific gravity of C₇₊ fraction are required to calculate pseudo-critical properties of a sweet natural gas using Stewart et al mixing rules. Following steps are guidance to this purpose.

1. Estimation of critical properties of C₇₊ fraction.

a. Estimation of boiling temperature.

$$T_{bc7+} = (4.5579M_{C7+}^{0.15178}\gamma_{C7+}^{0.15427})^3 \quad \text{B-1}$$

b. Calculation of pseudo-critical pressure of C₇₊ fraction.

$$P_{pc7+} = \exp \left[8.3634 - \frac{0.0566}{\gamma_{C7+}} - \left(0.24244 + \frac{2.2898}{\gamma_{C7+}} + \frac{0.1158}{\gamma_{C7+}^2} \right) \frac{T_{bc7+}}{1000} + \left(1.4685 + \frac{3.648}{\gamma_{C7+}} + \frac{0.47227}{\gamma_{C7+}^2} \right) \frac{T_{bc7+}^2}{10^7} - \left(0.42019 + \frac{1.6977}{\gamma_{C7+}^2} \right) \frac{T_{bc7+}^3}{10^{10}} \right] \quad \text{B-2}$$

c. Calculation of pseudo-critical temperature of C₇₊ fraction.

$$T_{pc7+} = (341.7 + 811\gamma_{C7+}) + (0.4244 + 0.1174\gamma_{C7+})T_{bc7+} + (0.4669 - 3.2623\gamma_{C7+}) \frac{10^5}{T_{bc7+}} \quad \text{B-3}$$

2. Calculation of correction factors for C₇₊ fraction.

$$F_j = \frac{1}{3} \left(\frac{yT_c}{P_c} \right)_{C7+} + \frac{2}{3} \left(\frac{y^2T_c}{P_c} \right)_{C7+} \quad \text{B-4}$$

$$\begin{aligned} \varphi_j = & 0.6081F_j + 1.1325F_j^2 - 14.004F_jy_{C7+} \\ & + 64.434F_jy_{C7+}^2 \end{aligned} \quad \text{B-5}$$

$$\begin{aligned} \varphi_k = & \left(\frac{T_c}{\sqrt{P_c}} \right)_{C7+} (0.3127y_{C7+} - 4.8156y_{C7+}^2 + \\ & 27.3751y_{C7+}^3) \end{aligned} \quad \text{B-6}$$

3. Calculation of pseudo-critical properties of the mixture.

a. Determination of J and K parameters.

$$J = \frac{1}{3} \sum_{i=1}^n \left(\frac{yT_c}{P_c} \right)_i + \frac{2}{3} \left[\sum_{i=1}^n \left(y \sqrt{\frac{T_c}{P_c}} \right)_i \right]^2 \quad \text{B-7}$$

$$K = \sum_{i=1}^n \left(\frac{yT_c}{\sqrt{P_c}} \right)_i \quad \text{B-8}$$

b. Correction of J and K parameters for C₇₊ fraction.

$$J' = J - \varphi_j \quad \text{B-9}$$

$$K' = K - \varphi_k \quad \text{B-10}$$

c. Calculation of pseudo-critical pressure and temperature.

$$T_{pc} = \frac{K'^2}{J'} \quad \text{B-11}$$

$$P_{pc} = \frac{T_{pc}}{J'} \quad \text{B-12}$$

Appendix C:

Parameters C1 to C5

Parameters C_1 to C_5 in Eq. 11 are calculated as follows:

$$C_1 = 0.96 + 0.008T_{pr} + \frac{0.22}{T_{pr}^2} \quad \text{C-19}$$

$$C_2 = 0.29 - 0.0635T_{pr} - \frac{0.865}{T_{pr}^2} \quad \text{C-20}$$

$$C_3 = \frac{0.00032 + 0.2T_{pr}^{-5.58}}{0.45 + T_{pr}^{-5.57}} \quad \text{C-21}$$

$$C_4 = \frac{-0.025 + 0.00013T_{pr}^{5.47}}{0.665 + T_{pr}^{5.47}} \quad \text{C-22}$$

$$C_5 = -0.0001 + \frac{9 * 10^{-5}}{1 - 6.466e^{(-1.815T_{pr})}} \quad \text{C-23}$$

And:

$$T_{pr} = \frac{T}{T_{pc}} \quad \text{C-24}$$

$$P_{pr} = \frac{P}{P_{pc}} \quad \text{C-25}$$

Derivatives C1 to C5

The details of derivatives in the Eq. 13 are as follows:

$$\left(\frac{\partial C_1}{\partial T_{pr}}\right)_p = 0.008 - \frac{0.44}{T_{pr}^3} \quad \text{C-26}$$

$$\left(\frac{\partial C_2}{\partial T_{pr}}\right)_p = -0.0635 + \frac{1.73}{T_{pr}^3} \quad \text{C-27}$$

$$\left(\frac{\partial C_3}{\partial T_{pr}}\right)_p = -\frac{0.5022T_{pr}^{-6.57} - 0.0017824T_{pr}^{-6.58} + 0.002T_{pr}^{-12.15}}{(0.45 + T_{pr}^{-5.57})^2} \quad \text{C-28}$$

$$\left(\frac{\partial C_4}{\partial T_{pr}}\right)_p = \frac{0.137223T_{pr}^{4.47}}{(0.665 + T_{pr}^{5.47})^2} \quad \text{C-29}$$

$$\left(\frac{\partial C_5}{\partial T_{pr}}\right)_p = \frac{0.001056e^{(-1.815T_{pr})}}{(1 - 6.466e^{(-1.815T_{pr})})^2} \quad \text{C-30}$$

Appendix D: Orkiszewski's method for the calculation of pressure gradient in a multiphase flow

Orkiszewski's method which covers all flow regimes (bubble, slug, transition and mist flow regimes) in vertical flow is as follows. Orkiszewski establishes some dimensionless parameters as boundaries for determination of the flow regimes and then applies Griffith's procedure for bubble flow, a modified form of Griffith and Wallies method for slug flow, a modified form of Griffith method combined with the Duns and Ros method for transition flow and the Duns and Ros method for mist flow regimes. At the following, it can be seen a comprehensive description of Orkiszewski method which is applied through this work for prediction of pressure loss in the case of a multiphase flow along a wellbore.

These boundaries are listed as follows.

5. Bubble flow: $q_g/q_t < L_b$
6. Slug flow: $q_g/q_t > L_b, v_{gd} < L_b$
7. Transition flow: $L_m > v_{gd} > L_s$
8. Mist flow: $v_{gd} > L_m$

The above dimensionless variables define as follows.

$$v_{gd} = \frac{q_g \left(\frac{\rho_l}{g\sigma} \right)^{0.25}}{A} \quad \text{D-1}$$

$$L_b = 1.071 - \left(\frac{0.2218 v_t^2}{d_h} \right) \quad \text{D-2}$$

But

$$L_b \geq 0.13$$

$$L_s = 50 + 36 \left(\frac{v_{gd} q_l}{q_g} \right) \quad \text{D-3}$$

$$L_m = 75 + 84 \left(\frac{v_{gd} q_l}{q_g} \right)^{0.75} \quad \text{D-4}$$

Where

V_{gd} = dimensionless gas velocity

V_t = total fluid velocity, ft/sec

q_g and q_l = gas and liquid flow rate, ft³/sec

ρ_l = liquid density, lbm/ft³

d_h = hydraulic pipe diameter, ft

σ = liquid surface tension, lbm/sec²

g = acceleration of gravity, ft/sec²

A = cross section area of wellbore, ft²

The term d_h which is called hydraulic diameter, and is written as follows.

$$d_h = \frac{4A}{P} \quad \text{D-5}$$

Where, A and P are cross section area (ft²) and wetted perimeter (ft) of the tube or duct. Therefore, Equation D-5 for a pipe can be written as follows:

$$d_h = \frac{4\pi r^2}{2\pi r} = 2r \quad \text{D-6}$$

Bubble flow

The following equation is applied for calculation of average fluid density.

$$\bar{\rho} = f_g \rho_g + (1 - f_g) \rho_l \quad \text{D-7}$$

Where the term f_g demonstrates the void gas fraction in the fluid, and can be calculated as follows.

$$f_g = \frac{1}{2} \left[1 + \frac{q_t}{v_s A} - \sqrt{\left(\frac{1 + q_t}{v_s A} \right)^2 - \frac{4q_g}{v_s A}} \right] \quad \text{D-8}$$

Where v_s is slip velocity in ft/sec, and Griffith suggested a value of 0.8 ft/sec for that (ORKISZEWSKI, 1967).

Therefore, the friction gradient (τ_f) for bubble flow regime is as follows.

$$\tau_f = \frac{f \rho_l v_l^2}{2g_c d_h} \quad \text{D - 9}$$

Where d_h is the hydraulic diameter in ft. This equation is based on single-phase liquid flow, and:

$$v_l = \frac{q_l}{A(1 - f_g)} \quad \text{D-10}$$

Where friction factor (f) in Equation D - 9 is the standard Moody friction factor and depends on the relative-roughness and the Reynolds number. The Reynolds number is calculated as follows.

$$N_{Re} = \frac{1488 \rho_l d_h v_l}{\mu_l} \quad \text{D-11}$$

Where μ_l shows the viscosity of liquid phase in centipoise (cp).

Slug flow

For the slug flow regime, the following equation is given for calculation of the average density of fluid.

$$\bar{\rho} = \frac{w_t + \rho_l v_b A}{q_t + v_b A} + \delta \rho_l \quad \text{D-12}$$

Where, q_t is the total velocity of gas and liquid in ft/sec. Also, in this equation, δ is a coefficient correlated from oilfield data, and the Griffith and Wallis relationship is given for calculation of the bubble rise or slip velocity, v_b .

$$v_b = C_1 C_2 \sqrt{g d_h} \quad \text{D-13}$$

Where, the terms C_1 and C_2 express the coefficient of bubble-rising for the rising of bubbles in the static and flowing column of fluid, respectively. The term C_1 is as a function of bubble Reynolds number (Equation D-14), and the term C_2 is a function of both bubble and liquid Reynolds number (Equation D-15). These terms are expressed in Figures Figure C3 and Figure C4 which are demonstrated experimentally by Griffith and Wallis.

$$N_{Re} = \frac{1488\rho_l d_h v_b}{\mu_l} \quad \text{D-14}$$

$$N_{Re} = \frac{1488\rho_l d_h v_t}{\mu_l} \quad \text{D-15}$$

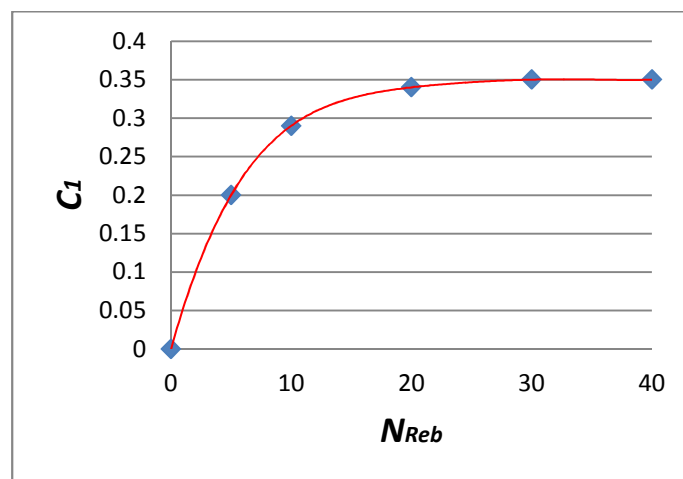


Figure C3. C_1 coefficient for bubbles rising in static liquid column vs. bubble Reynolds number.

When N_{ret} cannot read from Figure C4, following set of equations is used for calculation of v_b .

If $N_{reb} \leq 3000$, then

$$v_b = [0.546 + 8.74 \times 10^{-6} N_{re}] \sqrt{g d_h} \quad \text{D-16}$$

If $3000 \leq N_{reb} \leq 8000$, then

$$v_b = 0.5v_{bi} + \left(v_{bi}^2 + \frac{13.59\mu_l}{\rho_l\sqrt{d_h}} \right)^{0.5} \quad \text{D-17}$$

Where

$$v_{bi} = [0.251 + 8.74 \times 10^{-6}N_{re}] \sqrt{gd_h} \quad \text{D-18}$$

If $N_{reb} \geq 8000$, then

$$v_b = [0.35 + 8.74 \times 10^{-6}N_{re}] \sqrt{gd_h} \quad \text{D-19}$$

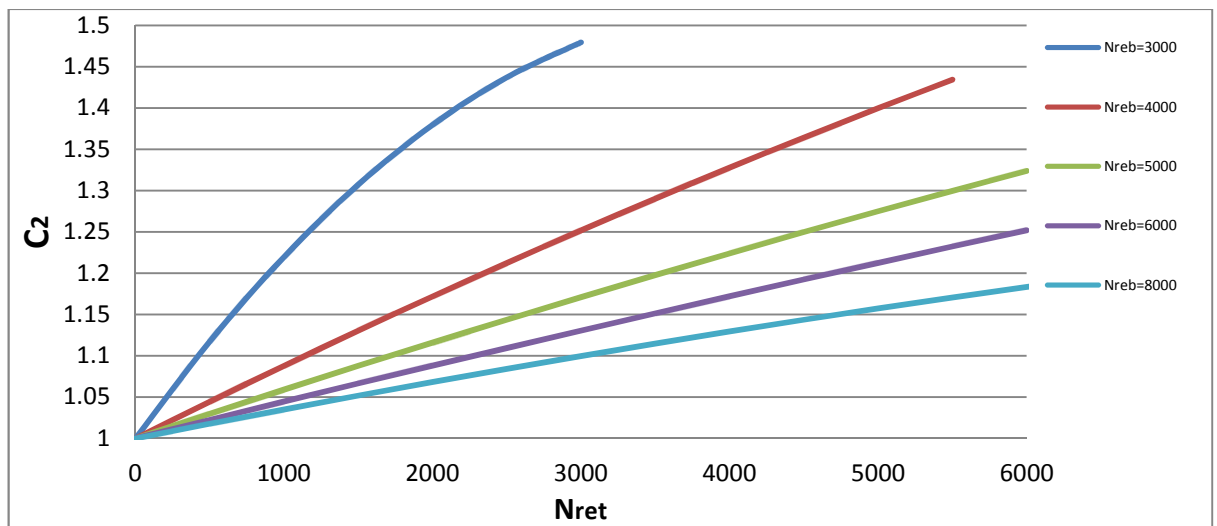


Figure C4. C2 coefficient vs. total Reynolds number.

Therefore, the calculation of friction loss gradient for slug flow regime using Orkiszewski's method is given as follows.

$$\tau_f = \frac{f\rho_l v_t^2}{2g_c d_h} \left(\frac{q_l + v_b A}{q_t + v_b A} + \delta \right) \quad \text{D-20}$$

Orkiszewski defined the parameter δ and called the liquid distribution coefficient which is as a function of hydraulic radius, liquid viscosity and total velocity. Following correlations and constraints are used to evaluate parameter δ .

If oil phase is continuous and $v_t < 10$.

$$\delta = \frac{0.0127}{d_h^{1.415}} \log(\mu_l + 1) - 0.284 + 0.167 \log v_t + 0.113 \log d_h \quad \text{D-21}$$

If oil phase is continuous and $v_t > 10$.

$$\delta = \frac{0.0274}{d_h^{1.371}} \log(\mu_l + 1) + 0.161 + 0.569 \log d_h - \log v_t \left[\frac{0.01}{d_h^{1.571}} \log(\mu_l + 1) + 0.397 + 0.63 \log d_h \right] \quad \text{D-22}$$

If water phase is continuous and $v_t < 10$.

$$\delta = \frac{0.013}{d_h^{1.38}} \log \mu_l - 0.681 + 0.232 \log v_t - 0.428 \log d_h \quad \text{D-23}$$

If water phase is continuous and $v_t > 10$.

$$\delta = \frac{0.045}{d_h^{0.799}} \log \mu_l - 0.709 - 0.162 \log v_t - 0.888 \log d_h \quad \text{D-24}$$

In order to eliminate pressure discontinuities between flow regimes; when, $\delta \geq -0.065v_t$ and $v_t > 10$, following correlation is used for evaluation of parameter δ .

$$\delta \geq -\frac{v_b A}{q_t + v_b A} \left(1 - \frac{\bar{\rho}}{\rho_l} \right) \quad \text{D-25}$$

Transition flow

The Duns and Ros method is used for evaluation of average fluid density ($\bar{\rho}$) and friction loss gradient (τ_f) for transition flow regime. In this method, the terms $\bar{\rho}$ and τ_f are firstly evaluated for slug and mist flow. Then linearly weighting of dimensionless parameters of gas velocity, v_{gD} , slug-transition boundary, L_s , and transition-mist boundary, L_M , (Equations D-26 and D-27) with the obtained values of ρ and τ_f for slug and mist flow regimes evaluate the terms $\bar{\rho}$ and τ_f for the transition flow regime.

$$\bar{\rho} = \left(\frac{L_M - v_{gD}}{L_M - L_S} \right) \bar{\rho}_S + \left(\frac{v_{gD} - L_S}{L_M - L_S} \right) \bar{\rho}_M \quad \text{D-26}$$

$$\bar{\tau}_f = \left(\frac{L_M - v_{gD}}{L_M - L_S} \right) \tau_{fS} + \left(\frac{v_{gD} - L_S}{L_M - L_S} \right) \tau_{fM} \quad \text{D-27}$$

Where letters M and S show mist and slug flow regimes, respectively.

Mist flow

In the case of mist flow regime, Equation D-7 is used for calculation of average fluid density ($\bar{\rho}$). However, as no slip is considered between phases, the void gas fraction (f_g) is calculated as follows.

$$F_g = \frac{q_g}{q_g + q_l} \quad \text{D-28}$$

The Duns and Ros method is used for calculation of friction loss gradient as follows.

$$\tau_f = \frac{f \rho_g v_{gs}^2}{2g_c d_h} \quad \text{D-29}$$

Where v_{gs} is superficial gas velocity and f is Moody friction factor as a function of Reynolds number.

$$N_{Re} = \frac{1488\rho_g d_h v_{gs}}{\mu_g} \quad \text{D-30}$$

Duns and Ros also developed a modification for relative roughness factor, ε/d_h . In their correlation, they applied the limit of $0.01 < \varepsilon/d_h < 0.5$ for roughness factor which is a function of liquid film wetting the pipe walls in mist flow regime. Therefore, following sets of equations and limitations are applied for calculation of the relative roughness factor, ε/d_h .

$$N = 4.52 \times 10^{-7} \left(\frac{v_{gs}\mu_l}{\sigma} \right)^2 \left(\frac{\rho_g}{\rho_l} \right) \quad \text{D-31}$$

When $N < 0.005$.

$$\frac{\varepsilon}{d_h} = \frac{34\sigma}{\rho_g v_{gs}^2 d_h} \quad \text{D-32}$$

When $N > 0.005$.

$$\frac{\varepsilon}{d_h} = \frac{174.8\sigma N^{0.302}}{\rho_g v_{gs}^2 d_h} \quad \text{D-33}$$

Appendix E: Flash Calculation Procedure

Suppose there are given a mixture of reservoir fluid at a given temperature and pressure which flows through a wellbore. Reservoir fluids normally contain hydrocarbon and non-hydrocarbon components, and hydrocarbon components range from methane to substances that may contain 100 carbon atoms (Firoozabadi, 1999). Understanding the equilibrium criteria for the given temperature and pressure along the wellbore may play a vital concept in the managing of an optimized production scenario. The flash calculation of multi-component mixture becomes necessary to apply for determination of number of moles in gas and liquid phase for a given temperature and pressure. Therefore, at the following, the procedure of flash calculation, which is performed for the simulation of multi-phase flow, has been described.

Formulation of Flash Calculation

For two phase mixture (Figure 3-8), the minimization of Gibbs free energy can be expressed as follows.

$$f_i^L(T, P, x) = f_i^V(T, P, x), \quad i = 1, \dots, c \quad \text{E-1}$$

The material balance is written as follows.

$$Fz_i = x_iL + y_iV, \quad i = 1, \dots, c \quad \text{E-2}$$

Where, the parameters F , L and V show the total mole number of the components in the feed, in the liquid phase, and in the gas phase, respectively.

Also, the sum of the mole fractions in the feed and the given phases are equal to unity as follows.

$$\sum_{i=1}^c x_i = \sum_{i=1}^c y_i = \sum_{i=1}^c z_i = 1 \quad \text{E-3}$$

Where, the parameters x_i , y_i and z_i express the mole fraction of the liquid, gas and feed.

Solution of Flash Calculation

Due to temperature and pressure loss along the production tubing and the complexity of flash calculation at any single point along the wellbore, the flash computation is a complex task. Therefore, to explore the mole fraction of gas, y_i , and liquid, x_i , phases, the Successive Substitution Iterative (SSI) technique and Newton-Raphson technique may apply.

Successive Substitution Iterative (SSI) technique

In this method, the equilibrium ratio is defined as follows.

$$K_i = y_i/x_i, \quad i = 1, \dots, c \quad \text{E-4}$$

Then

$$y_i = K_i x_i, \quad i = 1, \dots, c \quad \text{E-5}$$

The combination of Equations E-2 and E-5 can be expressed as follows.

$$Fz_i = x_i L + x_i K_i V, \quad i = 1, \dots, c \quad \text{E-6}$$

Also, it can be explained that:

$$L = F - V \quad \text{E-7}$$

Combining Equations E-6 and E-7 concludes as:

$$x_i = \frac{z_i}{1 + (K_i - 1)(V/F)} \quad i = 1, \dots, c \quad \text{E-8}$$

Similarly, for the vapour phase, it can be written as follows.

$$y_i = \frac{K_i z_i}{1 + (K_i - 1)(V/F)} \quad i = 1, \dots, c \quad \text{E-9}$$

The result of Equations E-8 and E-9 can be expressed as follows.

$$\sum_{i=1}^c \frac{(K_i - 1)z_i}{1 + (K_i - 1)(V/F)} = 0 \quad \text{E-10}$$

Equation E-10 is known as Rachford-Rice equation, and by defining $\alpha = (V/F)$, then the equation can be written as follows.

$$h(\alpha) = \sum_{i=1}^c \frac{(K_i - 1)z_i}{1 + \alpha(K_i - 1)} = 0 \quad \text{E-11}$$

From the definition of fugacity of component i in a phase, the fugacity of vapour, f_i^V and liquid f_i^L can be expressed in terms of the corresponding fugacity coefficients, ϕ_i^V and ϕ_i^L , respectively as follows.

$$f_i^V = y_i \phi_i^V P, \quad i = 1, \dots, c \quad \text{E-12}$$

$$f_i^L = x_i \phi_i^L P, \quad i = 1, \dots, c \quad \text{E-13}$$

The terms ϕ_i^V and ϕ_i^L in Equations E-12 and E-13 can readily be calculated using the PR-EOS. At equilibrium, E-4 may express as follows.

$$K_i = y_i/x_i = \phi_i^L / \phi_i^V, \quad i = 1, \dots, c \quad \text{E-14}$$

The two-phase flash can be solved iteratively using Equations E-4 to E-13. Now, it can be proceed with the iteration solution procedure as follows.

1. Guess the initial value for equilibrium ratio (k_i) at the given pressure, P , and temperature, T , using Wilson's correlation.

$$\ln K_i = 5.371(1 + \omega_i)[1 - T_{ci}/T] + \ln(P/P_{ci}) \quad \text{E-15}$$

Where, T_{ci} , P_{ci} and ω_i are the critical temperature, critical pressure and acentric factor of component i , respectively.

2. Using Newton-Raphson technique to solve α in Equation E-11. The technique will be described shortly.
3. The mole fractions of x_i and y_i can be solved using Equations E-8 and E-9, respectively.
4. Using PR-EOS to calculate compressibility factors of the vapour and liquid phases.
5. Using PR-EOS to calculate fugacity of the vapour and liquid phases.
6. Update K_i using the following equation.

$$K_i^{new} = K_i^{old} \exp[-\ln(f_i^V / f_i^L)] \quad \text{E-16}$$

7. Test the convergence according the following given tolerance.

$$(1/c) \sum_{i=1}^c [\ln(f_i^V / f_i^L)]^2 < 10^{-12} \quad \text{E-17}$$

Steps 2 to 7 repeats until the convergence criterion are satisfied.

Newton-Raphson Technique

Also, the Newton-Raphson technique is as following steps.

1. Calculate $h(\alpha)$ using Equation E-11.
2. Calculate $h'(\alpha)$ using following equation.

$$h'(\alpha) = - \sum_{i=1}^c \frac{(K_i - 1)^2 z_i}{[1 + \alpha(K_i - 1)]^2} = 0 \quad \text{E-18}$$

3. Update α as follows.

$$\alpha_i^{new} = \alpha_i^{old} - (h/h') \quad \text{E-19}$$

4. Test convergence as $|\alpha_i^{new} - \alpha_i^{old}| < 10^{-6}$.

The solution is in the interval of 0 and 1.

$$h(0) = \sum_{i=1}^c K_i z_i - 1 > 0 \quad \text{E-20}$$

And

$$h(1) = 1 - \sum_{i=1}^c (z_i/K_i) < 0 \quad \text{E-21}$$

Appendix F:

The WTP Simulator Codes

The following is a program for prediction of wellbore temperature profile along a production or injection wellbore. The program includes four sections as follows:

- Single phase liquid production
- Single phase gas production
- Multi-phase fluid production
- Injection wells

Definition of the Input Variables

a_pr	Parameter a in PR-EOS
ac_pr	Parameter ac in PR-EOS
AF	Acentric factor
alpha	Thermal diffusivity of earth (ft ² /hr)
Atbg	Surface area of tubing (ft ²)
b_pr	Parameter b in PR-EOS
Bg	Gas formation volume factor (ft ³ /scf)
chi_l	Liquid compositions
chi_o	Overall compositions
chi_v	Vapour compositions
cpa	Annulus fluid heat capacity (btu/(lbmole. F))
cpf	Wellbore fluid heat capacity (btu/(lbmole. F))
cpg	Heat capacity of gas (btu/(lbmole. F))
dgas	Gas density (lb/cu ft)
Dliq	Density of liquid (lb/cu ft)
Doil	Oil density (lb/cu ft)
dperf	Perforation interval (ft)

dtg	Geothermal temperature gradient (F/ft)
Dw	Water density (lb/cu ft)
dx	Length increment (ft)
dz_dx	dz/dx
dzdtp	dz/dtp
Ecsg	Casing emmissivity factor
Etbg	Tubing emmissivity factor
etbg	Emissivity of tubing
F	Time function
ff	Friction factor
Foil	Oil fraction
FP	Type of fluid phase
fug_l	Fugacity of liquid
fug_v	Fugacity of vapor
Fw	Water fraction
g	Earth acceleration gravity constant (ft/sec ²)
Gamag	Gas specific gravity (lbm/lbmole)
gc	Earth acceleration gravity constant (ft/sec ²)
J	778 ft.Lbf/btu
ka	Annulus fluid thermal resistivity (btu/hr.ft.F)
kcmt	Cement sheaths thermal resistivity (btu/hr.ft.F)
kg	Earth thermal resistivity (btu/hr.ft.F)
Kjt	Joule Thomson coefficient (F/psi)
ko	Overall thermal resistivity (btu/hr.ft.F)
lcs	Length of casing (ft)
Lb	Flow regime boundary definition, dimensionless
Lm	Flow regime boundary definition, dimensionless
Lperf	Length of perforation (ft)
Ls	Flow regime boundary definition, dimensionless
ltbg	Length of tubing (ft)
mf	Total mol fraction
mfgas	Gas mole fraction

mw	Molecular weight (lbm)
MWg	Gas molecular weight (lbm)
n_comp	Number of components
n_max	Maximum number of components
nc	Number of gas components
ncsg	Number of casing
Pc	Critical pressure (psia)
pi	Phi (π)
Ppseudo	Pesudo-critical pressure (psia)
pres	Reservoir pressure (psia)
q	Flow rate (bbl/d)
Qa	Annulus heat loss rate (btu/hr)
Qgas	Gas flow rate (ft ³ /day)
Qliq	Liquid flow rate (bbl/day)
Qo	Overall heat loss (btu/hr)
Qoil	Oil flow rate (bbl/day)
Qt	Total flow rate (bbl/day)
Qw	Water flow rate (bbl/day)
R	Universal gas constant
rey	Reynolds number
rg	Ground radius (ft)
rho_l	Density of liquid (lbm/ft ³)
rho_v	Density of vapour (lbm/ft ³)
ricsg	Inner radius of casing (ft)
ritbg	Inner radius of tubing (ft)
roa	Annulus fluid density (lb/cu ft)
rocmt	Outer radius of cement sheath (ft)
rocs	Outer radius of casing (ft)
rof	Wellbore fluid density (lb/cu ft)
Rog	Density of gas (lb/cu ft)
rotbg	Outer radius of tubing (ft)
SBC	Stephan-Boltzman-Constant

sggas	Specific gravity of gas (lbm/lbmole)
t	Steady-state time (day)
Tc	Critical Temperature (K)
TD	Total depth (ft)
Tg	Geothermal temperature (F)
Tgen	Generated heat (F)
Ticsg	Temperature @ inner casing radius (F)
Tocmt	Temperature @ outer cement sheath radius (F)
tp	Production duration (day)
Tpseudo	Pseudo-critical temperature (F)
Tr	Reservoir temperature (F)
Tres	Reservoir temperature (F)
TT	Temperature (F)
Tw	Wellbore temperature (F)
Uo	Overall heat transfer coefficient (Btu/hr.ft)
Vc	Critical volume
vcsg	Volume per foot of casing (ft ³ /ft)
Vg	Volume of gas fraction (ft ³)
visa	Annulus fluid viscosity (lb mass/(ft. hr))
visg	Gas viscosity (lbm/(ft. hr))
Vliq	Volume of liquid fraction (bbl)
Vs	Superficial gas velocity (ft/sec)
vtbg	Volume per foot of tubing (ft ³ /ft)
vttbg	Total volume of tubing (ft ³)
yCO2	Mole fraction of CO2
yH2O	Mole fraction of H2S
yH2S	Mole fraction of H2S
yN2	Mole fraction of N2
Z	Compressibility factor

List of Subroutines

subroutine WTP_SLP (FluidType)

subroutine WTP_SGP (FluidType)

subroutine WTP_Mixture (FluidType)

subroutine C_ConstantData (g, gc, SBC, pi, R)

subroutine C_TubingInfo (FluidType, ritbg, rotbg, vtbg, vttbg, ltbg, TD, etbg)

subroutine C_CasingInfo (FluidType, ncsg, ricsg1, rocsg1, vcsg1, vtcsg1, lcsg1, ricsg2, rocsg2, vcsg2, vtcsg2, lcsg2, ricsg3, rocsg3, vcsg3, vtcsg3, lcsg3)

subroutine C_Cmt_Ground_Data(rocmt1, rocmt2, rocmt3, rg)

subroutine L_WellboreFluidProp (rof, cpf)

subroutine L_ProductionData (vttbg, ltbg, t, q, Tw, Tg, tp, ff, dx, TT, Tr, dtg)

subroutine ProductionData (vttbg, ltbg, t, q, Tw, Tg, tp, dx, TT, Tr, P1, Vp, dtg)

subroutine C_AnnFluidProp (FluidType, ka, cpa, roa, visa)

subroutine C_ThermalProp (FluidType, kg, kcmt, Etbg, Ecsg, alpha)

subroutine fricHeatGen(rof, cpf, ff, pi, ritbg, q, vtbg, tp, gc, dx, Tgen)

subroutine L_TimeFunction (F, alpha, t, rocmt)

subroutine C_CmtFormIntTemp (ko, kg, F, rotbg, rocmt, Tg, Tw, Tocmt, A)

subroutine L_CmtHeatLossBTM(pi, kcmt, Ticsg, Tocmt, rocmt, rocsg, Qcmt)

subroutine C_CasingSurTemp (Ticsg, Tocmt, A, C, rocmt, rocsg, kcmt, Tw)

subroutine C_AnnulusHeatLoss (Qa, SBC, Ticsg, Tw, Etbg, Ecsg, rotbg, ricsg, Cpa, visa, ka, roa, g, pi)

subroutine C_CmtHeatLoss(pi, kcmt, Ticsg, Tocmt, rocmt, rocsg, Qcmt)

subroutine C_OverallHeatLoss (Uo, Qo, Tw, Ticsg, Tocmt, rotbg, rocmt, ricsg, rocsg, kcmt, Qa, pi)

subroutine C_ProdZone(nperf, dperf, Lperf)

subroutine Components(nc, MWg, Gamag, yN2, yCO2, yH2S, yH2O, AF, Tc, Pc, Vc, mf, mw, NC1, NC2, NC3, NC4, NC5)

subroutine PseudoPropKC(nc, mf, mw, Tc, Pc, NC1, NC2, NC3, NC4, NC5, Ppseudo, Tpseudo, yN2, yCO2, yH2S, yH2O)

subroutine PseudoPropUC(Gamag, MWg, Ppseudo, Tpseudo, yN2, yCO2, yH2S, yH2O)

subroutine ZFactorCalKC(TT, p1, z, Ppseudo, Tpseudo)

subroutine ZFactorCalUC(TT, P1, Z, Gamag, rog, Ppseudo, Tpseudo, dzdtp)

subroutine WellboreFluidPropKC (cpg, Gamag, rog, visg, MWg, P1, Z, R, TT, ritbg, Bg)

subroutine WellboreFluidPropUC (cpg, Gamag, rog, visg, P1, Z, TT, ritbg, Bg)

subroutine Gasspeed (q, TT, P1, R, ritbg, Atbg, MWg, Vg, Vs, Z)

subroutine FricFac(Gamag, visg, ritbg, q, ff)

subroutine GasProperties (P1, TT, ritbg, Z, Bg)

subroutine WellboreTempCalKC(n, cpg, Qo, Vg, d1, dx, g, gc, q, ritbg, dTw, TT, rog, Kjt, mf, nc, depth, Tc, Pc, Vc, Ppseudo, Tpseudo, AF, R, Gamag, Bg, ff, P1, dp, Z, Tw, Vs, TD, Pi, MWg, dperf, nperf, Lperf, Ko, Uo, Tg, dtg)

subroutine WellboreTempCalUC(n, cpg, Qo, Vg, d1, dx, g, gc, q, ritbg, dTw, TT, rog, Kjt, depth, Ppseudo, Tpseudo, R, Gamag, Bg, ff, P1, dp, Z, Tw, Vs, dzdtp, TD, Pi, MWg, dperf, nperf, Lperf, Ko, Uo, Tg, dtg, yN2, yCO2, yH2S)

subroutine M_ProdData(Qoil, Qgas, Qw, Qliq, Qt, Vliq, Tres, Pres, Doil, Dw, SGw, Cpm, t, VISliq, VISgas, Sigma, ltbg, Tg, dTg, Tw, P1, TT, dx, ritbg)

subroutine M_Components (Comp, yN2, yCO2, yH2S, yH2O, AF, Tc, Pc, Vc, mf, mw, CN1, CN2, CN3, CN4, nc)

subroutine FlashCalc(Comp, TT, P1, mf, AF, Tc, Pc, mw, mfgas, mfliq, Dgas, Dliq, nc)

subroutine M_WellboreTempCal(TT, P1, dPdx, yN2, yH2S, yCO2, yH2O, VISliq, VISgas, gc, g, pi, ritbg, Qgas, Qliq, Qt, Tgen, SGgas, etbg, dx, cpm, vtbg, Dm, Sigma, nc, mfgas, Tc, Pc, CN1, CN2, CN3, CN4, Vliq, Dliq)

subroutine JouleThomsonCoefKC(nc, P1, Z, cpg, rog, TT, Tc, Pc, Vc, R, AF, mf, Kjt)

subroutine JouleThomsonCoefUC(Z, dzdtp, cpg, rog, TT, Kjt)

subroutine Press_Loss(Gamag, Z, dx, TT, ff, q, P1, Bg, ritbg, dp)

subroutine TempPerf (q, Z, R, TT, gc, P1, MWg, Pi, ritbg, nperf, dperf, Kjt, TD, Tg, Lperf, dx, dtg)

subroutine alpha_calc(chi_o, xk_phase, alpha, n_comp, n_max)

subroutine cubic_1(a, b, c, z1, z2, z3)

subroutine flash_iterative(t, p, alpha, rho_l, rho_v, rho_m_l, rho_m_v, chi_v, chi_l, chi_o, fug_v, fug_l, xk_phase, d_fug_dx_v, d_fug_dp_v, d_fug_dx_l, d_fug_dp_l, omega, tc, pc, xm, dd, a_pr, b_pr, ac_pr, xk_pr, s, shi_par, err_max, err_l, delta, h, hi, v, da0_dx, db0_dx, dz_dx, n_comp, n_max, nt)

subroutine flash_newton(t, p, alpha, rho_l, rho_v, rho_m_l, rho_m_v, chi_v, chi_l, chi_o, fug_v, fug_l, xk_phase, d_fug_dx_v, d_fug_dp_v, d_fug_dx_l, d_fug_dp_l, omega, tc, pc, xm, dd, a_pr, b_pr, ac_pr, xk_pr, s, shi_par, err_max, err_l, delta, h, hi, v, da0_dx, db0_dx, dz_dx, x_j, f, xb, n_comp, n_max, nt)

subroutine m_fricfac(rey, ff, ritbg, etbg)

subroutine m_gasdensity(tres, pres, sggas, yn2, yco2, yh2s, yh2o, dgas, nc, mfgas, tc, pc, cn1, cn2, cn3, cn4)

subroutine gauss_jordan(a, b, n, n_max)

subroutine M_LiqProp(Qoil, Qw, Qliq, Doil, Vliq, Foil, Fw, Dw, Dliq, Pi, ritbg)

subroutine M_PhaseDet(Qgas, Qliq, Qt, ritbg, Dliq, sigma, g, Lm, Ls, FP, pi)

subroutine peng_rob_eos(t, p, chi, shi_par, i_phase, niv, rho, rho_mole, fug, d_fug, d_fug_dp, v, h, hi, omega, tc, pc, xm, dd, delta, a, b, ac, xk, da0_dx, db0_dx, dz_dx, s, n_comp, n_max)

subroutine M_PressLoss(Tres, Pres, FP, Dliq, dPdx, yN2, yH2S, yCO2, yH2O, VISliq, VISgas, gc, g, pi, ritbg, Qgas, Qliq, Qt, Vliq, Lm, Ls, wt, SGgas, etbg, dx, Dm, nc, mfgas, Tc, Pc, CN1, CN2, CN3, CN4)

subroutine M_PseudoPropKC(nc, mf, Tc, Pc, CN1, CN2, CN3, CN4, Ppseudo, Tpseudo, yN2, yCO2, yH2S, yH2O)

subroutine M_WellboreTempCal(Tres, Pres, dPdx, yN2, yH2S, yCO2, yH2O, VISliq, VISgas, gc, g, pi, ritbg, Qgas, Qliq, Qt, Tgen, SGgas, etbg, dx, cpm, vtbg, Dm, Sigm, nc, mfgas, Tc, Pc, CN1, CN2, CN3, CN4, Vliq, Dliq)

subroutine M_Zfactor(TT, P1, Z, Gamag, rog, Ppseudo, Tpseudo)

The WTP Simulator

```

!*****
!      Determination of type of fluid flowing through the wellbore
!*****

character(len=20) FluidType

print*, 'Enter type of flowing fluid through the wellbore'

print*, 'Enter Liquid, Gas or Mixture.'

read*, FluidType

Select case (FluidType)

    Case ('Liquid')

        call WTP_SLP (FluidType)

    Case ('Gas')

        call WTP_SGP (FluidType)

    case ('Mixture')

        call WTP_Mixture (FluidType)

end select

end

```

The WTP Simulator – Single Phase Liquid Production

```

!*****
Calculation of WTP for liquid fluid flow through the wellbore
!*****

subroutine WTP_SLP (FluidType)

real kg, ka, ko, kcm, ltbg, lcs1, lcs2, lcs3, l1, l2

open (51, file='HeatLossSLP.csv', status='unknown')

!=====

! Data entry section

!=====

```

```

call C_ConstantData (g, gc, SBC, pi, R)
call C_TubingInfo (FluidType, ritbg, rotbg, vtbg, vttbg, ltbg, TD, etbg)
!print*, 'Enter number of casings and liners'
read *, ncsbg

call C_CasingInfo (FluidType, ncsbg, ricsg1, rocsg1, vcsg1, vtcsg1, lcsbg1, ricsg2,
rocsg2,vcsg2, vtcsg2, lcsbg2, ricsg3, rocsg3, vcsg3, vtcsg3, lcsbg3)

call C_Cmt_Ground_Data(rocmt1, rocmt2, rocmt3, rg)

call L_ProductionData (vttbg, ltbg, t, q, Tw, Tg, tp, ff, dx, TT, Tr, dtg)

call L_WellboreFluidProp (rof, cpf)

call C_AnnFluidProp (FluidType, ka, cpa, roa, visa)

call C_ThermalProp (FluidType, kg, kcmt, Etbg, Ecsbg, alpha)

Depth=ltbg
l2=lcsbg2
l1=lcsbg1
ricsg=ricsg3
rocsg=rocsg3
rocmt=rocmt3

!   print*, 'Guess Koverall, Btu/(hr. ft. oF):'

!   read *, koverall   ! Overall thermal conductivity coefficient, Btu/(hr. ft. oF)

ko=0.4

!=====

!Calculation of heat generated in wellbore due to friction of flowing fluid

!=====

call fricHeatGen(rof, cpf, ff, pi, ritbg, q, vtbg, tp, gc, dx, Tgen)

write (51, '(6(A15,A),A15)') 'Depth (ft)',',',Tg (F)',',',Tw (F)',',', 'Koverall',',',
'Uoverall', ',','Qo (Btu/min)'

!=====

!Calculation section

```

```

!=====
100 call L_TimeFunction (F, alpha, t, rocmt)
10 call C_CmtFormIntTemp (ko, kg, F, rotbg, rocmt, Tg, Tw, Tocmt, A)
call C_CasingSurTemp (Ticsg, Tocmt, A, C, rocmt, rocs, kcmt, Tw)
call C_OverallHeatLoss (Uo, Qo, Tw, Ticsg, Tocmt, rotbg, rocmt, ricsg, rocs, kcmt,
Qa, pi)
call C_CmtHeatLoss(pi, kcmt, Ticsg, Tocmt, rocmt, rocs, Qcmt)
call L_Qo_HL (Uo, Qo, Tw, Ticsg, Tocmt, rotbg, rocmt, ricsg, rocs, kcmt, Qa, pi)
!=====
! Iteration Section
!=====
Q1 = abs (Qcmt - Qa)
if ((Q1.gt.0.02) .and. (Qa.gt.Qcmt)) then
  if (q1.gt.1) then
    ko=ko+0.001
    go to 10
  elseif (q1.gt.0.5) then
    ko=ko+0.0001
    go to 10
  else
    ko=ko+0.00001
    go to 10
  endif
elseif ((Q1.gt.0.02) .and. (Qa.lt.Qcmt)) then
  if (q1.gt.1) then
    ko=ko-0.001
    go to 10
  elseif (q1.gt.0.5) then

```

```

ko=ko-0.0001
go to 10
else
ko=ko-0.00001
go to 10
endif
else
write (51, '(5(f15.3,A),f15.3)') Depth,',', Tg,',',TT,',', Ko,',',Uo,',', Qo/60
endif

!=====
!Define the next step of calculation
!=====

if (depth .gt. 0) then
d1=depth
depth=depth-dx
if (depth .gt. 0)then
Tg=Tg-dx*dTg
TT=Tw+Tgen
if (TT.le.Tr) then
Tw=Tw-((Qo/60)/(rof*vtbg*cpf))+Tgen
TT=Tw
if (depth .ge. 12) then
ricsg=ricsg3
rocsg=rocsg3
rocmt=rocmt3
vtcsg=vtcsg3
elseif ((depth .ge. 11) .and. (depth .lt. 12)) then
ricsg=ricsg2

```

```

        rocsg=rocsg2
        rocmt=rocmt2
        vtcsg=vtcsg2
    else
        ricsg=ricsg2
        rocsg=rocsg2
        rocmt=rocmt2+rocm1
        vtcsg=vtcsg2
    endif
    go to 100
endif
Tw=Tw-((Qo/60)/(rof*vtbg*cpf))+Tgen
TT=Tw
go to 100
else
    depth=0
    Tg=Tg-d1*dTg
    Tw=Tw-((Qo/60)/(rof*vtbg*cpf))+(d1/dx)*Tgen
    TT=Tw
    Ko=0
    Uo=0
    Qo=0
    write (51, '(5(f15.3,A),f15.3)') Depth,',', Tg,',',TT,',', Ko,',',Uo,',', Qo/60
endif
endif
close(51)
end

```

The WTP Simulator – Single Phase Gas Production

```

!*****
!           Calculation of WTP for gas fluid flow through the wellbore
!*****

subroutine WTP_SGP (FluidType)

character(len=20) NC1, NC2, NC3, NC4, NC5, MixComp, FluidType
real kg, ka, ko, kcmt, ltbg, lcs1, lcs2, lcs3, l1, l2, MWg, Lperf
real Tc(16), Pc(16), Vc(16), mf(16), mw(16), AF(16)

open (unit=1, file='Data.csv', status='unknown')
open (unit=50, file='HeatLossSGP.csv', status='unknown')
open (unit=100, file='Cal.csv', status='unknown')

write (100, '(15A)') 'Gamag',',','Kjt',',','dp',',','Z',',','Bg',',','TT'

!=====

! Data entry section

!=====

call C_ConstantData (g, gc, SBC, pi, R)

call ProdZone(nperf, dperf, Lperf)

call C_TubingInfo (FluidType, ritbg, rotbg, vtbg, vttbg, ltbg, TD, etbg)

print*, 'Enter number of casings and liners'

read *, ncsg

call C_CasingInfo (FluidType, ncsg, ric1, roc1, vc1, vtc1, lc1, ric2,
roc2,vc2, vtc2, lc2, ric3, roc3, vc3, vtc3, lc3)

call C_Cmt_Ground_Data(rocmt1, rocmt2, rocmt3, rg)

call ProductionData (vttbg, ltbg, t, q, Tw, Tg, tp, dx, TT, Tr, P1, Vp, dtg)

call C_AnnFluidProp (FluidType, ka, cpa, roa, visa)

call C_ThermalProp (FluidType, kg, kcmt, Etbg, Ecsg, alpha)

```

```

print*, 'Are the components of gas mixture known?'
print*, 'Enter Yes or No.'
read*, MixComp
if (MixComp .eq. 'Yes') then
    print*, 'Enter number of components in the producing gas'
    read *, nc

    Call Components(nc, MWg, Gamag, yN2, yCO2, yH2S, yH2O, AF, Tc, Pc, Vc,
mf, mw, NC1, NC2, NC3, NC4, NC5)

    call PseudoPropKC(nc, mf, mw, Tc, Pc, NC1, NC2, NC3, NC4, NC5, Ppseudo,
Tpseudo, yN2, yCO2, yH2S, yH2O)

    call ZFactorCalKC(TT, p1, z, Ppseudo, Tpseudo)

    call WellboreFluidPropKC (cpg, Gamag, rog, visg, MWg, P1, Z, R, TT, ritbg, Bg)
else
    print*, 'Enter specific gravity of producing gas'
    read *, Gamag

    call PseudoPropUC(Gamag, MWg, Ppseudo, Tpseudo, yN2, yCO2, yH2S, yH2O)
    call ZFactorCalUC(TT, P1, Z, Gamag, rog, Ppseudo, Tpseudo, dzdtp)
    call WellboreFluidPropUC (cpg, Gamag, rog, visg, P1, Z, TT, ritbg, Bg)
endif

Depth=lrbg
l2=lrbg2
l1=lrbg1
ricsg=ricsg3
rocsg=rocsg3
rocmt=rocmt3

print*, 'Guess Koverall, Btu/(hr. ft. oF):'
read *, koverall    ! Overall thermal conductivity coefficient, Btu/(hr. ft. oF)
n=0

```

```

!=====
!Calculation section
!=====

call Gasspeed (q, TT, P1, R, ritbg, Atbg, MWg, Vg, Vs, Z)

call FricFac(Gamag, visg, ritbg, q, ff)

write (50, '(7(A15,A),A15)') 'Depth (ft)',',',Tg (F)',',',Tw (F)',',',Pw
(psi)',',',Koverall',',',Uoverall',',',Qo (Btu/min)',',',Z Factor'

100 call C_TimeFunction (F, alpha, t, rocmt)

!=====
!Calculation of heat generated in wellbore due to friction of flowing fluid
!=====

120 call C_CmtFormIntTemp (ko, kg, F, rotbg, rocmt, Tg, Tw, Tocmt, A)

call C_CasingSurTemp (Ticsg, Tocmt, A, C, rocmt, rocs, kcm, Tw)

call C_OverallHeatLoss (Uo, Qo, Tw, Ticsg, Tocmt, rotbg, rocmt, ricsg, rocs, kcm,
Qa, pi)

call C_CmtHeatLoss(pi, kcm, Ticsg, Tocmt, rocmt, rocs, Qcmt)

call OverallHeatLoss (Uo, Qo, Tw, Ticsg, Tocmt, rotbg, rocmt, ricsg, rocs, kcm,
Qa, pi)

!=====
! Iteration Section
!=====

Q1 = abs (Qcmt - Qa)

if ((Q1.gt.0.02) .and. (Qa.gt.Qcmt)) then
  if (q1.gt.1) then
    ko=ko+0.001
    go to 120
  elseif (q1.gt.0.5) then
    ko=ko+0.0001
    go to 120

```

```

else
    ko=ko+0.00001
    go to 120
endif

elseif ((Q1.gt.0.02) .and. (Qa.lt.Qcmt)) then
    if (q1.gt.1) then
        ko=ko-0.001
        go to 120
    elseif (q1.gt.0.5) then
        ko=ko-0.0001
        go to 120
    else
        ko=ko-0.00001
        go to 120
    endif
!else
! write (50, '(6(f15.3,A),f15.3)') Depth,',', Tg,',',TT,',',P1,',', Ko,',',Uo,',', Qo/60
endif

!=====
!Define the next step of calculation
!=====

if (depth .gt. 0) then
    d1=depth
    depth=depth-dx
    if (depth .gt. 0)then
        Tg=Tg-dx*dTg
        select case (MixComp)
            Case ('Yes')

```

```

call WellboreTempCalKC(n, cpg, Qo, Vg, d1, dx, g, gc, q, ritbg, dTw, TT,
rog, Kjt, mf, nc, depth, Tc, Pc, Vc, Ppseudo, Tpseudo, AF, R, Gamag, Bg, ff,
P1, dp, Z, Tw, Vs, TD, Pi, MWg, dperf, nperf, Lperf, Ko, Uo, Tg, dtg)

case ('No')

call WellboreTempCalUC(n, cpg, Qo, Vg, d1, dx, g, gc, q, ritbg, dTw, TT,
rog, Kjt, depth, Ppseudo, Tpseudo, R, Gamag, Bg, ff, P1, dp, Z, Tw, Vs,
dzdtp, TD, Pi, MWg, dperf, nperf, Lperf, Ko, Uo, Tg, dtg, yN2, yCO2,
yH2S)

end select

if (depth .ge. 12) then

    ricsg=ricsg3

    rocsg=rocsg3

    rocmt=rocmt3

    vtcsg=vtcsg3

elseif ((depth .ge. 11) .and. (depth .lt. 12)) then

    ricsg=ricsg2

    rocsg=rocsg2

    rocmt=rocmt2

    vtcsg=vtcsg2

else

    ricsg=ricsg2

    rocsg=rocsg2

    rocmt=rocmt2+rocm1

    vtcsg=vtcsg2

endif

go to 100

else

    n=2

    depth=0

    Tg=Tg-d1*dTg

```

```
select case (MixComp)
```

```
Case ('Yes')
```

```
call WellboreTempCalKC(n, cpg, Qo, Vg, d1, dx, g, gc, q, ritbg, dTw, TT,
rog, Kjt, mf, nc, depth, Tc, Pc, Vc, Ppseudo, Tpseudo, AF, R, Gamag, Bg, ff,
P1, dp, Z, Tw, Vs, TD, Pi, MWg, dperf, nperf, Lperf, Ko, Uo, Tg, dtg)
```

```
Case ('No')
```

```
call WellboreTempCalUC(n, cpg, Qo, Vg, d1, dx, g, gc, q, ritbg, dTw, TT,
rog, Kjt, depth, Ppseudo, Tpseudo, R, Gamag, Bg, ff, P1, dp, Z, Tw, Vs,
dzdtp, TD, Pi, MWg, dperf, nperf, Lperf, Ko, Uo, Tg, dtg, yN2, yCO2,
yH2S)
```

```
end select
```

```
Ko=0
```

```
Uo=0
```

```
Qo=0
```

```
write (50, '(7(f15.3,A),f15.3)') Depth,',', Tg,',',TT,',',P1,',', Ko,',',Uo,',',
Qo/60,',', Z
```

```
endif
```

```
endif
```

```
close(1)
```

```
close(50)
```

```
close(100)
```

```
return
```

```
end
```

The WTP Simulator – Mult-Phase Fluid Production

```
!*****
```

```
! Calculation of WTP for mixture of liquid and gas fluid flow through the wellbore
```

```
!*****
```

```
subroutine WTP_Mixture (FluidType)
```

```
character(len=20) FluidType
```

```
character(len=20) comp(16), CN1, CN2, CN3, CN4
```

```

real kg, ka, ko, kcmt, ltbg, lcs1, lcs2, lcs3, l1, l2
real Tc(16), Pc(16), Vc(16), mf(16), mw(16), AF(16)
real mfgas(16), mfliq(16), mftgas, mftliq
open (52, file='RHeatLossMP.csv', status='unknown')
open (45, file='RCompositions.csv', status='unknown')
!=====
! Data entry section
!=====
call C_ConstantData (g, gc, SBC, pi, R)
call C_TubingInfo (FluidType, ritbg, rotbg, vtbg, vttbg, ltbg, TD, etbg)
!print*, 'Enter number of casings and liners'
!read *, ncsg
ncsg=3
call C_CasingInfo (FluidType, ncsg, ricsg1, rocsg1, vcsg1, vtcs1, lcs1, ricsg2,
rocsg2,vcsg2, vtcs2, lcs2, ricsg3, rocsg3, vcsg3, vtcs3, lcs3)
call C_Cmt_Ground_Data(rocmt1, rocmt2, rocmt3, rg)
call C_AnnFluidProp (FluidType, ka, cpa, roa, visa)
call C_ThermalProp (FluidType, kg, kcmt, Etbg, Ecsg, alpha)
Depth=ltbg
l2=lcs2
l1=lcs1
ricsg=ricsg3
rocsg=rocsg3
rocmt=rocmt3
print*, 'Guess Koverall, Btu/(hr. ft. F):'
read *, koverall      ! Overall thermal conductivity coefficient
                        ! Btu/(hr. ft. F)
print*, 'Enter number of components of producing fluid'

```

```

read *, nc

call M_ProdData(Qoil, Qgas, Qw, Qliq, Qt, Vliq, Tres, Pres, Doil, Dw, SGw, Cpm,
t, VISliq, VISgas, Sigma, ltbg, Tg, dTg, Tw, P1, TT, dx, ritbg)

Call M_Components(Comp, yN2, yCO2, yH2S, yH2O, AF, Tc, Pc, Vc, mf, mw,
CN1, CN2, CN3, CN4, nc)

write (52, '(6(A15,A),A15)') 'Depth (ft)',',',Tg (F)',',',Tw (F)',',',Pw
(psi)',',',Koverall',',',Uoverall',',',Qo (Btu/min)'

call FlashCalc(Comp, TT, P1, mf, AF, Tc, Pc, mw, mfgas, mfliq, Dgas, Dliq, nc)

SGgas=Dgas/28.96

write (45,'(15A,A,f15.4,A,20A)')'Depth',',',Depth',',',ft'

write (45,'(15A)')'Component',',',V',',',L'

do i=1,nc

    write (45,'(15A,A,f15.8,A,f15.8)')Comp(i),',',mfgas(i),',',mfliq

enddo

mftgas=0.0

mftliq=0.0

do i=1,nc

    mftgas=mftgas+mfgas(i)*mw(i)

    mftliq=mftliq+mfgas(i)*mw(i)

enddo

write (45,'(15A,A,f15.8,A,f15.8)')",',',mftgas',',',mftliq

!=====

!Calculation section

!=====

100 call C_TimeFunction (F, alpha, t, rocmt)

10 call C_CmtFormIntTemp (ko, kg, F, rotbg, rocmt, Tg, Tw, Tocmt, A)

call C_CasingSurTemp (Ticsg, Tocmt, A, C, rocmt, rocs, kcm, Tw)

call C_AnnHeatLoss (Qa, SBC, Ticsg, Tw, Etbg, Ecs, rotbg, rics, Cpa, visa, ka,
roa, g, pi)

```

```

call C_CmtHeatLoss(pi, kcmt, Ticsg, Tocmt, rocmt, rocs, Qcmt)
call C_OverallHeatLoss (Uo, Qo, Tw, Ticsg, Tocmt, rothg, rocmt, ricsg, rocs, kcmt,
Qa, pi)!=====
! Iteration Section
!=====
Q1 = abs (Qcmt - Qa)
if ((Q1.gt.0.02) .and. (Qa.gt.Qcmt)) then
  if (q1.gt.1) then
    ko=ko+0.001
    go to 10
  elseif (q1.gt.0.5) then
    ko=ko+0.00001
    go to 10
  else
    ko=ko+0.00001
    go to 10
  endif
elseif ((Q1.gt.0.02) .and. (Qa.lt.Qcmt)) then
  if (q1.gt.1) then
    ko=ko-0.001
    go to 10
  elseif (q1.gt.0.5) then
    ko=ko-0.0001
    go to 10
  else
    ko=ko-0.00001
    go to 10
  endif
endif

```

```

else
    write (52, '(6(f15.3,A),f15.3)') Depth,',', Tg,',',TT,',',P1,',', Ko,',',Uo,',', Qo/60
endif

!=====

!Define the next step of calculation

!=====

if (depth .gt. 0) then
    d1=depth
    depth=depth-dx
    if(depth.lt.2800)then
        kg=kg+3.5
        kcmt=kcmt+3
    endif
    if(depth.lt.4000)then
        ka=0.05
    endif
    if (depth .gt. 0)then
        call M_WellboreTempCal(TT, P1, dPdx, yN2, yH2S, yCO2, yH2O, VISliq,
            VISgas, gc, g, pi, ritbg, Qgas, Qliq, Qt, Tgen, SGgas, etbg, dx, cpm, vtbg,
            Dm, Sigma, nc, mfgas, Tc, Pc, CN1, CN2, CN3, CN4, Vliq, Dliq)
        Tg=Tg-dx*dTg
        Tw=Tw-((Qo/60)/(Dm*vtbg*cpm))+Tgen
        TT=Tw
        Pw=P1
        if (depth .ge. 12) then
            ricsg=ricsg3
            rocsg=rocsg3
            rocmt=rocmt3
        endif
    endif
endif

```

```

    vtcsg=vtcsg3
elseif ((depth .ge. 11) .and. (depth .lt. 12)) then
    ricsg=ricsg2
    rocsг=rocsг2
    rocmt=rocmt2
    vtcsg=vtcsg2
else
    ricsg=ricsg2
    rocsг=rocsг2
    rocmt=rocmt2+rocml
    vtcsg=vtcsg2
endif
call FlashCalc(Comp, TT, P1, mf, AF, Tc, Pc, mw, mfgas, mfliq, Dgas, Dliq,
nc)
Qmliq=0.0
do i=1,nc
    Qmliq=Qmliq+((mf(i)-mfgas(i))/(mfliq(i)-mfgas(i)))*Qt*Dm
enddo
Qmgas=Qt*Dm-Qmliq
Qliq=Qmliq/(Dliq*5.615)
Qgas=Qmgas/(Dgas*5.615)
write (45,'(15A,A,f15.4,A,20A)')'Depth',',',Depth,',',ft'
write (45,'(15A)')'Component',',',V',',',L'
do i=1,nc
    write (45,'(15A,A,f15.8,A,f15.8)')Comp(i),',',mfgas(i),',',mfliq
enddo
mftgas=0.0
mftliq=0.0

```

```

do i=1,nc
    mftgas=mftgas+mfgas(i)*mw(i)
    mftliq=mftliq+mfgas(i)*mw(i)
enddo
write (45,'(15A,A,f15.8,A,f15.8)')',',mftgas,',',mftliq
go to 100
else
    depth=0
    Tg=Tg-d1*dTg
    call M_WellboreTempCal(TT, P1, dPdx, yN2, yH2S, yCO2, yH2O, VISliq,
        VISgas, gc, g, pi, ritbg,Qgas, Qt, Tgen, SGgas, etbg, dx, cpm, vtbg, Dm,
        Sigma, nc, mfgas, Tc, Pc, CN1, CN2, CN3, CN4, Vliq, Dliq)
    Tw=Tw-((Qo/60)/(Dm*vtbg*cpm))+Tgen
    TT=Tw
    Pw=P1
    Ko=0
    Uo=0
    Qo=0
    call FlashCalc(Comp, TT, P1, mf, AF, Tc, Pc, mw, mfgas, mfliq, Dgas, Dliq,
nc)
    Qmliq=0.0
    do i=1,nc
        Qmliq=Qmliq+((mf(i)-mfgas(i))/(mfliq(i)-mfgas(i)))*Qmt*Dm
    enddo
    Qmgas=Qmt*Dm-Qmliq
    Qliq=Qmliq/(Dliq*5.615)
    Qgas=Qmgas/(Dgas*5.615)
    write (45,'(15A,A,f15.4,A,20A)')'Depth',',',Depth,',',',ft'
    write (45,'(15A)')'Component',',',V',',',L'

```

```

do i=1,nc
  write (45,'(15A,A,f15.8,A,f15.8)')Comp(i),',',mfgas(i),',',mfliq
enddo
mftgas=0.0
mftliq=0.0
do i=1,nc
  mftgas=mftgas+mfgas(i)*mw(i)
  mftliq=mftliq+mfgas(i)*mw(i)
enddo
write (45,'(15A,A,f15.8,A,f15.8)')",',mftgas,',',mftliq
write (52, '(6(f15.3,A),f15.3)') Depth,',', Tg,',',TT,',',P1,',', Ko,',',Uo,',', Qo/60
endif
endif
close (52)
close (45)
end

```

The WTP Simulator – Injection Wells

```

!*****
!      Calculation of WTP for fluid injection through the wellbore
!*****
real kg, ka, ko, kcmt, ltbg, lcs1, lcs2, lcs3, l1, l2
open (51, file='HeatLossSLP.csv', status='unknown')
!=====
! Data entry section
!=====

```

```

call C_ConstantData (g, gc, SBC, pi, R)
call C_TubingInfo (FluidType, ritbg, rotbg, vtbg, vttbg, ltbg, TD, etbg)
print*, 'Enter number of casings and liners'
read *, ncsg

call C_CasingInfo (FluidType, ncsg, ricsg1, rocsg1, vcsg1, vtcsg1, lcs1, ricsg2,
rocsg2,vcsg2, vtcsg2, lcs2, ricsg3, rocsg3, vcsg3, vtcsg3, lcs3)

call C_Cmt_Ground_Data(rocmt1, rocmt2, rocmt3, rg)

call L_ProductionData (vttbg, ltbg, t, q, Tw, Tg, tp, ff, dx, TT, Tr, dtg)

call L_WellboreFluidProp (rof, cpf)

call C_AnnFluidProp (FluidType, ka, cpa, roa, visa)

call C_ThermalProp (FluidType, kg, kcmt, Etbg, Ecs1, alpha)

Depth=0
l2=lcs2
l1=lcs1
ricsg=ricsg1
rocsg=rocsg1
rocmt=rocmt1

print*, 'Guess Koverall, Btu/(hr. ft. oF):'
read *, koverall    ! Overall thermal conductivity coefficient
                    ! Btu/(hr. ft. oF)

ko=0.4

!=====
!Calculation of heat generated in wellbore due to friction of flowing fluid
!=====

write (51, '(6(A15,A),A15)') 'Depth (ft)',',',Tg (F)',',',Tw
(F)',',',Koverall',',',Uoverall',',',Qo (Btu/min)'

call fricHeatGen(rof, cpf, ff, pi, ritbg, q, vtbg, tp, gc, dx, Tgen)

!=====

```

!Calculation section

!=====

101 call L_TimeFunction (F, alpha, t, rocmt)

if (TT.gt.Tg) then

11 call C_CmtFormIntTemp (ko, kg, F, rotbg, rocmt, Tg, Tw, Tocmt, A)

call C_CasingSurTemp (Ticsg, Tocmt, A, C, rocmt, rocs, kcm, Tw)

call L_AnnulusHeatLossTop (Qa, SBC, Ticsg, Tw, Etb, Ecs, rotbg, rics, Cpa, visa, ka, roa, g, pi)

call L_CmtHeatLoss(pi, kcm, Ticsg, Tocmt, rocmt, rocs, Qcmt)

call C_OverallHeatLoss (Uo, Qo, Tw, Ticsg, Tocmt, rotbg, rocmt, rics, rocs, kcm, Qa, pi)

!=====

! Iteration Section

!=====

Q1 = abs (Qcmt - Qa)

if ((Q1.gt.0.02) .and. (Qa.gt.Qcmt)) then

if (q1.gt.1) then

ko=ko+0.001

go to 11

elseif (q1.gt.0.5) then

ko=ko+0.0001

go to 11

else

ko=ko+0.00001

go to 11

endif

elseif ((Q1.gt.0.02) .and. (Qa.lt.Qcmt)) then

```

if (q1.gt.1) then
  ko=ko-0.001
  go to 11
elseif (q1.gt.0.5) then
  ko=ko-0.0001
  go to 11
else
  ko=ko-0.00001
  go to 11
endif

else
  write (51, '(5(f15.3,A),f15.3)') Depth,',', Tg,',',TT,',', Ko,',',Uo,',', Qo/60
endif

!=====
!Define the next step of calculation
!=====

d1=depth
depth=depth+dx
Tg=Tg+dx*dTg
if (depth.le.(ltbg-dx)) then
  Tw=Tw-((Qo/60)/(rof*vtbg*cpf))+Tgen
  TT=Tw
  if (depth .ge. 12) then
    ricsg=ricsg3
    rocsg=rocsg3
    rocmt=rocmt3
    vtcs3=vtcs3

```

```

elseif ((depth .ge. 11) .and. (depth .lt. 12)) then
    ricsg=ricsg2
    rocsг=rocsг2
    rocmt=rocmt2
    vtcsg=vtcsg2
else
    ricsg=ricsg2
    rocsг=rocsг2
    rocmt=rocmt2+rocml
    vtcsg=vtcsg2
endif
go to 101
endif
endif

if (TT.eq.Tg) then
    TT=Tg
    Tw=TT
    Tg=Tg+dx*dTg
    go to 101
endif

if (TT.lt.Tg) then
12 call C_CmtFormIntTempBTM (ko, kg, F, rotbg, rocmt, Tg, Tw, Tocmt, A)
call C_CasingSurTemp (Ticsg, Tocmt, A, C, rocmt, rocsг, kcmt, Tw)
call L_AnnulusHeatLossBTM (Qa, SBC, Ticsg, Tw, Etbg, Ecsг, rotbg, ricsg, Cpa,
visa, ka, roa, g, pi)
call L_CmtHeatLossBTM(pi, kcmt, Ticsg, Tocmt, rocmt, rocsг, Qcmt)

```

call L_Qo_HL_BTM (Uo, Qo, Tw, Ticsg, Tocmt, rotbg, rocmt, ricsg, rocsg, kcmt,
Qa, pi)

!=====

! Iteration Section

!=====

Q1 = abs (Qcmt - Qa)

if ((Q1.gt.0.02) .and. (Qa.gt.Qcmt)) then

 if (q1.gt.1) then

 ko=ko+0.001

 go to 12

 elseif (q1.gt.0.5) then

 ko=ko+0.0001

 go to 12

 else

 ko=ko+0.00001

 go to 12

 endif

elseif ((Q1.gt.0.02) .and. (Qa.lt.Qcmt)) then

 if (q1.gt.1) then

 ko=ko-0.001

 go to 12

 elseif (q1.gt.0.5) then

 ko=ko-0.0001

 go to 12

 else

 ko=ko-0.00001

 go to 12

 endif

```

else
  write (51, '(5(f15.3,A),f15.3)') Depth,',', Tg,',',TT,',', Ko,',',Uo,',', Qo/60
endif

!=====
!Define the next step of calculation
!=====

d1=depth
depth=depth+dx
Tg=Tg+dx*dTg
if (depth.le.(lrbg-dx)) then
  Tw=Tw+((Qo/60)/(rof*vtbg*cpf))+Tgen
  TT=Tw
  if (depth .ge. 12) then
    ricsg=ricsg3
    rocsg=rocsg3
    rocmt=rocmt3
    vtcsg=vtcsg3
  elseif ((depth .ge. 11) .and. (depth .lt. 12)) then
    ricsg=ricsg2
    rocsg=rocsg2
    rocmt=rocmt2
    vtcsg=vtcsg2
  else
    ricsg=ricsg2
    rocsg=rocsg2
    rocmt=rocmt2+rocm1
    vtcsg=vtcsg2
  endif
endif

```

```

    go to 101
endif
endif
close(51)
end

```

The WTP Simulator – Subroutines

```

!           Enter constant information
subroutine C_ConstantData (g, gc, SBC, pi, R)
print*, 'Enter Acceleration Gravity Constant, ft/sec^2:'
read *, g
print*, 'Enter Acceleration Gravity Constant, ft/sec^2:'
read *, gc
print*, 'Enter Stephan-Boltzman Constant, Btu/(hr. ft^2. R):'
read *, SBC
print*, 'Enter Pi Constant:'
read *, Pi
print*, 'Enter Gas Constant, (ft^3.psia/(lbmol.R)):'
read *, R
return
end

subroutine C_TubingInfo (FluidType, ritbg, rotbg, vtbg, vttbg, ltbg, TD, etbg)
character (len=15) :: TBG(5), tbgsz, FluidType
real :: weit(5), dit(5), dot(5), vt(5)
real ltbg
open(unit=20, file='TBG_Data.txt', Status='OLD')
do i=1, 5

```

```

    read(20, '(A15, 4F15.4)') TBG(i), weit(i), dit(i), dot(i), vt(i)
enddo

print *, '***** Enter size and weight of tubing *****'

print *, 'For defining the size of tubing following rule should be considered.'

print *, '1. Enter letter "T" in capital'

print *, '2. Enter the size of casing followed by "'

print *, 'Some examples: T 4 1/2"'

!print*, 'tbgsiz='

!read *, tbgsiz

!print*, 'tbgweight='

!read*, tbgweight

!   print*, 'Enter the length of Tubing (ft):'

!   read *, ltbg

ltbg=18050

TD=ltbg

tbgsiz='T 3 1/2"'

tbgweight=9.2

do i=1, 5

    if((weit(i).eq.tbgweight).and.(TBG(i).eq.tbgsiz))then

        ditbg=dit(i)

        dotbg=dot(i)

        vtbg=vt(i)

    endif

enddo

!   print*, 'Enter the roughness of Tubing'

!   read *, etbg

etbg=0.0006

```

```

ritbg=ditbg/24    !Inner tubing radius (ft)
rotbg=dotbg/24    !Outter tubing radius (ft)
vtbg=vtbg*4.21    !unit volume of Casing (cu ft/ft)
vttbg=vtbg*ltbg   !Total volume of Tubing (cu ft)
print *,'
select case (FluidType)
  case ('Gas')
    write (50, '((20A,A),20A)')'Tubing',',','Information'
    write (50, '(6(20A,A),20A)') 'Size',',','Weigth (Lb/ft)',',','In Diameter (in)',',','Out
Diameter (in)',&
        ',','Capacity (bbl/ft)',',','Capacity (bbl/ft)',',','Depth (ft)'
    write      (50,      '(A15,      A,      5(f15.3,A),      f15.3)')
tbgsz,'',tbgweight,'',ritbg*2,'',rotbg*2,'',vtbg/4.21,'',etbg,'',ltbg
    write                                             (50,
'(7(A15,A),A15)')'*****',',','*****',',','*****',',','
*****',',','&
*****',',','&
*****',',','*****',',','*****',',','*****',',','*****
,
  case ('Liquid')
    write (51, '((20A,A),20A)')'Tubing',',','Information'
    write (51, '(6(20A,A),20A)') 'Size',',','Weigth (Lb/ft)',',','In Diameter (in)',',','Out
Diameter (in)',&
        ',','Capacity (bbl/ft)',',','Capacity (bbl/ft)',',','Depth (ft)'
    write      (51,      '(A15,      A,      5(f15.3,A),      f15.3)')
tbgsz,'',tbgweight,'',ritbg*2,'',rotbg*2,'',vtbg/4.21,'',etbg,'',ltbg
    write                                             (51,
'(7(A15,A),A15)')'*****',',','*****',',','*****',',','
*****',',','&
*****',',','&
*****',',','*****',',','*****',',','*****',',','*****
,
  case ('Mixture')

```

```

write (52, '((20A,A),20A)')'Tubing',',','Information'

write (52, '(6(20A,A),20A)') 'Size',',','Weigth (Lb/ft)',',','In Diameter (in)',',','Out
Diameter (in)',&

',','Capacity (bbl/ft)',',','Capacity (bbl/ft)',',','Depth (ft)'

write (52, '(A15, A, 5(f15.3,A), f15.3)')
tbgsz,','tbgsz,','ritbg*2,','rotbg*2,','vtbg/4.21,','etbg,','ltbg

write (52,
'(7(A15,A),A15)')'*****',',','*****',',','*****',',','
*****',',','&

'*****',',','*****',',','*****',',','*****
'

end select

close(20)

return

end

```

```

!           Enter wellbore fluid properties

subroutine L_WellboreFluidProp (rof, cpf)

print*, 'Enter heat capacity of wellbore fluid, (btu/(lb. F)):'
read *, Cpf

print*, 'Enter wellbore fluid API gravity, (API):'
read *, rof

rof=(141.5/(131.5+API))*62.4      !unit: (lb/cu ft)

print*, 'Enter velocity of wellbore fluid, (ft/min):'
read *, vf

return

end

subroutine C_CasingInfo (FluidType, ncsg, ricsg1, rocsg1, vcsg1, vtcs1, lcsg1,
ricsg2, rocsg2,&

```

```

vcsg2, vtcsg2, lcs2, ricsg3, rocsg3, vcsg3, vtcsg3, lcs3)

character (len=20) :: CSG_1, CSG_2, CSG_3, csg(8), FluidType
character (len=20) :: csgsize(ncsg)
real csgweight(ncsg), dicsg(ncsg), docsg(ncsg), vcsg(ncsg)
real wei(8), dic(8), doc(8), vc(8)
real lcs1, lcs2, lcs3

open(unit=10, file='CSG_Data.txt', Status='OLD')

do i=1, 8
  read(10, '(A20, 4F20.4)') csg(i), wei(i), dic(i), doc(i), vc(i)
enddo

print *, '***** Enter size and weight of casings *****'
print *, 'For defining the size of casing following rule should be considered.'
print *, '1. Enter letter "C" in capital'
print *, '2. Enter the size of casing followed by "'
print *, 'Some examples: C 13 3/8"'

do i=1, ncsg
  !print*, 'csgsize(i)='
  !read *, csgsize(i)
  !print*, 'csgweight(i)='
  !read*, csgweight(i)
enddo

csgsize(1)='C 13 3/8'
csgweight(1)=54.4

```

```
csgsize(2)='C 9 5/8'''
```

```
csgweight(2)=43.5
```

```
csgsize(3)='C 7'''
```

```
csgweight(3)=26.00
```

```
do k=1, ncsg
```

```
  do i=1, 8
```

```
    if((wei(i).eq.csgweight(k)).and.(csg(i).eq.csgsize(k)))then
```

```
      dicsg(k)=dic(i)
```

```
      docsg(k)=doc(i)
```

```
      vcsg(k)=vc(i)
```

```
    endif
```

```
  enddo
```

```
enddo
```

```
CSG_1=csgsize(1)
```

```
ricsg1=dicsg(1)/24      !Inner radius of casing no. 1, ft
```

```
rocsg1=docsg(1)/24     !Outer radius of casing no. 1, ft
```

```
vcsg1=vcsg(1)*4.21     !unit volume of Casing no 1, (cu ft/ft)
```

```
!  print*, 'Enter length of Casing 13 3/8" (ft):'
```

```
!  read *, lcs1
```

```
lcs1=480
```

```
vtcs1=vcsg1*lcs1
```

```
CSG_2=csgsize(2)
```

```
ricsg2=dicsg(2)/24     !Inner radius of casing no. 2, ft
```

```

rocs2=docsg(2)/24      !Outer radius of casing no. 2, ft
vcsg2=vcsg(2)*4.21    !unit volume of Casing no 2, (cu ft/ft)
!  print*, 'Enter length of Casing 9 5/8" (ft):'
!  read *, lcs2
lcs2=15000
vtcs2=vcsg2*lcs2

CSG_3=csgsize(3)
rics3=dicsg(3)/24     !Inner radius of casing no. 3, ft
rocs3=docsg(3)/24    !Outer radius of casing no. 3, ft
vcsg3=vcsg(3)*4.21   !unit volume of Casing no 3, (cu ft/ft)
!  print*, 'Enter length of Casing 7" (ft):'
!  read *, lcs3
lcs3=3000
vtcs3=vcsg3*lcs3

print *,''
select case (FluidType)
  case ('Gas')
    write (50, '(20A)')'Casings',',','information'
    write (50, '(11A)') 'Size',',','Weigth (Lb/ft)',',','In Diameter (in)',',','Out Diameter
(in)',',','Capacity (bbl/ft)',&
      ',','depth (ft)'
    write (50, '(A15, A, 4(f15.3,A), f15.3)')
    csgsize(1),',',csgweight(1),',',rics1*2,',',rocs1*2,',',vcsg1/4.21,',',lcs1
    write (50, '(A15, A, 4(f15.3,A), f15.3)')
    csgsize(2),',',csgweight(2),',',rics2*2,',',rocs2*2,',',vcsg2/4.21,',',lcs2
    write (50, '(A15, A, 4(f15.3,A), f15.3)')
    csgsize(3),',',csgweight(3),',',rics3*2,',',rocs3*2,',',vcsg3/4.21,',',lcs3

```



```

write
(7(A15,A),A15)'*****',,, '*****',,, '*****',,,
*****',,,&

```

```

*****',,, '*****',,, '*****',,, '*****'
,

```

```
end select
```

```
close(10)
```

```
return
```

```
end
```

```
subroutine Cmt_Ground_Data (rocmt1, rocmt2, rocmt3, rg)
```

```
print*, 'Enter outter diameter of cementing sheath (in):'
```

```
!read *, rocmt
```

```
!docmt1=30          !First casing
```

```
rocmt1=docmt1/24   !Outter cement sheath radius (ft)
```

```
docmt2=20          !Second casing
```

```
rocmt2=docmt2/24   !Outter cement sheath radius (ft)
```

```
docmt3=12          !Third casing
```

```
rocmt3=docmt3/24   !Outter cement sheath radius (ft)
```

```
print*, 'Enter the out_radius of Ground/Formation (ft):'
```

```
read *, rocmt
```

```
return
```

```
end
```

```
subroutine L_WellboreFluidProp (rof, cpf)
```



```

read *, Tw
Tr=Tw !Tr is the reservoir pressure and it's applied for comparison.
TT=Tw
print*, 'Enter geothermal temperature at bottom hole and surface(F):'
read *, Tg
Tgb=Tg !Geothermal temperature at the bottom
Tgs=70 !Geothermal temperature at the surface
tp=1440*vttbg/(q*5.615) !Production time (min)
!1 day = 1440 min
dx=ltbg/tp !Steps deffinition
dTg=(Tgb-Tgs)/ltbg !Geothermal change per each step
write (51, '(20A)')'Production and','reservoir','Information'
write (51, '(20A)') 'P duration (day)',',', 'P Rate (bbl/d)',',', 'T @ reservoir (F)',',', 'P @
reservoir (psi)'
write (51, '(3(f15.2,A),f15.2)') t,',',q,',',TT,',',P1
write (51, '(7(A15,A),A15)')'*****',',', '*****',',', '*****',',', '
*****',',',&
'*****',',', '*****',',', '*****',',', '*****'
'
return
end

```

```

subroutine ProductionData (vttbg, ltbg, t, q, Tw, Tg, tp, dx, TT, Tr, P1, Vp, dtg)
real ltbg
print*, 'Enter production time (Day(s)):'
read *, t ! Production time
print*, 'Enter production rate (MMscf/d):'
read *, q
print*, 'Enter reservoir pressure (psi):'

```

```

read *, p1
pr=p1
print*, 'Enter reservoir temperature (F):'
read *, Tw
Tr=Tw !Tr is the reservoir pressure and it's applied for comparison.
TT=Tw
print*, 'Enter geothermal temperature at bottom hole and surface(F):'
read *, Tg
Tgb=Tg !Geothermal temperature at the bottom
Tgs=75 !Geothermal temperature at the surface
tp=(vttbg*24*60)/(q*1000000) !Production time (min)
Vp=lbtg/tp !Production Speed (ft/min)
dx=100 !Steps definition
dTg=(Tgb-Tgs)/lbtg !Geothermal change per each step
write (50, '(20A)')'Production and','reservoir','Information'
write (50, '(20A)') 'P duration (day)',',', 'P Rate (bbl/d)',',', 'T @ reservoir (F)',',', 'P @
reservoir (psi)'
write (50, '(3(f15.2,A),f15.2)') t,',',q,',',TT,',',P1
write
(50,
'(7(A15,A),A15)')'*****',',', '*****',',', '*****',',',
'*****',',',&
'*****',',', '*****',',', '*****',',', '*****'
,
return
end

```

```

subroutine C_AnnFluidProp(FluidType, ka, cpa, roa, visa)
character(len=15) FluidType
real ka
print*, 'Enter Thermal conductivity coefficient of annulus fluid, btu/(hr. ft. F):'

```



```
if (t .ge. 7) then
```

```
  F=log(2*sqrt(alpha*(t*24))/rocmt)-0.29
```

```
else
```

```
  !print*, 'Enter f(t):'
```

```
  !read *, F
```

```
  F=1.0714e-09
```

```
end if
```

```
return
```

```
end
```

```
subroutine C_CmtFormIntTemp (ko, kg, F, rotbg, rocmt, Tg, Tw, Tocmt, A)
```

```
real kg, ko
```

```
A=ko/(log(rocmt/rotbg))
```

```
B=kg/F
```

```
Tocmt=(A*Tw+B*Tg)/(A+B)
```

```
return
```

```
end
```

```
subroutine C_AnnulusHeatLoss (Qa, SBC, Ticsg, Tw, Etbg, Ecsg, rotbg, ricsg, Cpa,
visa, ka, roa, g, pi)
```

```
real ka
```

```
Qr=(SBC*((Tw+460)**4-(Ticsg+460)**4))/((1/Etbg)+(rotbg/ricsg)*((1/Ecsg)-1))
```

```
Pr=(Cpa*visa)/ka
```

```
Beta=1/(Tw+460)
```

```
Gr=g*beta*((Tw+460)-(Ticsg+460))*(ricsg-rotbg)**3/((roa/visa)/3600)**2
```

```
Ra=Gr*Pr
```

```
fu=0.049*Ra**0.333*Pr**0.074 !fu means Nu
```

```
hm=(ka/(ricsg-rotbg))*fu
```

```
Qm=2*pi*hm*(Tw-Ticsg)
```

```
Qa=Qm+Qr
```

```
return
```

```
end
```

```
subroutine L_CmtHeatLoss(pi, kcmt, Ticsg, Tocmt, rocmt, rocsg, Qcmt)
```

```
real kcmt
```

```
real Tocmt
```

```
Qcmt=2*pi*kcmt*(Ticsg-Tocmt)/log(rocmt/rocsg)
```

```
return
```

```
end
```

```
subroutine C_OverallHeatLoss (Uo, Qo, Tw, Ticsg, Tocmt, rotbg, rocmt, ricsg,
rocsg, kcmt, Qa, pi)
```

```
real kcmt
```

```
rm=(ricsg-rotbg)/log(ricsg/rotbg)
```

```
havg=Qa/(2*pi*rm*(Tw-Ticsg))
```

```
Uo=((rotbg/(rm*havg))+rotbg*log(rocmt/rocsg)/kcmt)**(-1)
```

```
Qo=2*pi*rotbg*Uo*(Tw-Tocmt)
```

```
return
```

```
end
```

```
subroutine C_ProdZone(nperf, dperf, Lperf)
```

```
real Lperf
```

```
print*, 'Enter number of perforations per foot'
```

```
read *, nperf
```

```
print*, 'Enter length of production zone, (ft)'
```

```
read *, Lperf
```

```
print*, 'Enter diameter of perforation, (in)'
```

```
read *, dperf
```

```
return
```

```
end
```

```

subroutine Components (nc, MWg, Gamag, yN2, yCO2, yH2S, yH2O, AF, Tc, Pc,
Vc, mf, mw, NC1, NC2, NC3, NC4, NC5)

character(len=20) com(16), comp(nc), NC1, NC2, NC3, NC4, NC5

real mft, mmw(16), MWg, TTc(16), PPc(16), AAF(16), VVc(16)

real mw(nc), Tc(nc), Pc(nc), Vc(nc), AF(nc), mf(nc), YiMi(nc)

open (unit=20, file='Components_Data_File.txt', Status='old')

write (50, '(15A)') 'Component',',','Mole      ',',','Molecular',',','Yi*Mi',',','Tc      ',',','Pc
',',','Acentric',',','Vc'

write (50, '(15A)') '      ',',','Fraction',',','Weight',',','
',',','(R)',',','(psi)',',','Factor',',','ft^3/mole'

do i=1, 16

    read(20, '(A20, 4F20.4,F20.7)') com(i), mmw(i), TTc(i), PPc(i), AAF(i), VVc(i)

enddo

print *, 'For defining the name of a component foolowing rule should be considered.'

print *, '1. Enter letters in capital'

print *, '2. Enter i or n as the following if it is necessary.'

print *, 'Examples: N2, i-C4H10, n-C4H10'

print *, 'In this section, it is needed to enter the name and'

print *, 'mole fraction of each components.'

do i=1, nc

    print *, 'Enter the name of component',i

    print *, comp(i)

    read *, comp(i)

    print *, 'Enter the mole fraction of component', comp(i)

    print *, mf(i)

    read *, mf(i)

enddo

```

```

yN2=0.0
yCO2=0.0
yH2S=0.0
yH2O=0.0
MWg=0.0
mft=0.0
NC1='None'
NC2='None'
NC3='None'
NC4='None'
NC5='None'
do i=1, nc
  do k=1, 16
    if (comp(i)==com(k)) then
      comp(i)=com(k)
      mw(i)=mmw(k)
      Tc(i)=TTc(k)
      Pc(i)=PPc(k)
      AF(i)=AAF(k)
      Vc(i)=VVc(k)
      MWg=MWg+mf(i)*mw(i)
      YiMi(i)=mf(i)*mw(i)
      mft=mft+mf(i)
      write (50, '(A15,A,6(f15.4,A),f15.7)')
comp(i),',',mf(i),',',mw(i),',',YiMi(i),',',Tc(i),',',Pc(i),',',AF(i),',',Vc(i)
    if(comp(i)=='H2S') then
      NC1='H2S'
      yH2S=mf(i)

```



```

Tpseudo=0.0
if (NC5 .eq. 'None') then
  do i=1, nc
    Ppseudo=Ppseudo+(mf(i)*Pc(i))
    Tpseudo=Tpseudo+(mf(i)*Tc(i))
  enddo
else
!*****          Stewart et al method          *****
  print*, 'Enter specific gravity of C7+ component'
  print*, 'GamaC7+= '
  read *, Gamac7
  do i=1, nc
    yc7=mf(i)
    mwc7=mw(i)
  enddo
  do i=1, nc
    YY1=mf(i)*Tc(i)/Pc(i)
    Y1=Y1+YY1
    YY2=mf(i)*(Tc(i)/Pc(i))**0.5
    Y2=Y2+YY2
    YY3=mf(i)*Tc(i)/Pc(i)**0.5
    Y3=Y3+YY3
  enddo
  Tbc7=(4.5579*mwc7**0.15178*Gamac7**0.15427)**3
  Pppc71=(0.24244+(2.2898/Gamac7)+(0.11857/Gamac7**2))*(Tbc7/1000)
  Pppc72=(1.4685+(3.648/Gamac7)+(0.47227/Gamac7**2))*(Tbc7**2/10**7)
  Pppc731=(0.42019+(1.6977/Gamac7**2))*Tbc7**3
  Pppc732=Pppc731/10**5

```

```

Pppc73=Pppc732/10**5
Pppc7=exp(8.3634-(0.0566/Gamac7)-pppc71+Pppc72-Pppc73)
Tpc71=341.7+811*Gamac7
Tpc72=(0.4244+0.1174*Gamac7)*Tbc7
Tpc73=(0.4669-3.2623*Gamac7)*(10**5/Tbc7)
Tpc7=Tpc71+Tpc72+Tpc73
Fj=((yc7*Tpc7)/(3*Pppc7))+((2*yc7**2*Tpc7)/(3*Pppc7))
Saij=0.6081*Fj+1.1325*Fj**2-14.004*Fj*yc7+64.434*Fj*yc7**2
Saik=(Tpc7/Pppc7**0.5)*((0.3129*yc7)-(4.8156*yc7**2)+(27.3751*yc7**3))
corj1=(Y1/3)+(2*Y2**2/3)
corj=corj1-Saij
cork=Y3-Saik
Tpseudo=cork**2/corj
Ppseudo=Tpseudo/corj
endif

TTpseudo=Tpseudo
!Wichert and Aziz method
if ((NC1 .eq. 'H2S').or.(NC2 .eq. 'CO2')) then
  Acor=yH2S+yCO2
  Bcor=yH2S
  cor1=120*(Acor**0.9-Acor**1.6)+15*(Bcor**0.5-Bcor**4)
  Tpseudo=Tpseudo-cor1
  Ppseudo=Ppseudo*Tpseudo/(TTpseudo+Bcor*(1-Bcor)*cor1)
endif

if ((NC3 .eq. 'N2').or.(NC4 .eq. 'H2O')) then
  Tpscor=-246.1*yN2+400*yH2O
  Ppccor=-162*yN2+1270*yH2O
  Tpseudo=((Tpseudo-227.2*yN2-1.165*yH2O)/(1-yN2-yH2O))+Tpscor

```

```

    Ppseudo=((Ppseudo-493.1*yN2-3200*yH2O)/(1-yN2-yH2O))+Ppccor
endif
write (50, '(A15,A,f15.3,A,A15)')'Tpc = ',',',Tpseudo,',',',R'
write (50, '(A15,A,f15.3,A,A15)')'Ppc = ',',',Ppseudo,',',',Psia'
write (50, '(A15,5(A,A15))')'Impurities',',',',N2',',',',CO2',',',',H2S',',',',H2O',',',',C7+'
write (50, '(A15,5(A,f15.4))')'Mole Fraction',',',',yN2',',',',yCO2',',',',yH2S',',',',yH2O',',',',yC7
return
end

```

```

subroutine PseudoPropUC(Gamag, MWg, Ppseudo, Tpseudo, yN2, yCO2, yH2S,
yH2O)
real MWg
Ppseudo=0.0
Tpseudo=0.0
print*, 'Enter mole fraction of N2?'
read *, yN2
print*, 'Enter mole fraction of CO2?'
read *, yCO2
print*, 'Enter mole fraction of H2S?'
read *, yH2S
print*, 'Enter mole fraction of H2O?'
read *, yH2O
!***** Standing's correlations (1977) *****
Tpseudo=168+325*Gamag-12.5*Gamag**2      !psia
Ppseudo=677+15*Gamag-37.5*Gamag**2      !R
!Wichert and Aziz method
TTpseudo=Tpseudo
Acor=yH2S+yCO2
Bcor=yH2S

```

```

cor1=120*(Acor**0.9-Acor**1.6)+15*(Bcor**0.5-Bcor**4)
Tpseudo=Tpseudo-cor1
Ppseudo=Ppseudo*Tpseudo/(TTpseudo+Bcor*(1-Bcor)*cor1)
Tpscor=-246.1*yN2+400*yH2O
Ppccor=-162*yN2+1270*yH2O
Tpseudo=((Tpseudo-227.2*yN2-1.165*yH2O)/(1-yN2-yH2O))+Tpscor
MWg=Gamag*28.96                                !MWg: lbm/lbm.mole

write (50, '(A15,A,f15.3)')Tpc = ', ', Tpseudo
write (50, '(A15,A,f15.3)')Ppc = ', ', Ppseudo
write (50, '(A15,4(A,A15))')Impurities', ', ', 'N2', ', ', 'CO2', ', ', 'H2S', ', ', 'H2O'
write (50, '(A15,4(A,f15.4))')Mole Fraction', ', ', yN2, ', ', yCO2, ', ', yH2S, ', ', yH2O
return
end

```

```

subroutine ZFactorCalKC(TT, P1, Z, Ppseudo, Tpseudo)
    !Hall-Yarborough method for Z-factor calculation
    !Newton-Raphson iterative technique

    eps=1.0e-5
    y=0.01      !Firt guess
    Ppr=(P1+14.7)/(Ppseudo+14.7)
    tr=Tpseudo/(TT+460)
    A=0.06125*tr*exp(-1.2*(1-tr)**2)
    B=tr*(14.76-9.76*tr+4.58*tr**2)
    C=tr*(90.7-242.2*tr+42.4*tr**2)
    D=2.18+2.82*tr
    10 fy=(y+y**2+y**3-y**4)+(1-y)**3*(-(A*Ppr)-(B*y**2)+(C*y**D))
    u1=y+y**2+y**3-y**4
    du1=1+2*y+3*y**2-4*y**3

```

```

u2=(1-y)**3
du2=-3*(1-y)**2
u3=-(A*Ppr)-(B*y**2)+(C*y**D)
du3=-2*B*y+D*C*y**(D-1)
f1y=du1+(du2*u3+u2*du3)
if(abs(fy) .le. eps) then
    Z=A*Ppr/y
elseif ((fy .ne. 0).and.(f1y .ne. 0)) then
    y=y-(fy/f1y)
    goto 10
else
    print *,'Newton Raphson method do not converge.'
endif
return
end

```

```

subroutine ZFactorCalUC(TT, P1, Z, Gamag, rog, Ppseudo, Tpseudo, dzdtp)
    !Hall-Yarborough method for Z-factor calculation
    !Newton-Raphson iterative technique
    !Tpc=326+(315.7*(rog-.5))-(240*yn2)-(83.3*yco2)+(133.3*yh2s)
    !Ppc=678-(50*(rog-.5))-(206.7*yn2)+(440*yco2)+(606.7*yh2s)
    eps=1.0e-5
    y=0.01      !Firt guess
    Ppr=(P1+14.7)/(Ppseudo+14.7)
    Tpr=(TT+460)/Tpseudo
    tr=Tpseudo/(TT+460)
    A=0.06125*tr*exp(-1.2*(1-tr)**2)
    B=tr*(14.76-9.76*tr+4.58*tr**2)
    C=tr*(90.7-242.2*tr+42.4*tr**2)

```

```

D=2.18+2.82*tr
10 fy=(y+y**2+y**3-y**4)+(1-y)**3*(-(A*Ppr)-(B*y**2)+(C*y**D))
u1=y+y**2+y**3-y**4
du1=1+2*y+3*y**2-4*y**3
u2=(1-y)**3
du2=-3*(1-y)**2
u3=-(A*Ppr)-(B*y**2)+(C*y**D)
du3=-2*B*y+D*C*y**(D-1)
f1y=du1+(du2*u3+u2*du3)
if(abs(fy) .le. eps) then
    Z=A*Ppr/y
elseif ((fy .ne. 0).and.(f1y .ne. 0)) then
    y=y-(fy/f1y)
    goto 10
else
    print *,'Newton Raphson method do not converge.'
endif
C1=0.96+0.008*Tpr+(0.22/Tpr**2)
dC1dTpr=0.008-(0.44/Tpr**3)
C2=0.29-0.0635*Tpr-(0.865/Tpr**2)
dC2dTpr=(-0.0635)+(1.73/Tpr**3)
W1=0.00032+0.2*Tpr**(-5.58)
W2=0.45+Tpr**(-5.57)
C3=W1/W2
dW1dTpr=(-1.116)*Tpr**(-6.58)
dW2dTpr=(-5.57)*Tpr**(-6.57)
dC3dTpr=(dW1dTpr*W2-W1*dW2dTpr)/W2**2
W3=(-0.025)+0.00013*Tpr**5.47

```

```

W4=0.665+Tpr**5.47
C4=W3/W4
dW3dTpr=.0007111*Tpr**4.47
dW4Tpr=5.47*Tpr**4.47
dC4dTpr=(dW3dTpr*W4-W3*dW4Tpr)/W4**2
W5=1-6.466*exp(-1.815*Tpr)
C5=(-0.0001)+(0.00009/W5)
dW5dTpr=11.73579*exp(-1.815*Tpr)
dC5dTpr=(0.00009*(-dW5dTpr))/W5**2
Z1=C1+C2*Ppr+C3*Ppr**2+C4*Ppr**3+C5*Ppr**4
dZ1dTpr=dC1dTpr+dC2dTpr*Ppr+dC3dTpr*Ppr**2+dC4dTpr*Ppr**3+dC5dTpr*P
pr**4
dZdTp=0.055*dZ1dTpr/Tpseudo
rog=2.7*(P1+14.7)*Gamag/(Z*(TT+460))          !rog: lbm/ft^3
          !P1: psia
          !TT: R

return
end

```

```

subroutine WellboreFluidPropKC (cpg, Gamag, rog, visg, MWg, P1, Z, R, TT, ritbg,
Bg)
real MWg
print*, 'Enter heat capacity of wellbore fluid, (Btu/(lb.mole F)):'
read *, Cpg
rog=(P1+14.7)*MWg/(Z*R*(TT+460))          !lbm/ft^3
Atbg=3.14*ritbg**2
Bg=0.0282*Z*(TT+460)/(P1+14.7)
print*, 'Enter viscosity of wellbore fluid, lb.mass/(ft. hr):'
read *, visf

```

```

write (51, '(16A)') 'Thermal and',',',',physiactl Properties',',',',of production',',',',fluid'
write (50, '(16A)') 'Cp of Gas',',',',Gas density',',',',Gas viscosity',',',',Specific gravity'
write (50, '(16A)') 'Btu/(lbmole. F)',',',',lbm/cu. ft ',',',',lbm/(ft. hr)',',',',lbm/lbmole'
write (50, '(3(f15.2,A),f15.2)') Cpg,',',rog,',',visg,',',Gamag
return
end

```

```

subroutine WellboreFluidPropUC (cpg, Gamag, rog, visg, P1, Z, TT, ritbg, Bg)
print*, 'Enter heat capacity of wellbore fluid, (Btu/(lb.mole F)):'
read *, Cpg
Atbg=3.14*ritbg**2
Bg=0.0282*Z*(TT+460)/(P1+14.7)
print*, 'Enter viscosity of wellbore fluid, lb.mass/(ft. hr):'
read *, visf
write (51, '(16A)') 'Thermal and',',',',physiactl Properties',',',',of production',',',',fluid'
write (50, '(16A)') 'Cp of Gas',',',',Gas density',',',',Gas viscosity',',',',Specific gravity'
write (50, '(16A)') 'Btu/(lbmole. F)',',',',lbm/cu. ft ',',',',lbm/(ft. hr)',',',',lbm/lbmole'
write (50, '(3(f15.2,A),f15.2)') Cpg,',',rog,',',visg,',',Gamag
return
end

```

```

Subroutine Gasspeed (q, TT, P1, R, ritbg, Atbg, MWg, Vg, Vs, Z)
real MWg
Atbg=3.14*ritbg**2
Vm=Z*R*(TT+460)/(P1+14.7)           !Volume: cu ft/Lbm.mol
                                   !R=10.732 (psi. ft^3/Lbm.mol.R)
                                   !MWg: lbm/lbm.mol
Vg=(MWg/Vm)*(q*1000000/86400)      !Gas rate: Lbm/s
Vs=q*1000000/(Atbg*86400)         !Gas speed: scf/s

```

```
!write (1, '(A20,A,f15.3,A,A20)') 'Speed of gas',',',Vg,',',lbmass/s'
```

```
return
```

```
end
```

```
subroutine FricFac(Gamag, visg, ritbg, q, ff)
```

```
Rey=(20*Gamag*q*1000000)/(visg*ritbg*24)
```

```
if (Rey.le.2000)then
```

```
    ff=64/Rey
```

```
else
```

```
    ff=4*(2.28-4*log((0.0023/(ritbg*24)))+(21.25/Rey**0.9))**(-2)    !Jain and Swamee Equation
```

```
endif
```

```
!write (1, '(A20,A,f15.2)') 'Friction Factor',',',ff
```

```
Return
```

```
End
```

```
Subroutine GasProperties (P1, TT, ritbg, Z, Bg)
```

```
Atbg=3.14*ritbg**2
```

```
Bg=0.0282*Z*(TT+460)/(P1+14.7)    !ft^3/SCF
```

```
return
```

```
end
```

```
subroutine WellboreTempCalKC(n, cpg, Qo, Vg, d1, dx, g, gc, q, ritbg, dTw, TT, rog, Kjt, mf, nc, depth, Tc, Pc, Vc, Ppseudo, Tpseudo, AF, R, Gamag, Bg, ff, P1, dp, Z, Tw, Vs, TD, Pi, MWg, dperf, nperf, Lperf, Ko, Uo, Tg, dtg)
```

```
real Kjt, mf, Lperf, Ko, MWg
```

```
call JouleThomsonCoefKC(nc, P1, Z, cpg, rog, TT, Tc, Pc, Vc, R, AF, mf, Kjt)
```

```
if (d1 .eq. TD) call TempPerf (q, Z, R, TT, gc, P1, MWg, Pi, ritbg, nperf, dperf, Kjt, TD, Tg, Lperf, dx, dtg)
```

```
write (50, '(7(f15.3,A),f15.3)') Depth+dx,',', Tg+dx*dTg,',',TT,',',P1,',', Ko,',',Uo,',', Qo/60,',', Z
```

```
call Press_Loss(Gamag, Z, dx, TT, ff, q, P1, Bg, ritbg, dp)
```

```

n=n+1
dTW1=(1/cpg)*(Qo/3600)*(dx/Vg)
dTW2=(1/cpg)*g*dx/(778*gc)
dTW3=(1/cpg)*(Vs*Bg)**2/(2*778*gc)
dTW4=dTW1-dTW2+dTW3
dTW=(Kjt*dp)-dTW4
      !1hr=3600s      Qo: Btu/hr.ft
      !cpg: Btu/lbm.F  w: lbm/s
      !Cj: F/psi      gc: Lbm.ft/Lbf.s^2
      !dTf: F         g:ft/s^2
      !dz: ft         q: gas flow rate, cu ft/d
      !J: 778 ft.Lbf/Btu  A: TBG cross section
      !Bg: cu ft/scf    1 day=86400 sec

if (depth .lt. 0) then
  !Tw=TT-dTw
  Tw=Tw-(d1/dx)*dTw+1.7/n
else
  !Tw=Tw-(d1/dx)*dTw
  Tw=TT-dTw+1.7/n
endif

TT=Tw
P1=P1-dp
call ZFactorCalKC(TT, p1, z, Ppseudo, Tpseudo)
call GasProperties (P1, TT, ritbg, Z, Bg)
write (100, '(5(f15.4,A), f15.4)') Gamag,' ',Kjt,' ',dp,' ',Z,' ',Bg,' ',TT
return
end

```

```

subroutine WellboreTempCalUC(n, cpg, Qo, Vg, d1, dx, g, gc, q, ritbg, dTw, TT,
rog, Kjt, depth, Ppseudo, Tpseudo, R, Gamag, Bg, ff, P1, dp, Z, Tw, Vs, dzdtp, TD,
Pi, MWg, dperf, nperf, Lperf, Ko, Uo, Tg, dtg, yN2, yCO2, yH2S)
real Kjt, Lperf, Ko, MWg
call JouleThomsonCoefUC(Z, dzdtp, cpg, rog, TT, Kjt)
if (d1 .eq. TD) call TempPerf (q, Z, R, TT, gc, P1, MWg, Pi, ritbg, nperf, dperf, Kjt,
TD, Tg, Lperf, dx, dtg)
write (50, '(7(f15.3,A),f15.3)') Depth+dx,',', Tg+dx*dTg,',',TT,',',P1,',', Ko,',',Uo,',',
Qo/60,',', Z
call Press_Loss(Gamag, Z, dx, TT, ff, q, P1, Bg, ritbg, dp)
n=n+1
dTw1=(1/cpg)*(Qo/3600)*(dx/Vg)
dTw2=(1/cpg)*g*dx/(778*gc)
dTw3=(1/cpg)*(Vs*Bg)**2/(2*778*gc)
dTw4=dTw1-dTw2-dTw3
dTw=(Kjt*dp)-dTw4
      !1hr=3600s      Qo: Btu/hr.ft
      !cpg: Btu/lbm.F   w: lbm/s
      !Cj: F/psi      gc: Lbm.ft/Lbf.s^2
      !dTf: F         g:ft/s^2
      !dz: ft         q: gas flow rate, cu ft/d
      !J: 778 ft.Lbf/Btu  A: TBG cross section
      !Bg: cu ft/scf    1 day=86400 sec
if (depth .gt. dx) then
  Tw=TT-dTw+1.1/n
else
  Tw=Tw-(d1/dx)*dTw+1.1/n
endif
TT=Tw

```

```

P1=P1-dp
call ZFactorCalUC(TT, P1, Z, Gamag, rog, Ppseudo, Tpseudo, dzdtp, yN2, yCO2,
yH2S)
call GasProperties (P1, TT, ritbg, Z, Bg)
write (100, '(5(f15.4,A), f15.4)') Gamag,',',Kjt,',',dp,',',Z,',',Bg,',',TT
return
end

```

```

subroutine M_ProdData(Qoil, Qgas, Qw, Qliq, Qt, Vliq, Tres, Pres, Doil, Dw, SGw,
Cpm, tp, VISliq, VISgas, Sigma, ltbg, Tg, dTg, Tw, P1, TT, dx, ritbg)
real ltbg
Area=3.14*ritbg**2
print*, 'Enter reservoir temperature, F'
read *, Tres
Tw=Tres
TT=Tres
print*, 'Enter reservoir pressure, psig'
read *, Pres
P1=Pres
print*, 'Enter oil production rate @ separation condition, bbl/day'
read *, Qoil
print*, 'Enter gas production rate @ separation condition, Mscf/day'
read *, Qgas
print*, 'Enter water production rate @ separation condition, bbl/day'
read *, Qw
Qliq=Qoil+Qw
Vliq=5.615*Qliq/(86400*Area)    !Production liquid velocity, ft/sec
Qt=Qliq*5.615+Qgas*1000      !Total production flow rate, scf/day
print*, 'Enter API of produced oil'

```

```

read *, APIoil
SGoil=(APIoil+131.5)/141.5
Doil=SGoil*62.4
print*, 'Enter density of produced water, lbm/ft^3'
read *, Dw
SGw=Dw
print*, 'Enter heat capacity of mixture fluid, (btu/(lbm. F))'
read *, Cpm
print*, 'Enter viscosity of produced liquid phase, cp'
read *, VISliq
print*, 'Enter viscosity of produced gas phase, cp'
read *, VISgas
print*, 'Enter liquid surface tension, lbm/sec^2'
read *, Sigma
print*, 'Enter duration of productin, day'
read *, tp
print*, 'Enter geothermal temperature at the bottom hole(F):'
read *, Tg
Tgb=Tg          !Geothermal temperature at the bottom
print*, 'Enter geothermal temperature at the surface(F):'
read *, Tgs
Tgs=55          !Geothermal temperature at the surface
dx=100          !Steps deffinition
dTg=(Tgb-Tgs)/lbtg
write (52, '(3(A20,A), A20)') 'Production',',',',information',',',',at entry point',',',',to the
wellbore'
write (52, '(A20,A,A20)') 'Reservoir Temp (F)',',',',Reservoir Pres (psi)'
write (52, '(f20.4,A,f20.4)') Tres,',',',Pres

```

```
write (52, '(2(A20,A),A20)') 'Qoil (bbl/day)',',', 'Qwater (bbl/day)',',', 'Qgas
(Mscf/day)'
```

```
write (52, '(2(f20.4,A),f20.4)') Qoil,',', Qw,',', Qgas
```

```
write (52, '(7(A15,A),A15)') '*****',',', '*****',',', '*****',',', '*****',',',
*****',',', &
```

```
'*****',',', '*****',',', '*****',',', '*****',',',
'
```

```
return
```

```
end
```

```
subroutine M_Components (Comp, yN2, yCO2, yH2S, yH2O, AF, Tc, Pc, Vc, mf,
mw, CN1, CN2, CN3, CN4, nc)
```

```
character(len=20) com(16), comp(nc), CN1, CN2, CN3, CN4, CN5
```

```
real MWtot, mftot
```

```
real mmw(16), TTc(16), PPc(16), AAF(16), VVc(16)
```

```
real mw(nc), Tc(nc), Pc(nc), Vc(nc), AF(nc), mf(nc), YiMi(nc)
```

```
open (unit=20, file='Components_Data_File.txt', Status='old')
```

```
open (unit=21, file='Components_of_Fluid.txt', Status='old')
```

```
do k=1, 16
```

```
read(20, '(A20, 4F20.4,F20.7)') com(k), mmw(k), TTc(k), PPc(k), AAF(k),
VVc(k)
```

```
!mmw=Molecular weight (lbm/lbmole)
```

```
!TTC=Critical temperature (R)
```

```
!PPC=Critical pressure (psia)
```

```
!VVc=Critical molar volume (ft3/mole)
```

```
enddo
```

```
close(20)
```

```
do i=1, nc
```

```
read(21, '(A20, F20.4)') comp(i), mf(i)
```

```

enddo
close(21)
yN2=0.0
yCO2=0.0
yH2S=0.0
yH2O=0.2
MWtot=0.0
mftot=0.0
CN1='None'
CN2='None'
CN3='None'
CN4='None'
CN5='None'

write (52, '(3(A20,A), A20)') 'Components of','','producing fluid','','at entry
point','','to the wellbore'

write (52, '(7(A20,A), A20)') 'Component','','Mole fraction','','Molecular
weight','','','','Critical temp','','&

                                'Critical Press','','Critical volume','','Acentric factor'

write (52, '(6(A20,A), A20)') "','','','(lb/mole)','','(lb/mole)','','(R)','','&

                                '(psia)','','(cu ft/mole)'

do i=1, nc
  do k=1, 16
    if (comp(i)==com(k)) then
      comp(i)=com(k)
      mw(i)=mmw(k)
      Tc(i)=TTc(k)
      Pc(i)=PPc(k)
      AF(i)=AAF(k)
    end if
  end do
end do

```

```

Vc(i)=VVc(k)
MWtot=MWtot+mf(i)*mw(i)
YiMi(i)=mf(i)*mw(i)
mftot=mftot+mf(i)
write (52, '(A15,A,6(f15.4,A),f15.7)')
comp(i),',',mf(i),',',mw(i),',',YiMi(i),',',Tc(i),',',&
Pc(i),',',Vc(i),',',AF(i)
if(comp(i)=='H2S') then
  CN1='H2S'
  yH2S=mf(i)
endif
if(comp(i)=='CO2') then
  CN2='CO2'
  yCO2=mf(i)
endif
if(comp(i)=='N2') then
  CN3='N2'
  yN2=mf(i)
endif
if(comp(i)=='H2O') then
  CN4='H2O'
  yH2O=mf(i)
endif
if(comp(i)=='C7+') then
  CN5='C7+'
endif
endif
enddo

```



```

real fug_l(20)      ! liquid fugacity
real xk_phase(20)
real d_fug_dx_v(20,20), d_fug_dp_v(20)
real d_fug_dx_l(20,20), d_fug_dp_l(20)
real omega(20), tc(20), pc(20)
real xm(20), dd(20,20)
real a_pr(20,20), b_pr(20)
real ac_pr(20), xk_pr(20)
real shi_par(20), s(20)
real delta(20,20)
real h(20), hi(20)
real v(20)
real da0_dx(20), db0_dx(20), dz_dx(20)
!      newton -----
real x_j(20,20)
real f(20)
real xb(20,20)
real ttc(n_comp), ppc(n_comp), mw(n_comp), mf(n_comp), af(n_comp)
!      --- reading data file -----
n_max=20

t=((tt-491.67)/1.8)+273.15
p=p1*6894.7
do i=1,n_comp
    chi_o(i)=mf(i)
enddo
chi_o(n_comp) = 1.0
do ii=1,n_comp-1

```

```

    chi_o(n_comp) = chi_o(n_comp) - chi_o(ii)
enddo
do i=1,n_comp
    omega(i)=af(i)
    tc(i)=((ttc(i)-491.67)/1.8)+273.15
    pc(i)=ppc(i)*6894.7
    xm(i)=mw(i)
    xm(i)=0.001*xm(i)
enddo
!      ** dij: interaction coefficients =0 if i does not equal to j
!-----
open(unit=1,file='binary_interac_coeff.txt',status='old')
rewind 1
do ii=1,n_comp
    read(1,*) (dd(ii,kk),kk=1,n_comp)
enddo
close(1)
!      ** volume translation
!-----

open(unit=1,file='shi_par.txt',status='old')
rewind 1
read(1,*) i_vol_tran
do ii=1,n_comp
    read(1,*) shi_par(ii)
    if (i_vol_tran.eq.0) then
        shi_par(ii)=0.0d0

```

```

endif
enddo
close(1)
!-----
do i=1,n_comp
  do j=1,n_comp
    delta(i,j)=0.0
    if(i.eq.j) delta(i,j)=1.0
  enddo
enddo
enddo
! -----
err_max_iterative=1.0e-04

call flash_iterative (t, p,alpha, rho_l, rho_v, rho_m_l, rho_m_v,chi_v, chi_l, chi_o,
fug_v, fug_l, xk_phase,      d_fug_dx_v, d_fug_dp_v, d_fug_dx_l, d_fug_dp_l,
omega, tc, pc, xm, dd, a_pr, b_pr, ac_pr, xk_pr, s,shi_par, err_max_iterative,
err_1,delta, h, hi, v,da0_dx, db0_dx, dz_dx,      n_comp, n_max, nt_iterative)

err_max_newton=1.0e-12

call flash_newton (t, p, alpha, rho_l, rho_v, rho_m_l, rho_m_v,chi_v, chi_l, chi_o,
fug_v, fug_l, xk_phase, d_fug_dx_v, d_fug_dp_v, d_fug_dx_l, d_fug_dp_l, omega,
tc, pc, xm, dd, a_pr, b_pr, ac_pr, xk_pr, s,shi_par, err_max_newton, err_1,delta, h,
hi, v,da0_dx, db0_dx, dz_dx,x_j, f, xb,n_comp, n_max, nt_newton)

xmtv=0.0
xmtl=0.0

do ii=1,n_comp
  xmtv=xmtv+xm(ii)*chi_v(ii)
  xmtl=xmtl+xm(ii)*chi_l(ii)
enddo

open(25,file='rflash_test.csv')

write(25,*)           'cce=',                rho_v*(1.0-alpha)*xmtl/(rho_v*(1.0-
alpha)*xmtl+rho_l*alpha*xmtv)

write(25,*) ''

```

```

write(25,*) 'volume of vapor phase =',alpha*xmtv/rho_v
write(25,*) 'volume of liquid phase =',(1.0-alpha)*xmtl/rho_l
write(25,*) 'total volume=',alpha*xmtv/rho_v+(1.0-alpha)*xmtl/rho_l
write(25,*) 'cvd=',(1.0-alpha)*xmtl/rho_l/8.66493626e-05
rho_v=rho_v*.062428
rho_l=rho_l*.062428

open(unit=35, file='rflash_results.csv', status='unknown')
write (35, '(20a)') 'alpha',',','density of vapor',',','density of liquid'
write (35, '(2(f20.7,a),f20.7)') alpha',',',rho_v',',',rho_l
write (35, '(20a)') 'component',',',, v ',',',, l ',',',, k '
do ii=1,n_comp
    write (35, '(a,2(a,f7.5),a,f12.6)') comp(ii),',',chi_v(ii),',',chi_l(ii),',',xk_phase(ii)
enddo
close(35)
return
end

```

```

subroutine JouleThomsonCoefKC(nc, P1, Z, cp, rog, TT, Tc, Pc, Vc, R, AF, mf,
Kjt)
real Kjt, apr(nc), m(nc), aprim(nc), bpr(nc)
real Tc(nc), Pc(nc), Vc(nc), AF(nc), mf(nc)
deltaij=0.0
doubleapr=0.0
aapr=0.0
aprimpr=0.0
bbpr=0.0
do i=1, nc
    m(i)=0.37464+1.54226*AF(i)-0.26992*AF(i)**2

```

```

apr(i)=(0.45723553*R**2*Tc(i)**2/Pc(i))*(1+m(i)*(1-((TT+460)/Tc(i))**0.5))
aprim(i)=-m(i)*apr(i)/((1+m(i)*(1-
((TT+460)/Tc(i))**0.5))*((TT+460)*Tc(i))**0.5)
enddo
do i=1, nc
  do j=1, nc
    doubleapr=apr(i)*apr(j)
    deltaij=1-((2*(Vc(i)**(1/6)*Vc(j)**(1/6))/(Vc(i)**(1/3)+Vc(j)**(1/3))**3))**6
    aij=doubleapr**0.5*(1-deltaij)
    aapr=aapr+(mf(i)*mf(j)*aij)
    aprimpr=aprimpr+0.5*mf(i)*mf(j)*(1-
deltaij)*(((apr(j)/apr(i))**0.5*aprim(i))+((apr(i)/apr(j))**0.5*aprim(j)))
  enddo
enddo
do i=1, nc
  bpr(i)=0.077796074*R*Tc(i)/Pc(i)
  bbpr=bbpr+mf(i)*bpr(i)
enddo
Acappr=aapr*(P1+14.7)/(R*(TT+460))**2
Bcappr=bbpr*(P1+14.7)/(R*(TT+460))
dadtp1=(R*(TT+460))**2
dadtp2=aprimpr-(2*aapr/(TT+460))
dadtp=(P1+14.7)*dadtp2/dadtp1
dbdtp=-bbpr*(P1+14.7)/(R*(TT+460)**2)
dzdtp1=dadtp*(Bcappr-Z)
dzdtp2=dbdtp*(6*Bcappr*Z+2*Z_3*Bcappr**2-2*Bcappr+Acappr-Z**2)
dzdtp3=Acappr-2*Bcappr-3*Bcappr**2
dzdtp=(dzdtp1+dzdtp2)/(3*Z**2+2*(Bcappr-1)*Z+dzdp3)

```

```
Kjt=(1/(5.40395*cpg))*(TT/(Z*rog))*(dzdTp)  !1 Btu=5.40395 (psi. ft^3)
```

```
return
```

```
end
```

```
subroutine JouleThomsonCoefUC(Z, dzdtp, cpg, rog, TT, Kjt)
```

```
real Kjt
```

```
Kjt=(1/(5.40395*cpg))*(TT/(Z*rog))*(dzdTp)  !1 Btu=5.40395 (psi. ft^3)
```

```
!Kjt: F/psi
```

```
return
```

```
end
```

```
subroutine Press_Loss(Gamag, Z, dx, TT, ff, q, P1, Bg, ritbg, dp)
```

```
s=0.0375*Gamag*dx/(z*(TT+460))
```

```
s2=q*Bg*1000000*(TT+460)*Z
```

```
s1=0.000667*s2**2*ff/(ritbg*24)**5
```

```
P2=(P1**2-s1*(exp(s)-1))/exp(s)
```

```
P2=P2**0.5
```

```
dp=P1-P2
```

```
P1=P1-dp
```

```
Return
```

```
End
```

```
subroutine TempPerf (q, Z, R, TT, gc, P1, MWg, Pi, ritbg, nperf, dperf, Kjt, TD, Tg, Lperf, dx, dtg)
```

```
real MWg, Lperf, Kjt
```

```
q=q*1000000/(nperf*Lperf*86400)
```

```
dtbg=2*(ritbg*12)
```

```
dia=((dtbg**4)-(dperf**4))/(dtbg**4*dperf**4)
```

```
dPperf=1152*q**2*dia*(P1+14.7)*MWg/(pi*gc*Z*R*(TT+460))
```

```
dTperf=Kjt*dPperf
```

```
Tperf=TT-dTperf
```

```

write (50, '(3(f15.3,A),f15.3)') TD+3,',', Tg+dx*dTg,',',TT,',',P1
write (50, '(3(f15.3,A),f15.3)') TD+2,',', Tg+dx*dTg,',',Tperf,',',P1-dPperf
return
end

```

```

subroutine alpha_calc(chi_o,xk_phase,alpha,n_comp,n_max)
!implicit real*8(a-h,o-z)
real xk_phase(n_max),chi_o(n_max)
xk1= 0.0
do ii=1,n_comp
    xk1=max(xk1,xk_phase(ii))
enddo
xk2= 1.0e+20
do ii=1,n_comp
    xk2=min(xk2,xk_phase(ii))
enddo
alpha_0=1.0/(1.0-xk1)
alpha_1=1.0/(1.0-xk2)
do while (abs(alpha_1-alpha_0).ge.1.0e-06)

alpha=(alpha_0+alpha_1)/2.0
xh=0.0
do kk=1,n_comp
    xh=xh+(xk_phase(kk)-1.0)*chi_o(kk)/(1.0+alpha*(xk_phase(kk)-1.0))
enddo
if (xh.ge.0.0) then
    alpha_0=alpha
else
    alpha_1=alpha

```

```

endif
enddo
return
end

```

```

subroutine cubic_1(a, b, c, z1, z2, z3)
!   this subroutine solves and returns the roots of the
!   cubic equation: z**3 + a*z**2 + b*z + c = 0
!   (cf. Numerical Recipes, p. 179)
!IMPLICIT REAL*8(A-H,O-Z)
Pi = ACOS(-1.0)
Q = (A**2 - 3.0*B)/9.0
R = (2.0*A**3 - 9.0*A*B + 27.0*C)/54.0
IF(R.ge.0.0) THEN
    iSgnR = 1
ELSE
    iSgnR = -1
ENDIF
IF(R**2.lt.Q**3) THEN
!   CASE I: THREE REAL ROOTS
!       R**2 < Q**3
    Theta = ACos(R/Q/sqrt(Q))
    Z1 = -2.0*sqrt(Q)*cos(Theta/3.0) - a/3.0
    Z2 = -2.0*sqrt(Q)*cos((Theta + 2.0*Pi)/3.0) - a/3.0
    Z3 = -2.00*sqrt(Q)*cos((Theta - 2.0*Pi)/3.0) - a/3.0
ELSE
!   CASE II: ONE REAL ROOT, ONE COMPLEX CONJUGATE PAIR
!       R**2 > Q**3
!       (Note: we set Complex Roots equal to 0.0)

```

```

AAA = - iSgnR*(abs(R) + sqrt(R**2 - Q**3) )**(1.0/3.0)
IF(AAA.ne.0.0) THEN
    BBB = Q/AAA
ELSE
    BBB = 0.0
ENDIF

!      Z3 is Real
Z3 = (AAA + BBB) - A/3.0

!      Z1, Z2 should be Complex and a Conjugate Pair.
!      These are unneeded, so we set them equal to Zero.
ZImag = sqrt(3.0)/2.0*(AAA-BBB)
IF(abs(ZImag).eq.0.0) THEN
    Print*, "We Have a Problem, Im(Z1,Z2) = 0.0 ", ZImag
    STOP
ENDIF

Z1 = 0.0
Z2 = 0.0
ENDIF

RETURN

END

```

```

subroutine flash_iterative(t, p, alpha, rho_l, rho_v, rho_m_l, rho_m_v, chi_v, chi_l,
chi_o, fug_v, fug_l, xk_phase, d_fug_dx_v, d_fug_dp_v, d_fug_dx_l, d_fug_dp_l,
omega, tc, pc, xm, dd, a_pr, b_pr, ac_pr, xk_pr, s, shi_par, err_max, err_l,delta, h,
hi, v,da0_dx, db0_dx, dz_dx,n_comp, n_max, nt)

```

```

!implicit real*8(a-h,o-z)

```

```

real omega(n_max), tc(n_max), pc(n_max)

```

```

real xm(n_max), dd(n_max,n_max)

```

```

real a_pr(n_max,n_max), b_pr(n_max)

```

```

real ac_pr(n_max), xk_pr(n_max)

```

```

real chi_v(n_max) ! vapor composition
real chi_l(n_max) ! liquid composition
real chi_o(n_max) ! overall composition
real fug_v(n_max) ! vapor fugacity
real fug_l(n_max) ! liquid fugacity
real xk_phase(n_max)
real shi_par(n_max), s(n_max)
real d_fug_dx_v(n_max,n_max), d_fug_dp_v(n_max)
real d_fug_dx_l(n_max,n_max), d_fug_dp_l(n_max)
real delta(n_max,n_max)
real h(n_max), hi(n_max)
real v(n_max)
real da0_dx(n_max), db0_dx(n_max), dz_dx(n_max)
chi_o(n_comp) = 1.0
do ii=1,n_comp-1
    chi_o(n_comp) = chi_o(n_comp) - chi_o(ii)
enddo
err_1=1.0
alpha=0.5
nt=0
nt_max=10000
n_alpha=0
n_alpha_max=10
!           -- estimation of the ki factors --
do ii=1,n_comp
    xk_phase(ii)=exp(5.37*(1.0+omega(ii))*(1.0-tc(ii)/t))*pc(ii)/p
enddo
c_v=0.0

```

```

c_l=0.0
do ii=1,n_comp
  chi_v(ii)=chi_o(ii)*xk_phase(ii)
  chi_l(ii)=chi_o(ii)/xk_phase(ii)
  c_v=c_v+chi_v(ii)
  c_l=c_l+chi_l(ii)
enddo

do ii=1,n_comp
  chi_v(ii)=chi_v(ii)/c_v
  chi_l(ii)=chi_l(ii)/c_l
  xk_phase(ii)=chi_v(ii)/chi_l(ii)
enddo

write(25,*) "
write(25,*) 'iterative method:'
write(25,*) 'iteration number  alpha      error '
do while ((err_1.ge.err_max).and.(nt.le.nt_max))

call peng_rob_eos(t, p, chi_v, shi_par, 1, n_comp, rho_v, rho_m_v, fug_v,
d_fug_dx_v, d_fug_dp_v, v, h, hi, omega, tc, pc, xm, dd, delta, a_pr, b_pr, ac_pr,
xk_pr, da0_dx, db0_dx, dz_dx, s,n_comp, n_max)

call peng_rob_eos(t, p, chi_l, shi_par, 2, n_comp,rho_l, rho_m_l, fug_l,d_fug_dx_l,
d_fug_dp_l,v, h, hi,omega, tc, pc, xm, dd, delta,a_pr, b_pr, ac_pr, xk_pr, da0_dx,
db0_dx, dz_dx, s,n_comp, n_max)

do ii=1,n_comp
  xk_phase(ii)=xk_phase(ii)*fug_l(ii)/fug_v(ii)
enddo

call alpha_calc(chi_o,xk_phase,alpha,n_comp,n_max)

if (alpha.gt.1.0) then
  n_alpha=n_alpha+1
  alpha=1.0

```

```

endif
if (alpha.lt.0.0) then
  n_alpha=n_alpha+1
  alpha=0.0
endif
if (n_alpha.ge.n_alpha_max) err_1=0.0
c_v=0.0
c_l=0.0
do ii=1,n_comp
  chi_l(ii)=chi_o(ii)/&
  (1.0+alpha*(xk_phase(ii)-1.0))
  chi_v(ii)=xk_phase(ii)*chi_l(ii)
  c_v=c_v+chi_v(ii)
  c_l=c_l+chi_l(ii)
enddo
do ii=1,n_comp
  chi_v(ii)=chi_v(ii)/c_v
  chi_l(ii)=chi_l(ii)/c_l
enddo
if (err_1.ne.0.0) then
err_1=0.0

do ii=1,n_comp
  err_1=err_1+(fug_v(ii)/fug_l(ii)-1.0)**2
enddo
err_1=sqrt(err_1)
nt=nt+1
endif

```

```

write(25,25) nt,alpha,err_1
if (nt.eq.nt_max) then
  write(25,*) 'flash claculation did not converge !!!!!!'
  write(25,*) 'error=',err_1
  write(25,*) '-----'
endif
enddo

25 format(5x,i5,8x,f12.10,2x,e10.4)

return

end

```

```

subroutine flash_newton(t, p,alpha, rho_l, rho_v, rho_m_l, rho_m_v, chi_v, chi_l,
chi_o, fug_v, fug_l, xk_phase, d_fug_dx_v, d_fug_dp_v, d_fug_dx_l, d_fug_dp_l,
omega, tc, pc, xm, dd,a_pr, b_pr, ac_pr, xk_pr, s,shi_par, err_max, err_1, delta, h, hi,
v,da0_dx, db0_dx, dz_dx,x_j, f, xb,n_comp, n_max, nt)

```

```

!implicit real*8(a-h,o-z)

real omega(n_max), tc(n_max), pc(n_max)

real xm(n_max), dd(n_max,n_max)

real a_pr(n_max,n_max), b_pr(n_max)

real ac_pr(n_max), xk_pr(n_max)

real chi_v(n_max) ! vapor composition
real chi_l(n_max) ! liquid composition
real chi_o(n_max) ! overall composition

real fug_v(n_max) ! valpor fugacity
real fug_l(n_max) ! liquid fugacity

real xk_phase(n_max)

real shi_par(n_max), s(n_max)

real d_fug_dx_v(n_max,n_max), d_fug_dp_v(n_max)
real d_fug_dx_l(n_max,n_max), d_fug_dp_l(n_max)

real delta(n_max,n_max)

```

```

real h(n_max), hi(n_max)
real v(n_max)
real da0_dx(n_max), db0_dx(n_max), dz_dx(n_max)
real x_j(n_max,n_max)
real f(n_max)
real xb(n_max,n_max)
nt=0
nt_max=10000
if ((alpha.eq.0.0).or.(alpha.eq.1.0)) err_1=0.0
if (err_1.ge.err_max) then
  write(25,*) 'newton method:'
  write(25,*) 'iteration number   alpha       error '
endif
do while ((err_1.ge.err_max).and.(nt.le.nt_max))
call peng_rob_eos(t, p, chi_v, shi_par, 1, n_comp,&
  rho_v, rho_m_v, fug_v,&
  d_fug_dx_v, d_fug_dp_v,&
  v, h, hi,&
  omega, tc, pc, xm, dd, delta,&
  a_pr, b_pr, ac_pr, xk_pr,&
  da0_dx, db0_dx, dz_dx, s, &
  n_comp, n_max)
call peng_rob_eos(t, p, chi_l, shi_par, 2, n_comp,&
  rho_l, rho_m_l, fug_l,&
  d_fug_dx_l, d_fug_dp_l,&
  v, h, hi,&
  omega, tc, pc, xm, dd, delta,&
  a_pr, b_pr, ac_pr, xk_pr,&

```

```

    da0_dx, db0_dx, dz_dx, s, &
    n_comp, n_max)
do ii=1,n_comp
  do jj=1,n_comp
    dfi_dnj_v=0.0
    dfi_dnj_l=0.0
    do kk=1,n_comp
      dfi_dnj_v=dfi_dnj_v+d_fug_dx_v(ii,kk)*(delta(kk,jj)-chi_v(kk))
      dfi_dnj_l=dfi_dnj_l+d_fug_dx_l(ii,kk)*(delta(kk,jj)-chi_l(kk))
    enddo
    x_j(ii,jj)=dfi_dnj_v/alpha+dfi_dnj_l/(1.0-alpha)
  enddo
enddo
do ii=1,n_comp
  f(ii)=fug_v(ii)-fug_l(ii)
enddo
call gauss_jordan(x_j, xb, n_comp,n_max)
do ii=1,n_comp
  do jj=1,n_comp
    alpha=alpha-x_j(ii,jj)*f(jj)
  enddo
enddo
do ii=1,n_comp
  do jj=1,n_comp
    chi_v(ii)=chi_v(ii)-x_j(ii,jj)*f(jj)/alpha
  enddo
enddo
c_v=0.0

```

```

do ii=1,n_comp
  c_v=c_v+chi_v(ii)
enddo

do ii=1,n_comp
  chi_v(ii)=chi_v(ii)/c_v
enddo

do ii=1,n_comp
  chi_l(ii)=(chi_o(ii)-alpha*chi_v(ii))/(1.0-alpha)
enddo

c_l=0.0

do ii=1,n_comp
  c_l=c_l+chi_l(ii)
enddo

do ii=1,n_comp
  chi_l(ii)=chi_l(ii)/c_l
enddo

if (err_1.ne.0.0) then
  err_1=0.0

  do ii=1,n_comp
    err_1=err_1+(fug_v(ii)/fug_l(ii)-1.0)**2
  enddo

  err_1=sqrt(err_1)

  nt=nt+1
endif

write(25,25) nt,alpha,err_1

enddo

25 format(5x,i5,8x,f12.10,2x,e10.4)

return

```

```

end

```

```

subroutine m_fricfac(rey, ff, ritbg, etbg)
fc=0.0005
eps=0.0006
if (rey.le.2000)then
  ff=64/rey
elseif((rey.gt.2000).and.(rey.lt.4000))then
  !colebrook and white equation
10 ff1=(1/(1.74-2*log((2*etbg/(ritbg*24))*(18.7/(rey*fc**(-0.5))))))**2
  if((abs(fc-ff1)).lt.eps)then
    ff=ff1
  else
    fc=ff
    goto 10
  endif
endif
else
  ff=(1/(1.74-2*log(2*etbg/(ritbg*24))))**2 !nikuradse equation
endif
!write (1, '(a20,a,f15.2)') 'friction factor =',',',ff
!write (1,
return
end

```

```

subroutine m_gasdensity(tres, pres, sggas, yn2, yco2, yh2s, yh2o, dgas, nc, mfgas,
tc, pc, cn1, cn2, cn3, cn4)
character(len=20) cn1, cn2, cn3, cn4
real tc(16), pc(16), mfgas(16)
!ncompar=1
!if (compar.eq.1) then

```

```

    call m_pseudopropkc(nc, mfgas, tc, pc, cn1, cn2, cn3, cn4, ppseudo, tpseudo,
    yn2, yco2, yh2s, yh2o)

```

```

    call m_zfactor(tres, pres, z, sggas, dgas, ppseudo, tpseudo)

```

```

!   ncompar=ncompar+1

```

```

!endif

```

```

!   call pseudopropuc(sggas, mwg, ppseudo, tpseudo, yn2, yco2, yh2s, yh2o)

```

```

!   call m_zfactor(tres, pres, z, sggas, dgas, ppseudo, tpseudo)

```

```

!endif

```

```

return

```

```

end

```

```

subroutine gauss_jordan(a,b,n,n_max)

```

```

!implicit real*8(a-h,o-z)

```

```

real a(n_max,n_max), b(n_max,n_max)

```

```

parameter(nmax=50)

```

```

dimension indx(nmax),indxr(nmax),ipiv(nmax)

```

```

do j=1,n

```

```

    ipiv(j)=0

```

```

enddo

```

```

do i=1,n

```

```

    big=0.0

```

```

    do j=1,n

```

```

        if(ipiv(j).ne.1) then

```

```

            do k=1,n

```

```

                if (ipiv(k).eq.0) then

```

```

                    if (abs(a(j,k)).ge.big) then

```

```

                        big=abs(a(j,k))

```

```

                        irow=j

```

```

                        icol=k

```

```

        endif
        !elseif (ipiv(k).gt.1) then
            !pause 'singular matrix'
        endif
    enddo
endif
enddo
ipiv(icol)=ipiv(icol)+1
if(irow.ne.icol) then
    do l=1,n
        dum=a(irow,l)
        a(irow,l)=a(icol,l)
        a(icol,l)=dum
    enddo
    do l=1,n
        dum=b(irow,l)
        b(irow,l)=b(icol,l)
        b(icol,l)=dum
    enddo
endif
indxr(i)=irow
indxc(i)=icol
!if (a(icol,icol).eq.0.0d0) pause 'singular matrix'
pivinv=1.0/a(icol,icol)
a(icol,icol)=1.0
do l=1,n
    a(icol,l)=a(icol,l)*pivinv
enddo

```

```

do l=1,n
  b(icol,l)=b(icol,l)*pivinv
enddo
do ll=1,n
  if (ll.ne.icol) then
    dum=a(ll,icol)
    a(ll,icol)=0.0
    do l=1,n
      a(ll,l)=a(ll,l)-a(icol,l)*dum
    enddo
    do l=1,n
      b(ll,l)=b(ll,l)-b(icol,l)*dum
    enddo
  endif
enddo
enddo
do l=n,1,-1
  if (indxr(l).ne.indxc(l)) then
    do k=1,n
      dum=a(k,indxr(l))
      a(k,indxr(l))=a(k,indxc(l))
      a(k,indxc(l))=dum
    enddo
  endif
enddo
return
end

```

```

subroutine M_LiqProp(Qoil, Qw, Qliq, Doil, Vliq, Foil, Fw, Dw, Dliq, Pi, ritbg)

```

```

Area=Pi*ritbg**2
Foil=Qoil/(Qoil+Qw)
Fw=1-Foil
Qliq=Qoil+Qw           !Production liquid flow rate, bbl/day
Vliq=5.615*Qliq/(86400*Area)   !Production liquid velocity, ft/sec
Dliq=Doil*Foil+Dw*Fw       !Production liquid density, lbm/ft^3
return
end

```

```

subroutine M_PhaseDet(Qgas, Qliq, Qt, ritbg, Dliq, sigma, g, Lm, Ls, FP, pi)
character(len=20) FP
real Lb, Ls, Lm
Area=pi*ritbg**2           !Wellbore cross section area, (ft^2)
Vt=Qt/(86400*Area)        !Total velocity, ft/sec
Vgd=((Qgas*1000/8640)*(Dliq/(g*sigma))**0.25)/Area   !Dimensionless gas
velocity
Dh=2*ritbg                !Dh=2r, Hydraulic diameter of a circular tube, ft
Lb=1.071-(0.2218*Vt**2/Dh)   !Flow regime boundary, dimensionless
Ls=50+(36*Vgd*Qliq*5.615)/Qgas   !Flow regime boundary,
dimensionless

Lm=75+84*(Vgd*Qliq*5.615/Qgas)**0.75   !Flow regime boundary,
dimensionless

if (((Qgas/Qt).lt.Lbs).and.(Lb.ge.0.13)) then
    FP='Bubble flow'
elseif (((Qgas/Qt).gt.Lb).and.(Vgd.lt.Ls)) then
    FP='Slug flow'
elseif ((Vgd.lt.Lm).and.(Vgd.gt.Ls)) then
    FP='Transition flow'
elseif (Vgd.gt.Lm) then

```

```

    FP='Mist flow'
endif
return
end

```

```

subroutine peng_rob_eos(t, p, chi, shi_par, i_phase, niv, rho, rho_mole, fug, d_fug,
d_fug_dp, v, h, hi, omega, tc, pc, xm, dd, delta, a, b, ac, xk, da0_dx, db0_dx, dz_dx, s,
n_comp, n_max)

!implicit real*8(a-h,o-z)

real omega(n_max), tc(n_max), pc(n_max)

real xm(n_max), dd(n_max,n_max)

real delta(n_max,n_max)

real a(n_max,n_max), b(n_max)

real ac(n_max), xk(n_max)

real h(n_max), hi(n_max)

real fug(n_max), chi(n_max), shi_par(n_max)

real d_fug(n_max,n_max), d_fug_dp(n_max)

real s(n_max), v(n_max)

real da0_dx(n_max), db0_dx(n_max), dz_dx(n_max)

r=8.30549210

chi(n_comp)=1.0

do kk=1,n_comp-1
    chi(n_comp)=chi(n_comp)-chi(kk)
enddo

do i=1,n_comp
    if(omega(i).lt.0.50) then
        xk(i)=0.37464 + 1.54226*omega(i) -0.26992*omega(i)**2
    else

```

```

    xk(i)=0.3796 + 1.485*omega(i) -0.1644*omega(i)**2 +&
    0.01667*omega(i)**3
endif
ac(i)=0.45724 * r**2 * tc(i)**2/pc(i)
b(i)=0.07780 * r * tc(i)/pc(i)
enddo
do ii=1,n_comp
    a(ii,ii)=ac(ii)*(1.0+xk(ii)*(1.0-sqrt(t/tc(ii))))**2
enddo
do ii=1,n_comp
    do kk=1,n_comp
        a(ii,kk)=(1.0-dd(ii,kk))*sqrt(a(ii,ii)*a(kk,kk))
    enddo
enddo
aa=0.0
do ii=1,n_comp
    do kk=1,n_comp
        aa=aa+chi(ii)*chi(kk)*a(ii,kk)
    enddo
enddo
a0=aa*p/t**2/r**2
bb=0.0
do ii=1,n_comp
    bb=bb+chi(ii)*b(ii)
enddo
b0=bb*p/t/r
coef0 = -(a0*b0 - b0**2 - b0**3)
coef1 = a0 - 3.0*b0**2 - 2.0*b0

```

```

coef2 = -(1.0 - b0)
call cubic_1(coef2, coef1, coef0, z1, z2, z3)
z3 = max(z1,z2,z3)
z1 = min(z1,z2,z3)
if (z1.eq.0.0) z1=z3
if (i_phase.eq.1) z=z3
if (i_phase.eq.2) z=z1
!           liquid, single phase ==>
!   ----- total molar weight ---
xmt=0.0
do ii=1,n_comp
  xmt=xmt+xm(ii)*chi(ii)
enddo
!   ----- density ---
vm=r*t*z/p
c=0.0
do ii=1,n_comp
  c=c+chi(ii)*shi_par(ii)*b(ii)
enddo
vm=vm-c
rho=xmt/vm
rho_mole=1.0/vm
!   -----
!   ----- fugacity ---
do kk=1,n_comp
  x=b(kk)*(z-1.0)/bb - log(z-b0)
  xx=0
  do ii=1,n_comp

```

```

    xx=xx+chi(ii)*a(ii,kk)
enddo

x=x-a0*(2.0*xx/aa-b(kk)/bb)*log((z+(1.0+sqrt(2.0))*b0)/(z+(1.0-
sqrt(2.0))*b0))/b0/sqrt(2.0)/2.0

fug(kk)= exp(x) * p * chi(kk)
enddo

do i=1,n_comp
    s(i)=0.0
    do j=1,n_comp
        s(i)=s(i)+chi(j)*a(j,i)
    enddo
enddo

dz_da0=(b0-z)/(3.0*z**2-2.0*(1.0-b0)*z+(a0-2.0*b0-3.0*b0**2))
dz_db0=(-z**2+2.0*(3.0*b0+1.0)*z+(a0-2.0*b0-3.0*b0**2))/(3.0*z**2-2.0*(1.0-
b0)*z+(a0-2.0*b0-3.0*b0**2))

alpha=a0/b0
gamma=log((z+(1.0+sqrt(2.0))*b0)/(z+(1.0-sqrt(2.0))*b0))

if (niv.eq.n_comp-1) then
    do j=1,n_comp-1
        da0_dx(j)=p*2.0*(s(j)-s(n_comp))/r**2/t**2
        db0_dx(j)=p*(b(j)-b(n_comp))/r/t
        dz_dx(j)=dz_da0*da0_dx(j)+dz_db0*db0_dx(j)
    enddo
endif

if (niv.eq.n_comp) then
    do j=1,n_comp
        da0_dx(j)=p*2.0*s(j)/r**2/t**2
        db0_dx(j)=p*b(j)/r/t
    enddo
endif

```

```

dz_dx(j)=dz_da0*da0_dx(j)+dz_db0*db0_dx(j)
enddo
endif
! ----- fugacity derivatives :d_fugi/d_xj ---
if (niv.eq.n_comp-1) then
do i=1,n_comp-1
do j=1,n_comp-1
beta=2.0*s(i)/aa-b(i)/bb
d_alpha_dxj=(b0*da0_dx(j)-a0*db0_dx(j))/b0**2
d_beta_dxj=2.0*((a(i,j)-a(i,n_comp))*aa-&
2.0*s(i)*(s(j)-s(n_comp)))/aa**2+b(i)*(b(j)-b(n_comp))/bb**2
d_gamma_dxj=((dz_dx(j)+(1.0+sqrt(2.0))*db0_dx(j))/&
(z+(1.0+sqrt(2.0))*b0)-(dz_dx(j)+(1.0-sqrt(2.0))*db0_dx(j))/&
(z+(1.0-sqrt(2.0))*b0))

t1=(dz_dx(j)*bb-(z-1.0)*(b(j)-b(n_comp)))*b(i)/bb**2
t2=-((dz_dx(j)-db0_dx(j))/(z-b0)
t3=-d_alpha_dxj*beta*gamma/sqrt(2.0)/2.0
t4=-alpha*d_beta_dxj*gamma/sqrt(2.0)/2.0
t5=-alpha*beta*d_gamma_dxj/sqrt(2.0)/2.0
d_fug(i,j)=t1+t2+t3+t4+t5
! --- d_fugi/d_xj
d_fug(i,j)=fug(i)*&
(d_fug(i,j)+delta(i,j)/chi(i))
enddo
enddo
endif
if (niv.eq.n_comp) then

```

```

do i=1,n_comp
  do j=1,n_comp
    beta=2.0*s(i)/aa-b(i)/bb
    d_alpha_dxj=(b0*da0_dx(j)-a0*db0_dx(j))/b0**2
    d_beta_dxj=2.0*(aa*a(i,j)-s(i)*2.0*s(j))/aa**2+&
      b(i)*b(j)/bb**2

d_gamma_dxj=((dz_dx(j)+(1.0+sqrt(2.0))*db0_dx(j))/(z+(1.0+sqrt(2.0))*b0)-&
  (dz_dx(j)+(1.0-sqrt(2.0))*db0_dx(j))/(z+(1.0-sqrt(2.0))*b0))
  t1=(dz_dx(j)*bb-(z-1.0)*b(j))*b(i)/bb**2
  t2=-(dz_dx(j)-db0_dx(j))/(z-b0)
  t3=-d_alpha_dxj*beta*gamma/sqrt(2.0)/2.0
  t4=-alpha*d_beta_dxj*gamma/sqrt(2.0)/2.0
  t5=-alpha*beta*d_gamma_dxj/sqrt(2.0)/2.0
  d_fug(i,j)=t1+t2+t3+t4+t5
!
  --- d_fugi/d_xj
  d_fug(i,j)=fug(i)*(d_fug(i,j)+delta(i,j)/chi(i))
  enddo
enddo
endif

! ----- partial molar volumes ---
do i=1,n_comp
  v(i)=0.0
  do j=1,niv
    v(i)=v(i)+dz_dx(j)*(delta(i,j)-chi(j))
  enddo
  v(i)=v(i)*r*t/p

```

```

v(i)=v(i)+vm
enddo
!      ----- fugacity derivatives :d_fugi/d_p ---
!      ----- d_fugi/d_p=fi*vi/r/t
da0_dp=aa/r**2/t**2
db0_dp=bb/r/t
dz_dp=dz_da0*da0_dp+dz_db0*db0_dp
d_alpha_dp=(b0*da0_dp-a0*db0_dp)/b0**2
d_gamma_dp=((dz_dp+(1.0+sqrt(2.0))*db0_dp)/(z+(1.0+sqrt(2.0))*b0)-
(dz_dp+(1.0-sqrt(2.0))*db0_dp)/(z+(1.0-sqrt(2.0))*b0))
do i=1,n_comp
  beta=2.0*s(i)/aa-b(i)/bb
  t1=dz_dp*b(i)/bb
  t2=-(dz_dp-db0_dp)/(z-b0)
  t3=-beta*d_alpha_dp*gamma/sqrt(2.0)/2.0
  t4=-beta*alpha*d_gamma_dp/sqrt(2.0)/2.0
  d_fug_dp(i)=t1+t2+t3+t4
  d_fug_dp(i)=fug(i)*(d_fug_dp(i)+1.0/p)
enddo
if (niv.eq.n_comp-1) then
!      ----- enthalpy ---
daadt=0.0
do ii=1,n_comp
  do kk=1,n_comp
    daadt=daadt + chi(ii)*chi(kk)*a(ii,kk)*&
      (xk(ii)/(1.0+xk(ii)*(1.0-sqrt(t/tc(ii))))/sqrt(tc(ii))+xk(kk)/(1.0+xk(kk)*(1.0-
sqrt(t/tc(kk))))/sqrt(tc(kk)))
  enddo

```

```

enddo

daadt=-daadt/sqrt(t)/2.0

hm=r*t*(z-1.0)+(t*daadt-aa)*gamma/bb/sqrt(2.0)/2.0

! ----- enthalpy derivatives ---

do i=1,n_comp-1
  daa_dxi=2.0*(s(i)-s(n_comp))
  d_daadt_dxi=0.0
  do k=1,n_comp
    d_daadt_dxi=d_daadt_dxi+&
    chi(k)*a(i,k)*&
    (xk(i)/(1.0+xk(i)*(1.0-sqrt(t/tc(i))))/sqrt(tc(i)) +&
    xk(k)/(1.0+xk(k)*(1.0-sqrt(t/tc(k))))/sqrt(tc(k)) )-&
    chi(k)*a(n_comp,k)*(xk(n_comp)/(1.0+&
    xk(n_comp)*(1.0-sqrt(t/tc(n_comp))))/sqrt(tc(n_comp)) +&
    xk(k)/(1.0+xk(k)*(1.0-sqrt(t/tc(k))))/sqrt(tc(k)))
  enddo
  d_daadt_dxi=-d_daadt_dxi/sqrt(t)
  d_gamma_dxi=((dz_dx(i)+(1.0+sqrt(2.0))*db0_dx(i))/(z+(1.0+sqrt(2.0))*b0)-
  (dz_dx(i)+&
  (1.0-sqrt(2.0))*db0_dx(i))/(z+(1.0-sqrt(2.0))*b0))
  t1=r*t*dz_dx(i)
  t2=(((t*d_daadt_dxi-daa_dxi)*bb
  b(n_comp))/bb**2)*gamma/sqrt(2.0)/2.0 - (t*daadt-aa)*(b(i)-
  t3=((t*daadt-aa)/bb)*d_gamma_dxi/sqrt(2.0)/2.0
  hi(i)=t1+t2+t3
enddo

do i=1,n_comp
  h(i)=hm

```

```

do j=1,n_comp-1
    h(i)=h(i)+hi(j)*(delta(i,j)-chi(j))
enddo

h(i)=h(i)-p*v(i)

enddo

endif

return

end

```

```

subroutine M_PressLoss(Tres, Pres, FP, Dliq, dPdx, yN2, yH2S, yCO2, yH2O,
VISliq, VISgas, gc, g, pi, ritbg, Qgas, Qliq, Qt, Vliq, Lm, Ls, wt, SGgas, etbg, dx,
Dm, nc, mfgas, Tc, Pc, CN1, CN2, CN3, CN4)

character(len=20) FP, C
character(len=20) CN1, CN2, CN3, CN4

real Nrb, Nrel, Nre

real Tc(16), Pc(16), mfgas(16)

eps=0.0006

Area=Pi*ritbg**2

Vt=Qt/(86400*Area)           !Total fluid velocity, ft/sec
Vsl=Qliq/(86400*Area)       !Total fluid velocity, ft/sec
Vsg=Qgas/(86400*Area)       !Total fluid velocity, ft/sec

Select case (FP)

    Case ('Bubble flow')

        !The Griffith correlation

        Fgb=0.5*(1+(Qt/(0.8*Area))-(((1+(Qt/(0.8*Area)))**2)-
(4*Qgas+1000/(0.8*Area)))**(0.5)) !Gas fraction

        call M_GasDensity(Tres, Pres, SGgas, yN2, yCO2, yH2S, yH2O, Dgas, nc,
mfgas, Tc, Pc, CN1, CN2, CN3, CN4)

        Dmb=Dgas*Fgb+(1-Fgb)*Dliq           !Density of mixture,
lbm/ft^3

        Dm=Dmb

```

```

dh=2*ritbg                                !Hydraulic diameter, ft
Vliq=Qliq*5.615/(86400*Pi*ritbg**2*(1-Fgb))  !Velocity of
liquid, (ft/sec)
Reyb=1488*Dliq*dh*Vliq/VISliq
call M_FricFac(Reyb, ffb, ritbg, etbg)
FLGb=ffb*Dliq*Vliq**2/(2*gc*dh)           !Friction loss gradient
Wt=5.615*Qt*Dmb/86400                     !Total mass rate, lb/sec
dP1=Dmb+FLGb
dP2=Wt*Qgas/(4637*Area**2*Pres)
dPdx=(dP1/(1-dP2))*(dx/144)
Case ('Slug flow')
dh=2*ritbg
Vbguess=0.5*(g*dh)**0.5
Nre=1488*Dliq*Vliq*dh/VISliq
Nrel=1488*Dliq*Vt*dh/VISliq
10  Nrb=1488*Dliq*Vbguess*dh/VISliq
if (Nrb.lt.3000)then
  Vb=(0.546+8.74E-6*Nrel)*(g*dh)**0.5
elseif (Nrb.gt.8000)then
  Vb=(0.35+8.74E-6*Nrel)*(g*dh)**0.5
else
  Sai=(0.251+8.74E-6*Nrel)*(g*dh)**0.5
  Vb=0.5*(Sai+(Sai**2+(13.59*VISliq/(Dliq*dh**0.5))**0.5))
endif
if(abs(Vb-Vbguess).gt.eps)then
  Vbguess=Vb
  goto 10

```

```

endif

!print*, 'Determine phase continuity.'

!print*, 'Enter "Continuous oil" or "Continuous water".'

!read *, C

C='Continuous oil'

select case (C)

  Case ('Continuous oil')

    if(Vt.lt.10) Delta=(0.0127*log(VISliq+1)/dh**1.415)-
0.284+0.167*log(Vt)+0.113*Log(dh)

    if(Vt.gt.10) then

      X=-log(Vt)*((0.01*log(VISliq+1)/dh**1.571)+0.397+0.63*Log(dh))

      Delta=(0.0274*log(VISliq+1)/dh**1.371)+0.161+0.569*Log(dh)+X

    endif

  Case ('Continuous water')

    if(Vt.lt.10)Delta=(0.013*log(VISliq)/dh**1.38)-0.681+0.232*log(Vt)-
0.428*Log(dh)

    if(Vt.gt.10)Delta=(0.045*log(VISliq)/dh**0.799)-0.709-0.162*log(Vt)-
0.888*Log(dh)

  end select

  call M_GasDensity(Tres, Pres, SGgas, yN2, yCO2, yH2S, yH2O, Dgas, nc,
mfgas, Tc, Pc, CN1, CN2, CN3, CN4)

  Dms=((Dliq*(Vsl+Vb)+Dgas*Vsg)/(Vt+Vb))+Delta*Dliq

  Dm=Dms

  call M_FricFac(Nrel, ffs, ritbg, etbg)

  FLGS1=(((Qliq*5.615/86400)+Vb*Area)/((Qt*5.615/86400)+Vb*Area))+Delta

  FLGs=(ffs*Dliq*Vt**2/(2*gc*dh))*FLGS1 !Friction loss
gradient

  Wt=5.615*Qt*Dms/86400 !Total mass rate,
lb/sec

  dP1=Dms+FLGs

```

```

dP2=Wt*Qgas/(4637*Area**2*Pres)
dPdx=(dP1/(1-dP2))*(dx/144)
case ('Transition flow')
  dh=2*ritbg
  Vbguess=0.5*(g*dh)**0.5
  Nre=1488*Dliq*Vliq*dh/VISliq
  Nrel=1488*Dliq*Vt*dh/VISliq
100  Nrb=1488*Dliq*Vbguess*dh/VISliq
  if (Nrb.lt.3000)then
    Vb=(0.546+8.74E-6*Nrel)*(g*dh)**0.5
  elseif (Nrb.gt.8000)then
    Vb=(0.35+8.74E-6*Nrel)*(g*dh)**0.5
  else
    Sai=(0.251+8.74E-6*Nrel)*(g*dh)**0.5
    Vb=0.5*(Sai+(Sai**2+(13.59*VISliq/(Dliq*dh**0.5))**0.5))
  endif
  if(abs(Vb-Vbguss).gt.eps)then
    Vbguess=Vb
    goto 100
  endif
!print*, 'Determine phase continuity.'
!print*, 'Enter "Continuous oil" or "Continuous water".'
!read *, C
C='Continuous oil'
select case (C)
  Case ('Continous oil')
    if(Vt.lt.10)
      Delta=(0.0127*log(VISliq+1)/dh**1.415)-
0.284+0.167*log(Vt)+0.113*Log(dh)

```

```

if(Vt.gt.10) then
    X=-log(Vt)*((0.01*log(VISliq+1)/dh**1.571)+0.397-0.63*Log(dh))
    Delta=(0.0274*log(VISliq+1)/dh**1.371)+0.161+0.569*Log(dh)+X
endif

Case ('Continuous water')

    if(Vt.lt.10)Delta=(0.013*log(VISliq)/dh**1.38)-0.681+0.232*log(Vt)-
0.428*Log(dh)

    if(Vt.gt.10)Delta=(0.045*log(VISliq)/dh**0.799)-0.709-0.162*log(Vt)-
0.888*Log(dh)

end select

call M_GasDensity(Tres, Pres, SGgas, yN2, yCO2, yH2S, yH2O, Dgas, nc,
mfgas, Tc, Pc, CN1, CN2, CN3, CN4)

Dms=((Dliq*(Vsl+Vb)+Dgas*Vsg)/(Vt+Vb))+Delta*Dliq

call M_FricFac(Nrel, ffs, ritbg, etbg)

FLGs=(ffs*Dliq*Vt**2/(2*gc*dh))*(((Qliq+Vb*Area)/(Qt+Vb*Area))+Delta)
!Friction loss gradient

!The Duns and Ros correlation

Fgm=Qgas/(Qgas+Qliq)                                !Gas fraction

Dmm=(1-Fgm)*Dliq+Fgm*Dgas

dh=2*ritbg                                           !Hydraulic diameter, ft

Vsgas=(Qgas*1000)/(86400*Area)                        !Superficial
velocity of gas (ft/sec)

Reym=1488*Dgas*dh*Vsgas/VISgas

call M_FricFac(Reym, ffm, ritbg, etbg)

FLGm=ffm*Dgas*Vsg**2/(2*gc*dh)!Density of mixture, lbm/ft^3

Dmt=((Lm-Vgd)/(Lm-Ls))*Dms+((Vgd-Ls)/(Lm-Ls))*Dmm

Dm=Dmt

FLGt=((Lm-Vgd)/(Lm-Ls))*FLGs+((Vgd-Ls)/(Lm-Ls))*FLGm    !Friction
loss gradient

Wt=5.615*Qt*Dmt/86400                                !Total mass rate, lb/sec

```

```

dP1=Dmt+FLGt
dP2=Wt*Qgas/(4637*Area**2*Pres)
dPdx=(dP1/(1-dP2))*(dx/144)
case ('Mist flow')
!The Duns and Ros correlation
Fgm=Qgas/(Qgas+Qliq) !Gas fraction
call M_GasDensity(Tres, Pres, SGgas, yN2, yCO2, yH2S, yH2O, Dgas, nc,
mfgas, Tc, Pc, CN1, CN2, CN3, CN4)
Dmm=(1-Fgm)*Dliq+Fgm*Dgas !Density of mixture,
lbm/ft^3
Dm=Dmm
dh=2*ritbg !Hydraulic diameter, ft
Vsgas=(Qgas*1000)/(86400*Area) !Superficial velocity of
gas (ft/sec)
Reym=1488*Dgas*dh*Vsgas/VISgas
call M_FricFac(Reym, ffm, ritbg, etbg)
FLGm=ffm*Dgas*Vsg**2/(2*gc*dh) !Friction loss gradient
Wt=5.615*Qt*Dmm/86400 !Total mass rate, lb/sec
dP1=Dmm+FLGm
dP2=Wt*Qgas/(4637*Area**2*Pres)
dPdx=(dP1/(1-dP2))*(dx/144)
end select
return
end

```

```

subroutine M_PseudoPropKC(nc, mf, Tc, Pc, CN1, CN2, CN3, CN4, Ppseudo,
Tpseudo, yN2, yCO2, yH2S, yH2O)
character(len=20) CN1, CN2, CN3, CN4
real mf(nc), Tc(nc), Pc(nc)
Ppseudo=0.0

```

```

Tpseudo=0.0
do i=1, nc
  Ppseudo=Ppseudo+(mf(i)*Pc(i))
  Tpseudo=Tpseudo+(mf(i)*Tc(i))
enddo
TTpseudo=Tpseudo
!Wichert and Aziz method

if ((CN1 .eq. 'H2S').or.(CN2 .eq. 'CO2')) then
  Acor=yH2S+yCO2
  Bcor=yH2S
  cor1=120*(Acor**0.9-Acor**1.6)+15*(Bcor**0.5-Bcor**4)
  Tpseudo=Tpseudo-cor1
  Ppseudo=Ppseudo*Tpseudo/(TTpseudo+Bcor*(1-Bcor)*cor1)
endif

if ((CN3 .eq. 'N2').or.(CN4 .eq. 'H2O')) then
  Tpscor=-246.1*yN2+400*yH2O
  Ppccor=-162*yN2+1270*yH2O
  Tpseudo=((Tpseudo-227.2*yN2-1.165*yH2O)/(1-yN2-yH2O))+Tpscor
  Ppseudo=((Ppseudo-493.1*yN2-3200*yH2O)/(1-yN2-yH2O))+Ppccor
endif

return

end

```

```

subroutine M_WellboreTempCal(Tres, Pres, dPdx, yN2, yH2S, yCO2, yH2O,
VISliq, VISgas, gc, g, pi, ritbg,Qgas, Qliq, Qt, Tgen, SGgas, etbg, dx, cpm, vtbg,
Dm, Sigm,nc, mfgas, Tc, Pc, CN1, CN2, CN3, CN4, Vliq, Dliq)

character(len=20) FP

character(len=20) CN1, CN2, CN3, CN4

```

```

real Ls, Lm
real Tc(16), Pc(16), mfgas(16)
Area=Pi*ritbg**2
Vt=Qt/Area
!call MP_LiqProp(Qoil, Qw, Qliq, Doil, Vliq, Foil, Fw, Dw, Dliq, Pi, ritbg)
call M_PhaseDet(Qgas, Qliq, Qt, ritbg, Dliq, sigma, g, Lm, Ls, FP, pi)
call M_PressLoss(Tres, Pres, FP, Dliq, dPdx, yN2, yH2S, yCO2, yH2O, VISliq,
VISgas, gc, g, pi, ritbg,&
                Qgas, Qliq, Qt, Vliq, Lm, Ls, wt, SGgas, etbg, dx, Dm, nc, mfgas, Tc, Pc,
                CN1, CN2, CN3, CN4)
Qgen=Qt*dPdx*dx/(86400*5.40935)                !Unit: Btu/min
Tgen1=Qgen/(Dm*vtbg*cpm)                       !Unit: F
Tgen=Tgen1*100/(Vt*60)
Pres=Pres-dPdx
if (FP.eq.'Mist flow') Tgen=0
return
end

```

```

subroutine M_Zfactor(TT, P1, Z, Gamag, rog, Ppseudo, Tpseudo)
    !Hall-Yarborough method for Z-factor calculation
    !Newton-Raphson iterative technique
    eps=1.0e-5
    y=0.01    !Firt guess
    Ppr=(P1+14.7)/(Ppseudo+14.7)
    Tpr=(TT+460)/Tpseudo
    tr=Tpseudo/(TT+460)
    A=0.06125*tr*exp(-1.2*(1-tr)**2)
    B=tr*(14.76-9.76*tr+4.58*tr**2)
    C=tr*(90.7-242.2*tr+42.4*tr**2)

```

```

D=2.18+2.82*tr
10 fy=(y+y**2+y**3-y**4)+(1-y)**3*(-(A*Ppr)-(B*y**2)+(C*y**D))
u1=y+y**2+y**3-y**4
du1=1+2*y+3*y**2-4*y**3
u2=(1-y)**3
du2=-3*(1-y)**2
u3=-(A*Ppr)-(B*y**2)+(C*y**D)
du3=-2*B*y+D*C*y**(D-1)
f1y=du1+(du2*u3+u2*du3)
if(abs(fy) .le. eps) then
    Z=A*Ppr/y
elseif ((fy .ne. 0).and.(f1y .ne. 0)) then
    y=y-(fy/f1y)
    goto 10
else
    print *,'Newton Raphson method do not converge.'
endif
rog=2.7*(P1+14.7)*Gamag/(Z*(TT+460))      !rog: lbm/ft^3
                                           !P1: psia
                                           !TT: R

return
end

```
